ЖУРНАЛ
ПРИКЛАДНОЙ ХИМИИ

Volume 32, No. 5

May, 1959

JOURNAL OF
APPLIED CHEMISTRY
OF THE USSR

(ZHURNAL PRIKLADNOI KHIMII)

IN ENGLISH TRANSLATION

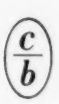

CONSULTANTS BUREAU, INC.

Chemistry Collections

IN ENGLISH TRANSLATION

Consultants Bureau's chemistry collections, a unique venture in the translation-publishing field, consist of articles on specialized subjects, selected by specialists in each field, from Soviet chemical journals published in translation by CB. These collections are then presented in symposium form.

Periodically we shall issue new collections taken from the latest volumes of our journals, not only on subjects already covered but also on those which prove most valuable to current scientific research. The following is one of the most recent additions to our list of collections (information on forthcoming titles available on request).

SOVIET RESEARCH IN FUSED SALTS (1956)

42 papers taken from the following Soviet chemistry journals, 1956: Soviet Journal of Atomic Energy; Journal of General Chemistry; Journal of Applied Chemistry; Bulletin of the Academy of Sciences, USSR, Division of Chemical Sciences; Proceedings of the Academy of Sciences, USSR, Chemistry Section. The entire collection consists of one volume, in two sections.

I	Systems (23 papers)	$ 30.00
II	Electrochemistry: Aluminum and Magnesium, Corrosion, Theoretical; Thermodynamics; Slags, Mattes (19 papers)	20.00
THE COMPLETE COLLECTION		$ 40.00

also available in translation . . .

SOVIET RESEARCH IN FUSED SALTS (1949-55)

125 papers taken from the following Soviet chemistry journals, 1949-55: Journal of General Chemistry; Journal of Applied Chemistry; Bulletin of Academy of Sciences, USSR, Div. Chemical Sciences; Journal of Analytical Chemistry. Sections of this collection may be purchased separately as follows:

Structure and Properties (100 papers)	$110.00
Electrochemistry (8 papers)	20.00
Thermodynamics (6 papers)	15.00
Slags and Mattes (6 papers)	15.00
General (5 papers)	12.50
THE COMPLETE COLLECTION	$150.00

NOTE: Individual papers from each collection are available at $7.50 each. Tables of contents sent upon request.

CB collections are translated by bilingual scientists, and include all photographic, diagrammatic and tabular material integral with the text. Reproduction is by multilith process from "cold" type; books are staple bound in durable paper covers.

CONSULTANTS BUREAU, INC.

227 WEST 17TH STREET, NEW YORK 11, N. Y.

Volume 32, No. 5

May, 1959

JOURNAL OF
APPLIED CHEMISTRY
OF THE USSR

(ZHURNAL PRIKLADNOI KHIMII)

A publication of the Academy of Sciences of the USSR

IN ENGLISH TRANSLATION

Year and issue of first translation:
Vol. 23, No. 1 January 1950

	U. S. and Canada	*Foreign*
Annual subscription	*$60.00*	*$65.00*
Annual subscription for libraries of nonprofit academic institutions	*20.00*	*25.00*
Single issue	*7.50*	*7.50*

Copyright 1960
CONSULTANTS BUREAU ENTERPRISES, INC.
227 West 17th Street, New York, N. Y.

Editorial Board
(ZHURNAL PRIKLADNOI KHIMII)

P. P. Budnikov, S. I. Vol'fkovich, A. F. Dobrianskii,
O. E. Zviagintsev, N. I. Nikitin (Editor in Chief),
G. V. Pigulevskii, M. E. Pozin, L. K. Simonova
(Secretary), V. V. Skorchelletti, N. P. Fedot'ev

Note: The sale of photostatic copies of any portion of this copyright translation is expressly prohibited by the copyright owners.

Printed in the United States of America

JOURNAL OF APPLIED CHEMISTRY OF THE USSR

Volume 32, Number 5 May, 1959

CONTENTS

	PAGE	RUSS. PAGE
Modification of Potassium Metaphosphate by Means of Salt Additions. S. I. Vol'fkovich and T. A. Ban'shchikova	963	941
Crystallization of Calcium Sulfate from Solutions of Wet-Process Phosphoric Acid. E. V. Khamskii and M. L. Chepelevetskii	970	948
Use of p-Phenylenediamine as Oxidation Inhibitor for Ammonium Sulfite–Bisulfite Solutions. B. A. Chertkov	975	952
Oxidation of Ammonium Sulfite–Bisulfite Solutions in the Extraction of SO_2 from Flue Gases. B. A. Chertkov	983	960
A Study of the Factors Influencing Formation of Sulfides from Metal Oxides by the Action of Sulfur Dioxide. V. V. Pechkovskii	988	966
Combined Removal of CO_2 from Nitrogen–Hydrogen Mixtures and Production of Ammonium Carbonates. S. N. Ganz, G. I. Vilesov, S. I. Gorbman, and S. B. Leibovich	992	969
A Study of the Rate of Conversion of $CaSO_4$ into $(NH_4)_2SO_4$ in Conjunction with Absorption of NH_3 and CO_2 under Conditions of High Turbulence. S. N. Ganz, S. B. Leibovich, and S. I. Gorbman	998	975
Action of Acid Solutions on Vitreous Lithium Silicates. S. K. Dubrovo	1001	979
A Study of the Optical Properties of Sodium Aluminoborosilicate Glasses. A. A. Appen and Gan' Fu-si (Kan Fu-si)	1006	983
A Study of the Optical Properties of Potassium Aluminoborosilicate Glasses. A. A. Appen and Gan' Fu-si (Kan Fu-si)	1013	991
Effect of Common Salt on the Solubility of Sodium Antimonate, Stannate, and Arsenate in Aqueous Caustic Soda Solution. G. G. Urazov, B. M. Lipshits, and V. S. Lovchikov.	1017	995
Investigation of the Conversion of Carbon Monoxide by Steam under Pressure. V. I. Atroshchenko and B. Bibr.	1020	997
Effect of the Height of the Foam Layer on a Sieve Plate on Absorption of Carbon Dioxide by Alkali Solutions. M. E. Pozin, B. A. Kopylev, and É. Ya. Tarat.	1027	1004
Absorption of Carbon Dioxide by Caustic Soda Solutions under Foam Conditions. M. E. Pozin, B. A. Kopylev, and É. A. Tarat	1033	1011
Surface Resistance in Absorption Processes. M. Kh. Kishinevskii and L. A. Mochalova.	1039	1016
Some Questions of the Analogy between Diffusional and Thermal Processes. A.A.Medvedev and P. G. Romankov	1044	1021
Bubbling of Air through a Layer of Viscous Liquid. I. P. Levsh and O. B. Balandina	1051	1029

CONTENTS (continued)

	PAGE	RUSS. PAGE
Interfacial Tension in Certain Sulfide–Silicate Systems at a High Temperature. V. L. Kheifets and A. B. Sheinin	1062	1039
Preparation and Certain Properties of Thin Silica Dielectric Films. N. N. Tvorogov.	1065	1043
Stability of Electrolyte Foams. V. G. Gleim, I. K. Shelomov and B. R. Shidlovskii.	1069	1046
A Study of the Oxidation of Aluminum Powder in Aqueous Alcoholic Solutions. L. I. Virin	1073	1050
Effect of Sulfur Compounds on the Current Efficiency for Magnesium in the Electrolysis of Carnallite. S. A. Pushkareva	1079	1056
Electrolytes for Electrochemical Polishing of Steel. G. P. Maitak and G. S. Tret'yakova	1083	1060
The Cause of Luster in Electrolytic Nickel Deposits. A. V. Pamfilov and R. M. Morgart	1089	1066
Sodium Salicylate as Inhibitor of Steel Corrosion in Neutral Media. E. V. Bogatyreva and S. A. Balezin	1094	1071
The Role of Diffusion in Hydrolysis of Polysaccharides in a Heterogeneous Medium. A. A. Konkin and E. A. Shukalova	1099	1076
Effect of Acid Concentration on the Hydrolysis Rate of Polysaccharides. L. I. Novikova and A. A. Konkin	1104	1081
Polymerization of Styrene in Presence of 1,1'-Bis-Hydroperoxodicyclohexyl Peroxide and Cobalt Naphthenate. R. K. Gavurina, P. A. Medvedeva, Sh. G. Yanovskaya, and L. O. Visleneva	1109	1086
Study of the Chemical Structure of Emulsion-Polymerized Divinyl Rubbers Made at + 50 and – 35°. A. I. Yakubchik, S. K. Zykova, and V. M. Vlasova	1115	1092
Epoxy Resins Based on Diphenylolethane (4,4'-Dihydroxydiphenylmethylmethane) and Phenol–Acetaldehyde Resins. G. L. Yukhnovskii and Zu Khva-den	1124	1100
Waterproofing of Paper by Alkyl Acetoxysilanes and Siloxanes. M. G. Voronkov, V.P. Davydova, and N. P. Grishanina	1130	1106
Dehydrogenation of Higher Paraffin Hydrocarbons over Carbon Catalysts. I. B. Rapoport, B. K. Nefedov, and S. G. Grakhova	1137	1112
Dehydrogenation of Paraffin Hydrocarbons over Chromium Oxide–Alumina Catalysts I. B. Rapoport and B. K. Nefedov	1145	1121
Oxidation of Acenaphthene to Naphthalic Anhydride. G. P. Petrenko and M. M. Dashevskii	1150	1126
Preparation of Formaldehyde by Oxidation of Methane, Catalyzed by Nitrogen Oxide. N. S. Enikolop'yan, N. A. Kleimenov, L. V. Karmilova, A. M. Markevich, and A. B. Nalbandyan	1156	1132
Reactions of Metals with Organic Thio and Thiophosphorus Additives in Oils. G. V. Vinogradov, M. M. Kusakov, P. I. Sanin, E. A. Razumovskaya, and A. V. Ul'yanova	1160	1136
Joint Polycondensation of Phenoxyacetic Acid and p-Chlorophenol with Formaldehyde. A. A. Vansheidt, N. N. Kuznetsova, and Z. I. Kulikova	1166	1142

CONTENTS (continued)

	PAGE	RUSS. PAGE
Catalytic Condensation of Compressed Acetylene with Aromatic Amines in the Liquid Phase. N. S. Kozlov and S. Ya. Chumakov	1173	1149
Brief Communications		
Studies of the Tempering of Porcelain. A. I. Avgustinik and V. M. Loginov	1177	1154
Possible Use of the PGF-2 Gas Analysis Apparatus as a Universal Instrument for Rapid Estimation of the Explosion Hazards of Various Vapor–Gas–Air Media. A. N. Baratov	1181	1157
Reduction of Nickel and Cobalt Ferrites by Hydrogen. M. G. Zhuravleva, V. N. Bogoslovskii, and G. I. Chufarov	1184	1159
Films of Semiconducting Tin Dioxide with Increased Conductivity. A. Ya. Kuznetsov, A. V. Kruglova, and B. P. Kryzhanovskii	1186	1161
Textile-Based Membrane Semiultrafilters. S. G. Mokrushin and V. I. Borisikhina	1189	1163
Corrosion Resistance of Certain Electrodeposited Alloys under Near-Tropical Conditions. N. P. Fedot'ev, P. M. Vyacheslavov, E. G. Kruglova, and S. Ya. Grilikhes.	1191	1165
Corrosion of Metals in Thionyl Chloride. V. A. Titov, Yu. A. Babkin, and I. M. Balandin	1195	1167
Influence of the Structure of Alcohols on the Film-Forming Properties of their Esters. Z. I. Edlinskii (Z. Jedlinski)	1198	1169
Combination of the Ester Interchange, and Polycondensation Reactions in Synthesis of Polyethylene Terephthalate. B. V. Petukhov and A. A. Konkin	1201	1171
Preparation of Lactic Acid Esters. R. M. Gel'dshtein	1204	1173
Alkylation of Avtol-6 (Lubricating Oil) Distilled by Chlorinated Paraffin in Presence of Dry Gumbrin and Gaseous Hydrogen Chloride. I. F. Radzevenchuk	1206	1174
Preparation of Propionic Acid from Acrylonitrile. I. N. Nazarov and G. A. Shvekhgeimer	1209	1177
Reactions of Nitro Olefins with Barbituric Acid. V. A. Kon'kova and V. V. Perekalin	1211	1178
Book Review		
W. L. Faith, D. B. Keyes, and R. L. Clark, Industrial Chemicals, Second Edition, New York, Wiley, 1957, 844	1213	1180

MODIFICATION OF POTASSIUM METAPHOSPHATE BY MEANS OF SALT ADDITIONS

S. I. Vol'fkovich and T. A. Ban'shchikova

The M. V. Lomonosov University, Moscow

The high concentration of nutrient substances in potassium metaphosphate – 39.87% K_2O and 60.13% P_2O_5, – make this compound a promising highly concentrated compound fertilizer for soils deficient in both elements. A very attractive property of metaphosphates is that they can be prepared to have different mobilities in soil; in accordance with requirements, they can be produced in forms soluble in water or citrates, or in almost insoluble form. Potassium metaphosphates may also be of interest for water softening and as components of detergents and special phosphate glasses.

Although metaphosphates of sodium and, to a smaller extent, of potassium were studied as early as the first half of the 19th century by Graham, Maddrell Fleitmann, and Lindbom), systematic and extensive studies of the properties, methods of preparation, and structure of various polymeric forms of the metaphosphates, of particular interest in agriculture, were undertaken only during the past 25-35 years (by Pascal, Britske, Thilo and others).

The method of preparation of potassium metaphosphate by decomposition of potassium chloride at high temperatures by orthophosphoric acid has long been known [1-5], but conditions in which different polymers and modifications are formed have not been studied sufficiently.

The present paper deals with a study of the conditions for preparation of potassium metaphosphates of practical importance by thermal dehydration of monopotassium orthophosphate (KH_2PO_4), and addition of small amounts of other salts to the product in order to modify its properties; mainly to confer solubility in water and ammonium citrate solution, as such solubility is a criterion of the rate and degree of assimilation of the product by plants.

The experiments on preparation of potassium metaphosphate were conducted over two temperature ranges: 320-330° and 960-1000°; two different dehydration products were obtained.

Experiments on preparation of potassium metaphosphate at 320-330° and 960-1000°; two different dehydration products were obtained.

Experiments on preparation of potassium metaphosphate at 320-330° were carried out in a TG-3 electric crucible furnace; the temperature was measured by means of a Chromel – Alumel thermocouple with an MP-28 millivoltmeter (accuracy grade 1), and checked by means of a LATR instrument. A weighed sample of potassium orthophosphate was poured through a funnel into a prepared nickel basin* which was in a furnace heated 20° above the experimental temperature. The experimental dehydration temperature was established within 2-3 minutes. At the end of the experiment the basin was removed from the furnace and cooled in air.

Experiments on preparation of potassium metaphosphate at 960-1000° were carried out in a muffle furnace with automatic regulation; at the end of an experiment, the crucible was taken out of the furnace and the

*As nickel reacted with the reaction products under the experimental conditions, the basin was previously coated on the inside with a thin film of the meta salt.

contents were poured out rapidly onto an aluminum surface (for air chilling) or into a vessel with petrolatum (for oil chilling). After oil chilling, the product was washed with benzene and dried in air.

The products were analyzed for total P_2O_5 and water-soluble * and citrate-soluble P_2O_5 by the method used in the Scientific Research Institute of Fertilizers and Insectofungicides [6].

The starting material was pure potassium orthophosphate, prepared by neutralization of phosphoric acid with potassium carbonate, containing 51.87% P_2O_5. The other reagents were of chemically pure or analytical grades.

In the first series of experiments, on dehydration of KH_2PO_4 at 320-330°, the effect of the heating time on the solubility of the product in water and ammonium citrate solution was studied. This series of experiments showed that with increase of the heating time of the original salt in the furnace from 10 to 60 minutes, and hence with increasing dehydration, the solubility of the product in water is decreased approximately 5-fold (from 55-56% to 9-13%), and in ammonium citrate solution, approximately 2.5-fold (from 38-37% to 20-22%).

The optimum heating time at 320-330°, with a layer about 1 cm thick, was 15-16 minutes. This resulted in 98.8% dehydration of the original ortho salt, and the product contained 81.8% P_2O_5 in available form. **

If KH_2PO_4 was 92% dehydrated (in 10 minutes), the product was completely soluble in water. Thus, if a small percentage of water remains in the product, it retains its solubility in water, which is very important in practice.

In the next series of experiments, additions of various salts were tested in order to obtain a completely available product with 100% dehydration of KH_2PO_4. It is known from the work of Andre [7] and from earlier experiments carried out in the Scientific Research Institute of Fertilizers and Insectofungicides and MGU that addition of magnesium salts prevents retrogradation of water-soluble phosphoric acid in fertilizers.

We tested the following additives: KCl, NaCl, $CaCl_2$, $MgCl_2$, $MgCl_2 \cdot 6H_2O$, $MgSO_4$, MgO, CaO, in amounts from 1 to 10%. The choice of the additives was based on crystallochemical considerations and on the fact that some of them are present in native potassium salts (sylvinite, carnallite, and others). Some of these substances gave positive results in preliminary experiments (conducted jointly with Zh. V. Kirillova in 1955).

The results of these experiments are given in Tables 1-3.

It follows from these data that the best results are obtained with addition of calcium oxide which, at 98% dehydration, gives a product with an average content of 97.1% available P_2O_5. The next in order of effectiveness is magnesium sulfate, which gives 92.6% available P_2O_5 at 99% dehydration. Next in order are calcium and magnesium chlorides, and magnesium oxide.

It must be noted that additions of CaO, $MgCl_2$, MgO, $CaCl_2$, $MgSO_4$, while increasing the total contents of available P_2O_5 by 3 to 13%, cause a redistribution of the amounts of water-soluble and citrate-soluble P_2O_5; the content of water-soluble P_2O_5 is increased 3 to 3.8-fold. Comparison of the products with and without added salts shows that the amounts of water-soluble and citrate-soluble P_2O_5 change places, i.e., in the former case most of the P_2O_5 (67-81%) is obtained in the water-soluble form.

Additions of KCl and NaCl produced no practical effects; addition of 5% NaCl doubled the content of water-soluble P_2O_5, but the total content of available P_2O_5 fell by 5%. Additions of 1 or 3% of CaO and $MgCl_2$ were also ineffective.

In subsequent experiments, with additives the amounts of CaO and $MgCl_2$ were increased to 7.5%.

The experiments show that with 7.5% additions the best results are again obtained with calcium oxide: at 97% dehydration the product contained 98.5% available P_2O_5 and about 75% water-soluble P_2O_5.

In experiments with 10% additions, a completely water-soluble product was obtained with addition of $MgCl_2$. At 98.3% dehydration, 100% of the P_2O_5 is water soluble.

* The term "water-soluble P_2O_5" is taken as the amount of P_2O_5 determined in an aqueous extract made by dissolution of a sample of the salt as in the method for determination of available P_2O_5.

** Available P_2O_5 is the sum of water- and citrate-soluble P_2O_5.

TABLE 1

Effects of Added Salts on the Solubility of Potassium Metaphosphate. Additives were introduced in 5% amounts, temperature 320-330°, heating time 15 minutes

Additive	Total P_2O_5 content of product (%)	Degree of dehydration of salt (%)	Contents of			$\frac{\text{available } P_2O_5}{\text{total } P_2O_5}$ (%)
			water-soluble P_2O_5 (%)	citrate-soluble P_2O_5 (%)	available P_2O_5 (%)	
No additive	59.1	98.3	11.8	38.3	50.1	84.7
	59.4	98.7	13.2	36.8	49.9	83.5
KCl	57.7	100.0	8.6	37.5	46.1	82.5
	56.0	98.1	11.3	38.8	50.1	87.0
NaCl	57.3	100.0	26.4	18.9	45.3	79.0
	57.6	100.0	23.7	22.1	45.8	79.5
$CaCl_2$	55.4	97.2	46.0	5.0	51.0	92.0
	55.4	97.2	42.2	8.1	50.3	91.0
CaO	56.0	98.0	28.5	26.5	55.0	98.3
	56.0	98.0	32.7	20.8	53.5	95.5
	56.2	98.6	37.8	13.9	53.7	95.6
	55.5	97.3	43.2 *	11.8	55.0	99.0
$MgCl_2 \cdot 6H_2O$	54.3	95.5	36.9	10.3	47.2	87.0
	53.6	94.2	41.1	8.5	49.6	92.5 **
$MgCl_2$	56.0	98.0	36.2	11.2	47.4	84.6
	55.8	97.9	35.6	14.0	49.6	89.0
$MgSO_4$	56.2	98.5	42.4	10.3	52.7	94.9
	56.8	99.5	34.2	17.1	51.3	90.3
MgO	55.6	97.5	40.7	8.5	49.5	89.0
	56.1	98.5	38.7	11.4	49.8	88.9
	53.8	94.5	40.9	9.2	50.1	93.0

*Aqueous extracts from samples with added CaO and $CaCl_2$ were turbid.

**Duration of experiments with addition of $MgCl_2$ $6H_2O$ — 30 minutes.

TABLE 2

Effects of Added Salts on the Solubility of Potassium Metaphosphate.
Additives were introduced in 7.5% amounts, temperature 320-330°, heating time 15 minutes.

Additive	Total P_2O_5 content of product (%)	Degree of dehydration (%)	Contents of			$\frac{\text{available } P_2O_5}{\text{total } P_2O_5}$ (%)
			water-soluble P_2O_5 (%)	citrate-soluble P_2O_5 (%)	available P_2O_5 (%)	
$MgCl_2$	53.9	97.4	50.0	2.4	52.4	97.4
	54.4	98.0	44.3	5.3	49.6	91.4
MgO	52.0	94.0	51.2	1.6	52.8	100.0
	51.8	93.6	47.1	5.3	52.4	100.0
$CaCl_2$	55.5	100.0	40.3	10.5	50.8	91.7
	52.6	95.0	45.6	5.4	51.0	97.0
CaO	53.1	96.0	37.9	15.2	53.1	100.0
	54.0	97.4	42.6	9.8	52.4	97.0

TABLE 3

Effects of Added Salts on the Solubility of Potassium Metaphosphate. Additives were introduced in 10% amounts, temperature 320-330°, heating time 15 minutes

Additive	Total P_2O_5 content of product (%)	Degree of dehydration (%)	Contents of water-soluble P_2O_5 (%)	Contents of citrate-soluble P_2O_5 (%)	Contents of available P_2O_5 (%)	available P_2O_5 / total P_2O_5 (%)
$MgCl_2$	53.1	98.5	53.1	Not determined	53.7	100.0
	52.9	98.0	52.7	Same	52.7	100.0
MgO	51.0	95.0	44.1	7.6	51.7	100.0
	51.2	95.3	43.9	4.3	48.2	94.4
$CaCl_2$	51.3	95.3	49.0	2.2	51.2	100.0
	51.4	95.5	47.1	4.0	51.1	99.5
CaO	51.9	96.5	40.6	12.0	52.6	100.0
	51.8	96.3	36.2	14.6	50.8	98.5

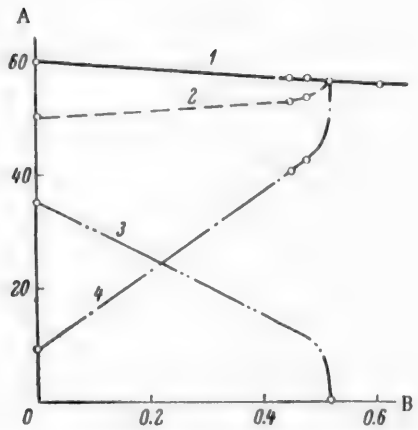

Fig. 1. Solubility of potassium metaphosphate as a function of the amount of water left after dehydration: A) P_2O_5 content (%); B) water content (moles); P_2O_5 content (%): 1) total, 2) available, 3) citrate-soluble, 4) water-soluble.

In experiments with additions of magnesium chloride hexahydrate the degree of dehydration was lower, but the proportion of available P_2O_5 was higher than in experiments with anhydrous magnesium chloride. This, together with the results of the preceding experiments with different times of heating of KH_2PO_4, suggested experiments on partial dehydration of the salt in order to obtain soluble products.

The results are given in Fig. 1.

These experiments showed that a completely water-soluble product is obtained when the original monopotassium phosphate is 48% dehydrated, i.e., when about half the water content is retained in the product. This product was hygroscopic, with a hygroscopicity of over 10 points on Pestov's scale [8]. It seems that the partial dehydration as the result of exposure of the salt for different times at 320° did not yield a salt of definite composition, but a mixture of phosphates of different degrees of hydration was obtained.

In experiments on dehydration of monopotassium orthophosphate at 960-1000°, the effects of additives and chilling on the solubility of the product were studied. The results are given in Table 4.

The experiments showed that chilling in air does not result in uniform rapid cooling of the whole melt; part was obtained in the form of a transparent glass and the rest in the form of opaque white glass. In experiments with chilling in petrolatum the product was obtained in the form of small spheroidal granules.

The following additives were tested: Fe_2O_3, Al_2O_3, NaCl, KCl, $MgCl_2$, $CaCl_2$, SiO_2. Experiments with oil chilling showed that a completely water-soluble product is obtained with 3% amounts of the following additives: $CaCl_2$, Al_2O_3, $MgCl_2$, NaCl. The same additives in 1% amounts may probably give a soluble product if the melt is dispersed more finely in the oil during chilling. 1% of Fe_2O_3 is enough to give a completely water-soluble product. Addition of only 0.5% Fe_2O_3 resulted in a glassy product containing 100% of water-soluble P_2O_5; it became devitrified after some time.

TABLE 4

Effect of Additives on the Solubility of Potassium Metaphosphate. Temperature 960-1000°, heating time 15 minutes, air chilling

Additive	Amount added (%)	P_2O_5 in product (%) Mixture	Degree of dehydration (%)	Contents of available P_2O_5 (%) water-soluble	citrate-soluble	total	available P_2O_5 / total P_2O_5 (%)
No additive	—	60.2	100.0	8.2	39.7	47.9	79.7
	—	59.6	99.2	7.8	41.3	49.2	81.8
NaCl	1	58.2	98.0	13.7	44.2	57.9	98.5
	1	59.1	99.2	12.0	41.5	53.5	89.6
	5	56.8	99.5	56.8	—	56.8	100.0
	5	56.8	99.5	56.8	—	56.8	100.0
$MgCl_2$	1	59.0	99.2	18.1	38.9	57.0	96.8
	1	59.1	99.2	15.1	40.0	55.1	93.1
	5	57.5	100.0	57.5	—	57.5	100.0
	5	56.8	99.5	56.8	—	56.8	100.0
SiO_2	5	57.2	100.0	57.2	—	57.2	100.0
	5	57.2	100.0	57.2	—	57.2	100.0

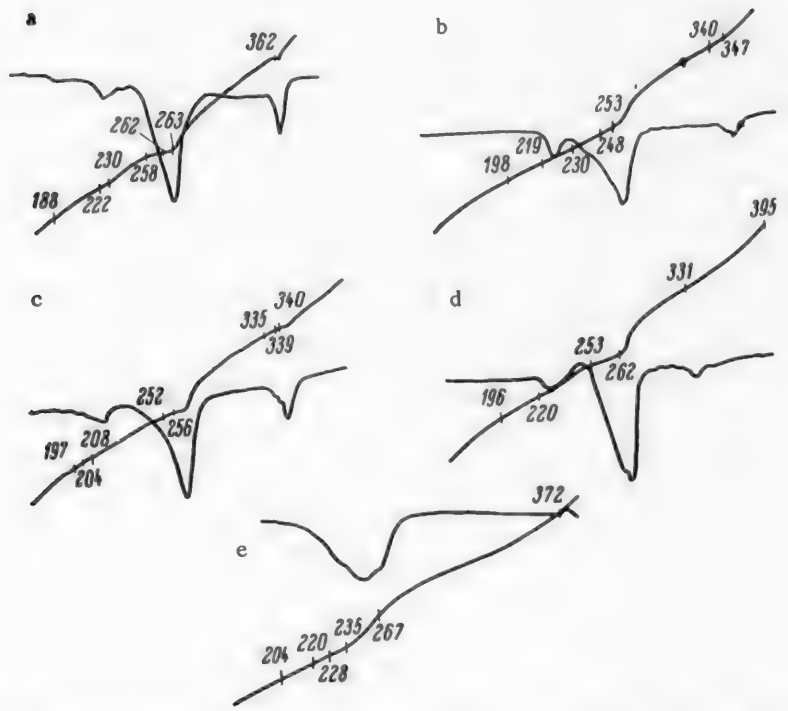

Fig. 2. Thermograms of KH_2PO_4 dehydration: a) without additive, b) 7.5% $MgCl_2$, c) 7.5% $CaCl_2$, d) 7.5% CaO, e) 7.5% MgO.

Addition of SiO_2 gave a completely water-soluble product only if not less than 5% was added. No effect was produced by addition even of 5% KCl.

The products formed at 320-330° and 960-1000° were investigated to determine whether they can be used as water-softening agents. The so-called "barium number" was determined in accordance with the existing tentative technical specifications for metaphosphates.

The experiments confirmed literature reports that the product made at 320-330° does not bind Ba or Ca ions. The samples contained 56.2 and 55.9% P_2O_5 and had activities of 6.8-8%.

Metaphosphates made at 960-1000° had the following characteristics: the product with addition of 1% Fe_2O_3 had 67% activity, with 2% – 68.7%, and with 3% – 53%.

Sodium metaphosphate prepared under analogous conditions had 84.6% activity. A product containing equal amounts of KPO_3 and $NaPO_3$ had 81.5% activity; a product containing 30% $NaPO_3$ and 70% KPO_3, had 78% activity.

According to the 1954 tentative technical specifications, sodium hexametaphosphate should have not less than 76% activity by the barium chloride method. Therefore the product obtained at 320-330° is unsuitable for water softening; the product made at 960-1000° with addition of 1% Fe_2O_3 is suitable, but is somewhat less active than sodium metaphosphate.

In practice, a mixed product consisting of potassium and sodium metaphosphates made from native sylvinite may be used in the production of water-softening agents.

For investigation of the influence of added salts on the dehydration of monopotassium orthophosphate, the process was studied thermographically.

A Kurnakov pyrometer with automatic recording of the heating curves was used for the investigation. The furnace with the test sample of salt was heated up uniformly ("linearly"). The salt samples were contained in Stepanov vessels about 3 ml in capacity. The furnace was heated up at a rate of 2° per minute. Aluminum oxide was used as the reference standard. The differential thermocouple was connected to the galvanometer in such a manner that endothermal processes gave deflections in the direction of the abscissa axis in the recorded graphs.

The vessel containing the salt was weighed before and after the heating. The degree of dehydration reached during the experiment was found from the loss in weight, and the final product was analyzed for total P_2O_5.

Thermograms were obtained for the dehydration of pure potassium orthophosphate and with 7.5% additions of calcium and magnesium chlorides and oxides (Fig. 2).

SUMMARY

1. The effects of various additives in potassium metaphosphate made at 320-330° were studied; the greatest effects were produced by calcium oxide and magnesium chloride. With 5% of calcium oxide, 97.1% P_2O_5 passed into available form; of this, 75% P_2O_5 was in the water-soluble form (at 98% dehydration). Under laboratory conditions the product was nonhygroscopic and free-flowing. This product can be used as a highly-concentrated compound fertilizer for acid and neutral soils.

2. Partial dehydration of monopotassium phosphate yields a completely water-soluble product on removal of about one half of its water; this gives a mixture of polyphosphates of different degrees of dehydration. The hygroscopicity of this product is over 10 points on the Pestov scale, i.e., it is not very suitable in practice as a fertilizer. When over 48% water is removed, the amounts of water-soluble and available P_2O_5 in the product gradually decrease.

3. When potassium metaphosphates are made at 960-1000°, a completely water-soluble product may be obtained by addition of 1% Fe_2O_3 to the ortho salt. The same result is obtained on addition of 3% $CaCl_2$, $MgCl_2$, NaCl, Al_2O_3 or 5% SiO_2.

Chilling is required for the formation of a water-soluble product; chilling in oil is more effective than air chilling.

In tests of the suitability of potassium metaphosphate as a component of detergents it was found that the product made with addition of 1% Fe_2O_3 had 67% activity (by the barium chloride method), whereas a product containing equal amounts of KPO_3 and $NaPO_3$ had 81.5% activity, which is nearly as high as the activity of $NaPO_3$ used industrially.

4. Thermographic investigation of dehydration of monopotassium phosphates, with and without various additives, up to 400° showed that most of the additives slightly lower the final dehydration temperature (by 15-30°) without influencing the main course of the process.

LITERATURE CITED

[1] B. H. Baskerwill, Ind. Eng. Ch. 34, 1 (1942).

[2] S. L. Madorsky and K. G. Clark, Ind. Eng. Ch. 32, 2, 244 (1940).

[3] É. V. Britske, A. A. Lezhnev and N. E. Pestov, J. Chem. Ind. 7, 1, 4 (1930).

[4] W. Hazen and W. H. Ross, U. S. Patents: a) 1456850 (1923); b) 1456831 (1923).

[5] S. I. Vol'fkovich, Bull. Acad. Sci. USSR, Div. Chem. Sci. 6, 673 (1957).*

[6] B. V. Mikhal'chuk (editor), Methods of Analysis and Control in Sulfuric Acid and Superphosphate Production [in Russian] (1955).

[7] L. K. Andre, Chem. et. Ind. 73, 3, 531 (1955).

[8] N. E. Pestov, Physicochemical Properties of Granular and Powdered Chemical Products [in Russian] (Izd. AN SSSR, 1947).

Received December 20, 1958.

*Original Russian pagination. See C. B. translation.

CRYSTALLIZATION OF CALCIUM SULFATE FROM SOLUTIONS OF WET-PROCESS PHOSPHORIC ACID

E. V. Khamskii and M. L. Chepelevetskii

The Prof. Ya. V. Samoilov Scientific Institute for Fertilizers and Insectofungicides

Studies of the crystallization of calcium sulfate from phosphoric acid solutions are closely connected with the production of H_3PO_4 by the sulfuric acid wet process.

The technology of this process is largely determined by the hydrate form in which the calcium sulfate crystallizes. Accordingly, a distinction is made between the dihydrate, hemihydrate, and anhydrite methods of acid production [1]. The main condition in the production of phosphoric acid by the dihydrate method is absence of calcium sulfate hemihydrate in the solid phase at the end of the extraction process. It is necessary to conform to this condition in order to avoid "setting" of the slurry during washing on the filters. Therefore for the dihydrate process it is necessary to know at what temperatures and P_2O_5 concentrations the solid phase reaching the filters consists of $CaSO_4 \cdot 2H_2O$, only.

It is known from earlier publications [2,3] that over a wide range of H_3PO_4 concentrations and temperatures the first substance to be precipitated is the metastable $CaSO_4 \cdot 0.5\ H_2O$, which is converted either into the dihydrate or into anhydrite, according to the crystallization conditions. Thus, the possibility of obtaining wet-process acid by the dihydrate method is determined by the time required for the conversion $CaSO_4 \cdot 0.5\ H_2O \rightarrow$ $\rightarrow CaSO_4 \cdot 2H_2O$. Since the time required for this conversion increases with increasing P_2O_5 content in the liquid phase [2], there is a limiting concentration for each temperature at which all the hemihydrate is converted into the dihydrate during the extraction time.

Since the above-mentioned investigations were performed with solutions of chemically pure H_3PO_4, with equimolecular CaO/SO_3 ratio in the liquid phase, it was necessary to test the above considerations under conditions resembling production conditions more closely. In the production of phosphoric acid, calcium sulfate crystallizes in presence of a number of impurities and, as a rule, in presence of excess $Ca^{\cdot\cdot}$ or SO_4'' ions in the liquid phase; moreover, under production conditions, crystallization takes place in the presence of large amounts of crystals already formed.

Nevertheless, as was shown by Gibbs [4], the probability of formation of any particular phase is determined by the change of free energy in its formation, while the latter in its turn depends considerably both on the presence of impurities and on the presence of seed crystals.

Tammann [5] also noted that the presence of impurities may lead to total disappearance of the nuclei of one metastable phase and to increase of the stability of another.

In the conditions of the wet process for phosphoric acid, both the hemihydrate and the dihydrate of calcium sulfate are metastable phases. It was therefore to be expected that impurities, and excess of either crystal-forming ion ($Ca^{\cdot\cdot}$ or SO_4'') may have significant effects on the probability of formation and the stability of these hydrates, and that the crystallization of calcium sulfate under technical conditions differs from its crystallization in chemically pure solutions.

Accordingly, the purpose of the present investigation was to study the crystallization of calcium sulfate under approximately the technological conditions, in order to obtain phosphoric acid of high concentration by the dihydrate process.

EXPERIMENTAL

Experiments on crystallization of calcium sulfate were carried out in a glass vessel fitted with a stirrer, kept at constant temperature to the nearest ±0.05°. The reagents used were flotation apatite, wet-process phosphoric acid, chemically pure phosphoric and sulfuric acids, fluosilicic and hydrofluoric acids, calcium carbonate, ammonium hydroxide of analytical reagent grade, and pure ferric hydroxide.

The experiments were conducted as follows. A solution of phosphoric acid heated to the required temperature was put in the vessel, and apatite and sulfuric acid were introduced with continuous stirring; to keep the concentration of the liquid phase constant throughout the experiment, the calculated amount of water was added. In a number of experiments, a solution of monocalcium phosphate in sulfuric acid was put into the reaction vessel instead of apatite.

Samples of the liquid and solid phases were taken at definite time intervals. The phases were separated by filtration on suction filters. After the separation, the solid phase was washed with ethyl acetate until neutral to methyl orange, and dried at room temperature until the ester odor disappeared. The liquid phase was analyzed for P_2O_5, CaO and SO_3, and the solid phase for water of crystallization. The refractive indices of some of the solid-phase samples were determined.

P_2O_5 was determined by the photocolorimetric method, SO_3 by precipitation of SO_4'' as $BaSO_4$, and CaO by Chapman's method. For determination of the water of crystallization the samples were dried to constant weight under an infrared lamp. The refractive indices were determined by the immersion method.

The experimental data presented below represent the results of studies of three problems.

The problem in the first series of experiments was to determine the degree of hydration of the calcium sulfate initially precipitated during crystallization from solutions of wet-process phosphoric acid.

The results of these experiments are summarized in Table 1.

TABLE 1

Contents of Water of Crystallization in Calcium Sulfate Samples 2-3 Minutes after Precipitation from Phosphoric Acid Solutions at 70°

Composition of liquid phase	Solid phase			
	refractive indices		content of H_2O of crystallization (%)	composition of solid phase
	Ng	Np		
Sol. of chem. pure ..... H_3PO_4, P_2O_5 35%	1.577	1.556	6.61	Hemihydrate
same. ..... H_3PO_4, P_2O_5 35%, Fe_2O_3 1%, SO_3 1%, Al_2O_3 0.3%, F 0.9%, SiO_2 0.4%	1.532 1.577	1.523 1.556	11.41	Mixture of dihydrate and hemihydrate
Sol. chem. pure H_3PO_4, P_2O_5 35%, Fe_2O_3 1.5%, SO_3 1.5%, Al_2O_3 0.6%, F 0.9%, SiO_2 0.4%	1.532	1.523	18.01	Dihydrate with admixture of hemihydrate
Sol. chem. pure H_3PO_4, P_2O_5 35%, Fe_2O_3 2.7%, SO_3 2.7%, Al_2O_3 1.6%, F 1%, SiO_2 0.5%	1.532	1.523	20.21	Dihydrate
Sol. of wet-process. ..... H_3PO_4, P_2O_5 35%, Fe_2O_3 0.3%, SO_3 2.5%, Al_2O_3 1%, F 1.44%, SiO_2 0.6%	1.532	1.523	19.48	Dihydrate

The data in Table 1 show that under technical conditions, in contrast to solutions of chemically pure H_3PO_4, calcium sulfate dihydrate is precipitated first.

It is clear from Table 1 that the change in the order of phase crystallization in the transition from chemically pure to technical H_3PO_4 solution is caused by the presence of impurities.

The second series of experiments consisted of a study of the crystallization of calcium sulfate from solutions of wet-process phosphoric acid of different concentrations (as P_2O_5), at different temperatures, and with different CaO/SO_3 ratios in the liquid phase.

The purpose of these experiments was to determine the degree of hydration of calcium sulfate precipitated under different conditions, with different compositions of the medium, and at different temperatures. The water of crystallization in the precipitates was determined 15-20 minutes after the start of crystallization. The results are given in Table 2.

TABLE 2

Contents of Water of Crystallization in Calcium Sulfate Precipitates 15-20 Minutes After Precipitation from Wet-Process Phosphoric Acid Solutions at Different Temperatures

Temperature (°C)	Composition of liquid phase (%)				Water of crystallization in solid phase (%)	Composition of solid phase
	P_2O_5	CaO	SO_3	CaO/SO_3 (molar)		
70	38.0	0.25	0.51	0.7	20.2	Gypsum
	39.1	0.24	0.52	0.7	16.3	Mixture of gypsum and hemihydrate
	40.0	0.25	0.54	0.7	7.4	Hemihydrate with admixture of gypsum
75	35.0	0.01	3.10	0.004	20.2	Gypsum
80	35.0	0.02	3.10	0.010	19.0	Gypsum with admixture of hemihydrate
82.5	35.0	0.02	3.20	0.009	12.5	Mixture of gypsum and hemihydrate
85	35.0	0.05	3.20	0.3	11.8	
87.5	35.0	0.06	3.40	0.3	7.4	Hemihydrate with admixture of gypsum
80	35.0	0.95	0.25	5.4	20.1	Gypsum
82.5	35.0	0.95	0.26	5.3	15.8	Mixture of gypsum and hemihydrate
85.0	35.0	0.97	0.26	5.3	13.5	
87.5	35.0	0.99	0.20	7.0	9.0	Hemihydrate with admixture of gypsum

TABLE 3

Contents of Water of Crystallization in the Solid Phase Formed During Extraction of H_3PO_4 with Different CaO/SO_3 Ratios in the Liquid Phase

Temperature (°C)	Composition of liquid phase (%)				Water of crystallization in solid phase (%)	Composition of solid phase
	P_2O_5	CaO	SO_3	CaO/SO_3		
60	39.2	0.04	2.10	0.03	6.9	Hemihydrate
		0.11	1.10	0.14	6.5	
		0.76	0.22	5.0	17.5	Gypsum with admixture of hemihydrate
		0.96	0.25	5.4	19.6	
70	36.4	0.07	2.74	0.04	18.7	Gypsum
	36.4	0.56	0.42	1.8	20.1	
	38.1	0.05	3.31	0.014	5.7	Hemihydrate
	38.1	0.64	0.43	2.1	13.6	Mixture of gypsum and hemihydrate

It follows from the data in Table 2 that with increase of the CaO/SO_3 ratio calcium sulfate can crystallize as the dihydrate in more highly concentrated phosphoric acid solutions and at higher temperatures.

In the third series of experiments the technological conditions for production of phosphoric acid were simulated and the composition of the solid phase at the end of the extraction was studied.

For this purpose the water of crystallization was determined in samples of the solid phase taken 8 hours after the start of each experiment. The results are given in Table 3.

The data in Table 3 show that increase of the CaO/SO_3 ratio in the liquid phase increases stability of the dihydrate in solutions of wet-process phosphoric acid.

DISCUSSION OF RESULTS

The results show that the presence of impurities in solutions of wet-process phosphoric acid favors crystallization of calcium sulfate in the dihydrate form.

Increase of the CaO/SO_3 ratio in the liquid phase is a necessary condition for increasing the stability of calcium sulfate dihydrate. The action mechanism of the impurities in this case evidently consists of a decrease of the change of free energy in the formation of $CaSO_4 \cdot 2H_2O$ and an increase of the change of free energy in the formation of $CaSO_4 \cdot {}^1/_2 H_2O$. This example demonstrates once again the important role of impurities in solution in the formation of new phases and production of real crystals with modified properties.

The influence of the CaO/SO_3 ratio on the degree of hydration of crystallizing calcium sulfate may be explained as follows.

Increase of the content of calcium ions in solution results in partial neutralization of the hydrogen ions of phosphoric acid and, in consequence, in an increase of the vapor pressure of the solution. The latter effect favors formation of $CaSO_4 \cdot 2H_2O$. Moreover, increase of the calcium ion concentration leads to increased contents of phosphate ions and admixtures of other anions in the solid phase as the result of formation of a limited solid solution. A solid solution of calcium phosphate and sulfate is formed more easily if the sulfate crystallizes as $CaSO_4 \cdot 2H_2O$. This is because $CaSO_4 \cdot 2H_2O$ and $CaHPO_4 \cdot 2H_2O$ crystallize in the same monoclinic crystal system, while $CaSO_4 \cdot {}^1/_2H_2O$ crystallizes in the hexagonal system. The increased stability of the dihydrate with increase of the calcium ion concentration in the solution can also be attributed to the creation of favorable conditions for the formation of these solid solutions.

These results alter the existing concepts of the physicochemical principles of the dihydrate process of phosphoric acid production. If the first substance to be precipitated during the extraction is $CaSO_4 \cdot 2H_2O$ (and not the hemihydrate, as is the case in solutions of chemically pure H_3PO_4), then the formation of acid by the dihydrate process is determined not by the kinetics of the $CaSO_4 \cdot {}^1/_2 H_2O \rightarrow CaSO_4 \cdot 2H_2O$ conversion but by conditions which favor primary crystallization of calcium sulfate in the dihydrate form. The discovery of the influence of CaO/SO_3 ratio on the crystallization of calcium sulfate opens up new possibilities for regulation of the wet extraction process by variations of the amounts of sulfuric acid and phosphate rock fed into the digesters. The above experimental results show that phosphoric acid of relatively high concentration can be obtained by the dihydrate method. For example, if the digestion is effected at 70° with a molar CaO/SO_3 ratio of the order of 2.0-2.8 in the liquid phase of the first digester, an acid product containing 34-38% P_2O_5 and over can be obtained.

SUMMARY

1. At temperatures of 60-80°, under definite conditions, the first substance to be precipitated from solutions of wet-process phosphoric acid may be calcium sulfate dihydrate.

2. Increase of the CaO/SO_3 ratio in H_3PO_4 solutions favors crystallization of calcium sulfate as the dihydrate, and increases the stability of the latter.

3. It is shown that wet-process phosphoric acid containing 34-38% P_2O_5, can be made by the dihydrate method.

LITERATURE CITED

[1] S. K. Voskresenskii, J. Appl. Chem. 27, 669 (1954).*

[2] A.A.Taperova and M. N. Shul'gina, J. Appl. Chem. 23, 32 (1950).*

[3] A. A. Taperova and M. N. Shul'gina, J. Appl. Chem. 18, 521 (1945).

[4] J. W. Gibbs, Fundamentals of Statistical Mechanics [Russian translation] (Moscow—Leningrad, 1946).

[5] G. Tammann, Manual of Heterogeneous Equilibria [Russian translation] (ONTI, Chem. Theoret. Press, Leningrad, 1935).

Received December 21, 1957.

*Original Russian pagination. See C. B. translation.

USE OF p-PHENYLENEDIAMINE AS OXIDATION INHIBITOR FOR AMMONIUM SULFITE – BISULFITE SOLUTIONS

B. A. Chertkov

In the ammonia cyclic process for removal of SO_2 from flue gases, about 0.1% by weight of technical p-phenylenediamine is added to the liquor to inhibit oxidation [1,2].

The choice of p-phenylenediamine as the oxidation inhibitor for ammonium sulfite–bisulfite solutions was based on the work of Zil'berman and Ivanov [3], who found that p-phenylenediamine was the most effective substance in protecting sodium sulfite and bisulfite solutions, which are analogous in properties, against oxidation.

According to the most widely held theory, the mechanism of inhibitor action is that its molecules terminate the oxidation chain reaction taking place in the reaction volume, and prevent initiation of new chains [4,5]. In Kashtanov's opinion, the inhibitor forms a complex compound with the most active molecules of the reagent, which have considerably higher polarity than the average measured value [6].

There are also other theories to explain the mechanism of inhibitor action in the oxidation of solutions, but as yet there is no generally accepted theory which satisfactorily explains all the observed phenomena, and in particular, instances of the so-called "inversion of catalysis." It is therefore impossible to approach the selection of oxidation inhibitors on a scientific basis, and such selection can usually be made only on the basis of pilot or plant trials.

We carried out preliminary tests of p-phenylenediamine under the conditions of the cyclic ammonia process for extraction of SO_2 from gases in an experimental unit, with pure gases and solutions [7]. These tests confirmed that p-phenylenediamine is highly effective as an oxidation inhibitor for ammonium sulfite – bisulfite solutions.

However, the effectiveness of this inhibitor was much lower under industrial conditions [1]. The high degree of oxidation of the liquor (at the initial operating stages in the industrial unit up to 20% of all the absorbed SO_2 was converted into ammonium sulfate) suggested that the action of the inhibitor is paralyzed by volatile ash or other impurities in the flue gas entering the liquor.

Laboratory investigations were carried out in this connection (by S. M. Golyand, T. K. Krapivina, and R. A. Berdyanskaya in the Scientific Research Institute of Gas Purification, by T. D. Averbukh and N. P. Bakina in the Ural Chemical Scientific Research Institute, and by the present author in a sulfur-recovery unit); the results, although somewhat contradictory, showed that there is no selective adsorption of inhibitor on ash particles, but ash apparently has a catalytic effect, opposite to the action of the inhibitor, on the process.

A similar effect was observed by Rice [4], who found that removal of dust from the reaction system led to sharp retardation of the oxidation of sodium sulfite, and therefore he ascribed catalytic activity to the dust particles.

In order to obtain quantitative data necessary for comparative evaluation of inhibitor efficiency under different conditions, we carried out an additional study of the process in relation to the problems of the cyclic ammonia process for removal of SO_2 from flue gases.

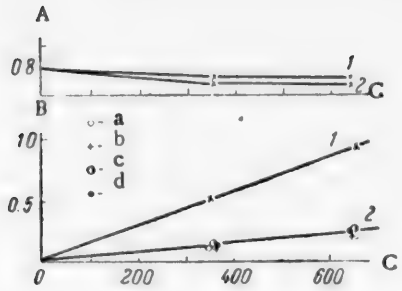

Fig. 1. Effect of additions of p-phenylenediamine on the oxidation rate of ammonium sulfite–bisulfite solution in air: temperature 22°; initial concentration NH_3 eff(C_{init}) 8 moles/liter, S/C_{init} 0.8, thiosulfate concentration 0; A) S/C ratio, B) $(NH_4)_2SO_4$ concentration (moles/liter), C) time (hours); 1) without inhibitor, 2) with inhibitor; contents of p-phenylenediamine (in g/liter): a) 3, b) 2, c) 1, d) 0.5.

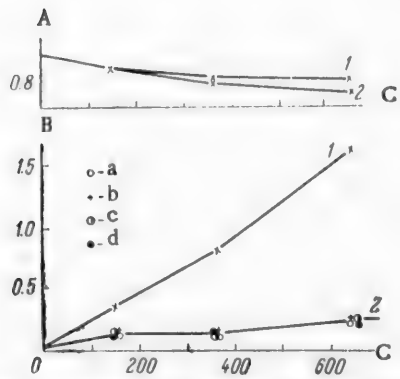

Fig. 2. Effect of additions of p-phenylenediamine on the oxidation rate of ammonium sulfite–bisulfite solution in air: temperature 22°, C_{init} 8.9 moles/liter, S/C_{init} 0.91, thiosulfate concentration 0; designations as in Fig. 1.

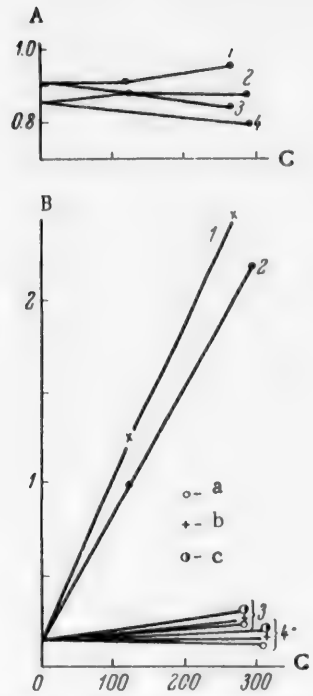

Fig. 3. Effect of additions of p-phenylenediamine on the oxidation rate of ammonium sulfite-bisulfite solution in air: temperature 22°, C_{init} 7.90 moles/liter, S/C_{init} 0.86 and 0.92, thiosulfate concentration 0.25 mole/liter; 1) without inhibitor, S/C 0.92; 2) the same, S/C 0.86; 3) with inhibitor, S/C 0.92; 4) the same, S/C 0.86; remaining designations as in Fig. 2.

EXPERIMENTAL•

The static method described earlier [2] was used for determination of the inhibiting effect of p-phenylenediamine. All the experiments were conducted under identical conditions (at room temperature, in the air); only the initial solution composition and amount of inhibitor added were varied. The effectiveness of inhibitor action was estimated from the increase of the amount of $(NH_4)SO_4$ in a sample of liquor or from the rate of oxygen absorption G_{O_2} (in g/m²·hour) which is equivalent to it.

Fig. 1 shows the effectiveness of the inhibitor action of p-phenylenediamine in the oxidation of pure, artificially prepared ammonium sulfite–bisulfite solution with initial S/C ratio•• of 0.8.

•The experimental work was performed by D. L. Puklina and T. I. Pekareva.

•• The S/C ratio represents the SO_2/NH_{3eff} molar ratio in solution. At S/C = 0.8 the composition of the solution is close to the composition of the regenerated liquor in the ammonia cyclic process for recovery of SO_2 from flue gases.

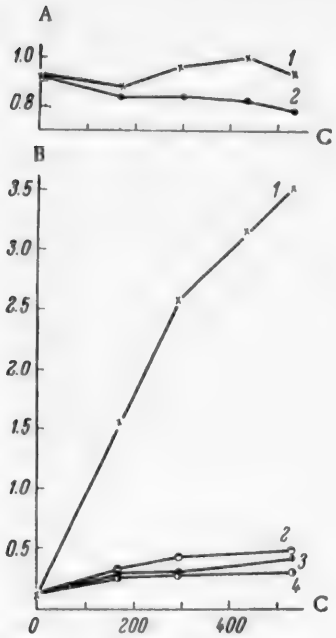

Fig. 4. Effect of additions of p-phenylenediamine on the oxidation rate of ammonium sulfite–bisulfite solution in air: temperature 22°, C_{init} 8 moles/liter, S/C_{init} 0.91, thiosulfate concentration 0.25 mole/liter; inhibitor contents (g/liter): 1) without inhibitor, 2) 0.25, 3) 0.5, 4) 1; remaining designations as in Fig. 1.

It follows from Fig. 1 that addition of the inhibitor lowers the oxidation rate of the solution approximately 4 to 5-fold as compared with a sample without inhibitor. Inhibitor additions of 3, 2, 1, and 0.5 g/liter produce almost the same effect.

It should be noted that a solution of this initial composition is oxidized rather slowly even without added inhibitor, because of the low S/C ratio and the high total concentration of the solution [2]. This is also shown by the continuous decrease of the S/C ratio of the solution during oxidation, also shown in Fig. 1.

Fig. 2. represents the effect of p-phenylenediamine on the oxidation of a solution differing from the previous one by having a higher S/C ratio,* equal to 0.91. In this instance, as was to be expected, the original solution was oxidized much more rapidly, but despite this the retarding effect of the inhibitor was as strong as before.

Fig. 3. represents the action of p-phenylenediamine in the oxidation of pure solutions containing, in addition to sulfite–bisulfite, 0.25 mole per liter of thiosulfate, which is known to be a powerful positive catalyst in the oxidation of such solutions [2]. Despite the sharp increase in the oxidation rates of the original solutions, the inhibiting effect of p-phenylenediamine was still very strong. Addition of 1 g p-phenylenediamine per liter decreased the oxidation rate approximately 10-fold.

The effects of additions of 1, 0.5, and 0.25 g of the inhibitor per liter in the oxidation of a solution containing 0.25 mole of thiosulfate per liter are compared in Fig. 4. Decrease of inhibitor concentration in this range results in some weakening of the inhibitor effect, but the effect is still very large even at the lowest inhibitor concentration.

Thus, the action of p-phenylenediamine is not confined to inhibition of the direct oxidation of ammonium sulfite–bisulfite by molecular oxygen; it also paralyzes the catalytic activity of ammonium thiosulfate which is inevitably present in the working liquor of sulfur-recovery plants.

A fuller picture of the oxidation of the working liquor (filtered free of ash) in contact with air is shown in Figs. 5-7.

In these graphs, Curve A represents the decrease of ammonia content combined as sulfite and bisulfite, while Curve C represents the increase of ammonia combined as sulfate.

It follows from Fig. 5 that oxidation of a liquor of initial S/C ratio 0.78, containing 1.37 g of p-phenylenediamine per liter, proceeds very slowly. The concentrations of ammonium thiosulfate and trithionate also remain almost unchanged; this shows that the reactions of spontaneous decomposition are also very slow under these conditions.

Fig. 6 shows an instance of almost total inhibition of oxidation of the liquor during 2000 hours on addition of 3.2 g of the inhibitor per liter.

Fig. 7 represents another instance in which the working liquor was oxidized relatively rapidly with an inhibitor content of 1.05 g/liter. In this instance rapid oxidation was favored by the high initial S/C ratio of the solution, which rose rapidly to 1 and over,** and this in turn accelerated spontaneous decomposition. Under these conditions the retarding effect of the inhibitor was much weaker.

*At S/C = 0.91 the composition of the solution is close to the composition of the saturated liquor in the ammonia cyclic process for recovery of SO_2 from flue gases.

**This cannot occur in the cyclic process of SO_2 absorption.

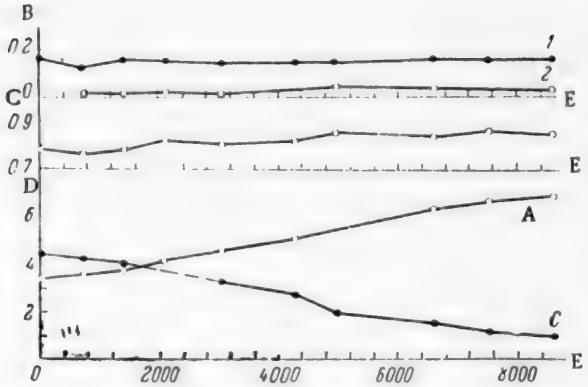

Fig. 5. Course of oxidation and composition variations of the working liquor in contact with air: temperature 20-22°, inhibitor content 1.37 g/liter; B) contents of $(NH_4)_2S_2O_3$ (Curve 1) and $(NH_4)_2S_3O_6$ (Curve 2) (in moles/liter); C) S/C ratio; D) NH_3 present as ammonium sulfate (Curve A) and as ammonium sulfite and bisulfite (Curve C)(in moles/liter); E) time (hours).

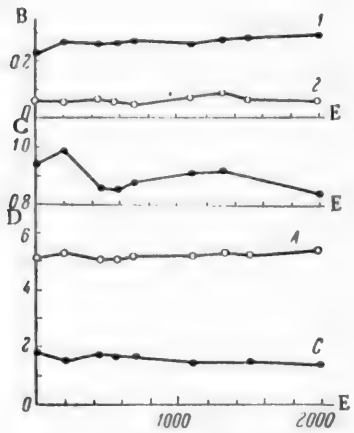

Fig. 6. Course of oxidation and composition variations of the working liquor in contact with air: temperature 20-22°, inhibitor content 3.2 g/liter; designations as in Fig.5.

The results of all these experiments are summarized in Table 1, where the rate of oxygen absorption G_{O_2} (in g/m^2· hour) is the measure of the oxidation rate of the solution.

Estimations of the inhibitor effectiveness from the data in Table 1 show that apart from the experiment with a high S/C ratio (average of 0.94 over the experiment), in which G_{O_2} was lowered only 3 to 4-fold as the result of addition of the inhibitor, the decreases of G_{O_2} were 6 to 10-fold in all the experiments.

The action of p-phenylenediamine proved equally effective under conditions of cyclic extraction of SO_2 from gases in a pilot unit (with pure gases and solutions) [7]. Data characterizing the oxidation of the working liquor in this unit are presented in Table 2.

The operation of the plant can be divided into two periods which differ substantially. In the first period, without inhibitor, the percentage oxidation of the absorbed SO_2 was high, and consequently the NH_{3eff} concentration in the absorbent liquor was low. In the second period, with inhibitor, the percentage oxidation was low and the NH_{3eff} concentration in the absorbent liquor was high.

A noteworthy fact is that the values of G_{O_2} both during the first and during the second operating periods in the pilot unit differ little in absolute magnitude from the values given above, found in studies of the action of p-phenylenediamine under static conditions (in the cold).

This indicates that this inhibitor, in contrast to many others, retains its stability during the periodic temperature variations inherent in the cyclic process. It can also be concluded that the oxidation rate of the solution apparently depends little on the hydrodynamic process conditions, as the oxidation is determined by the relatively slow chemical reaction in the liquid phase [8].

The following method was used to determine the influence of ash and other impurities present in flue gas on the effectiveness of p-phenylenediamine.

The flue gas was drawn through two parallel samples of solution. To one sample, 1 g of the inhibitor per liter was added at the start of the experiment. The remaining experimental conditions were identical for the two samples.

The results are plotted in Fig. 8.

In presence of ash, the inhibiting effect of p-phenylenediamine was weaker than before; the oxidation rate of the solution containing inhibitor was lowered only 2 to 2.5-fold as compared with the solution without inhibitor.

This result confirms the hypothesis that in presence of fine ash particles with a large surface area

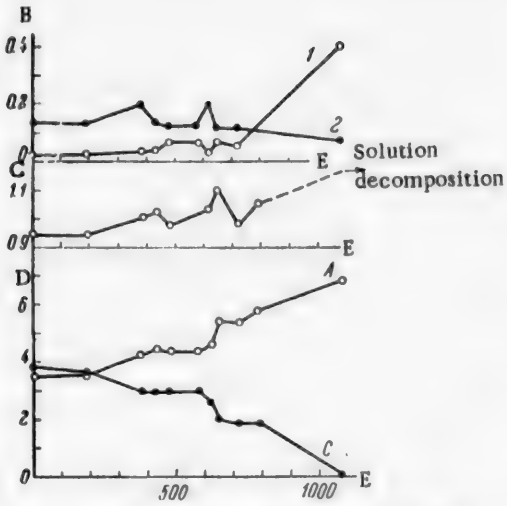

Fig. 7. Course of oxidation and composition variations of the working liquor in contact with air: temperature 20-22°, inhibitor content 1.05 g/liter; designations as in Fig. 5.

the positive catalytic effect of the impurities which are always present in the liquor is stimulated, and the inhibitor action is therefore diminished. This makes it easier to understand why the percentage oxidation of SO_2 is higher during the first operating periods of industrial units for extraction of SO_2 from flue gases. The principal cause is undoubtedly the high ash content of the working liquor.

In conclusion, we consider the questions, important in practice, of the duration of inhibitor action under industrial conditions, the extent of inhibitor losses in the production cycle, and the possible conversion of the inhibitor into an inactive oxidized form. For this purpose we use the material balance for the inhibitor, determined for one operating period of a unit for the extraction of SO_2 from glue gases (Table 3)

The material balance was based on the following data: 1) amount of inhibitor introduced into the system (D) during a definite time interval; 2) initial and final volumes of the working liquor in the system over this time interval (U_1 and U_2); 3) losses of working liquor during this time interval (U_{lost}); 4) content of the active form of the inhibitor in the liquor, as determined by analysis (a_{act}).

TABLE 1

Summary of Average Experimental Data on Oxidation of Ammonium Sulfite–Bisulfite Solutions (Free of Ash) in Air

S/C ratio	Concentration (moles/liter)		Value of G_{O_2} (g/m² · hour)	Value of S/C during experiment	Concentration (moles/liter)		Value of G_{O_2} (g/m² · hour)
	NH_3 eff	$(NH_4)_2S_2O_3$			NH_3 eff	$(NH_4)_2S_2O_3$	
Without inhibitor							
0.86	6.8	0	1.02	0.77	8.2	0	0.17
0.81	5.1	0	1.32	0.885	7.9	0.29	0.26
0.79	7.3	0	0.64	0.875	7.6	0.26	0.28
0.935	5.5	0.22	4.0	0.83	8.0	0.28	0.09
0.935	5.4	0.26	3.9	0.94	3.8	0.16	1.05
0.87	5.85	0.24	3.2	0.88	2.9	0.25	0.48
0.95	1.45	0.30	1.8	0.83	2.2	0.17	0.47
				0.80	3.5	0.15	0.39
				0.78	4.4	0.16	0.32
With added inhibitor 1—1.4 g/liter				0.88	1.6	0.32	0.13
				0.855	1.5	0.22	0.21
0.85	7.5	0	0.19	0.835	1.2	0.26	0.11
0.78	7.2	0	0.16				

If the calculated total inhibitor contents in the liquor at the start and end of each time interval are denoted by a_1 and a_2, the equation for the material balance of the inhibitor can be written as follows:

$$U_1 \cdot a_1 + D = U_2 \cdot a_2 + U_{lost} \cdot \frac{a_1 + a_2}{2},$$

from which a_2 can always be found when a_1 is known:

TABLE 2

Oxidation of Working Liquor in the Pilot Unit (Cyclic Process)

Linear gas vel. in absorbers (m/sec)	Liquor rate in absorbers (m^3/m^2·hour)	Content of NH_3eff in sol. (moles/liter)	Liquor regeneration temp. (°C)	Addition of p-phenylenediamine (%)	Degree of oxidation of absorbed SO_2 (%)	Value of G_{O_2} (g/m^2·hour)	Note
0.7	3.0	2.5	87	Nil	18.5	0.73	Surface area of packing in absorbers 900 m^2; thiosulfate concentration in solution 0-0.05 mole/liter; 0.3% of SO_2 by volume in the income gas; oxygen content of incoming gas 20% by volume.
1.0	3.0	2.6	84	Nil	17	0.80	
1.0	3.0	2.25	91	Nil	21	1.20	
1.4	3.0	6.6	99	0.1*	2	0.16	
1.4	1.7	6.0	101	0.05**	2.1	0.17	
0.6	2.2	7.2	107	0.005**	1.5***	0.22	
0.6	2.0	7.6	107	0.01**	0.7***	0.10	

*Inhibitor added at start of two-week operating period.

**Inhibitor added daily.

***Incoming gas contained 1.2% SO_2.

$$a_2 = \frac{a_1\left(U_1 + \frac{U_{lost}}{2}\right) + D}{U_2 + \frac{U_{lost}}{2}}.$$

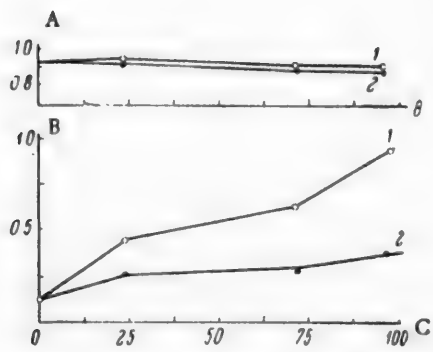

Fig. 8. Effect of added p-phenylenediamine on the oxidation rate of the working liquor in contact with flue gas contaminated with ash: A) S/C ratio, B) concentration of $(NH_4)_2SO_4$ (moles/liter), C) time (hours); 1) without inhibitor, 2) with inhibitor, 1 g/liter.

The difference between a_2 and a_{act} gives the content of inhibitor in inactive form in the liquor.

The liquor loss U_{lost} was found from the ammonia balance for the unit. This loss includes all forms of liquor loss in the unit – in the ash filtration section, with ammonium sulfate crystals, in spray from absorbers, mechanical loss, etc. The average loss was 5.3 m^3 of liquor per 24 hours, or about 220 liters/hour.

The concentration of the active form of the inhibitor in the working liquor was determined by the method worked out by R. A. Berdyanskaya in the Scientific Research Institute of Gas Purification. The principle of the method is based on the formation of a blue color when weakly acid solutions of p-phenylenediamine are mixed with aniline and ferric choride; the color intensity is determined colorimetrically. Oxidation products of p-phenylenediamine do not give this color.

The material balance in Table 3 shows that p-phenylenediamine retains its activity for a long time in industrial ammonium sulfite–bisulfite liquors. The inevitable and fairly

TABLE 3

Inhibitor Balance in a Working Unit for Extraction of SO_2 from Flue Gases

Time from start of operation (days)	Amt. of inhibitor added from start of operation (kg)	Volume of liquor in system (m^3)	Liquor loss during period of operation (m^3)	Calc. inhibitor concentration in liquor (g/liter)	Total amt. of inhibitor lost with liquor from start (kg)	Analyt. cont. of active inhibitor in liquor (g/liter)	Content of inactive inhibitor (by difference) (g/liter)	Inhibitor activity (%)
0	43	55	—	0.8	—	0.85	0	100
4	79	127	21.2	0.51	13.5	0.5	0	100
6	99	126	10.6	0.63	19.6	—	—	—
9	144	121	15.9	0.93	31.8	0.6	0.33	65
11	174	142	10.6	0.93	41.8	0.6	0.33	65
13	204	124	10.6	1.21	53.3	0.56	0.65	46
15	234	123	10.6	1.34	66.9	0.82	0.52	61
16	249	129	5.3	1.35	74.1	0.876	0.47	65
18	279	135	10.6	1.40	88.9	0.750	0.65	54
19	294	122	5.3	1.60	96.9	0.795	0.80	50
20	309	121	5.3	1.70	105.7	0.875	0.82	52
22	339	115	10.6	1.85	124.4	1.07	0.78	58
26	382	142	15.9	1.62	151.9	1.07	0.55	66
32	506	145	31.8	2.10	210.9	—	—	—
41	633	140	47.7	2.27	318.9	1.27	1.0	56
45	716	145	21.2	2.4	367.9	1.40	1.0	58
49	776	140	21.2	2.55	421	1.47	1.08	58
53	836	139	21.2	2.60	476	1.45	1.15	56

considerable losses of liquor in the production cycle lead to corresponding losses of inhibitor, and to the need for continous replenishment. It follows from Table 3 that during 53 days of continuous operation of the unit somewhat more than one half of the inhibitor consumed was removed from the system with lost liquor.

The inhibitor retains 100% activity only at the start of the period (for a few days). This is followed by partial transformation (apparently, oxidation) of the inhibitor into an inactive form. However, this process eventually becomes stabilized. It follows from Table 3 that, at the ratio between inhibitor losses and addition of fresh portions observed for the unit in question, an average of 60% of the total inhibitor content in the liquor was in the active and 40% in the inactive form.

SUMMARY

1. The inhibiting effects of small amounts of p-phenylenediamine on oxidation of ammonium sulfite – bisulfite solutions were studied, and it was found that p-phenylenediamine is most effective when added to pure solutions, not contaminated with solid impurities. In presence of solid impurities, for example if the liquor is contaminated with volatile ash from flue gases, the inhibitor efficiency of p-phenylenediamine is reduced 3 to 4-fold.

2. It was also found that p-phenylenediamine can exert an inhibiting effect for a long time both under static conditions and in the cyclic process for extraction of SO_2 from dilute gases, when the liquor is in continuous circulation and is subjected to alternate heating and cooling.

LITERATURE CITED

[1] A. P. Andrianov and B. A. Chertkov, J. Chem. Ind. 7, 10 (1954).

[2] B. A. Chertkov, J. Appl. Chem. 30, No. 10, 1496 (1957).*

[3] Ya. I. Zil'berman and P. T. Ivanov, J. Chem. Ind. 4, 541 (1940).

*Original Russian pagination. See C. B. translation.

[4] K. C. Bailey, Retardation of Chemical Reactions (Goskhimizdat, 1940). [Russian translation].

[5] T. D. Averbukh, J. Chem. Ind. 11, 14 (1948).

[6] L. I. Kashtanov and A. N. Oleshchuk, J. Gen. Chem. 2, 182 (1938); L. I. Kashtanov and L. N. Sokolova, J. Gen. Chem. 8, 1484 (1951);* L. I. Kashtanov and N. V. Kazanskaya, J. Phys. Chem. 9, 1547 (1954); L. I. Kashtanov and N. V. Kazanskya, Trans. S. Ordzhonikidze Moscow Eng. - Econ. Inst. 1, 139; L. I. Kashtanov and M. I. Darykina, Trans. S. Ordzhonikidze Moscow Eng.-Econ. Inst.1, 143.

[7] B. A. Chertkov, Trans. Sci. Res. Inst. Gas Purification, 1 (Goskhimizdat, 1957).

[8] B. A. Chertkov, J. Appl. Chem. 32, No.1, 78 (1959).*

Received October 3, 1957.

*Original Russian pagination. See C. B. translation.

OXIDATION OF AMMONIUM SULFITE–BISULFITE SOLUTIONS IN THE EXTRACTION OF SO_2 FROM FLUE GASES

B. A. Chertkov

In the previous communications [1-3] we considered the influence of various factors – solution composition, temperature, and others – on the rate of oxidation of ammonium sulfite–bisulfite. It was found experimentally that the degree of oxidation of the solution increases with increase of the relative content of bisulfite in the solution (the S/C ratio), temperature, and partial pressure of oxygen in the gas phase. It was also shown that at a definite concentration of the sulfite–bisulfite solution the degree of oxidation reaches a maximum value, and it decreases continuously both at higher and at lower concentrations. At the same time it was established that the oxidation reaction can be accelerated appreciably by the catalytic action of ammonium thiosulfate which gradually accumulates in the solution, and that this action of thiosulfate can be inhibited and the oxidation reaction greatly retarded by addition of an inhibitor (p-phenylenediamine). However, the presence of solid impurities in the solution and, in particular, contamination by volatile ash from flue gases, may lower sharply the effect of the inhibitor.

In the actual operating conditions of a gas purification plant, in addition to the above factors, hydrodynamic factors also operate, and the over-all oxidation of the absorbent solution is a complex function of a number of variables.

It was of interest to compare our experimental data and the relationships derived from them with the actual course of oxidation of ammonium sulfite–bisulfite liquors under industrial conditions. In this paper such a comparison is made for the oxidation of the working liquor in a unit for the extraction of SO_2 from flue gases by the ammonia cyclic process [4].

The oxidation product of ammonium sulfite–bisulfite is ammonium sulfate $(NH_4)_2SO_4$, which is used as a fertilizer after removal from the liquor. Without going into details of the technological process of SO_2 extraction from gases by the ammonia cyclic process, we merely note here that the accumulating ammonium sulfate is removed from the system by evaporation of a part of the working liquor in a vacuum evaporator. As a result of the increase of the total salt concentration in the liquor, ammonium sulfate, which is the least soluble component, separates out in the solid phase and is then removed by centrifugation.

In an ideal cyclic process, the amount of crystalline $(NH_4)_2SO_4$ obtained over a definite time interval can serve as a measure of the rate of oxidation of the absorbent solution. In actual practice, the industrial process is accompanied by losses of liquor, with which some ammonium sulfate is also lost from the system. However, these losses can be taken into account fairly accurately from the ammonia balance for the plant.

Thus, the total amount of ammonium sulfate formed by oxidation of the absorbent liquor during absorption of SO_2 from the gas can be determined from the amount of crystalline $(NH_4)_2SO_4$ obtained, its losses in the production cycle, and from the results of analytical determinations of the changes of $(NH_4)_2SO_4$ content in the working liquor over a definite time interval.

Such balances for ammonium sulfate formation were calculated for different periods of plant operation. The final results of one such balance are presented in the diagram.

The diagram shows that the oxidation rate of the liquor in this unit was, in general, uniform. The average rate of $(NH_4)_2SO_4$ formation remained constant during prolonged time intervals under definite conditions of

absorber operation. Data on the oxidation of the liquor and on the operating conditions in the absorbers for all the investigated periods are summarized in the table.

In addition to the average daily increases of $(NH_4)_2SO_4$ content, the table contains the values, equivalent to these, of the rate of oxygen absorption G_{O_2} in $g/m^2 \cdot$ hour, calculated per unit surface area of the absorber packing.

It follows from the table that during the first three operating periods of the sulfur recovery unit the oxidation proceeded at the highest rate, and G_{O_2} reached a value of 1.1 $g/m^2 \cdot$ hour. This is because the temperature of the liquor in the absorber was higher than during the other periods, and also because of the higher ash content, in presence of which the inhibitor could not exert its full retarding effect. The low rate of oxidation of the liquor during the next (fourth) operating period is due to the fact that during this period the thiosulfate concentration of the liquor was at its lowest, and the liquor was least contaminated with ash. The fact that the saturated liquor leaving the absorber had a lower S/C ratio than during the other operating periods was also significant. The higher oxidation rate of the liquor during the fifth period, apart from the causes already indicated, was mainly due to the fact that during this period the liquor in the absorber was saturated to higher S/C ratios than during the preceding periods.

In the subsequent operating periods, the liquor temperature in the absorbers was lower, and this led to some decrease of the oxidation rate, despite the fact that the thiosulfate content of the working liquor rose appreciably.

If we disregard the sixth period, when the lower oxidation rate was due to the low total salt concentration in the liquor at the start of the period (accumulation of the liquor) and to the low thiosulfate content, we see that during the remaining seven periods the average oxidation rate of the liquor varied within very narrow limits, and corresponded to an average oxygen absorption rate of 0.75 $g/m^2 \cdot$ hour.

In view of the fact that the operating conditions of the absorbers during these periods are the most typical of the ammonia cyclic process for extraction of SO_2 from flue gases, this average value can be taken with every justification as a reliable measure of the oxidation rate of ammonium sulfite–bisulfite liquor under industrial conditions.

Let us now consider how the oxidation rate of the liquor can vary with changes in different conditions of absorption of SO_2 from gases. Variation of the percentage SO_2 content of the gas cannot in itself influence the oxidation of the liquor but, since there is an optimum liquor concentration in the cyclic process for any given SO_2 concentration in the gas [5], such variation would have an indirect influence through variations of the liquor composition.

Alteration of the percentage content of oxygen in the gas, for example, if the process was changed to absorption of SO_2 from waste gases in nonferrous metallurgical processes, should produce a proportional change of G_{O_2} [2] with the liquor composition indicated in the table.

Alteration of the linear gas velocity in the absorber cannot influence the oxidation rate of the liquor, as in the absorption of oxygen, which is a sparingly soluble gas, liquid-film resistance is the principal factor and gas-film resistance may be disregarded.

Increase of the liquor rate in the absorber decreases the resistance of the liquid film and should therefore favor more rapid transfer of oxygen from the boundary layer into the main bulk of the liquid. However, since the over-all oxidation process is determined by the relatively slow reaction between sulfite–bisulfite and dissolved oxygen, the concentration gradient of the latter in the liquid phase is probably very low and the influence of the liquor rate in this instance may be assumed to be the same as in simple physical absorption. According to Ramm [6], the mass-transfer coefficient in the liquid film (K_L) is a power function of the liquor rate (Γ), where the power of Γ may vary from 0.33 (for a wetted-wall absorber) to 0.67 (for a packed absorber). Therefore, hydrodynamic factors can only have an influence if the liquor rate in the absorber is increased considerably. However, this may not be necessary if the liquor is recirculated through the absorption sections.

The small role of hydrodynamic factors is also confirmed by the fact that the average rate of absorption of oxygen in the absorber (0.75 $g/m^2 \cdot$ hour) is close to the values obtained in a laboratory study of the oxidation process under static conditions [3].

Data on the Oxidation of the Working Liquor in a Sulfur Recovery Unit

Operation periods	Dates	Liquor characteristics						Temperature of liquor leaving the absorber (°C)	Average increase of $(NH_4)_2SO_4$ content (kg-moles/day)	Number of working absorbers	Rate of oxygen absorption G_{O_2} (g/m²·hour)	Notes
		contents (moles/liter)			ash content (g/liter)	S/C for liquor at top of absorber	S/C for liquor at bottom of absorber					
		NH_3tot	NH_3eff	$(NH_4)_2S_2O_3$								
1	25 III —13 V 1952	7.25	3.6	0.06—0.25	8.3	0.79	0.88	38—30	41.0	1	0.91	Linear gas velocity in total section of absorbers during all periods was 1.1-1.3 m/second; liquor rate in absorbers, 4-4.5 m³/m²·hour; packing area in each absorber, 30,000 m²; SO_2 content of incoming flue gas, 0.3-0.4%; oxygen content of incoming flue gas, 8-12%; inhibitor content of liquor, 0.5-1.5 g/liter.
2	15 IX —10 XI 1952	8.25	4.0	0.03—0.10	3.5	0.79	0.89	35—35	35.5	1	0.79	
3	29 XI — 7 I 1952	6.8	3.2	0.03—0.10	4.5	0.80	0.90	35—34	49.5	1	1.11	
4	30 VIII—12 IX 1953	5.0—8.0	2.5—5	0.01—0.04	1.1	0.78—0.82	0.83—0.90	28—40	22.5	1	0.50	
5	12 IX —27 IX 1953	7.0—9.0	2.8—4.5	0.04—0.07	2.3	0.78—0.82	0.87—0.96	28—38	55.5	1	1.24	
6	6 XI —13 XI 1955	2 —7.5	1 —4.8	0.01—0.07	1.05	0.79—0.82	0.9 —0.92	18—28	34.3	2	0.38	
7	13 XI —30 XI 1955	7.5—9.7	3.3—4.5	0.07—0.29	1.85	0.79—0.82	0.93—0.96	17—24	78.8	2	0.88	
8	30 XI —22 XII 1955	9.5	2.7—4.3	0.29—0.42	2.0	0.79—0.82	0.90—0.96	23—28	63.7	2	0.71	
9	22 XII —28 XII 1955	9.5—10	2.9—4.3	0.42—0.52	1.9	0.79—0.82	0.91—0.96	23—26	70.0	2	0.78	
10	16 I — 3 II 1957	7.0—9.5	3.4—4.6	0.10—0.26	1.94	0.79—0.82	0.92—0.95	20—22	65.0	2	0.72	
11	3 II —22 II 1957	9.5	3.7—4.6	0.26—0.35	2.0	0.79—0.82	0.86—0.96	21—24	49.5	2	0.55	
12	22 II — 2 III 1957	9.5	3.6—4.2	0.35—0.34	3.12	0.79—0.82	0.95—0.96	20—22	67.5	2	0.75	
13	12 III — 3 IV 1957	9.0	3.5—4.1	0.15—0.27	2.03	0.79—0.82	0.93—0.97	20—22	72.4	2	0.80	

Variations of salt concentrations in the liquor may have different effects on the oxidation process. When the NH_{3tot} and NH_{3eff} concentrations are raised above the values given in the table, the oxidation rate should fall owing to the lower solubility of oxygen in more highly concentrated salt solutions. With decrease of the NH_{3eff} concentration the oxidation rate should first rise, and after passing through a maximum (2.5 moles NH_{3eff} per liter) it should fall sharply because the determining factor is then no longer access of oxygen but the rate of the reaction between sulfite–bisulfite and dissolved oxygen [1]. However, dilute solutions cannot be used in the cyclic process for extraction of SO_2 from gases.

Increase of the thiosulfate content of the liquor, say to 0.5 mole/liter, might in itself produce a sharp increase of oxidation rate [1]. However, in presence of sufficient inhibitor (1 g/liter) thiosulfate does not exert a catalytic effect, and this factor may be disregarded. From this point of view an increase of the ash content, which weakens the action of the added inhibitor, is undesirable.

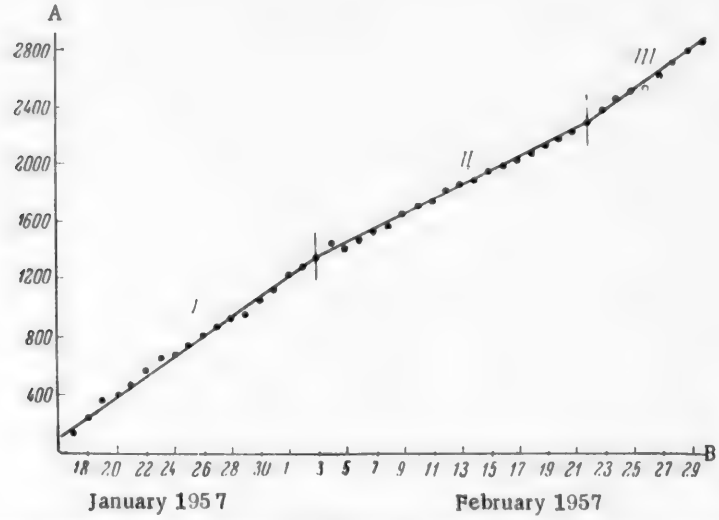

Progressive accumulation of $(NH_4)_2SO_4$ in the system: A) total amount of $(NH_4)_2SO_4$ in the system (kg-moles), B) time (days); average rates of $(NH_4)_2SO_4$ formation during different periods (in kg-moles/day): I) 65, II) 49.5, III) 67.5.

Variation of the S/C ratio of the saturated liquor can have an appreciable effect on the oxidation rate only if this ratio is varied over a wide range [1]. Since in the normal cyclic process the S/C ratio of the saturated liquor approaches the theoretical limit (S/C = 1 for pure bisulfite) with any initial SO_2 concentration in the gas, the influence of this factor is confined to a comparatively narrow region, in which the variations of oxidation rate are inconsiderable.

Increase of the liquor temperature in the absorber should also have an accelerating influence on the oxidation process [2].

To summarize the above, it may be concluded that the following factors should have the greatest effects on the oxidation process in the absorption of SO_2 from gases: partial pressure of oxygen in the gas, ammonium sulfite – bisulfite concentration in the liquor, S/C ratio in the resultant concentrated liquor, and the liquor temperature in the absorber.

Since the effects of all these factors can be determined quantitatively with the aid of the relationships established by us earlier [1,2], it is possible to use the average oxidation rate of a liquor, determined in the unit described above, as a starting point for determining the degree of oxidation in absorption of SO_2 from gases by the ammonia process under any other operating conditions.

The amount of sulfate formed by oxidation in any method of extraction of SO_2 from gases is generally compared with the total amount of SO_2 formed in unit time. The degree of oxidation so found is a relative value which depends on the SO_2 concentration in the gas and the total gas rate in the absorber. It is obvious that the greater the total amount of SO_2 absorbed in the apparatus, the less is the degree of oxidation under otherwise constant conditions. Since hydrodynamic factors do not play any appreciable role in oxidation of the working liquor but are known to have a very strong influence on the rate of SO_2 absorption, the lowest degree of oxidation may be attained in an absorber in which absorption of SO_2 is the most intensive.

From this point of view, a high-rate bubbling absorber operated under foam conditions should have considerable advantages over a packed absorber. In fact, our investigations [7] showed that the rate of SO_2 absorption from flue gas was 10 to 15 times as high (calculated per unit absorber volume) in an experimental bubbling absorber operated under foam conditions as in a packed absorber, while the rate of oxygen absorption increased only to 2 to 3-fold. As a result, the degree of oxidation was roughly one fifth that found under analogous conditions in the packed absorber. It follows that replacement of packed absorbers by bubbling equipment, apart from the other known advantages, would make it possible to extract SO_2 from dilute gases by the ammonia process with a much lower yield of ammonium sulfate, with corresponding saving of ammonia.

In that case it would quite likely be possible to abandon the use of the relatively costly oxidation inhibitor – p-phenylenediamine.

SUMMARY

Practical data on the oxidation of ammonium sulfite–bisulfite in the extraction of SO_2 from flue gases in packed absorbers were analyzed. The average rate of absorption of oxygen from the gas (G_{O_2}) under the most typical conditions of the ammonia cyclic process was calculated, and the possible variation limits of this rate with changes in the absorber operating conditions were considered. It is shown that the degree of oxidation of the absorbed SO_2 can be lowered considerably if the absorption is effected in a bubbling absorber operated under foam conditions.

LITERATURE CITED

[1] B. A. Chertkov, J. Appl. Chem. 30, No. 10, 1496 (1957).*

[2] B. A. Chertkov, J. Appl. Chem. 32, No. 1, 78 (1959).*

[3] B. A. Chertkov, J. Appl. Chem. 32, No. 5, 952 (1959).*

[4] A. P. Andrianov and B. A. Chertkov, J. Chem. Ind. 7, 10 (1954).

[5] B. A. Chertkov, Trans. Sci. Res. Inst. Gas Purification [in Russian] (Goskhimizdat, 1957).

[6] V. M. Ramm, Absorption Processes in Chemical Industry [in Russian] (Goskhimizdat, 1951).

[7] B. A. Chertkov, Bull. Tech. and Econ. Inf. State Committee on Chemistry 5, 7 (1958).

Received May 3, 1957.

*Original Russian pagination. See C. B. translation.

A STUDY OF THE FACTORS INFLUENCING FORMATION OF SULFIDES FROM METAL OXIDES BY THE ACTION OF SULFUR DIOXIDE

V. V. Pechkovskii

The A. M. Gor'kii State Institute, Perm'

Sulfide formation forms the basis of many operations in chemical technology and ferrous and nonferrous metallurgy [1-4].

It was shown earlier [5] that when sulfur dioxide reacts with metal oxides in a reducing atmosphere the roasting products contain various sulfur compounds, including sulfides. Certain factors which influence the rate and extent of sulfide formation were studied; these included the temperature, amount of carbon in the original mixture, and the physicochemical properties of the metal oxides.

The purpose of the present investigation was to study the influence of various factors on the conversion of metal oxides to sulfides by the action of sulfur dioxide in a reducing atmosphere. The rate and extent of interaction of sulfur dioxide with metal oxides in presence of carbon were studied in relation to the concentration of sulfur dioxide, the kind and particle size of the carbonaceous material used, the crystallochemical structure of the metal oxide, contents of various additives in the original mixture, and the duration of the experiment.

The analytical procedures and characteristics of the materials used are described in the preceding paper [5]. Pure dry nitrogen was used as a diluent for 100% sulfur dioxide for producing gas mixtures of definite composition. The carbonaceous materials used were blood charcoal, semicoke made from Zhurino coal, Kuznetsk coal from the 3-3 bis pits, blast-furnace coke, and birchwood charcoal from Syava.

TABLE 1
Characteristics of the Carbonaceous Materials Used

Materials	Ash	Sulfur	Volatiles
Wood charcoal	1.8	0.4	9.4
Kuznetsk coal	10.5	0.5	18.0
Semicoke	8.0	0.5	14.0
Coke	12.8	0.6	0.7

The characteristics of the carbonaceous materials used are given in Table 1.

Mixtures containing 30-31% carbon were prepared. Except when otherwise stated, the duration of each experiment was 15 minutes, and the particle size of the powdered metal oxides and carbonaceous materials was less than 0.078 mm.

The principal experimental results are given in Tables 2-6.

TABLE 2

Variation of the Degree of Conversion of Metal Oxides to Sulfides with the SO_2 Concentration in the Gas Phase at 750°. Carbonaceous material – blood charcoal

Metal oxide	Degree of conversion to sulfide (%) at SO_2 concentration (vol.%)				
	10.0	30.0	50.0	75.0	100.0
Mn_2O_3	46.4	55.7	66.1	64.4	72.0
ZnO	16.8	22.0	28.3	33.7	39.4
Fe_2O_3	6.5	10.6	14.8	15.2	23.1

TABLE 3

Effects of Temperature and SO_2 Concentration on the Degree of Conversion of Metal Oxides to Sulfides. Carbonaceous material–blood charcoal

Temperature (°C)	Degree of conversion to sulfide (%) at SO_2 concentration (vol.%)							
	5	20	5	20	5	20	5	20
	Mn_2O_3		ZnO		Co_3O_4		Fe_2O_3	
650	16.6	25.6	3.2	4.5	5.0	5.7	1.7	2.5
700	19.0	41.7	5.1	8.3	6.4	9.7	2.5	5.1
750	20.1	61.8	10.5	19.2	10.1	18.3	4.9	11.1
800	21.2	65.0	16.2	38.8	15.5	44.6	5.2	25.1
850	24.8	66.4	20.8	70.0	25.7	86.5	7.4	61.3
900	—	67.1	23.0	87.4	34.2	97.4	—	75.0

TABLE 4

Effect of the kind of Carbonaceous Material on the Degree of Conversion of Metal Oxides to Sulfides at 850° and 20% SO_2 Concentration

Metal oxide	Degree of conversion to sulfide (%) with carbonaceous material			
	wood charcoal	Kuznetsk coal	semi-coke	coke
Co_2O_3	87.2	85.4	83.0	6.7
Mn_2O_3	77.8	72.6	72.4	22.8
ZnO	75.7	67.5	78.1	5.1

The data in Tables 2 and 3 lead to the conclusion that the degree of conversion decreases steadily with decrease of sulfur dioxide concentration in the gas phase from 100 to 20%. The degree of conversion of metal oxides to sulfides falls sharply with decrease of SO_2 concentration in the gas phase from 20 to 5%. The rate and extent of conversion of metal oxides in gaseous mixtures containing less than 5% SO_2 are relatively low.

Data giving an indication of the relative reactivity of different carbonaceous materials are contained in Tables 3 and 4. It was found that the relative reactivity of different carbonaceous materials in the reaction in question varies somewhat with the kind of metal oxide, temperature, and SO_2 concentration in the gas phase. At 850° and 20% sulfur dioxide in the gas phase, the carbonaceous materials used can be arranged in the following sequence of decreasing reactivity in this reaction: wood charcoal, blood char, semicoke, Kuznetsk coal, coke. It must be noted that the first four of these carbonaceous materials have fairly high reactivity in the conversion of metal oxides to sulfides by the action of sulfur dioxide. Coke, on the other hand, has low reactivity. The conversion of metal oxides to sulfides by sulfur dioxide in presence of coke begins to occur at an appreciable rate only at temperatures above 850-900°.

It was further found that the crystal form of the metal oxide has a considerable influence on the conversion process. Thus, at 850° with 10% SO_2 in the gas phase, the degree of conversion of powdered Mn_2O_3 reagent and native pyrolusite from Chiatura was 59.1 and 33% respectively.

It follows that native pyrolusite, which has a denser structure and a less reactive surface, is converted to sulfide to a considerably lower degree than Mn_2O_3 reagent.

In order to determine the effect of various impurities on the conversion process, special experiments were carried out on the conversion of mixtures of metal oxides and carbon in presence of various additives. The additives tested were powdered oxides of iron, chromium, manganese, and cobalt, and also ferruginous bauxite from Kustanai. It was found that 5-7% additions of iron, chromium, or cobalt oxides have no practical effect on the conversion of zinc oxide to sulfide by the action of sulfur dioxide. Addition of manganese oxide in the form of Mn_2O_3 reagent increases somewhat the degree of conversion of zinc and cobalt oxides, while ferruginous bauxite decreases it.

It is known [4] that ferruginous bauxite catalyzes the reaction

$$SO_2 + 2CO \rightleftarrows 2CO_2 + 1/2S_2 + 52330 \text{ cal.}$$

The degree of conversion of sulfur dioxide to elemental sulfur decreases with rise of temperature. This probably accounts for the decrease in the degree of conversion of metal oxides to sulfides by sulfur dioxide in presence of bauxite at temperatures above 750-800°.

It was found that the rate and extent of conversion of metal oxides to sulfides by sulfur dioxide in a reducing atmosphere depends on the particle size of the carbonaceous material used. However, the nature of the relationship between the rate and extent of conversion and particle size varies somewhat with the temperature and with the kind of carbonaceous material.

It follows from the data in Table 5 that when cobalt and zinc oxides are roasted with Kuznetsk coal the degree of conversion decreases if the particle size of the coal is greater than 0.25 mm. When the same oxides are roasted with wood charcoal, the degree of conversion decreases only if the particle size of the charcoal is greater than 1.0 mm.

TABLE 5

Effect of Grain Size of the Carbonaceous Material on the Degree of Conversion of Metal Oxides with 10% SO_2 Concentration

Carbonaceous material	Temperature (°C)	Co_2O_3				ZnO			
		Degree of conversion of oxide (%) with particle size (mm)							
		0.25	0.5	1.0	2.0	0.25	0.5	1.0	2.0
Kuznetsk coal	750	9.9	10.9	11.7	11.7	6.4	6.5	6.3	6.1
	900	35.4	32.2	30.6	27.0	29.2	26.8	24.1	20.8
Wood charcoal	750	25.8	26.0	27.1	27.8	24.6	25.3	26.6	27.2
	900	42.1	47.2	50.3	41.9	40.2	41.3	44.5	40.1

TABLE 6

Effect of Duration of the Experiment on the Degree of Conversion of Metal Oxides at 10% SO_2 Concentration. Carbonaceous material—blood charcoal

Metal oxide	Temperature (°C)	Degree of conversion of oxide (%) with particle size (mm)			
		15	30	45	60
Co_2O_3	650	4.9	7.9	11.8	16.4
	850	60.5	78.5	79.0	80.0
ZnO	650	3.5	4.8	5.3	6.0
	850	52.6	79.3	79.5	79.5

The less pronounced decrease of the degree of conversion with increase of particle size of the carbonaceous material which is found with wood charcoal is due to the fact that the latter has a more developed internal surface than Kuznetsk coal. The reason for the increase of the degree of conversion with increase of particle size of wood charcoal from 0.25 to 1.0 mm is that in the hearth-roasting conditions used, increase of particle size leads to better contact between the solid particles and the gas phase both on the surface of the layer and within it.

Data on the effect of duration of the experiment on the degree of conversion are presented in Table 6. It is seen that in the region of fairly high conversions the reaction of metal oxides with sulfur dioxide in a reducing atmosphere proceeds rapidly during the first 20-30 minutes, after which the reaction rate falls sharply.

It can be concluded from these experimental results that the rate and extent of conversion of metal oxides to sulfides by sulfur dioxide in presence of carbon depends on numerous factors, which include temperature, concentration of sulfur dioxide, amount, kind, and particle size of the carbonaceous material used, the physical and physicochemical properties of the metal oxides, presence of impurities, and roasting time.

LITERATURE CITED

[1] M. E. Pozin, Technology of Mineral Salts [in Russian] (Goskhimizdat, 1949).

[2] M. A. Pavlov, Metallurgy of Pig Iron [in Russian] II (Metallurgy Press, 1949).

[3] V. I. Smirnov, Metallurgy of Copper and Nickel [in Russian] (Metallurgy Press, 1950).

[4] A. V. Avdeeva, Gas Sulfur [in Russian] (Goskhimizdat, 1950).

[5] V. V Pechkovskii, J Appl. Chem. 30, 825 (1957)*

Received March 5, 1958.

*Original Russian pagination. See C. B. translation.

COMBINED REMOVAL OF CO_2 FROM NITROGEN–HYDROGEN MIXTURES AND PRODUCTION OF AMMONIUM CARBONATES*

S. N. Ganz, G. I. Vilesov, S. I. Gorbman, and S. B. Leibovich

The present communication contains experimental data on the kinetics of separate and joint absorption of NH_3 and CO_2 in relation to the physicochemical and hydrodynamic process conditions. This series of experiments determines the degree and rate of CO_2 absorption, and therefore the technical and economic feasibility of this process.

The absorption process was studied in horizontal high-speed rotary absorbers. Details of these absorbers and their performance are described in earlier papers [1-4].

EXPERIMENTAL

The study of the absorption of NH_3 and CO_2 with formation of ammonium carbonates under conditions of high turbulence was performed in the following sequence.

First the effects of peripheral disk speed, volumetric gas rate, and NH_3 concentrations in the gas and liquid phases on the rate of absorption of NH_3 in water were studied. Next the effects of peripheral disk speed, volumetric gas rate, CO_2 concentration in the gas, and NH_3 concentration in the liquid on the rate of absorption of CO_2 by aqueous ammonia solutions were studied.

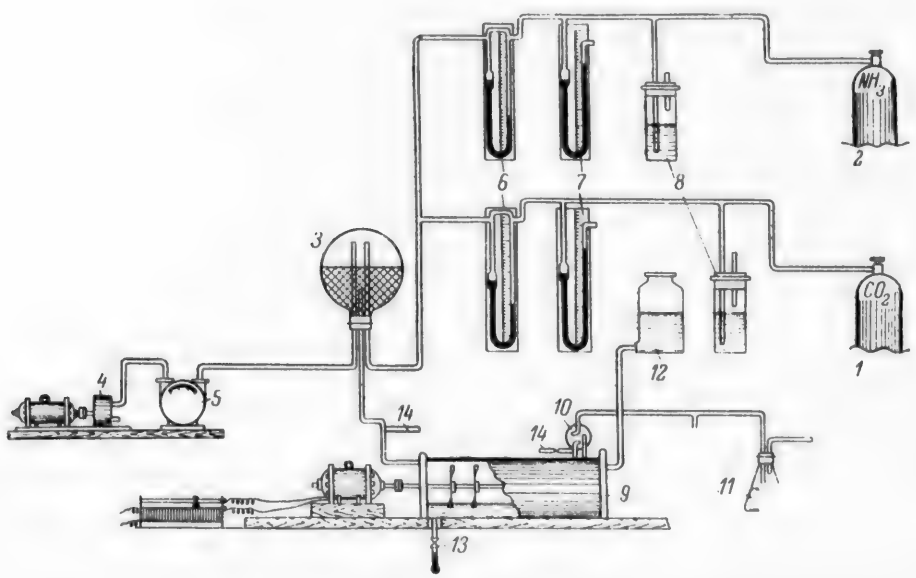

Fig. 1. Equipment for combined absorption of CO_2 and NH_3 in mechanical absorbers.

*Communication I.

In a separate series of experiments the combined absorption of NH_3 and CO_2 by water was studied in relation to the concentrations of these components in the gas phase and the contents of ammonium carbonates in the liquid phase. The apparatus used for studying absorption processes is shown schematically in Fig. 1.

NH_3 and CO_2 were fed from the cylinders 1 and 2 into the mixer 3, where they were mixed with air supplied from the blower 4 through the meter 5. The amounts of CO_2 and NH_3 were measured by the flow meters 6, the gas pressures were indicated by the manometers 7, while the gas pressures were maintained steady by means of the manostats 8. The gas mixture passed from the mixer to the absorber 9 and then through the trap 10 and hydraulic seal 11 into the atmosphere. The absorbent liquor entered the absorber from the header 12 and was removed through the outlet 13. Gas samples for determinations of NH_3 or CO_2 were taken at the absorber entry and exit through the stopcocks 14. Samples of liquid leaving the absorber were taken for analysis from the outlet 13.

The NH_3 and CO_2 contents of the gas were determined by the evacuated bulb method; here NH_3 was absorbed in 45% H_2SO_4, and CO_2 in 20% NaOH solution.

In separate absorption of NH_3 or CO_2, one of the gas cylinders was disconnected from the system.

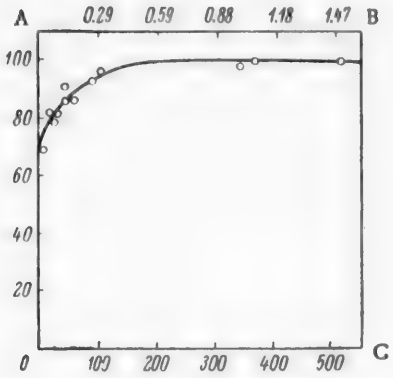

Fig. 2. Variation of the degree of absorption of NH_3 by water with peripheral disk speed: NH_3 concentration in gas 7.25%, P = 749 mm, w_G = 500 $m^3/m^3 \cdot$ hour, t = 17.6°; A) degree of absorption (%), B) peripheral disk speed (m/second), C) shaft speed (rpm).

Absorption of ammonia. In the first series of experiments the degree of absorption of NH_3 by water was studied in relation to shaft speed (or peripheral disk speed). The temperature was maintained in the range of 17-18°, P_{atm} = 749 mm. The volumetric gas rate was 500 m^3 gas/m^3 absorbent per hour. The results of these experiments are plotted in Fig. 2. It can be seen that the absorption rate rises rapidly with increase of peripheral disk speed and at n = 250 rpm it reaches 100%. The time of phase contact decreases with increase of the volumetric gas rate, and the degree of absorption falls somewhat. This is illustrated by the experimental data in Fig. 3. To increase the degree of absorption of NH_3 at gas rates higher than 500 $m^3/m^3 \cdot$ hour the disk speed must be increased to 850-900 rpm (which is equivalent to a peripheral disk speed on about 2.5 m/second in the model absorber). Under such conditions, with 8.3% NH_3 in the gas and 6% NH_3 in the liquid phase, at t = 17.6° and P = 748 mm, the degree of absorption fell to 93.5% at volumetric rate w = 2500 $m^3/m^3 \cdot$ hour.

In packed towers a similar degree of adsorption is attainable under the same conditions at volumetric gas rates of the order of 60-62 $m^3/m^3 \cdot$ hour.

Therefore, under conditions of high turbulence the output per unit volume of the absorber is approximately 2500/(60–62) = 40 to 41-fold the output of packed towers.

It follows that in the absorption of a readily soluble gas the hydrodynamic conditions also play an important part in accelerating the process.

Under conditions of high turbulence at n_{disk} = 850 rpm and w = 500 $m^3/m^3 \cdot$ hour, the degree of absorption of NH_3 is independent of its concentration in the gas. Under these conditions at t = 17.7° and P = 748 mm, NH_3 at any concentration (down to the lowest) is absorbed completely by water. Increase of the NH_3 concentration in the liquid phase lowers the absorption rate because of a decrease in the driving force of the process.

Absorption of CO_2. The apparatus used for studying the rate of absorption of CO_2 was the same as that used for NH_3 (Fig. 1). In the first series of experiments the effect of peripheral disk speed on the degree and rate of CO_2 absorption was studied. The absorbent was aqueous ammonia containing 7.4% NH_3. The process was conducted at t = 18° and P = 753 mm. The gas rate was 500 $m^3/m^3 \cdot$ hour, with 11.8% CO_2 in the gas.

The results of the experiments are presented in Fig. 4. It is seen that under constant conditions the degree of absorption rises rapidly with increase of shaft speed and at n = 2000 rpm (v_d = 5.2 m/second) it reaches a

maximum (98.5%). Further increase of shaft speed does not alter this result. Values of the absorption coefficient calculated from these data are plotted in Fig. 5.

The effect of volumetric gas rate was studied at n = 1850-1900 rpm (peripheral disk speed v_d = 4.5-5 m/second), CO_2 content of gas 10.7%, NH_3 content of solution 7.14%, t = 18.5° and P = 746 mm. The results of the experiments are presented in Fig. 6.

As was to be expected, increase of the volumetric gas rate decreases the degree of absorption owing to a decrease in the time of phase contact.

The effect of CO_2 concentration in the gas on the absorption rate was studied at a gas rate of 500 m^3/m^3 · hour, peripheral disk speed 4.5 m/second, t = 17°, P = 756 mm, and 8.5-9% NH_3 in the solution. The results are plotted in Fig. 7, where it is seen that the curve has a pronounced maximum corresponding to 11% CO_2 in the gas.

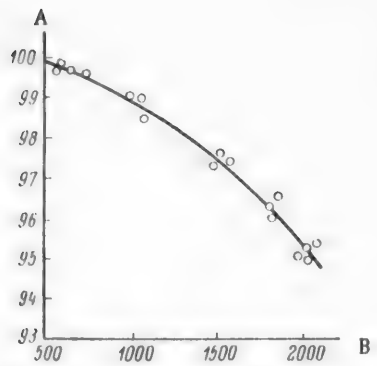

Fig. 3. Variation of the degree of absorption of NH_3 by water with the volumetric gas rate: NH_3 concentration in gas 8.3%, n = 850 rpm, t = 17.6°; A) degree of absorption (%), B) gas rate (m^3/m^3 · hour).

The characteristic curvature of the graph in Fig. 7 indicates that the highest rate of the process is attainable at 1:1 ratio of NH_3 to CO_2, which is the stoichiometric ratio. Thus, with 8.5% NH_3 in the solution, its molar concentration must be 8.5/17 = 0.5.

This NH_3 concentration in solution corresponds to the maximum on the absorption curves with 11-11.5% CO_2 in the gas, which is also equal to 11.2/22.4 = 0.5 mole. Therefore the reaction $NH_3 + CO_2 + H_2O = NH_4HCO_3$ • proceeds at the greatest rate.

This finding is confirmed by another series of experiments, in which the CO_2 concentration was kept constant at 10.5%, while the NH_3 concentration in solution was varied from 2 to 13%. This series of experiments was conducted at w_G = 500 m^3/m^3 hour, v_d = 4.5 m/second, t = 21°, and P = 748 mm.

The data, plotted in Fig. 8, also give a curve with a well-defined maximum at 8% NH_3 concentration in solution.

It is easy to see that here again the molar ratio NH_3 : CO_2 = 1 : 1, as 8 g/17 of NH_3 in solution = 0.47 mole, just as 10.5 liters/22.4 of CO_2 in the gas = 0.47 mole. However, as will be clear from the experiments detailed below, the highest reaction rate at NH_3 : CO_2 = 1 : 1 is found at low concentrations of ammonium carbonates in solution. The CO_2 pressure in solution increases with increase of their concentration, and in that case the extent and rate of reaction should increase in presence of excess ammonia in the gas.

Combined absorption of NH_3 and CO_2. In connection with the method adopted [1] for removal of CO_2 from nitrogen–hydrogen mixtures it is of considerable interest to study the kinetics of simultaneous absorption of NH_3 and CO_2 in the same apparatus, as this would simplify the technological process considerably. The experimental unit shown in Fig. 1 was therefore used for studying the kinetics of NH_3 and CO_2 absorption with these gases introduced simultaneously (through separate tubes) into the absorber in such a manner that CO_2 and NH_3 were mixed only in the absorber. The investigation was performed under the following constant conditions: v_d = 4.5 m/second, NH_3 concentration in gas 16.2%, CO_2 concentration in gas 8.1%. The results of this series of experiments are plotted in Fig. 9, and the absorption coefficients calculated from these data are given in Fig. 10.

It follows from these results that variations of the degrees and rates of combined absorption of NH_3 and CO_2 with volumetric gas rate differ relatively little from the corresponding values in separate absorption of CO_2 by aqueous ammonia.

•If ammonium carbonates are absent from solution or are present in small amounts only.

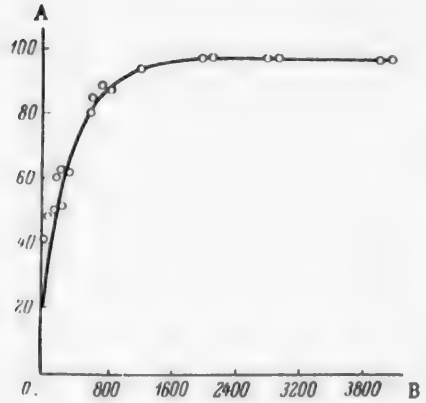

Fig. 4. Variation of the degree of absorption of CO_2 by aqueous ammonia with peripheral disk speed: w = 500 $m^3/m^3 \cdot$ hour, NH_3 concentration in solution 7.4%, CO_2 11.8%, P = 735 mm; A) degree of absorption (%), B) shaft speed (rpm).

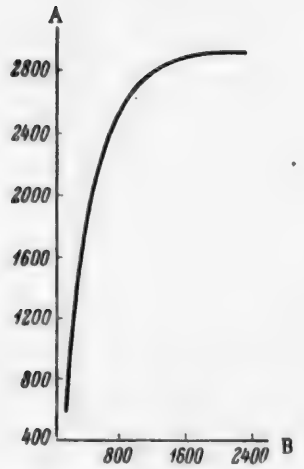

Fig. 5. Variation of the coefficient of absorption of CO_2 by aqueous ammonia with peripheral disk speed: w= 500 $m^3/m^3 \cdot$ hour, NH_3 concentration in solution 7.4%, CO_2 11.8%, P = = 785 mm; A) absorption rate coefficient (kg $CO_2/m^3 \cdot$ hour atmos), B) shaft speed (rpm).

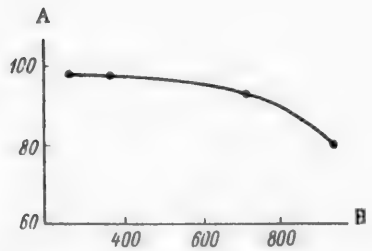

Fig. 6. Variation of the degree of absorption of CO_2 by aqueous ammonia with volumetric gas rate: NH_3 concentration in solution 7.14%, CO_2 in gas 10.7%, n = 1850 rpm, P = 746 mm; A) degree of absorption (%), B) volumetric gas rate ($m^3/m^3 \cdot$ hour).

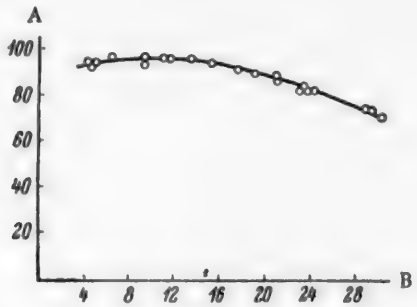

Fig. 7. Variation of the degree of absorption of CO_2 by aqueous ammonia with CO_2 concentration in the gas: w_G = 500 $m^3/m^3 \cdot$ hour, NH_3 concentration = 8.5-9%, t = 12.74°, n= 1850 rpm, P=756 mm; A) degree of absorption (%), B) CO_2 concentration (%).

From the point of view of profitability, transport of the product, and utilization of the ammonium carbonates, it is very important to study the rates of absorption of CO_2 and NH_3 in relation to the concentration of ammonium carbonates in solution. A series of experiments was carried out for this purpose on the combined absorption of CO_2 and NH_3 in the following volume proportions in the gas: $NH_3 : CO_2 = 1 : 1$ and $NH_3 : CO_2 = 2 : 1$.

Experiments on the absorption of these gases were performed separately with solutions of $(NH_4)_2CO_3$ and NH_4HCO_3, with initial salt contents of 20 to 420 g/liter in the liquid phase. Under these conditions, the degree of absorption of NH_3 was only slightly lower than the degree of absorption of NH_3 in water, and these results are therefore not given here.

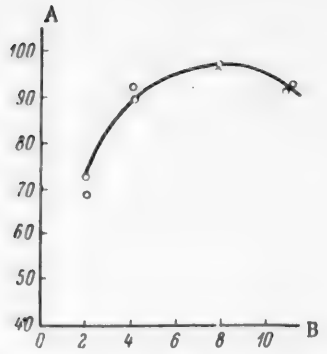

Fig. 8. Variation of the degree of absorption of CO_2 by aqueous ammonia with the NH_3 concentration in solution: w_G = 500 $m^3/m^3 \cdot$ hour, CO_2 concentration 10.5%, P = 760 mm, v_d = 4.5 m/second, t = 21.5°; A) degree of CO_2 absorption (%), B) NH_3 content of solution (%).

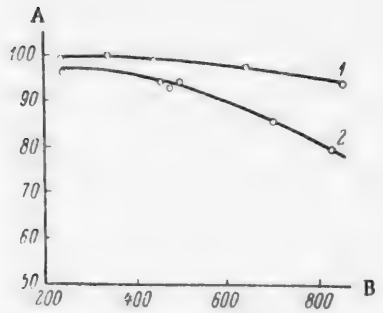

Fig. 9. Effect of volumetric gas rate on the combined absorption of CO_2 and NH_3 gases by water: CO_2 concentration in gas 8.1%, NH_3 in gas 16.2%, v_d = 4.5 m/second, P = = 745.8 mm, t = 22.5°; A) degree of absorption of CO_2 or NH_3 (%), B) gas rate ($m^3/m^3 \cdot$ hour); curves: 1) NH_3, 2) CO_2.

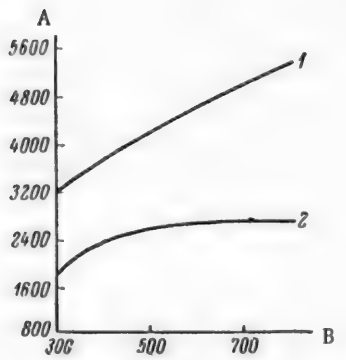

Fig. 10. Effect of volumetric gas rate on the coefficients of absorption of gaseous CO_2 and NH_3 in water: CO_2 concentration in gas 8.1%, NH_3 in gas 16.2%, n = 1850 rpm, P = 745.8 mm, t = 23.05°; A) absorption rate coefficient (kg/$m^3 \cdot$ hour $\cdot$ atmos), B) gas rate ($m^3/m^3 \cdot$ hour); curves: 1) NH_3, 2) CO_2.

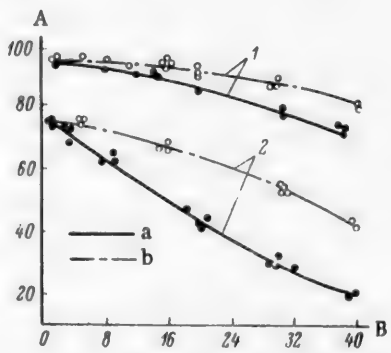

Fig. 11. Variation of the degree of absorption of CO_2 with concentrations of $(NH_4)_2CO_3$ and NH_4HCO_3 in solution (in combined absorption of CO_2 and NH_3); concentration of CO_2 8%, NH_3 8.16%, w= 500 $m^3/m^3 \cdot$ hour, n = 1850 rpm, t_{av} = 35-36°, P = 756 mm; A) degree of absorption of CO_2 (%), B) salt concentration C $\cdot$ 10 (g/liter); a) NH_4HCO_3, b) $(NH_4)_2CO_3$. Ratio NH_3 : CO_2 : 1) 2 : 1, 2) 1 : 1.

With regard to the variations of the degree of absorption of CO_2 with the concentration of ammonium carbonates and with the NH_3 : CO_2 in the gas, Fig. 11 shows that these variations are considerable. In this figure, the continuous lines represent absorption of $CO_2 + NH_3$ by $(NH_4)_2CO_3$, and the broken lines, by NH_4HCO_3.

It follows from this graph that under equal conditions the degree of absorption falls with increasing concentration of ammonium carbonates in solution, because of the increasing concentration of ammonium carbonates in solution, because of the increasing viscosity of the solution and increasing pressures of NH_3 and CO_2 in solution.

It follows from these experiments that at high concentrations of carbonates in the liquid phase the best results are obtained with the use of excess ammonia.

SUMMARY

1. Absorption of CO_2 from the gas phase by aqueous ammonia solutions proceeds at a high rate under conditions of high turbulence. The degree of absorption is also high under such conditions.

2. Analogously, the combined absorption of NH_3 and CO_2 with formation of carbonates also proceeds at a high rate.

3. At low concentrations of ammonium carbonates in solution the absorption proceeds at the highest rate at molar concentration ratio $NH_3 : CO_2 = 1 : 1$ as the process involves primary formation of NH_4HCO_3. At high contents of ammonium carbonates in the liquid phase absorption of CO_2 is most complete in presence of excess NH_3 in the gas.

4. It follows from these experimental results that relatively little power is required for effective removal of CO_2 from nitrogen–hydrogen mixtures with simultaneous production of ammonium carbonates. It then becomes unnecessary to absorb CO_2 in water, and power consumption for compression of the gas is reduced sharply.

LITERATURE CITED

[1] S. N. Ganz and S. B. Kravchinskaya, J. Appl. Chem. 28, No. 2 (1955).*

[2] S. N. Ganz and S. I. Kapturova, J. Appl. Chem. 28, No. 6 (1955).*

[3] S. N. Ganz, J. Appl. Chem. 29, 1018 (1956).**

[4] S. N Ganz and M. A. Lokshin, Trans. Dnepropetrovsk Inst. Chem. Tech. 5 (1956).

Received September 12, 1957.

*See C. B. translation.

**Original Russian pagination. See C. B. translation.

A STUDY OF THE RATE OF CONVERSION OF $CaSO_4$ INTO $(NH_4)_2SO_4$ IN CONJUNCTION WITH ABSORPTION OF NH_3 AND CO_2 UNDER CONDITIONS OF HIGH TURBULENCE*

S. N. Ganz, S. B. Leibovich, and S. I. Gorbman

The Dnepropetrovsk Institute of Chemical Technology

One rational method for removal of CO_2 from nitrogen–hydrogen mixture is to combine this process with conversion of $CaSO_4$ into ammonium sulfate. This method is promising because the removal of CO_2 from the gas is accompanied by production of a valuable fertilizer without consumption of sulfuric acid. This process has been adopted industrially in certain countries and has been studied by numerous workers both in the USSR and abroad [1].

Since the conversion of calcium sulfate and absorption of CO_2 are slow under the usual conditions, to accelerate these processes we used horizontal rotary reactors in which the gas and liquid phases were intensively mixed. These reactors are of analogous design to the high-speed rotary absorbers, descriptions of which with relevant design calculations were published earlier [2-5].

EXPERIMENTAL

In the first series of experiments, we studied the effect of hydrodynamic conditions in the apparatus on the rate of conversion of $CaSO_4$ by 10% ammonium carbonate solution. After the optimum conditions had been found, the rate of conversion of $CaSO_4$ was studied when this process was carried out in conjunction with absorption of CO_2 and NH_3. The experiments were performed in a large laboratory unit described and illustrated in the preceding paper [6]. The hydrodynamic conditions in the absorber were varied by variations of the disk speed, and in the first series of experiments also by variations of the gas rate. The degrees of absorption of NH_3 and CO_2 were determined from the concentrations of these gases at the absorber entry and exit. The gases were analyzed by the evacuated flask method [6].

The degree of conversion of $CaSO_4$ was found from the amount of $(NH_4)_2CO_3$ converted and the amount of $(NH_4)_2SO_4$ formed. The content of the latter in solution was determined by the formaldehyde method [7].

RESULTS OF THE INVESTIGATIONS

In the first series of experiments, the effect of agitation intensity on the conversion rate of $CaSO_4$ was studied. A solution containing 116 g of $(NH_4)_2CO_3$ per liter was poured into a horizontal rotary reactor with 4 disks attached to a horizontal shaft, and finely powdered $CaSO_4 \cdot 2H_2O$ was then added, the amount being 100 g calculated as 100% $CaSO_4$. Each experiment was continued for 3 minutes, and the $(NH_4)_2SO_4$ and $(NH_4)_2CO_3$ contents of the liquid phase were then determined.

From the results the degree of $CaSO_4$ conversion was calculated; the values are plotted in Fig. 1** It is seen that the conversion of $CaSO_4$ greatly increases with increased turbulence of the system, which is determined by the disk speed. The degree of $CaSO_4$ conversion rises sharply with shaft speed and at n = 400-500 rpm (peripheral

*Communication II.

**In each separate experiment fresh portions of $(NH_4)_2CO_3$ solution and $CaSO_4 \cdot 2H_2O$ were introduced as the disk speed was changed.

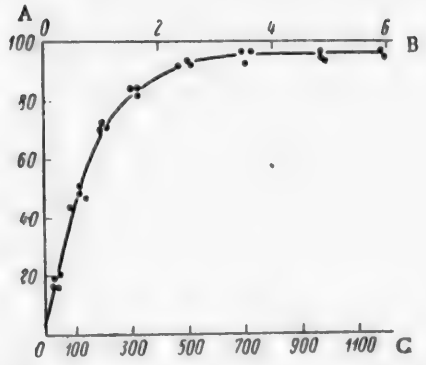

Fig. 1. Variation of the degree of conversion of $CaSO_4$ by $(NH_4)_2CO_3$ solution with shaft speed or peripheral disk speed, with 116 g/liter of $(NH_4)_2CO_3$ and 100 g/liter of $CaSO_4$ in the liquor; t = 30°, P = 750 mm, duration of each experiment 3 minutes; A) degree of conversion (%), B) peripheral disk speed (m/second), C) shaft speed (rpm).

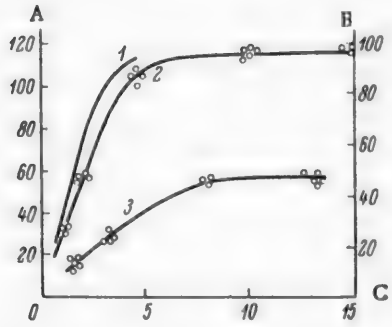

Fig. 2. Variation of the degree of conversion of $CaSO_4$ into $(NH_4)_2SO_4$ with the duration of the experiment, with 8.4% NH_3 in solution, CO_2 content 10.6%, P = 750 mm; $CaSO_4$ content of original liquor 126 g/liter, t = 27°C; A) degree of $CaSO_4$ conversion (g/liter), B) degree of $CaSO_4$ conversion (%), C) duration of experiment (minutes); volumetric gas rate ($m^3/m^3 \cdot$ hour): 1) 700, 2) 500, 3) 250.

disk speed v_d = 2-2.5 m/second) it reaches 90-94% within 3 minutes of phase contact.

Further increase of the disk speed leads to only a slight increase of the degree of conversion.

For example, with a phase contact time of 3 minutes the amount of $CaSO_4$ converted is 24 g/liter at 50 rpm, and 94 g/liter at 500 rpm. Accordingly, in the second case the amount of $CaSO_4$ converted into ammonium sulfate is increased 94/24 ≈ ≈3.9-fold. It follows that if sulfuric acid is replaced by gypsum in the production of ammonium sulfate the process can be accelerated by increasing the turbulence of the system. The acceleration of the process is probably the consequence of mechanical removal of the diffusion film of insoluble $CaCO_3$ formed in the surface of the gypsum particles by the reaction

$$CaSO_4 + (NH_4)_2CO_3 = CaCO_3 + (NH_4)_2SO_4. \quad (1)$$

In conditions of laminar flow, the thickness of the $CaCO_3$ layer on the gypsum particles increases as the reaction proceeds, and the reaction rate slows down as a result.

With intensive agitation of the interacting phases, the protective $CaCO_3$ layer is continuously destroyed and the surface of the $CaSO_4$ particles is renewed, so that the reaction rate increases. The bend in the curve in Fig. 1 (n = 500 rpm) indicates that the agitation regime attained at this degree of conversion is the most rational, as the maximum effect is produced with the least expenditure of energy for agitation.

In the subsequent experiments, we studied the rate of absorption of CO_2 when this process was combined with conversion of gypsum.

In these experiments an aqueous suspension of gypsum in the rotary reactor was saturated with ammonia to a content of 8.4% NH_3. The ammoniacal suspension of gypsum was then used for absorption of CO_2 from gas under the following conditions: n_{shaft} = 1200 rpm, t = 27.5-28.0°, P = 750 mm, $CaSO_4$ content of ammoniacal liquor 126 g/liter, CO_2 content of gas 10.6%. The experiments were performed at three different gas rates: 250, 500, and 700 $m^3/m^3 \cdot$ hour. The results showed that the degree of CO_2 absorption decreases as gypsum is consumed in the reaction. The absorption of CO_2 at w = 250 $m^3/m^3 \cdot$ hour virtually ceases at the 12th minute because of the complete conversion of the gypsum and NH_3 present in the liquor.

These experiments also showed that the degree of CO_2 absorption falls with increase of the volumetric gas rate.

Analogous experiments were performed under the same conditions to study the effect of the volumetric gas rate on the conversion rate of $CaSO_4$. The results of these experiments are given in Fig. 2. It is seen that increase of the volumetric gas rate accelerates the conversion of $CaSO_4$ considerably, owing to increase of the molar CO_2 concentration and higher turbulence of the system.

The last series of experiments was concerned with the influence of $CaSO_4$ and $(NH_4)_2CO_3$ concentrations in the liquor on the degree of $CaSO_4$ conversion at n = 1200 rpm, t = 25°, and P = 750 mm. The concentrations of $CaSO_4 \cdot H_2O$ and $(NH_4)_2CO_3$ used are given below.

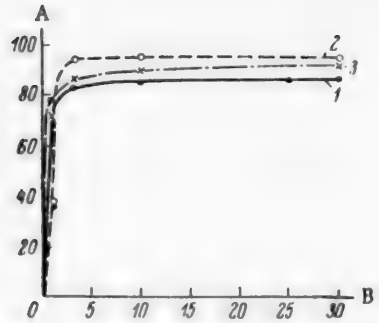

Fig. 3. Variation of the degree of conversion of $CaSO_4$ into $(NH_4)_2SO_4$ with the duration of the experiment at t = 23°, P = 750 mm, n = 1200 rpm, v_d = 6 m/second; A) degree of $CaSO_4$ conversion (%), B) duration of experiment (minutes); contents of $CaSO_4$ and $(NH_4)_2CO_3$ respectively (in g/liter): 1) 6.3 and 5.7, 2) 63 and 57, 3) 126 and 115.6.

$CaSO_4 \cdot H_2O$	$(NH_4)_2CO_3$
6.3	5.7
63	57
126	115.6

The results obtained at these concentrations are plotted in Fig. 3, where the duration of the experiment (in minutes) is taken along the abscissa axis and the degree of $CaSO_4$ conversion along the ordinate axis. It follows from these results that the highest rate corresponds to the average concentrations represented by Curve 3 (64 g $CaSO_4$ and 57 g $(NH_4)_2CO_3$ per liter).

Comparison of the values on Curve 2 of Fig. 3 with the values on the curve in Fig. 1 shows that decrease of temperature from 30° (Fig. 1) to 23° (Fig. 3) leads to a decrease of the degree of conversion under otherwise similar conditions. Increase of temperature has a favorable effect on this process. Experiments showed that the optimum temperatures are in the 28-38° range. Above and below this range the rate of $CaSO_4$ conversion decreases. At temperatures below 25-28° the reaction rate falls, while at temperatures above 38-40° the CO_2 and NH_3 pressures in solution and the gas viscosity increase.

SUMMARY

1. It was shown in a study of the rate of conversion of gypsum into ammonium sulfate in conjunction with removal of CO_2 from the gas that the gypsum conversion rate increases considerably under conditions of high turbulence. This is accompanied by a high degree of CO_2 absorption with almost complete conversion of $CaSO_4$ into ammonium sulfate.

2. The experimental data presented in this paper, and the method used, may also be of interest to the coke by-product industry in relation to the removal of NH_3 and CO_2 from coke-oven gas.

LITERATURE CITED

[1] Trans. Sci. Res. Inst. Fertilizers and Insectofungicides 101 (1939); 160 (1958).

[2] S. N. Ganz and S. B. Kravchinskaya, J. Appl. Chem. 28, No. 2 (1955).*

[3] S. N. Ganz and S. I. Kapturova, J. Appl. Chem. 28, No. 6 (1955).*

[4] S. N. Ganz, J. Appl. Chem. 29, 1018 (1956).**

[5] S. N. Ganz and M. A. Lokshin, Trans. Dnepropetrovsk Inst. Chem. Tech. 5 (1956).

[6] S. N. Ganz, G. I. Vilesov, S. I. Gorbman, and S. B. Leibovich, J. Appl. Chem. 32, No. 5, 960 (1959).**

[7] A. P. Groshev, Technical Analysis [in Russian] (Goskhimizdat, 1953).

Received September 12, 1957.

*See C.B. Translation.

**Original Russian pagination. See C. B. Translation.

ACTION OF ACID SOLUTIONS ON VITREOUS LITHIUM SILICATES

S. K. Dubrovo

The extent and nature of chemical breakdown of vitreous silicates by aqueous solutions depend on many factors. The most important of these are the state of the silica in the glass, which depends on the composition of the glass, the hydrogen-ion concentration of the acting solution, the nature of the reaction products on the glass surface and in solution, which determine secondary reactions, etc.

In a study of the action of aqueous solutions on vitreous sodium silicates, we regarded the primary process to be exchange of sodium ions in the glass with hydrogen ions from solution [1]. In the case of lithium silicate glasses there may be an analogous reaction represented by the scheme

$$Li^+(Si_nO_m)^- + H^+ \rightleftarrows H(Si_nO_m) + Li^+.$$

In principle, the character of chemical attack should be the same for lithium as for sodium silicate glasses. However, in view of the different ionic radii of lithium and sodium in the silicates, the difference between the rates of attack should increase with increasing contents of alkali metal oxides in the glasses.

There is hardly any information in the literature on the chemical durability of simple lithium silicate glasses.

The purpose of the present investigation was to study the decomposition of glassy lithium silicates in acid solutions in relation to the silica contents of the glasses, and to compare the results with the chemical durability of sodium silicate glasses.

EXPERIMENTAL

The lithium silicates studied were in the composition range with $Li_2O : SiO_2$ ratios from 1:1.4 to 1:5, which corresponded to Li_2O contents between 16.7 and 41.7 molar %.

Method of investigation. The preparation of these glasses was described earlier [2]. The investigations were performed mostly with powders separated between sieves with 110-140 μ holes, washed free from dust fractions in alcohol and dried at 110°.

At this grain size the total calculated surface area of 1 g of the powder was from 192 to 209 cm^2 (according to the density of the glass). With glasses of high chemical resistance 1 g samples were taken, and with less resistant glasses, 0.5 g samples. In the case of unstable glasses plates 10-15 cm^2 in area were used, in order to keep the composition of the acting solution as constant as possible. The experiments were performed in quartz beakers at 40°, with 120 ml of liquid stirred by means of a quartz stirrer. The stirring rate was such that the powder remained in suspension and was uniformly washed by the liquid. Samples were taken after 1, 2, 4, and 6 hours. Before a sample was filtered. The chemical durability of lithium glasses was studied by determinations of the amounts of glass components dissolved in a definite time. These amounts were then calculated as moles of the corresponding oxides per 1 cm^2 of the original glass surface (n_{Li_2O}, n_{SiO_2}). The process was also characterized in terms of $\alpha = \frac{n_{SiO_2}}{x n_{Li_2O}}$, which represents the fraction of silica which passed into solution from the layer of glass attacked by the solution. Here x represents the silica content of the original glass, the composition of which is

expressed as $Li_2O \cdot xSiO_2$. The amount of silica in solution was determined by the colorimetric method described earlier [1]. Lithium oxide was also determined colorimetrically, by means of the FEK-M colorimeter, by the ferricyanide method described by Forster [3]. Special experiments were carried out to test the effect of silicic acid in solution on the accuracy of lithium determinations.

TABLE 1

Action of Hydrochloric Acid Solutions on Lithium Silicates

Molar ratio		Components, α	$n \cdot 10^4$ (in moles/cm^2) during time (hours):				Acid concentration (normality)
Li_2O	SiO_2		1	2	4	6	
1	1.4	Li_2O	17	26	33	40	0.1
		SiO_2	0.06	0.06	0.07	0.07	
		α	0.002	0.002	0.002	0.001	
		Li_2O	31	42	56	128	1
		SiO_2	Not detected				
1	1.7	Li_2O	3.07	3.97	5.98	8.0	0.1
		SiO_2	—	—	0.01	0.01	
		α	—	—	0.001	0.001	
1	2	Li_2O	0.70	0.98	1.65	1.83	0.1
		SiO_2	—	—	—	0.006	
		α	—	—	—	0.001	
1	2	Li_2O	0.96	1.1	2.0	2.0	1
		SiO_2	Not detected				
1	2.3	Li_2O	0.16	0.29	0.55	0.59	0.1
		SiO_2	—	—	0.005	0.006	
1	3	Li_2O	0.11	0.15	0.25	0.33	0.1
		SiO_2	—	—	0.001	0.001	
1	3	Li_2O	0.22	0.27	0.34	0.44	1
		SiO_2	Not detected				
1	4	Li_2O	0.19	0.22	0.30	0.30	0.1
		SiO_2	Not detected				
1	5	Li_2O	0.19	0.20	0.23	0.30	0.1
		SiO_2	Not detected				

Chemical durability of vitreous lithium silicates in hydrochloric acid solutions. The effects of 0.1 N and 1 N hydrochloric acid solutions on the above-named lithium silicates were studied. The results are presented in Table 1 and in Fig. 1 and 2. It follows from Table 1 and Fig. 1 that the rate at which lithium oxide goes into solution from bisilicate and from glasses of higher silica contents (1 : 3, 1 : 4, 1: 5) falls with time. This indicates that a residual protective layer is formed on the surface of these glasses. It is seen in Fig. 2 that the plot of the logarithm of the amount of lithium oxide dissolved against the silica content of the glass is a smooth curve without any inflections corresponding to special points on the phase diagram for the system Li_2O-SiO_2. With increase of the silica content of the glass from 58 to 70 molar % the amount of dissolved lithium oxide increases, but further increase of the silica content has almost no effect on the leaching rate.

It is clear from Table 1 that the amount of silica dissolved out of lithium silicate glasses is very small. Even with such a relatively unstable glass as 1: 1.4 the fraction of silica dissolved out of the attacked layer does not exceed 0.2% ($\alpha = 0.002$). With the 1:3 composition and with glasses of higher silica contents SiO_2 was not detected at all in the solution.

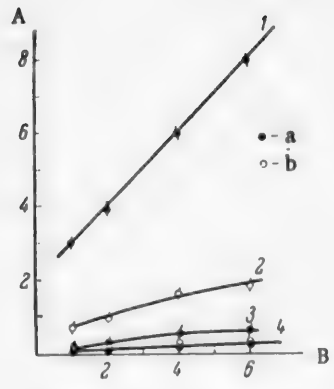

Fig.1. Action of 0.1 N hydrochloric acid solution at 40° on vitreous lithium silicates: A) values of $n_{Li_2O} \cdot 10^{-6}$ (moles/cm^2) B) time (hours); molar ratio of Li_2O to SiO_2: 1) 1:1.7, 2) 1:2, 3) 1:2.3, 4) 1:3, 1:4 and 1:5.

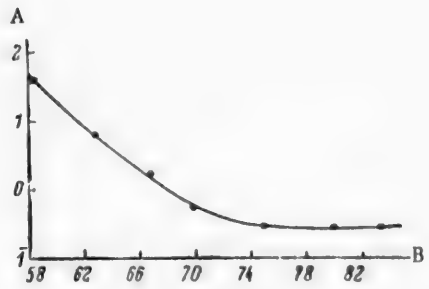

Fig. 2. Variation of the amount of Li_2O dissolved out during 6 hours with the composition (in the action of 0.1 N hydrochloric acid on lithium silicates): A) values of log $n_{Li_2O} \cdot 10^{-6}$, B) SiO_2 contents (molar %).

Increase of the hydrochloric acid concentration from 0.1 to 1 N increases the amount of lithium oxide dissolved; the extent of this increase is greater for glasses of lower stability. Silica is not dissolved out to any appreciable extent by the action of 1 N hydrochloric acid on lithium glasses under these conditions.

Thus, lithium silicate glasses are characterized by leaching out of lithium oxide with formation of hydrated silica on the glass surface. The leached-out glass layer contains water, the amount of which is ~16% in the case of 1:1.4 glass.

Comparison of chemical durability of vitreous lithium and sodium silicates in acid solutions. The durability of lithium and sodium glasses in hydrochloric acid solutions was compared in experiments performed under the same conditions. For clearer comparison, we calculated (with certain assumptions) the depth of the attacked glass layer and the thickness of the residual silica layer.

The depth of the attacked layer was calculated from the amount of dissolved lithium oxide (n_{Li_2O}) by means of the formula used earlier for soda glasses [1]:

$$\rho_{Li_2O} = \frac{n_{Li_2O} \cdot M \cdot 100}{a \cdot d},$$

where M is the molecular weight of Li_2O, a is the Li_2O content (in wt. %), and d is the density of the glass. Similarly it is possible to calculate ρ_{SiO_2}, which represents the decrease in the thickness of the residual silica layer as the result of partial dissolution. The difference between these values ($\rho = \rho_{Li_2O}$) represents the thickness of the residual layer on the glass surface.

Since the amounts of SiO_2 dissolved are negligible in comparison with Li_2O when acids act on lithium glasses, it may be assumed in practice that $\rho = \rho_{Li_2O}$. In the case of sodium silicates ρ_{SiO_2} need only be taken into account for glasses containing less than 65% silica.

Of course, these calculations are conventional, as they involve a number of assumptions to which attention was drawn in our investigation of sodium glasses [1]. However, the results demonstrate very clearly the relative chemical durability of vitreous lithium and sodium silicates. The depths of attack of these glasses by the action of 0.1 N hydrochloric acid solution during 6 hours are compared in Table 2.

These results indicate that vitreous lithium silicates are more resistant to acids than sodium silicates of the corresponding molecular composition. The difference between the depths of corrosion decreases with increasing silica contents.

DISCUSSION OF RESULTS

If the action of aqueous solutions on alkali silicates is regarded as a process which causes breakdown of Si–O–Me and Si–O–Si, linkages, the forces of attraction between the cations and oxigen must be taken into consideration. These forces are represented by the equation $\frac{z_c \cdot z_O}{a^2}$, where z_c is the valence of the cation,

z_O is the valence of oxygen, and $\underline{a}$ is the interionic distance ($r_c + r_O$). Assuming the ionic radii in silicates to be 0.78 A for lithium, 0.98 A for sodium, and 1.33 A for potassium, we find the following values for the forces of attraction: 0.45, 0.37, and 0.27 respectively. Of course, we cannot assume a strict quantitative connection between the chemical durability of alkali silicates and the strength of the Me–O bonds in them, but undoubtedly the corrosion of simple silicates should diminish with increase of this strength. It follows that lithium silicates should have higher chemical durability than the corresponding sodium and potassium silicates.

With increase of the lithium content in silicates the number of Si–O–Si linkages broken down increases. This weakens the resistance of the the silicon–oxygen framework to the corrosive action of chemical reagents, as in the case of sodium silicates. However, since the lithium ion has a stronger field of force than other alkali-metal ions, its bond strength with singly-bonded oxygens should favor greater strength of the structure as a whole.

It follows from literature data and our results [2-4] that lithium glasses are more closely packed than the corresponding sodium glasses. It is therefore to be expected that ions should diffuse more slowly into solution from lithium glasses than from glasses with a more open structure. This fact should also increase the chemical durability of lithium glasses.

Our experimental results are consistent with the foregoing considerations.

TABLE 2

Depth of Corroded Glass Layers (in μ) in the Action of 0.1 N Hydrochloric Acid Solution During 6 Hours

Composition (molar %)			ρR_2O	ρSiO_2	Π
Li_2O	Na_2O	SiO_2			
37.1 *	—	62.9	3.4	—	3.4
—	37.1	62.9	130	30	100
33.3	—	66.7	1.2	—	1.2
—	33.3	66.7	69	0.07	69
30.3	—	69.7	0.4	—	0.4
—	30.3	69.7	39	—	39
25	—	75	0.3	—	0.3
—	25	75	8.0	—	8.0
20	—	80	0.3	—	0.3
—	20	80	1.9	—	1.9

*Under the action of hydrochloric acid during 4 hours.

SUMMARY

1. The corrosion of vitreous lithium silicates with $Li_2O : SiO_2$ ratios from 1:1 to 1:5 in hydrochloric acid solutions was studied; it was found that a plot of the logarithm of the amount of lithium oxide dissolved out against the silica content of the glass gives a smooth curve s without any inflections corresponding to special points on the phase diagram for the system $Li_2O–SiO_2$.

2. Lithium silicate glasses are characterized by leaching out of lithium oxide with formation of a layer of hydrated silica on the glass surface.

3. Vitreous lithium silicates are attacked to a smaller depth by acid solutions in a given time than sodium glasses of the corresponding molecular composition. The difference between the acid resistances of these glasses diminishes with increasing silica content.

LITERATURE CITED

[1] S. K. Dubrovo and Yu. A. Shmidt, Bull. Acad. Sci. USSR, Div. Chem. Sci. 4, 597 (1953).*

[2] S. K. Dubrovo and Yu. A. Shmidt, J. Appl. Chem. 32, No. 4, 742 (1959).*

*Original Russian pagination . See C.B.Translation.

[3] C. F. Forster, Analyst 79, 943, 629 (1954).

[4] H. Moore, P. W. McMillan, J. Soc. Glass Techn. 40, 193, 66 (1956).

Received July 4, 1958.

A STUDY OF THE OPTICAL PROPERTIES OF SODIUM ALUMINOBOROSILICATE GLASSES*

A. A. Appen and Gan' Fu-si (Kan Fu-si)

Among the oxides introduced into glass, Al_2O_3 and B_2O_3 are of special significance, as boron and aluminum ions each have two coordination numbers (3.4 and 4.6 respectively), and boron–oxygen and aluminum–oxygen tetrahedrons often replace isomorphously silicon–oxygen tetrahedrons. The simultaneous presence of Al_2O_3 and B_2O_3 in glass results in peculiar variations of properties with composition. This effect has been named the aluminoborate anomaly [1]. As is known, borosilicate, aluminosilicate, and aluminoborosilicate glasses are widely used in practice. Systematic studies of the properties of glasses containing Al_2O_3 and B_2O_3 are of importance both in practice and in theory, as they give better insight into certain questions of glass structure.

The optical properties of sodium aluminosilicate glasses containing up to 6% Al_2O_3 were systematically studied by Faick and Young [2]. It was found that the refractive index increases as silica is replaced by alumina (equal percentages by weight). Morey and Merwin [3] determined the refractive indices of certain glasses with high alumina contents.

The optical properties of sodium borosilicate glasses had been studied earlier by Turner [4], English [5], and others. Detailed data were obtained by Turner and Wang [6]. As silica is replaced by boron oxide, the curves showing variations of refractive index pass through maxima, but the position of the maximum varies with the Na_2O content. The average dispersion remains almost unchanged, while the Abbé number first increases and then remains almost constant.

Investigations of the optical properties of glasses containing Al_2O_3 and B_2O_3 simultaneously have only recently been started. It has been reported [1] that in certain glasses n_D and $n_F - n_C$ decrease as silica is replaced by alumina. This is an unusual effect which has been given the name of the aluminoborate anomaly [7].

We studied the optical properties of three series of glasses.

I. $16\,Na_2O \cdot yB_2O_3 \cdot xAl_2O_3$. $(84-x-y)\,SiO_2$, where $x=0, 4, 8, 12$; $y=0, 4, 8, 12, 16, 20, 24, 32$. The Na_2O content was constant. Silica was replaced by alumina or boric anhydride at different $\frac{Na_2O}{B_2O_3}$ ratios

II. $(32-y)\,Na_2O \cdot yB_2O_3 \cdot xAl_2O_3$ $(68-x)SiO_2$, where $x=0, 4, 8, 12$; $y=0, 4, 8, 12, 16, 20, 24, 28, 32$. The $\frac{Na_2O}{B_2O_3}$ ratio was varied and silica was replaced by alumina, or at constant contents of Al_2O_3 and SiO_2 sodium oxide was replaced by boric anhydride.

III. $(20-y)\,Na_2O \cdot yB_2O_3 \cdot xAl_2O_3 \cdot (80-x)SiO_2$, where $x=0, 4, 8, 12$; $y=0, 4, 8, 12$. The composition was varied as in the second series, but the SiO_2 contents were higher.

The oxide contents of the glasses are expressed in molar percentages.

About seventy different glasses were prepared. The glasses were melted in a platinum crucible in a Silit furnace. The melts were stirred vigorously by means of a platinum stirrer in order to attain a high degree of homogeneity. The glasses were carefully annealed.

*Communication I in the series on the aluminoborate anomaly of properties of silicate glasses.

Pure reagents were used in preparation of the batches. To diminish errors due to volatilization of alkali, the basic alkali silicate glasses were melted first, and the other components were then added. Possible volatilization of B_2O_3 was also taken into account when the batches were made up. The results of check analyses showed that in most instances the difference between the synthetic and analytical compositions of the glasses was negligibly small.

The optical constants of the glasses were determined at different wavelengths by means of the Pulfrich refractometer, and densities were determined by hydrostatic weighing. The accuracy was to within $\pm 1 \cdot 10^{-4}$, in the refractive index determinations, and to within $\pm 1 \cdot 10^{-3}$ in the density determinations.

In this paper we present a brief account of the results obtained in investigations of the refractive index n_D, mean dispersion $n_F - n_C$, density d, and molecular refraction MR.

EXPERIMENTAL RESULTS

The results are expressed in terms of the relative changes (differences) in the properties, Δn_D and Δd, in the diagrams, while the corresponding data for the original glasses are presented in Table 1.

TABLE 1

Refractive Indices and Densities of the Original Glasses

Glass composition	n_D	d
Series I		
16 Na_2O · 84 SiO_2	1.486	2.361
16 Na_2O · 4 B_2O_3 · 80 SiO_2	1.4970	2.414
16 Na_2O · 8 B_2O_3 · 76 SiO_2	1.5096	2.467
16 Na_2O · 12 B_2O_3 · 72 SiO_2	1.5150	2.488
16 Na_2O · 16 B_2O_3 · 68 SiO_2	1.5193	2.498
16 Na_2O · 20 B_2O_3 · 64 SiO_2	1.5194	2.482
16 Na_2O · 24 B_2O_3 · 60 SiO_2	1.5190	2.476
16 Na_2O · 32 B_2O_3 · 52 SiO_2	1.5151	2.419
Series II		
32 Na_2O · 68 SiO_2	1.5049	2.494
28 Na_2O · 4 B_2O_3 · 68 SiO_2	1.5093	2.497
24 Na_2O · 8 B_2O_3 · 68 SiO_2	1.5138	2.505
20 Na_2O · 12 B_2O_3 · 68 SiO_2	1.5183	2.513
16 Na_2O · 16 B_2O_3 · 68 SiO_2	1.5193	2.498
12 Na_2O · 20 B_2O_3 · 68 SiO_2	1.5064	2.402
8 Na_2O · 24 B_2O_3 · 68 SiO_2	1.4817	2.239
4 Na_2O · 28 B_2O_3 · 68 SiO_2	1.463	2.131
32 B_2O_3 · 68 SiO_2	1.456	2.120
Series III		
20 Na_2O · 80 SiO_2	1.493	2.386
16 Na_2O · 4 B_2O_3 · 80 SiO_2	1.4970	2.414
12 Na_2O · 8 B_2O_3 · 80 SiO_2	1.5007	2.411
8 Na_2O · 12 B_2O_3 · 80 SiO_2	1.4913	2.340

For aluminosilicate glasses, as a rule, the refractive index increases continuously as silica is replaced by alumina, but it must be pointed out that the effect of n_D increase is greater with increase of SiO_2 content (Fig. 1).

For aluminoborosilicate glasses, the variations of n_D and other properties present a more complex picture. In the first series, at low $\frac{Na_2O}{B_2O_3}$ (<2) ratios, the refractive index decreases as silica is replaced by alumina (Fig. 2), and the effect of n_D decrease is intensified with decrease of the $\frac{Na_2O}{B_2O_3}$ ratio. However, when the the Al_2O_3 content exceeds the Na_2O content, further replacement of SiO_2 by Al_2O_3 results in an increase of n_D.

Minima appear on the curves (Curves 7,8). When the ratio $\frac{Na_2O}{B_2O_3}=4$ there is an appreciable maximum in the course of n_D (Curve 2).

As silica is replaced by boric anhydride, maxima appear, as a rule, on the curves for n_D (Fig. 3). Introduction of alumina makes the maximum less sharp, and its position shifts toward lower B_2O_3 contents.

The density variations follow the same course as the variations of refractive index, but the relative accuracy of the density determinations is lower (Fig. 4 and 5). The points at which the maxima appear on the curves for variations of n_D and $\underline{d}$, respectively, do not coincide. The maximum appears somewhat earlier on the curve for the density variations. Table 2 gives the positions of the maximum at different Al_2O_3 contents.

TABLE 2

Positions of the Maxima on Replacement of SiO_2 by B_2O_3 in Glasses of Series I

Glass characteristics	n_D				d			
Al_2O_3 content of glass (%)	0	4	8	12	0	4	8	12
Position of maximum (% B_2O_3)	20	18	17	15	17	15	8	–

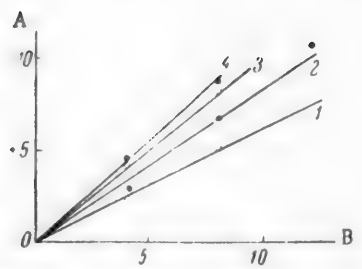

Fig. 1. Variations of refractive-index difference with chemical composition of glasses in the system $Na_2O \cdot Al_2O_3 \cdot SiO_2$ on replacement of SiO_2 by Al_2O_3: A) $\Delta n_D \cdot 10^3$; B) x (molar % Al_2O_3).
1) $32Na_2O \cdot xAl_2O_3 \cdot (68-x)\,SiO_2$,
2) $20Na_2O \cdot xAl_2O_3 \cdot (80-x)\,SiO_2$,
3) $16Na_2O \cdot xAl_2O_3 \cdot (84-x)\,SiO_2$,
4) $13Na_2O \cdot xAl_2O_3 \cdot (87-x)\,SiO_2$.

As silica is replaced by alumina the mean dispersion grows continuously at all $\frac{Na_2O}{B_2O_3}$ ratios, but it remains almost unchanged as silica is replaced by boron oxide.

As silica is replaced by alumina the molecular refraction increases linearly and the $\frac{Na_2O}{B_2O_3}$ ratio does not affect MR. As silica is replaced by boric anhydride, MR is unchanged at first, in the 13-17% B_2O_3 range there is a weak inflection, and after that MR increases continuously.

In the second series of glasses the variations of optical properties follow a different course. As silica is replaced by alumina, n_D increases so long as the ratio $\frac{Na_2O}{B_2O_3}>3$ (Fig. 6, Curves 1, 2, 3). With decrease of the $\frac{Na_2O}{B_2O_3}$ ratio the n_D increase weakens and becomes almost zero at $\frac{Na_2O}{B_2O_3}=3$. After this, n_D begins to decrease (Curves 4, 5, 6). On further decrease of the $\frac{Na_2O}{B_2O_3}$ ratio, Δn_D becomes zero for the second time (Curve 7) and then becomes positive again ($\frac{Na_2O}{B_2O_3}<\frac{1}{3}$, Curves 8, 9). It should be noted that when silica is replaced by alumina in alkali-free or low-alkali aluminoborosilicate glasses, n_D increases much more than it does for aluminosilicate glasses.

As silica is replaced by alumina, the mean dispersion increases; with decrease of the $\frac{Na_2O}{B_2O_3}$ ratio, the increase $n_F - n_C$ is greater (Fig. 7).

As silica is replaced by alumina or as sodium oxide is replaced by boron oxide, MR increases linearly and the $\frac{Na_2O}{B_2O_3}$ ratio has little effect on MR (Fig. 8)

We studied the third series in order to determine the influence of SiO_2 contents on variations of the optical properties. In the second series, as silica is replaced by alumina, variations of the $\frac{Na_2O}{B_2O_3}$ ratio influence only

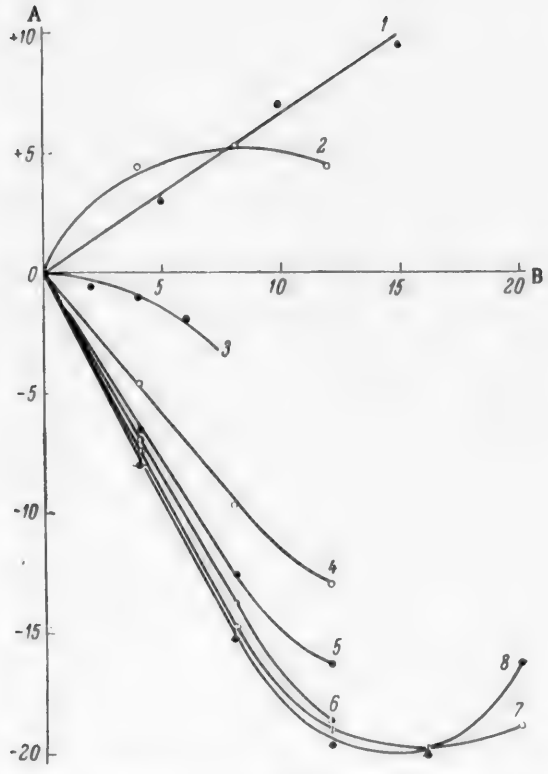

Fig. 2. Variations of refractive-index difference with chemical composition of the first series of glasses, $16Na_2O \cdot yB_2O_3 \cdot xAl_2O_3 \cdot (84-x-y)SiO_2$, on replacement of SiO_2 by Al_2O_3: A) $\Delta n_D \cdot 10^3$; B) x (molar % Al_2O_3); 1) y = 0, 2) y = 4, 3) y = 8, 4) y = 12, 5) y = 16, 6) y = 20, 7) y = 24, 8) y = 32.

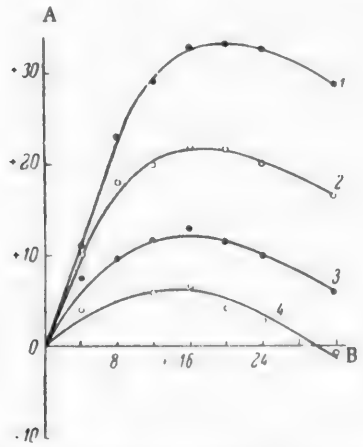

Fig. 3. Variations of refractive-index difference with chemical composition of the first series of glasses, $16Na_2O \cdot yB_2O_3 \cdot xAl_2O_3 \cdot (84-x-y)SiO_2$ by B_2O_3: A) $\Delta n_D \cdot 10^3$, B) y (molar % B_2O_3); 1) x = 0, 2) x = 4, 3) x = 8, 4) x = 12.

the rate of increase or decrease of n_D or $\underline{d}$, and there are no maxima on the curves. In the third series the variations follow a different course. The curves for variations of n_D and $\underline{d}$ have both maxima and minima, the positions of which depend on the $\frac{Na_2O}{B_2O_3}$ ratio. Variations of n_D are shown in Fig. 9.

DISCUSSION OF RESULTS

In aluminosilicate glasses, the aluminum ion acquires on oxygen from Na_2O, and forms a tetrahedron (AlO_4) which enters the structural network and joins gaps in the network where sodium ions are situated ($\equiv Si-O_{Na+}^{Na+}O-Si\equiv$). As a result, n_D and $\underline{d}$ increase, but only slightly. In borosilicate glasses the boron ion also acquires an oxygen from Na_2O and its coordination number changes from three (BO_3) to four (BO_4). On addition of alumina to a borosilicate glass, the glass structure becomes more complex. The ratio $\frac{r_{B^{3+}}}{r_{O^{2-}}}$ lies beyond the limits favorable for tetrahedron formation [8], and therefore, if the content of Na_2O is sufficient, the (AlO_4) tetrahedron is more stable than the (BO_4) tetrahedron. This means that oxygen is utilized primarily in transferring aluminum into the glass framework. As silica is replaced by alumina, if the $\frac{Na_2O}{B_2O_3}$ ratio is low, the (AlO_4) tetrahedron enters the framework in place of the (BO_4) tetrahedron, while boron acquires coordination number three. As a result, n_D and $\underline{d}$ decrease strongly. If the $\frac{Na_2O}{B_2O_3}$ ratio is high, the (AlO_4) tetrahedrons enter the framework without altering the coordination of boron, which retains the coordination number of four. Therefore n_D and $\underline{d}$ increase as SiO_2 is replaced by Al_2O_3. At intermediate $\frac{Na_2O}{B_2O_3}$ ratios the n_D and $\underline{d}$ curves have maxima or the decreases or increases of n_D and $\underline{d}$ are diminished. If the glass contains very little Na_2O or much alumina (more than soda), not all the Al^{3+} ions can enter the framework, and some act as modifiers, i.e., they retain a coordination number of six, which should increase n_D and $\underline{d}$. This accounts for the minima on Curves 7, 8 (Fig. 2) and 4 (Fig. 9). The (AlO_4) and (BO_4) tetrahedrons bear additional electric charges, and apparently they cannot become joined directly but are separated by (SiO_4) tetrahedrons

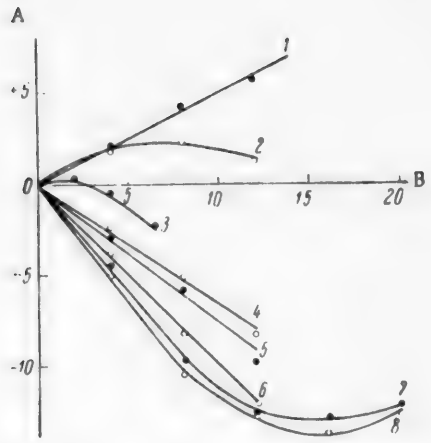

Fig. 4. Variations of density difference with chemical composition of the first series of glasses, $16Na_2O \cdot yB_2O_3 \cdot xAl_2O_3 \times (84-x-y)SiO_2$ on replacement of SiO_2 by Al_2O_3: A) $\Delta d \cdot 10^2$, B) x (molar% Al_2O_3); 1) y = 0, 2) y = 4, 3) y = 8, 4) y = 12, 5) y = 16, 6) y = 20, 7) y = 24, 8) y = 32.

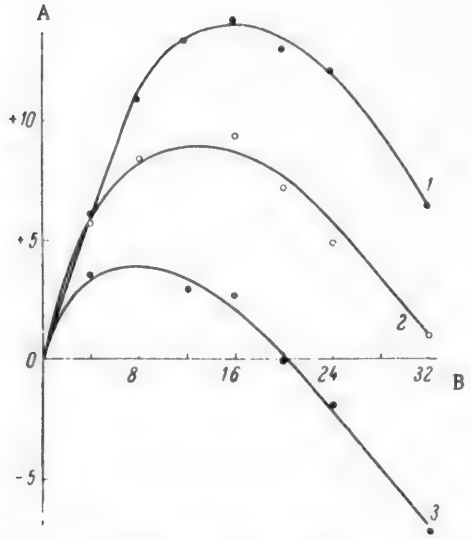

Fig. 5. Variations of density difference with chemical composition of the first series of glasses, $16Na_2O \cdot yB_2O_3 \cdot xAl_2O_3 \cdot (84-x-y)SiO_2$ on replacement of SiO_2 by B_2O_3: A) $\Delta d \cdot 10^2$, B) y (molar % B_2O_3); 1) x = 0, 2) x = 4, 3) x = 8.

or (BO_3) triangles. The silicon ion also tends to combine with oxygen, and therefore, in aluminosilicate glasses, change of the coordination number of boron depends not only on the $\frac{Na_2O}{B_2O_3}$ ratio and the amount of Al_2O_3, but also on the SiO_2 content. This influence of SiO_2 is revealed when the results for the properties of glasses of the second and third series are compared.

When silica is replaced by alumina, or sodium oxide by boric anhydride, the molecular refraction increases linearly all the time. This shows that molecular refraction conforms satisfactorily to the additivity rule. Molecular refraction is almost uninfluenced by changes in the glass structure.

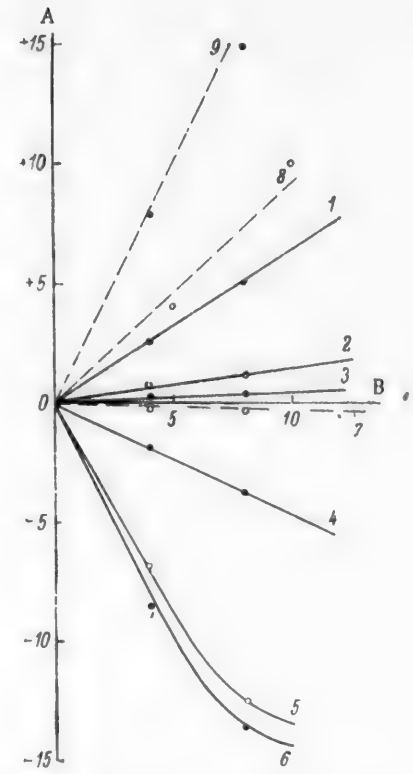

Fig. 6. Variations of refractive-index difference with chemical composition of the second series of glasses, $(32-y) \cdot Na_2O \cdot yB_2O_3 \cdot xAl_2O_3 \cdot (68-x)SiO_2$, on replacement of SiO_2 by Al_2O_3: A) $\Delta n_D \cdot 10^3$, B) x (molar % Al_2O_3); 1) y = 0, 2) y = 4, 3) y = 8, 4) y = 12, 5) y = 16, 6) y = 20.

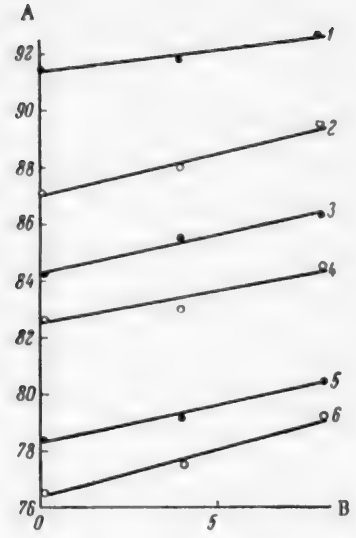

Fig. 7. Variations of mean dispersion with chemical composition of the second series of glasses, (32−y) $Na_2O \cdot yB_2O_3 \cdot xAl_2O_3 \cdot (68-x)SiO_2$ on replacement of SiO_2 by Al_2O_3: A) $(n_F-n_C) \cdot 10^4$, B) x (molar % Al_2O_3); 1) y = 0, 2) y = 4, 3) y = 8, 4) y = 12, 5) y = 16, 6) y = 20.

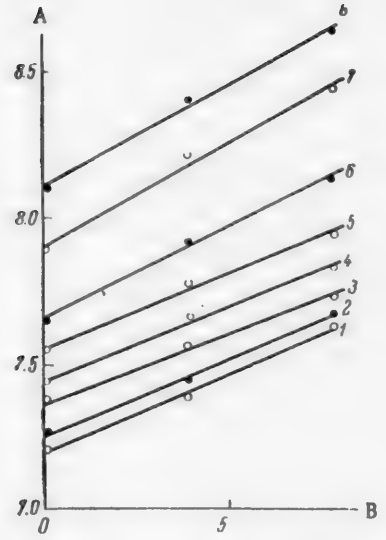

Fig. 8. Variations of molecular refraction with chemical composition of the second series of glasses,(32−y) $Na_2O \cdot yB_2O_3 \cdot xAl_2O_3 \cdot (68-x)SiO_2$, on replacement of SiO_2 by Al_2O_3: A) MR, B) x (molar % Al_2O_3); 1) y = 0.2) y = 4, 3) y = = 8, 4) y = 12, 5) y = 16, 6) y = 20, 7) y = 24, 8) y = 28.

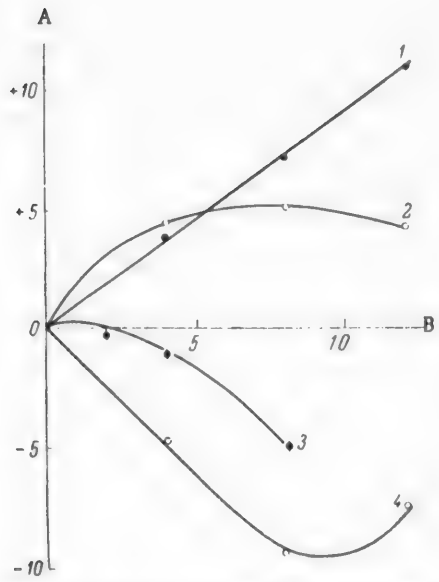

Fig. 9. Variations of refractive-index difference with chemical composition of the third series of glasses, (20−y) $Na_2O \cdot yB_2O_3 \cdot xAl_2O_3 \cdot (80-x)SiO_2$, on replacement of SiO_2 by Al_2O_3: A) $\Delta n_D \cdot 10^3$, B) x (molar % Al_2O_3); 1) y = 0.2, 2) y = 4 3) y = 8, 4) y = 12.

SUMMARY

1. The aluminoborate anomaly of the optical properties of sodium aluminoborosilicate glasses was studied, and the variations of refractive index, mean dispersion, density, and molecular refraction at different $\frac{Na_2O}{B_2O_3}$ ratios and silica contents were determined.

2. The appearance of maxima and minima on the curves for the properties (n_D and $\underline{d}$) and changes of sign of Δn_D and Δd from plus to minus and back to plus are attributed to changes in the coordination numbers of B^{3+} and Al^{3+} ions; the influence of silica is also emphasized.

3. Variations of molecular refraction conform satisfactorily to the additivity rule.

LITERATURE CITED

[1] A. A. Appen. Travaux du IV Congres international du Verre, Paris (1956).

[2] C. Faick and J. Young, J. Research Natl. Bureau Standards 14, 133 (1935).

[3] G. W. Morey. The Properties of Glass. N.Y. (1954).

[4] W. E. S. Turner and F. Winks, J. Soc. Glass. Techn. 9, 389 (1925).

[5] S. English and W. E. S. Turner, J. Soc. Glass. Techn. 7, 155 (1923).

[6] T. H. Wang and W. E. S. Turner, J. Soc. Glass. Techn. 29, 390 (1945).

[7] E. I. Galant and A. A. Appen, J. Appl. Chem. 31, 1741 (1958).*

[8] K. S. Evstrop'ev and N. A. Toropov, Chemistry of Silicon and Physical Chemistry of Silicates [in Russian] (Industrial Construction Press, 1956).

Received July 12, 1958.

*Original Russian pagination. See C. B. Translation.

A STUDY OF THE OPTICAL PROPERTIES OF POTASSIUM ALUMINO-BOROSILICATE GLASSES •

A. A. Appen and Gan' Fu-sI (Kan Fu-si)

Peculiarities in the variations of optical properties and density of sodium aluminoborosilicate glasses were described in our first communication [1]. Potassium aluminoborosilicate glasses were studied in the present investigation. These experiments were carried out in order to determine the influence of the nature of alkali elements on the manifestation of the aluminoborate anomaly of glass properties.

In contrast to soda glasses, potash glasses have high viscosity in the melted state, and it is therefore difficult to obtain homogeneous samples, especially with high alumina contents. The density of some of the glasses was determined by the pycnometric method, and the refractive index by the immersion method.

There are as yet no systematic data in the literature on the optical properties of potassium aluminosilicate, borosilicate, and aluminoborosilicate glasses.

Two series of glasses were studied, corresponding to the same molecular composition as the sodium glasses.

I. 16 $K_2O \cdot yB_2O_3 \cdot xAl_2O_3 \cdot (84-x-y)SiO_2$, where x = 0, 4, 8, 12; y = 0, 4, 8, 12, 16, 20, 24, 32.

II. $(32-y)\,K_2O \cdot yB_2O_3 \cdot xAl_2O_3\ (68-x)SiO_2$, where x = 0, 4, 8; y=0, 4, 8, 12, 16, 24, 28.

The results are expressed in terms of relative changes in the properties, Δd and Δn_D, in the diagrams, while values of n_D and d for the original glasses are given in Table 1.

TABLE 1

Refractive Indices and Densities of the Original Glasses

Series I			Series II		
glass composition	n_D	d	glass composition	n_D	d
16 $K_2O \cdot 84\ SiO_2$	1.490	2.358	32 $K_2O \cdot 68\ SiO_2$	1.507	2.46
16 $K_2O \cdot 4\ B_2O_3 \cdot 80\ SiO_2$	1.4980	2.403	28 $K_2O \cdot 4\ B_2O_3 \cdot 68\ SiO_2$	1.5076	2.468
16 $K_2O \cdot 8\ B_2O_3 \cdot 76\ SiO_2$	1.5065	2.445	24 $K_2O \cdot 8\ B_2O_3 \cdot 68\ SiO_2$	1.5097	2.459
16 $K_2O \cdot 12\ B_2O_3 \cdot 72\ SiO_2$	1.5125	2.473	16 $K_2O \cdot 16\ B_2O_3 \cdot 68\ SiO_2$	1.5153	2.477
16 $K_2O \cdot 16\ B_2O_3 \cdot 68\ SiO_2$	1.5153	2.477	8 $K_2O \cdot 24\ B_2O_3 \cdot 68\ SiO_2$	1.481	2.217
16 $K_2O \cdot 20\ B_2O_3 \cdot 64\ SiO_2$	1.5154	2.463	4 $K_2O \cdot 28\ B_2O_3 \cdot 68\ SiO_2$	1.465	2.121
16 $K_2O \cdot 24\ B_2O_3 \cdot 60\ SiO_2$	1.5140	2.444	32 $B_2O_3 \cdot 68\ SiO_2$	1.456	2.12
16 $K_2O \cdot 32\ B_2O_3 \cdot 52\ SiO_2$	1.5086	2.387			

The general picture of variations of the optical properties of potash glasses is very similar to that of the soda glasses.

•Communication II in the series on the aluminoborate anomaly of properties of silicate glasses.

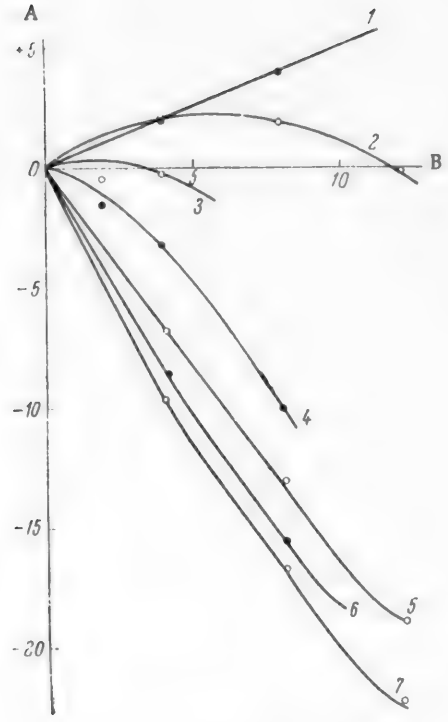

Fig. 1. Variations of refractive-index difference with chemical composition of the first series of glasses, $16K_2O \cdot yB_2O_3 \cdot xAl_2O_3 \cdot (84-x-y)SiO_2$, on replacement of SiO_2 by B_2O_3: A) $\Delta n_D \cdot 10^3$, B) x (molar % Al_2O_3); 1) y = 0, 2) y = 4, 3) y = 8, 4) y = 12, 5) y = 16, 6) y = 20, 7) y = 24.

TABLE 2

Positions of Maxima on Replacement of SiO_2 by B_2O_3 in Potash Glasses of Series I

Glass characteristics	n_D			d		
Al_2O_3 content of glass (%)	0	4	8	0	4	8
Position of maximum (% B_2O_3)	18	14	12	16	12	8

The refractive indices, mean dispersions, and densities are lower in the potash than in the soda glasses, while molecular refractions are higher.

In the first series, at low $\frac{K_2O}{B_2O_3}$ ratios, the refractive index decreases sharply on replacement of silica by alumina, i.e., the aluminoborate anomaly is very pronounced (Fig. 1, Curves 4-7). With increase of the $\frac{K_2O}{B_2O_3}$ ratio the decrease of refractive index becomes less and at $\frac{K_2O}{B_2O_3} = 4$ a maximum appears (Curve 2). In absence of B_2O_3 replacement of SiO_2 by Al_2O_3 produces a continuous increase of n_D as usual (Curve 1).

As silica is replaced by boric anhydride, very distinct maxima appear on the curves for refractive index changes (Fig. 2). Introduction of alumina makes the maximum diffuse, and its position is shifted in the direction of lower B_2O_3 contents.

Density variations follow roughly the same course as the refractive index variations, but the positions of the maxima on the curves for changes of n_D and $\underline{d}$ do not coincide (Fig. 3, 4). The maxima appear somewhat earlier on the density curves (Table 2).

It should be noted that the changes of the properties are more pronounced in potash than in soda glasses.

As silica is replaced by alumina the mean dispersion remains almost unchanged at all $\frac{K_2O}{B_2O_3}$ ratios (Fig. 5), while the molecular refraction increases linearly (Fig. 6).

On replacement of silica by boric anhydride the mean dispersion decreases a little, while molecular refraction is almost unchanged at first and then increases.

In the second series of potash glasses, replacement of silica by alumina produces the same complex effects as those observed in the corresponding soda glasses. At very high $\frac{K_2O}{B_2O_3}$ ratios or in absence of B_2O_3, n_D increases (Fig. 7, Curve 1). At $\frac{K_2O}{B_2O_3}$ ratios approximately between 6 and 1/3, n_D decreases (Curves 3, 4). At lower $\frac{K_2O}{B_2O_3}$ ratios, the refractive index increases again (Curve 5). The density variations follow the same course, while the mean dispersion remains constant and molecular dispersion increases linearly.

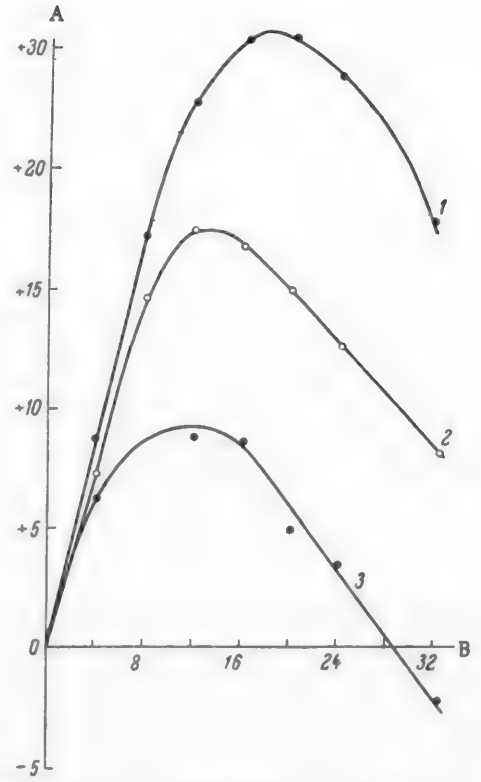

Fig. 2. Variations of refractive-index difference with chemical composition of the first series of glasses, $16K_2O \cdot yB_2O_3 \cdot xAl_2O_3 \cdot (84-x-y)SiO_2$ on replacement of SiO_2 by B_2O_3: A) $\Delta n_D \cdot 10^3$, B) y (molar % B_2O_3); 1) x = 0, 2) x = 4, 3) x = 8.

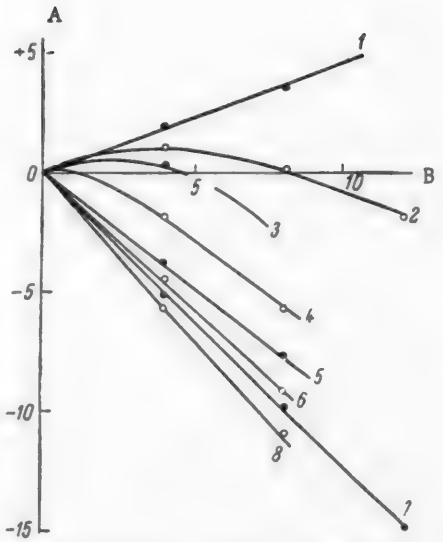

Fig. 3. Variations of density difference with chemical composition of the first series of glasses, $16K_2O \cdot yB_2O_3 \cdot xAl_2O_3 \cdot (84-x-y)SiO_2$, on replacement of SiO_2 by Al_2O_3: A) $\Delta d \cdot 10^2$, B) x (molar % Al_2O_3) 1) y = 0, 2) y = 4, 3) y = 8, 4) y = 12, 5) y = 16, 6) y = 20 7) y = 24, 8) y = 32.

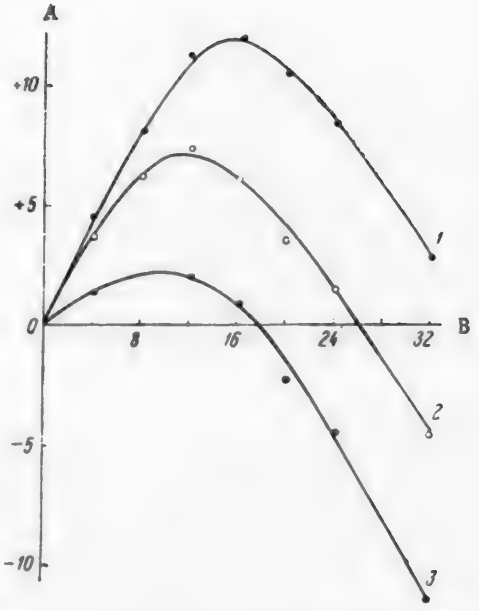

Fig. 4. Variations of density difference with chemical composition of the first series of glasses, $16K_2O \cdot yB_2O_3 \cdot xAl_2O_3 \cdot (84-x-y) \cdot SiO_2$, on replacement of SiO_2 by B_2O_3: A) $\Delta d \cdot 10^2$, B) y (molar % B_2O_3); 1) x = 0, 2) x = 4, 3) x = 8.

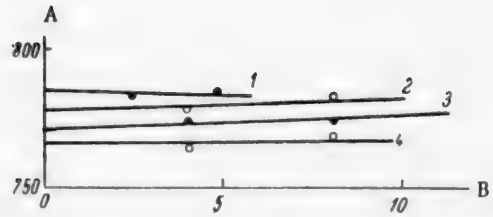

Fig. 5. Variations of mean dispersion with chemical composition of the first series of glasses, 16 $K_2O \cdot yB_2O_3 \cdot xAl_2O_3 \cdot (84-x-y)\,SiO_2$, on replacement of SiO_2 by Al_2O_3; A) $(n_F - n_C \cdot 10^4)$, B) x (molar % Al_2O_3); 1) y = 8, 2) y = 16, 3) y = 24, 4) y = 32.

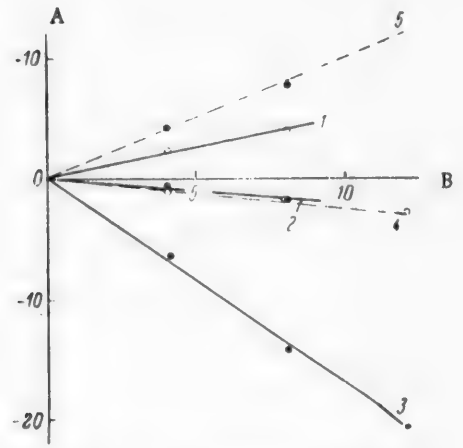

Fig. 7. Variations of refractive-index difference with chemical composition of the second series of glasses, $(32-y) \cdot K_2O \cdot yB_2O_3 \cdot xAl_2O_3 \cdot (68-x)\,SiO_2$ on replacement of SiO_2 by Al_2O_3: A) $\Delta n_D \cdot 10^3$, B) x (molar % Al_2O_3); 1) y = 0, 2) y = 4, 3) y = 16, 4) y = 24, 5) y = 28.

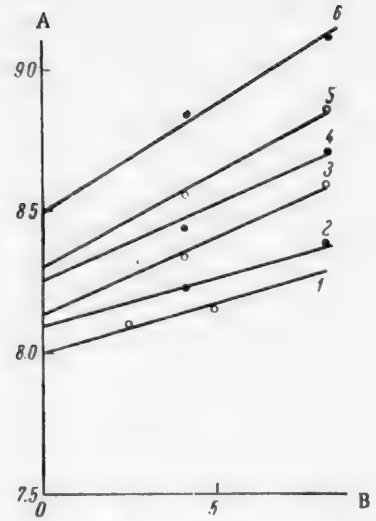

Fig. 6. Variations of molecular refraction with chemical composition of the first series of glasses, 16 $K_2O \cdot yB_2O_3 \cdot xAl_2O_3 \cdot (84-x-y) \cdot SiO_2$, on replacement of SiO_2 by Al_2O_3: A) MR, B) x (molar % Al_2O_3); 1) y = 8, 2) y = 12, 3) y = 16, 4) y = =20, 5) y = 24, 6) y = 32.

The reason for the resemblance between the properties of potash and soda glasses is that the difference between the strengths of Na–O and K–O bonds is not large [2]. The potassium ion gives up oxygen more easily, and therefore the maxima are more distinct and earlier on the curves for variations of n_D, and $\underline{d}$ of potash glasses The causes of the aluminoborate anomaly were discussed in the first communication.

SUMMARY

The aluminoborate anomaly of properties of potash silicate glasses was studied and it was found that the variations of the optical properties and density of potash and soda glasses on replacement of silica by alumina and boric anhydride conform to similar laws.

LITERATURE CITED

[1] A. A. Appen and Kan Fu-si, J. Appl. Chem. 32, No. 5, 983 (1959).*

[2] K. H. San, J. Am. Ceram. Soc. 30, 277 (1947).

Received September 29, 1958.

*Original Russian pagination. See C. B. translation.

EFFECT OF COMMON SALT ON THE SOLUBILITY OF SODIUM ANTIMONATE, STANNATE, AND ARSENATE IN AQUEOUS CAUSTIC SODA SOLUTION

G. G. Urazov, B. M. Lipshits, and V. S. Lovchikov

The use of a melted mixture of caustic soda, common salt, and potassium nitrate for removal of arsenic, tin, and antimony from lead has led to improved results in lead refining and has made it possible to extract the impurities in the form of useful products.

A study of the oxidation of arsenic, tin, and antimony has shown that common salt does not take part in the reactions, lowers the chemical activity of the alkaline melts, and increases the oxidation time of the impurities. Therefore the use of common salt in alkaline refining of lead is undesirable from the pyrometallurgical standpoint. For a full evaluation of the role of common salt in this refining process it was necessary to study the influence of this salt on hydrometallurgical processing of the melts. We therefore studied the solubilities of sodium arsenate, stannate, and antimonate in aqueous caustic soda solutions containing sodium chloride.

Technical caustic soda containing up to 6% Na_2CO_3 is used in lead refining. During hydrometallurgical treatment of the melts the carbonate is dissolved, and its concentration in solution increases somewhat as the result of carbonation of the caustic soda. Therefore in the course of these investigations we also studied the influence of sodium carbonate on the solubilities of the above-named salts.

EXPERIMENTAL

The materials used in the investigations were caustic soda free from sodium carbonate, sodium chloride of chemically pure grade, and sodium antimonate arsenate, and stannate which we prepared.

The salt solubilities were studied in glass vessels immersed in a thermostat with a toluene thermoregulator by means of which the water temperature in the apparatus could be regulated to within ± 0.1°. Alkali solution and the salts were put in the vessels, and the liquids were stirred at strictly constant temperature until analytical data for consecutive samples coincided, which showed that equilibrium had been reached. The side tube of the apparatus was firmly corked during the experiments.

Data on the influence of common salt and sodium carbonate on the solubility of sodium antimonate in water and in aqueous alkali are presented in Table 1.

The solubility of sodium antimonate in water is 0.10% at 25°, and 0.58% at 75°. Common salt lowers the solubility of sodium antimonate in water, In the simultaneous presence of caustic soda and common salt in solution, the main salting-out effect is exerted by caustic soda. Since the liquors in hydrometallurgical treatment of the alkaline melts contain caustic soda, the common salt present in them cannot have a significant influence on the solubility of sodium antimonate.

The presence of sodium carbonate in solution lowers the solubility of sodium antimonate both at 25° and at 75°. In solutions containing 350 g NaOH per liter,sodium carbonate has no practical effect on the solubility of sodium antimonate. The effects of common salt and sodium carbonate on the solubility of sodium stannate in aqueous alkaline solutions are given in Table 2.

At 25° the solubility of sodium stannate in water is 27.7%. Increase of temperature by 50° lowers its solubility down to 21.78°. Common salt lowers the solubility of sodium stannate in water. In solutions containing 350 g NaOH per liter,common salt has almost no effect on the solubility of this salt. The effects of sodium carbonate are similar.

TABLE 1

Solubility of Sodium Antimonate in Water and in Aqueous Solutions of Caustic Soda, Common Salt, and Sodium Carbonate

Temperature (°C)	Contents in solution (g/liter)			Contents in solution (wt.%)	
	NaOH	NaCl	Na_2CO_3	$NaSbO_3$	including Sb
25	—	—	—	0.1000	0.064
	85	—	—	0.0030	0.0019
	350	—	—	0.0230	0.0150
	—	85	—	0.0123	0.0078
	—	300	—	0.0053	0.0034
	—	—	20	0.0158	0.0100
	—	—	85	0.0053	0.0034
	85	85	—	0.0030	0.0019
	350	85	—	0.0220	0.0140
	350	85	20	0.0270	0.0170
75	—	—	—	0.580	0.370
	85	—	—	0.031	0.020
	350	—	—	0.066	0.040
	—	85	—	0.034	0.020
	—	300	—	0.063	0.040
	—	—	20	0.033	0.021
	—	—	85	0.027	0.017
	85	85	—	0.028	0.018
	350	85	—	0.071	0.046
	350	85	20	0.070	0.042

TABLE 2

Solubility of Sodium Stannate in Water and in Aqueous Solutions of Caustic Soda, Common Salt, and Sodium Carbonate

Temperature (°C)	Contents in solution (g/liter)			Contents in solution (wt.%)	
	NaOH	NaCl	Na_2CO_3	Na_2SnO_3	including Sn
25	—	—	—	27.70	15.46
	85	—	—	14.30	8.00
	350	—	—	0.48	0.27
	—	85	—	24.30	13.50
	—	300	—	12.00	6.70
	—	—	20	25.50	14.20
	—	—	85	20.40	11.30
25	85	85	—	10.80	6.20
	350	85	—	0.48	0.27
	350	85	20	0.45	0.25
75	—	—	—	21.78	13.10
	85	—	—	13.10	7.31
	350	—	—	0.52	0.29
	—	85	—	17.00	9.50
	—	300	—	6.20	3.40
	85	85	—	9.70	5.40
	350	85	—	0.45	0.25
	350	85	20	0.45	0.25

TABLE 3

Solubility of Sodium Arsenate in Water and in Aqueous Solution of Caustic Soda and Common Salt

Temperature (°C)	Contents in solution (wt.%)			
	NaOH	NaCl	Na_3AsO_4	including As
25	0	0	13.80	5.50
	0	8.10	4.88	1.76
	6.10	8.06	1.70	0.61
	12.47	8.00	0.94	0.34
	14.60	8.04	0.78	0.28
75	5.90	0	24.95	8.99
	5.61	1.77	24.54	8.85
	5.81	3.77	24.10	8.68
	5.96	5.83	23.52	8.48

Variations of the solubility of sodium arsenate with the concentrations of caustic soda and common salt in solution are detailed in Table 3.*

Common salt lowers the solubility of sodium arsenate in water. In simultaneous presence of NaOH and NaCl in solution caustic soda has the main salting-out effect on sodium arsenate.

Temperature has a significant effect on the solubility of sodium arsenate; in observations of saturated solutions it was found that, on cooling, sodium arsenate is not deposited but forms a crystalline structure, and the solution completely loses its fluidity.

SUMMARY

1. In aqueous caustic soda solutions, common salt has almost no effect on the solubilities of sodium antimonate, stannate, and arsenate. Therefore its presence is not necessary in solution in the conversion of melts formed in the alkali refining of lead for removal of arsenic, tin, and antimony.

2. Sodium carbonate has almost no effect on the solubilities of sodium antimonate and stannate in concentrated aqueous alkaline solutions.

*V. I. Milent'eva took part in these experiments.

LITERATURE CITED

[1] G. G. Urazov, V. S. Lovchikov, and B. M. Lipshits, Bull. Tech. Econ. Inf. Acad. Sci. USSR 7, 9 (1957).

Received April 14, 1958.

INVESTIGATION OF THE CONVERSION OF CARBON MONOXIDE BY STEAM UNDER PRESSURE

V. I. Atroshchenko and B. Bibr

The V. I. Lenin Polytechnic Institute, Khar'kov

The production of hydrogen by conversion of carbon monoxide by steam is of great theoretical and practical importance:

$$CO + H_2O \rightleftarrows H_2 + CO_2, \quad \Delta H^0_{25^\circ} = -9838 \text{ cal} \tag{1}$$

The significance of this reaction is increasing because of the utilization of spent natural gas as a source of hydrogen.

It is known that if the conversion process is effected under pressure, the cost of hydrogen is reduced and the output of the equipment is raised. Moreover, in this conversion method it is possible to use the pressure of the natural gas itself, and costs are lowered still further in consequence.

Despite the importance of the use of pressure in conversion of carbon monoxide, the literature does not contain any data on the kinetics of this process.

Kul'kova and Temkin [1], who studied the conversion of CO under atmospheric pressure, proposed the following equation to represent the kinetics of the process:

$$-\frac{dp_{CO}}{d\tau} = k_1 p_{CO}\left(\frac{p_{H_2O}}{p_{H_2}}\right)^{\beta} - k_2 p_{CO_2}\left(\frac{p_{H_2}}{p_{H_2O}}\right)^{1-\beta}. \tag{2}$$

Replacing in this equation the final partial pressures by the initial partial pressures, and introducing the excess coefficients u, s, v, and the degree of conversion α, equal to $\frac{p^0_{CO} - p_{CO}}{p^0_{CO}}$ we have,

$$p_{CO} = p^0_{CO} - \alpha p^0_{CO}; \quad p_{CO_2} = p^0_{CO_2} + \alpha p^0_{CO}; \quad p_{H_2O} = p^0_{H_2O} - \alpha p^0_{CO}; \quad p_{H_2} = p^0_{H_2} + \alpha p^0_{CO},$$

$$u = \frac{p^0_{H_2}}{p^0_{CO}}, \quad s = \frac{p^0_{H_2O}}{p^0_{CO}}, \quad v = \frac{p^0_{CO_2}}{p^0_{CO}},$$

$$\frac{d\alpha}{d\tau} = k_1 (1-\alpha)\left(\frac{s-\alpha}{u+\alpha}\right)^{\beta} - k_2 (v+\alpha)\left(\frac{u+\alpha}{s-\alpha}\right)^{1-\beta} \tag{3}$$

It follows from Equation (3) that variations of the total pressure P do not affect the reaction rate.

The same conclusion follows from the kinetic equation proposed by Kirillov [2] for the conversion rate of CO under normal pressure:

$$-\frac{dp_{CO}}{d\tau} = k_1 p_{H_2O}\left(\frac{p_{CO}}{p_{CO_2}}\right)^{\beta} - k_2 p_{H_2}\left(\frac{p_{CO_2}}{p_{CO}}\right)^{\gamma}, \quad (4)$$

$$\frac{d\alpha}{d\tau} = k_1(s-\alpha)\left(\frac{1-\alpha}{v+\alpha}\right)^{\beta} - k_2(u+\alpha)\left(\frac{v+\alpha}{1-\alpha}\right)^{\gamma}. \quad (5)$$

However, it is known from literature data [3,4] and from plant practice that the influence of pressure is more complex, and Equations (2) and (4) are not applicable to the process under pressure.

The literature contains a number of papers [3-5] the authors of which studied the activity of catalysts for conversion of CO under pressure, but no general relationships were derived.

We have attempted to study the kinetics of conversion of carbon monoxide by steam under increased pressure.

RESULTS OF INVESTIGATIONS

The raw material for the conversion studies was industrial water gas containing 30-36% CO, 50-36% H_2, 4-10% N_2 + CH_4, 5-8% CO_2, traces of oxygen, and about 3 g of sulfur compounds per cubic meter.

The crude gas was purified by means of caustic soda and alkaline pyrogallol solutions in a special unit, and passed through a furnace containing heated copper turnings at 500°. It was then passed through absorbers containing $KMnO_4$ and NaOH solutions and dried over solid caustic soda in a tower. The last traces of impurities were removed in filters containing active carbon.

The compressed gas passed through a regulating valve of the GIAP (State Institute of the Nitrogen Industry) type (Fig. 1) into a large buffer vessel and filters containing active carbon and caustic potash. The filters were connected to the line of a GIAP regulator, operating on the principle of a mercury manometer, which closes the contacts of the regulating valve coil. This maintained the pressure in the unit constant to within a few centimeters of mercury. The dry gas, freed from oil and iron carbonyl, was passed into a saturator about 30 liters in capacity, filled with distilled water and heated 2-3° higher than the temperature required for saturation with water vapor. The heating was regulated automatically. The gas entering the saturator was in the form of fine bubbles which actively agitated the water. The saturated gas with a small excess of water vapor passed through a coil saturator-condenser with a tube length of about 3 meters. Excess water vapor was condensed in this coil, the temperature of which was accurately maintained by means of an ultrathermostat. The vapor–gas mixture passed through a heating tube into the contact column lined with a porcelain tube, containing 25 ml of catalyst in the form of 3× 3 mm cylinders. The catalyst temperature was kept constant to within ± 3°. The converted gas was cooled in a condenser, the excess condensed water was separated off in a separator, and the gas, after reduction to atmospheric pressure, passed through a flow meter and was analyzed. All the parts of the apparatus in contact with hot gas were made from stainless steel.

The catalyst column contained industrial high-temperature catalyst consisting of 30% Fe_2O_3, 2.5% Cr_2O_3, 61% MgO, 1% K_2O and 1.5% Al_2O_3, bulk density 1.26 g/ml, free volume 42%.

The steam–gas ratio was checked by measurements of the water collected in the separator.

The compositions of the crude, purified, and converted gas were determined by means of the VTI gas analysis apparatus. The degree of conversion of carbon monoxide was found from the amounts of carbon monoxide present before and after conversion.

Data on variations of the degree of conversion with time are presented in Table 1. The equilibrium degree of conversion (Table 1) was calculated on the assumption of ideal behavior of the components, which is quite permissible in practical calculations in the pressure range studied [1,5].

For comparison of our data with literature data [3,4] we used the method of Atwood et al. [3], who compared the activity of catalysts by means of the ratio $\frac{k_{e,\,p}}{k_{e,\,1}}$, calculated from the equation

$$k_e = V(R+1)\log\frac{1}{1-CO_t}, \quad (6)$$

where k_e is the rate constant; V is the volumetric velocity of the dry gas at 60° F and P = 1 atmos; R is the vapor–gas ratio; CO_t is the ratio of converted carbon monoxide to the fraction capable of reacting at equilibrium

$$CO_t = \frac{\alpha}{\alpha'}; \qquad V(R+1) = \frac{3600 \cdot 288.56 \cdot 0.42 \cdot P}{\tau \cdot T}.$$

Results calculated for 700° K are given in Table 2 and Fig. 2. Our results conform to the same general relationship as was found by the above-named authors [3], although they used a low-temperature catalyst.

However, it is clear that Equation (6) can be used only for comparing different catalysts, and it does not represent the kinetics of the process.

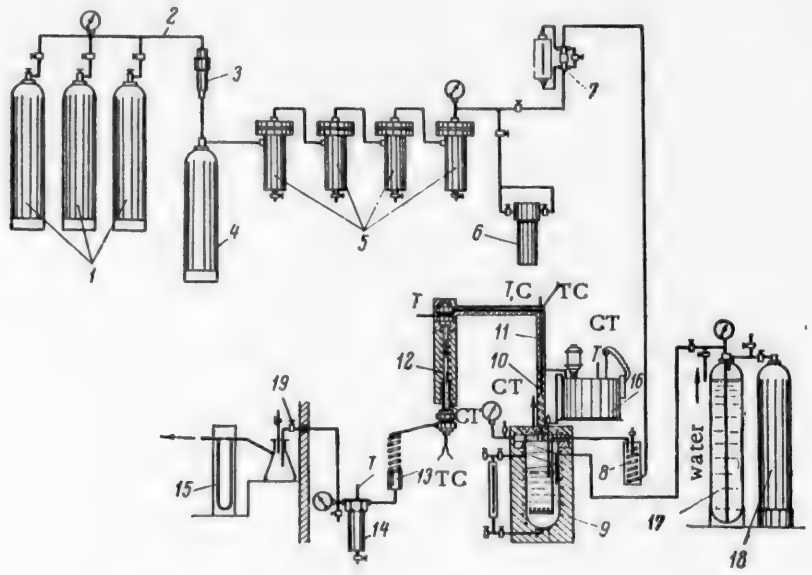

Fig. 1. Diagram of unit for CO conversion: 1) cylinders with pure gas, 2) distributor tube, 3) regulating valve, 4) intermediate vessel, 5) filters, 6) pressure regulator, 7) flow meter, 8) gas preheater, 9) saturator, 10) coil condenser, 11) superheater, 12) converter, 13) condenser, 14) separator, 15) flow meter, 16) thermostat, 17) cylinder with distilled water, 18) nitrogen cylinder, 19) throttle valve, CT) contact thermometer, T) thermometer, TC) thermocouple.

For determination of the reaction-rate constant we used the equation derived earlier [6] for the rate of conversion of carbon monoxide by steam:

$$-\frac{dp_{CO}}{d\tau} = k_1 \frac{p_{CO} - p'_{CO}}{p_{H_2}} \sqrt{p_{H_2O}}; \tag{7}$$

$$k_1 = \frac{V\sqrt{p^0_{CO}}}{\tau}\left[\frac{u+\alpha'}{\sqrt{s-\alpha'}} \ln \frac{(\sqrt{s-\alpha}+\sqrt{s-\alpha'})(\sqrt{s}-\sqrt{s-\alpha'})}{(\sqrt{s-\alpha}-\sqrt{s-\alpha'})(\sqrt{s}+\sqrt{s-\alpha'})} - 2(\sqrt{s}-\sqrt{s-\alpha})\right] \tag{8}$$

where k_1 is the rate constant ($second^{-1}$); τ is the contact time (seconds), equal to $\frac{\mu \cdot 3600 \cdot P \cdot 273}{T \cdot V \cdot (R+1)}$; μ is the free volume of the catalyst; P is the total pressure (abs. atmos); T is the absolute temperature (°K); p_i are the partial pressures of the components at τ (atmos); p^0_i are the initial partial pressures of the components

TABLE 1

Temperature T (°K)	Pressure P (atmos, abs.)	steam:gas ratio	Steam–gas mixture p^0_{CO}	$p^0_{H_2}$	$p^0_{N_2+CH_4}$	$p^0_{H_2O}$	Equilibrium conversion α	Contact time τ (sec)	Conversion α	Rate constant k_1 (sec^{-1})
578	6	2.010	0.675	1.132	0.186	4.007	0.9858	0.882	0.0782	0.050
								0.601	0.0401	0.040
								0.431	0.0212	0.028
660	6	1.913	0.697	1.171	0.192	3.940	0.9601	0.878	0.468	0.528
								0.421	0.280	0.538
700	6	3.152	0.491	0.824	0.135	4.555	0.9768	0.624	0.400	0.362
	6	1.974	0.676	1.136	0.186	4.002	0.9455	0.841	0.676	1.09
								0.424	0.417	0.913
	6	3.304	0.471	0.791	0.132	4.606	0.9693	0.595	0.713	1.06
								0.281	0.418	0.858
								0.157	0.257	0.803
	11	1.844	1.295	2.122	0.451	7.132	0.9724	0.797	0.502	0.872
								0.565	0.380	0.791
	11	3.986	0.717	1.285	0.204	8.794	0.9736	0.461	0.535	0.917
								0.295	0.434	1.02
								0.209	0.350	1.02
	21	1.880	2.422	3.783	1.086	13.709	0.9450	1.510	0.590	0.840
								1.086	0.420	0.648
								0.795	0.305	0.560
740	6	2.036	0.669	1.123	0.184	4.024	0.9269	0.832	0.812	1.96
								0.416	0.633	2.07
								0.274	0.428	1.59
	6	3.389	0.463	0.776	0.128	4.633	0.9538	0.532	0.881	2.38
								0.287	0.720	2.26
								0.143	0.469	1.93
	11	1.894	1.272	2.087	0.442	7.199	0.9227	0.781	0.712	1.94
								0.560	0.634	2.07
	21	1.900	2.405	3.757	1.079	13.759	0.9260	1.570	0.827	2.08
								1.113	0.725	1.88
								0.779	0.529	1.37
780	6	2.099	0.655	1.100	0.181	4.064	0.9056	0.818	0.890	4.21
								0.394	0.783	3.87
								0.260	0.600	2.94
	6	3.329	0.469	0.788	0.129	4.614	0.9406	0.496	0.940	3.49
								0.292	0.821	3.53
								0.159	0.635	3.29
	11	1.936	1.254	2.055	0.436	7.255	0.9003	0.762	0.819	3.44
								0.563	0.769	3.54
	11	3.831	0.740	1.327	0.210	8.723	0.9488	0.476	0.880	3.22
								0.281	0.731	2.94
								0.206	0.610	2.69
	21	1.911	2.379	3.895	0.940	13.786	0.9005	1.530	0.866	3.27
								1.048	0.836	3.74
								0.767	0.770	3.58
820	6	2.120	0.651	1.093	0.179	4.077	0.8803	0.825	0.854	3.29
								0.381	0.825	5.54
								0.260	0.745	5.21

TABLE 1 (Cont'd)

Temperature T (°K)	Pressure P (atmos, abs.)	steam:gas ratio	Steam—gas mixture				Equilibrium conversion α'	Contact time τ (sec)	Conversion α	Rate constant k_1 (sec^{-1})
			p^0_{CO}	$p^0_{H_2}$	$p^0_{N_2+CH_4}$	$p^0_{H_2O}$				
820	6	3.408	0.461	0.773	0.127	4.639	0.9199	0.493	0.912	4.67
								0.294	0.892	5.36
								0.149	0.765	5.98
	11	1.868	1.266	2.170	0.400	7.164	0.8661	0.751	0.841	5.45
								0.554	0.812	5.61
	11	3.799	0.743	1.332	0.217	8.708	0.9327	0.447	0.893	4.48
								0.269	0.875	6.39
								0.202	0.745	4.55
	21	1.930	2.364	3.871	0.932	13.833	0.8740	1.454	0.862	4.96
								0.998	0.850	6.03
								0.735	0.840	7.24
700	1	1.688	0.134	0.224	0.014	0.628	0.9288	0.549	0.809	1.48
								0.274	0.658	1.58

at $\tau = 0$ (atmos); p'_{CO} is the equilibrium partial pressure of carbon monoxide; $u = \frac{p^0_{H_2}}{p^0_{CO}}$; $s = \frac{p^0_{H_2O}}{p^0_{CO}}$; $\alpha = \frac{p^0_{CO} - p'_{CO}}{p^0_{CO}}$ is the degree of conversion; $\alpha' = \frac{p^0_{CO} - p'_{CO}}{p^0_{CO}}$ is the equilibrium degree of conversion.

The rate constants calculated from Equation (8) are given in Table 1. As the values are satisfactorily constant, it follows that Equation (7) satisfactorily describes the conversion of carbon monoxide by steam at increased pressures.

Analysis of Equation (7) makes it possible to determine the effect of pressure on the reaction rate.

By means of transformations leading to calculation of the rate constant, Equation (7) can be put into the form

$$\frac{d\alpha}{d\tau} = k_1 p_{CO}^{0-0.5} (\alpha' - \alpha)(s - \alpha)^{0.5} (u + \alpha)^{-1}. \quad (9)$$

For the process under normal pressure $p^0_{CO} = \frac{\%\,CO}{100(R+1)}$, and at higher pressures $p^0_{CO} = \frac{\%CO \cdot P}{100(R+1)}$, where % CO is the amount of carbon monoxide in the dry converted gas.

It follows that

$$w = \frac{d\alpha}{d\tau} = k_1 \left[\frac{\%\,CO \cdot P}{100(R+1)} \right]^{-0.5} (\alpha' - \alpha)(s - \alpha)^{0.5} (u + \alpha)^{-1}; \quad (10)$$

$$w = w_0 \frac{1}{\sqrt{P}}, \quad (11)$$

where w_0 is the reaction rate at P = 1 atmos, and w is the reaction rate at a higher pressure P (in atmos).

It follows from Equation (11) that the reaction rate is inversely proportional to the square root of the pressure.

TABLE 2

Temperature T (°K)	Pressure P (atmos)	Steam–gas mixture p^0_{CO}	$p^0_{H_2}$	$p^0_{N_2+CH_4}$	$p^0_{H_2O}$	Steam–gas ratio R	V (R + 1)	CO_l	$k_{e,p}$	$\frac{k_{e,P}}{k_{e,1}}$
700	1	0.134	0.224	0.014	0.628	1.688	1145	0.871	1110	1.00
							2280	0.708		
	6	0.676	1.136	0.186	4.002	1.974	4450	0.715	2330	2.09
							8820	0.441		
	11	1.295	2.122	0.451	7.132	1.844	8600	0.516	2660	2.39
							12130	0.391		
	21	2.422	3.783	1.086	13.709	1.880	8670	0.624	3570	3.21
							12050	0.444		
							16460	0.323		

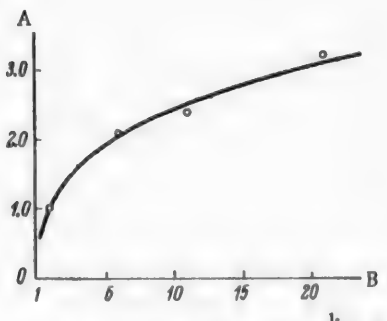

Fig. 2. Variation of the ratio $\frac{k_{e,p}}{k_{e,1}}$ with pressure: A) values of $\frac{k_{e,p}}{k_{e,1}}$, B) pressure (atmos).

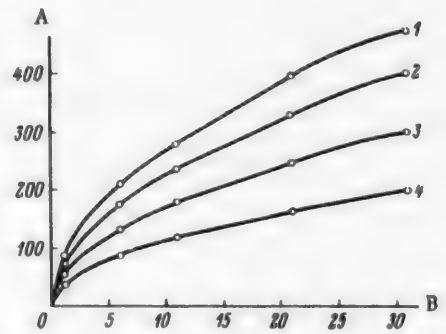

Fig. 3. Effect of pressure on catalyst productivity at various degrees of conversion: A) productivity Z, B) pressure (atmos); 1) α = 0.95, 2) α = 0.80, 3) α = 0.60, 4) α = 0.4.

The productivity of the catalyst, expressed as the product of the space velocity of the steam–gas mixture, the fraction of carbon monoxide in the mixture, and the degree of conversion, is

$$Z = V_{cm} \cdot \frac{\%\,CO}{100\,(R+1)} \cdot \alpha. \tag{12}$$

Putting $V_{cm} = \frac{273\,\mu \cdot 3600 \cdot P}{\tau \cdot T}$, we have

$$Z = \frac{273 \cdot \mu \cdot 3600 \cdot P}{\tau \cdot T} \times \frac{\%\,CO}{100\,(R+1)} \cdot \alpha. \tag{13}$$

Equating values of τ from Equations (13) and (8), we have

$$Z = \frac{273 \cdot \mu \cdot 3600 \cdot P \cdot k_1 \cdot \alpha}{T\left[\frac{u+\alpha'}{\sqrt{s-\alpha'}} \ln \frac{(\sqrt{s-\alpha}+\sqrt{s-\alpha'})(\sqrt{s}-\sqrt{s-\alpha'})}{(\sqrt{s-\alpha}-\sqrt{s-\alpha'})(\sqrt{s}+\sqrt{s-\alpha'})} - 2(\sqrt{s}-\sqrt{s-\alpha})\right]} \times \sqrt{\frac{\%\,\mathrm{CO} \cdot P}{(1+R)\,100}}. \quad (14)$$

Under constant conditions (equal gas composition, steam–gas ratio, reaction temperature, and degree of conversion) all the terms except the pressure are constant, and Equation (14) becomes

$$Z = Z_0 \sqrt{P}. \quad (15)$$

When P = 1 atmos, $Z = Z_0$, where Z_0 is the productivity at atmospheric pressure. It follows that the productivity per unit of catalyst is directly proportional to the square root of the total pressure.

This relationship is shown graphically in Fig. 3, from which it follows that the productivity is increased sharply if the pressure is raised to 5-10 atmos. At higher pressures, the productivity rises almost uniformly. It may be concluded on technical and economic grounds [5] that increase of pressure above 30 atmos is of little advantage.

It follows from Table 2 that the effects of pressure are the same with high-temperature and low-temperature catalysts.

SUMMARY

The conversion of carbon monoxide by steam was studied with the use of water gas and an industrial catalyst at elevated pressures (5, 10, and 20 atmos), and it was found that the rate of conversion of carbon monoxide is satisfactorily represented by the equation

$$-\frac{dp_{CO}}{d\tau} = k_1 \frac{p_{CO} - p'_{CO}}{p_{H_2}} \sqrt{p_{H_2O}}.$$

The experimental results are in agreement with available literature data on the activity of other catalysts.

LITERATURE CITED

[1] N. V. Kul'kova and M. I. Temkin, J. Phys. Chem. 23, 695 (1939).

[2] I. P. Kirillov, Trans. Ivanovo Inst. Chemical Technology 5, 46 (1950).

[3] K. Atwood, M. R. Arnold and E. G. Appel, Ind. Eng. chem. 42, 1601 (1950).

[4] C. Padovani, and A. Lotteri, J. Soc. Chem. Ind. 56, 391 (1937).

[5] G. Natta, and R. Rigamonti, Chim. Ind. (It.) 18, 623 (1936).

[6] B. Bibr, Candidate's Dissertation [in Russian] (Khar'kov, 1957).

Received January 6, 1958.

EFFECT OF THE HEIGHT OF THE FOAM LAYER ON A SIEVE PLATE ON ABSORPTION OF CARBON DIOXIDE BY ALKALI SOLUTION

M. E. Pozin, B. A. Kopylev, and E. Ya. Tarat

The Lensoviet Technological Institute, Leningrad

The hydrodynamic conditions in a gas–liquid system on a sieve plate (grid) of an absorber are determined by the linear velocities of the gas and liquid, the amount of liquid on the plate, the grid design (hole diameter, open section, etc.), and the physical properties of the components of the system. The hydrodynamic conditions, in turn, determine the turbulence of the streams and consequently the rates of heat and mass transfer.

In this paper we consider the hydrodynamic regime under which the layer of liquid on the plate is completely converted to foam when the gas passes through it (the foam regime).

It is generally considered [1] that the foam height H and the hydraulic resistance ΔP of the foam layer on the grid characterize the hydrodynamic operating conditions.

The dependence of H and ΔP on a number of determining factors – gas velocity $\underline{w}$, liquid rate $\underline{i}$, height of the overflow weir h_b, density of the liquid γ_L, and viscosity μ, was studied in earlier investigations [2-5]. The influence of H on the rates of heat transfer and mass transfer in different gas–liquid systems was determined [2,6,7], mainly for easily soluble gases. Below are given values of H and ΔP when air containing different amounts of CO_2 is passed through NaOH solution, and these values are correlated with the rate of absorption of CO_2.

EXPERIMENTAL*

Experimental procedure. Experiments on absorption of carbon dioxide by caustic soda solution under the foam regime were performed in an apparatus (Fig. 1) consisting of a glass column of d = 36 mm, separated into two parts by a horizontal vinyl resin grid. The perforated part of the grid was equal to the cross section of the apparatus, 0.001 m^2. The grid had holes 2 mm in diameter with their centers 5 mm apart; this corresponds to an open section S_0 = 17%. The section above the grid had four overflow compartments for removal of foam. During an experiment, one of the compartments was connected to a vessel for foam breaking, while the others were plugged with corks. In this manner the height of the overlow weir h_b could be varied; by such variations, and by supply of different amounts of liquid into the column (variations of flow rate $\underline{i}$) it was possible to vary the foam height $\underline{H}$ between 100 and 400 mm at a given gas velocity (w) in the apparatus. The flow rate was calculated relative to the diameter of the overflow compartment, and expressed in $m^3/m \cdot$ hour. With overflow compartments 20 mm in diameter a liquid feed rate Q = 20 liters per hour corresponds to a flow rate i = 1 $m^3/m \cdot$ hour. This apparatus was coupled with a laboratory unit, described earlier [8], for carbonation of soda solutions, additionally fitted with heaters for the gas and caustic soda solution. Carbon dioxide was absorbed in 3 N NaOH solution containing on the average 6% CO_2 (by volume), at gas and liquid temperatures of ~ 60°.

The analytical methods used were the same as in the previous investigation [8].

*L. Ya. Tereshchenko and P. M. Karaseva took part in the experimental work.

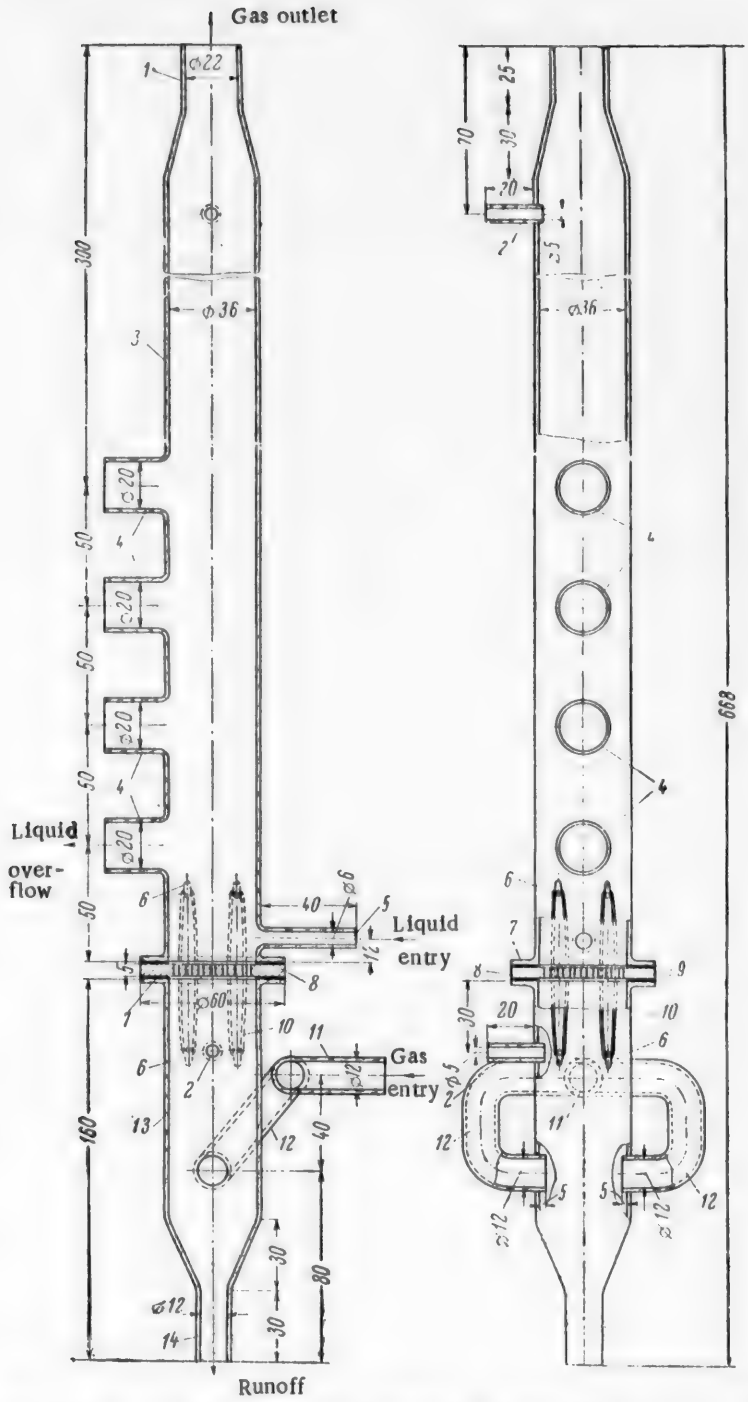

Fig. 1. Laboratory model of foam absorber with weirs of different heights: 1) gas outlet, 2) branch for pressure measurement, 3) column above grid, 4) overflow compartments, 5) liquid inlet, 6) stop catches, 7) flange, 8) grid, 9) gasket, 10) rubber tightening, 11) gas entry, 12) gas inlet tube, 13) column below grid, 14) runoff tube.

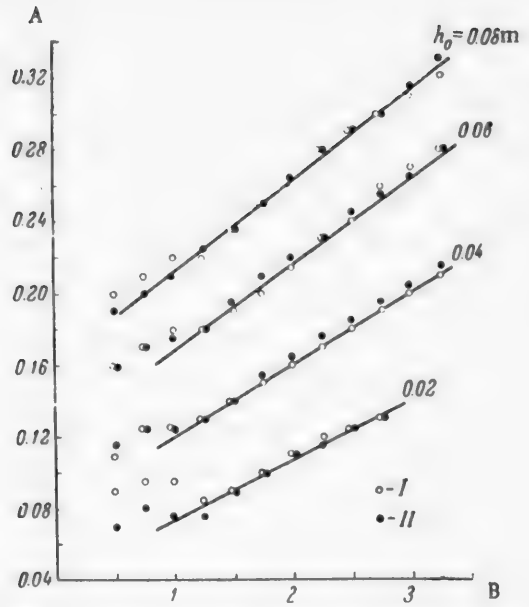

Fig. 2. Foaming in the system air–water at 18°: A) foam height H (m), B) gas velocity $\underline{w}$ in full section of the apparatus (m/second); continuous lines represent calculated values; I) experimental data for standard model, 5/2 grid (S_0 = 12.8%); II) experimental data for model of d = 36 mm, 5/2 grid (S_0 = 17.0%).

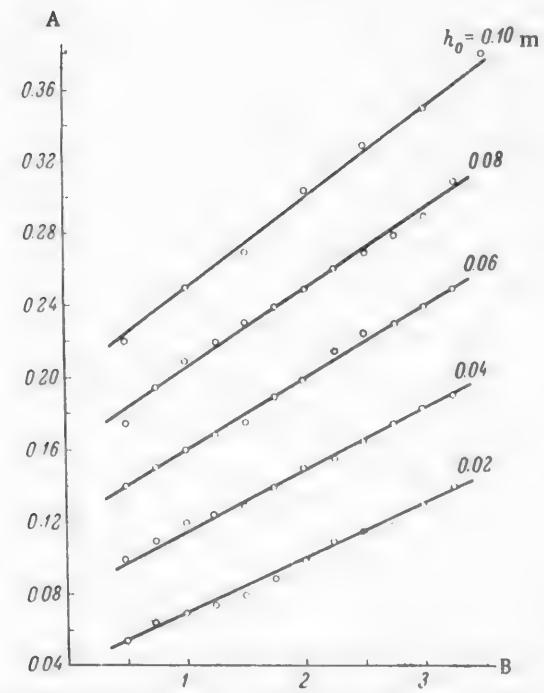

Fig. 3. Foaming in the system air–3 N NaOH solution at 60° with 5/2 grid: A) foam height H (m), B) gas velocity $\underline{w}$ in full section of the apparatus (m/second).

In measurements of the foam height H, spray above the upper level of the gas–liquid system was not taken into account. The values of ΔP were calculated by subtraction of the resistance of the dry grid from the total hydraulic resistance of the tray in the apparatus.

In analysis of the experimental results, average values for several duplicate experiments were calculated. The characteristics of CO_2 absorption – the absorption coefficient K per 1 m^2 of grid, and the efficiency η of a single tray – were calculated from analytical data for the gas phase by means of the formulas given earlier [9]. In calculations of K, it was assumed that the equilibrium CO_2 pressure over NaOH solution is zero.

EXPERIMENTAL RESULTS

It was found in preliminary experiments that the foaming conditions in the small apparatus used are the same as in the standard model 75 cm^2 in cross section (Fig. 2) [2], and that variation of the CO_2 concentration in the gas from 0 to 15% has no influence on foaming.

Foaming of NaOH solution was studied with air passed through 3 N NaOH solution at temperatures from 18 to 80°. The gas velocity $\underline{w}$ was varied from 0.5 to 3.5 m/second, and the height h_0 of the original liquid layer from 20 to 100 mm.

Foaming in NaOH solution. It follows from Fig. 3 that variations of foam height H with $\underline{w}$ at different values of h_0 are represented by a group of straight lines corresponding to the equation

$$H = 0.25\, w\,(h_0 + 0.1) + 2h_0.$$

It may be noted that the applicability ranges of Equation (1) were fairly wide, namely: for $\underline{w}$ between 0.5 and 3.5 m/second, and for h_0 between 0.02 and 0.1 m. H increases slightly with increase of temperature (Fig. 4).

It follows from Fig. 5 that at constant gas velocity the hydraulic resistance of the foam layer is proportional to its height, which varies with h_0. The straight lines in Fig. 5 are parallel. The higher the gas velocity in the apparatus, the less is the density and hydraulic resistance of the foam, because at a higher gas velocity a foam layer of given height is formed from a smaller amount of liquid (at smaller h_0) than at a lower gas velocity. Therefore the higher the linear gas velocity, the lower do the ΔP–H curves lie.

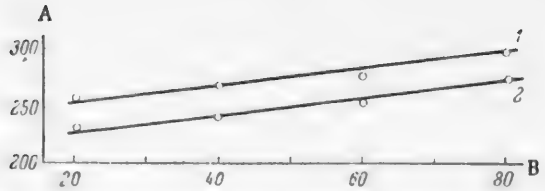

Fig. 4. Effect of temperature on foam height with 5/2 grid, w = 2.0 m/second, i = 5 m^3/m·hour, h_b = 100 mm; A) foam height H (mm), B) temperature (°C); concentration of NaOH solution (g-equiv/liter): 1) 1.0, 2) 3.0.

The generalized empirical equation for calculation of ΔP in the system under consideration is of the form

$$\Delta P = 400H - 20w + 30 \ (mmH_2O) \qquad (2)$$

Effects of foam height on the absorption coefficient and tray efficiency. It is known [1,2] that the height H of the foam layer on the grid is one of the basic characteristics of the foam regime determining the coefficient of absorption and the extent of the absorption process, i.e., tray efficiency.

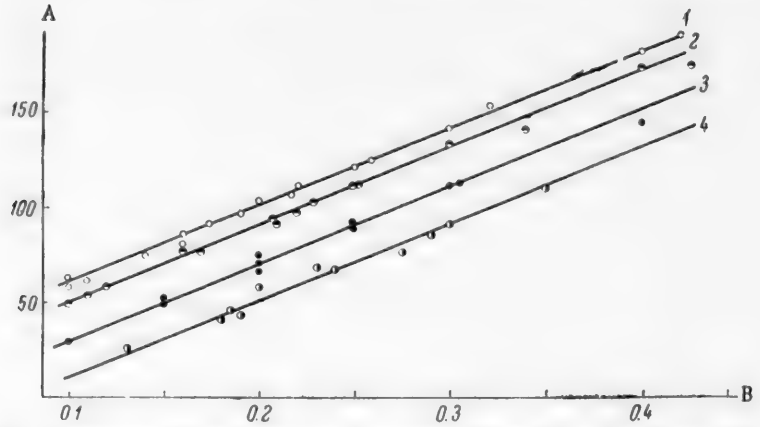

Fig. 5. Variation of the hydraulic resistance of foam with foam height at 60°, 5/2 grid, 3 N NaOH solution: A) foam resistance ΔP (mm H_2O), B) foam height H (m); gas velocity w in apparatus (in m/second): 1) 0.5, 2) 1.0, 3) 2.0, 4) 3.0.

Fig. 6 represents variations of the absorption coefficient K per 1 m^2 of grid (tray) area with H at different values of w. Variations of H at constant w were effected by variations of the weir height and the amount of liquid fed into the apparatus. It is clear from Fig. 6 that the coefficient of absorption of CO_2 by NaOH solution at a given gas velocity is proportional to the foam height in the range of foam heights studied. The equation for calculation of K in terms of H and w is of the form:

$$K = 200w(H + 2) + 2400H. \qquad (3)$$

Some indication of the turbulence of the foam layer may be given by its hydraulic resistance ΔP. This value in its turn, may serve as a tentative criterion of the rate of operation of the equipment.

In Fig. 7, K is plotted against ΔP (at different heights of the foam layer on the grid). The relationship is represented by straight lines for different values of w, such that

$$K = 6.75\Delta P + 580w - 260. \qquad (4)$$

This shows that the absorption rate (analogously to the rate of heat transfer) in the foam apparatus is proportional to the energy expended in foaming of the system.

To derive an equation for the efficiency of absorption of the CO_2 by alkali solution as a function of the foam height, we use the expression [9]

$$\eta = \frac{2K}{2v + K}, \qquad (5)$$

where v is the flow rate of an inert (unabsorbed) gas (in m/hour).

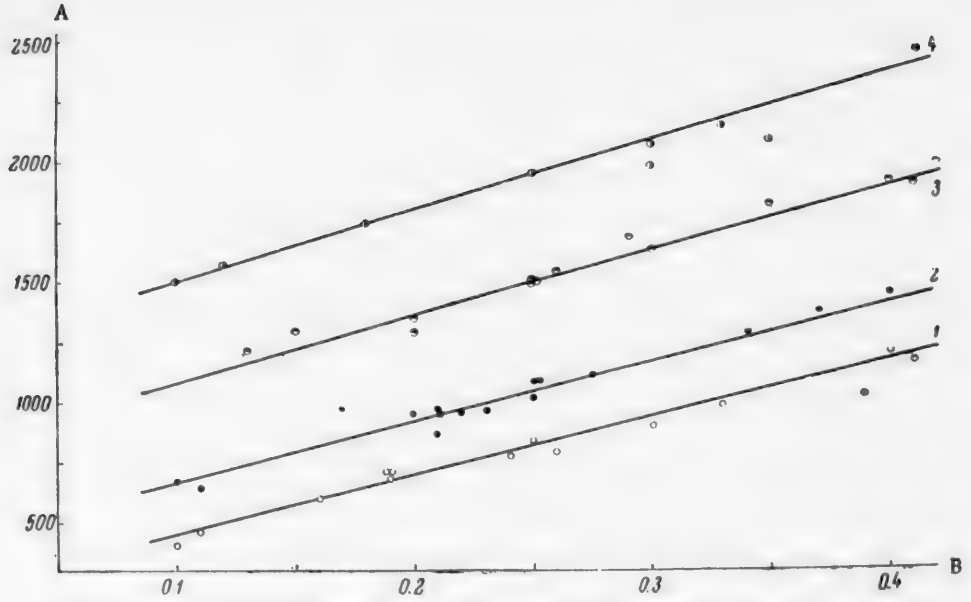

Fig. 6. Effect of foam height on the coefficient of absorption of carbon dioxide at 60°, 5/2 grid, 3 N NaOH solution, 6% CO_2 in gas: A) absorption coefficient K (in kg/m^2 · hour · kg/m^3), B) foam height H (in m); gas velocity w in apparatus (in m/second): 1) 0.5, 2) 1.0, 3) 2.0, 4) 3.0.

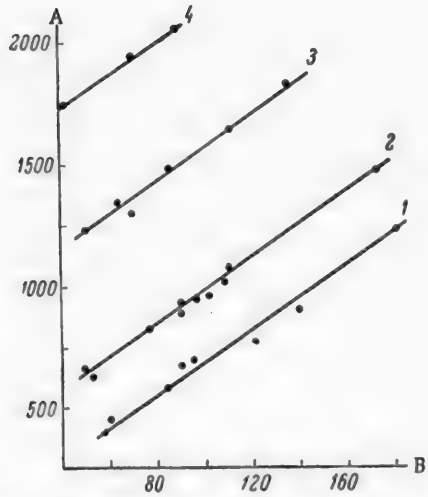

Fig. 7. Variation of the coefficient of absorption of carbon dioxide with the hydraulic resistance of the foam at 60°, 3 N NaOH solution, 6% CO_2 in gas: A) absorption coefficient K (in kg/m^2 · hour · kg/m^3), B) foam resistance ΔP (in mm H_2O); gas velocity w, in apparatus (in m/second): 1) 0.5, 2) 1.0, 3) 2.0, 4) 3.0.

For a gas containing 6% CO_2,

$$v = 3600w\,(1 - 0.06) \approx 3400w, \tag{6}$$

and hence

$$\eta = \frac{2K}{6800w + K}. \tag{7}$$

Substituting the value of K from Equation (3) into Equation (7) we have

$$\eta = 2\,\frac{12H + w\,(H + 2)}{12H + w\,(H + 36)}. \tag{8}$$

Fig. 8 shows variations of η with H, calculated from Equation (8), for different gas velocities in the apparatus. The experimental data (points on the curves) fit satisfactorily on the calculated lines.

Equation (3) is empirical and therefore, like Equation (8), it is applicable only to conditions analogous to those described above.

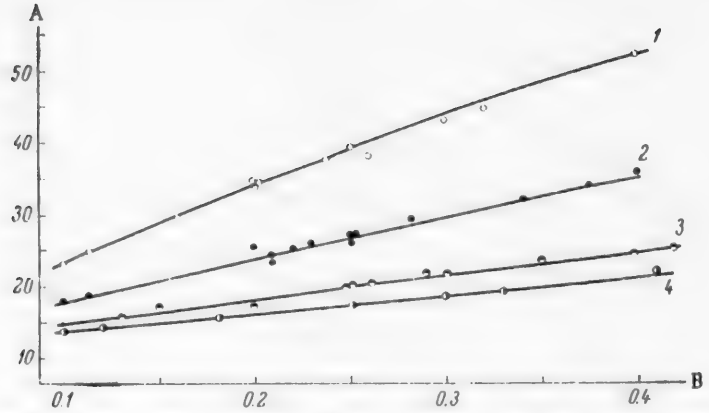

Fig. 8. Variation of the degree of absorption (efficiency) of carbon dioxide with foam height at 60°, 3 N NaOH solution, 6% CO_2 in gas: A) degree of absorption (efficiency) η (%), B) foam height H (m); gas velocity $\underline{w}$ in apparatus (in m/second): 1) 0.5, 2) 1.0, 3) 2.0, 4) 3.0.

SUMMARY

1. The efficiency of a single tray of a foam apparatus in absorption of carbon dioxide by 3 N alkali solution at 60° is in the range of 0.15-0.5 for gas velocities from 0.5 to 3 m/second.

2. The coefficient of absorption of carbon dioxide is between 500 and 2500, in accordance with the gas velocity and the amount of liquid supplied to the grid.

3. Under the experimental conditions used (3 N NaOH solution, 6% CO_2 in the gas, temperature 60°) the coefficient of absorption of carbon dioxide varies in proportion to the foam height, which varies at a given linear gas velocity with the amount of liquid on the grid tray (of the apparatus).

4. The foam regime is very effective in absorption of carbon dioxide from gases by caustic soda solutions; it ensures a high rate of the process, which can therefore be carried out in an absorber of small dimensions.

LITERATURE CITED

[1] M. E. Pozin, I. P. Mukhlenov, and É. Ya. Tarat, J. Appl. Chem. 30, No. 1, 45 (1957).*

[2] M. E. Pozin, I. P. Mukhlenov, E. S. Tumarkina, and É. Ya. Tarat, The Foam Method for Treatment of Gases and Liquids [in Russian] (Goskhimizdat, 1955).

[3] M. E. Pozin, I. P. Mukhlenov, E. S. Tumarkina, and É. Ya. Tarat, J. Appl Chem. 27, No. 1, 13 (1954).*

[4] M. E. Pozin and I. P. Mukhlenov, Proc. Acad. Sci. USSR, new series, 2, No. 2, 393 (1953).

[5] M. E. Pozin and E. S. Tumarkina, J. Appl. Chem. 27, No. 11, 1170, 1180 (1954).*

[6] M. E. Pozin I. P. Mukhlenov, and É. Ya. Tarat, J. Appl. Chem. 30, No. 2, 393 (1953).*

[7] M. E. Pozin and É. Ya. Tarat, J. Appl. Chem. 31, No. 9, 1332 (1958).*

[8] M. E. Pozin, B. A. Kopylev, and É. Ya. Tarat, J. Appl. Chem. 30, No. 5, 674 (1957).*

[9] M. E. Pozin, J. Appl. Chem. 25, No. 10, 1032 (1952).*

Received October 3, 1957.

*Original Russian pagination. See C. B. Translation.

ABSORPTION OF CARBON DIOXIDE BY CAUSTIC SODA SOLUTIONS UNDER FOAM CONDITIONS

M. E. Pozin, B. A. Kopylev, and É. A. Tarat

The Lensoviet Technological Institute, Leningrad

Caustic soda solutions are widely used in deep-cooling units in the production of synthetic ammonia for final purification of the gas, and in many other cases when a high degree of removal of carbon dioxide from gases is required.

This process is effected in cumbersome packed towers or bubbling absorbers.

Available data on the absorption of carbon dioxide by 3 N NaOH solution at 60° [1], and also on the absorption of various other gases [2-7], show that absorption of carbon dioxide by alkali solution proceeds much more rapidly under foam conditions than in scrubbers or bubbling absorbers. It was desired in this connection to determine the optimum process conditions for the foam regime. The chemistry and mechanism of this process, and its rate under different conditions, have not been studied sufficiently as yet

The mechanism of the process depends on the conditions of CO_2 diffusion in the gas and liquid phases, diffusion of the reaction products from the surface into the bulk of the liquid, and diffusion of hydroxyl ions toward the reaction zone [8].

The carbonate formed differs from sodium hydroxide in solubility in water, rate of interaction with CO_2, diffusion rate, etc. The poor solubility of CO_2 in the surface (carbonate) liquid hinders diffusion of the absorbed component from the gas phase.

The available literature data on the rate of absorption of CO_2 by NaOH solutions [8-14] refer to different conditions; the results obtained are contradictory and different explanations are offered for the mechanism of the process. Such data cannot be used for selection of the optimum conditions, such as temperature and solution concentration, for the process in the foam apparatus.

The purpose of this work was to study the rate of absorption of CO_2 by NaOH solutions under foam conditions in relation to physicochemical and hydrodynamic conditions—concentrations of CO_2 in the gas phase and NaOH in solution, temperature, linear gas velocity, liquid flow rate, etc.

The experimental results are presented below; they characterize the rate and degree of absorption of carbon dioxide by caustic soda solutions in the foam apparatus under various conditions.

EXPERIMENTAL RESULTS

The results given below were obtained in the absorption of carbon dioxide by caustic soda solutions in a model foam apparatus described earlier [1].

Fig. 1 represents variations of the absorption coefficient K calculated per 1 m^2 of grid (tray) area *, and of the efficiency η of a single tray, with the initial concentration C_{in} of CO_2 in the gas. Methods for calculation

*The experimental conditions in this and subsequent cases are given in the figure captions.

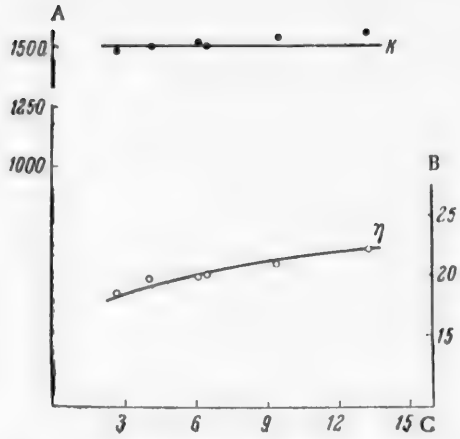

Fig. 1. Effects of carbon dioxide concentration in the gas on K and η: A) absorption coefficient K (in kg /m^2· hour · kg/ m^3), B) degree of absorption (efficiency) η (%), C) initial concentration C_{in} of CO_2 in the gas (vol. %); 5/2 grid; gas velocity w = 2.0 m/second, liquid rate i = 5 m^3/m · hour, weir height h_b = 100 mm, 3 N NaOH solution, t = 60°.

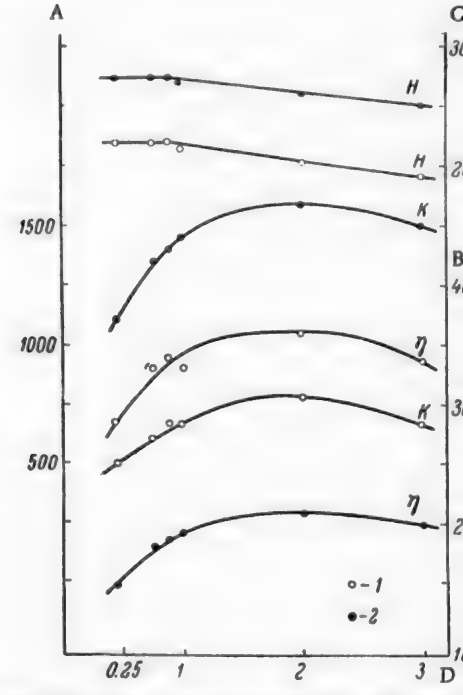

Fig. 2. Effects of concentration of the caustic soda solution on K, η, and H: A) absorption coefficient K (in kg / m^2 ·hour · kg/m^3), B) degree of absorption (efficiency) η (%), C) foam height H (mm), D) concentration of NaOH solution (in g-equiv/ liter); gas velocity $\underline{w}$ in apparatus (m/second): 1) 0.5; 2) 2.0; 5/2 grid, i = 5 m^3/m · hour, h_b = 100 mm, C_{in} = 6%, t = 60°.

of K and η have been described previously [1-7]. It may be seen that under otherwise constant conditions K is almost independent of C_{in} in the range of 2 to 15%. This shows that the absorption rate is determined in this instance by the resistance of the gas phase. The values of η increase somewhat with increase of C_{in}, as η increases with decrease of $\underline{w}$.

Variations of the absorption characteristics of carbon dioxide in the foam apparatus with the NaOH content in solution are plotted in Fig. 2. It is seen that the coefficient of absorption and degree of absorption of CO_2 (efficiency) increase with increase of NaOH concentration from 0.25 N to 2 N. This is because, at relatively low NaOH concentration from 0.25 N to 2 N. This is because, at relatively low NaOH concentrations in solution, the driving force of the process is determined by diffusion conditions in the liquid as well as in the gas phase. It must be noted that K and η increase in this concentration range, despite the fact that the foam height diminishes somewhat (under otherwise equal conditions) with increase of NaOH concentration owing to changes in the physical properties of the solutions – increases of density, viscosity, and surface tension.

The curves for K as a function of NaOH concentration follow this course at all gas velocities studied (0.5-2 m/second); this is in good agreement with literature data on absorption of CO_2 in packed towers [13].

The effect of the degree of carbonation of NaOH solution on the absorption of CO_2 is shown in Fig. 3. At up to 25% carbonation of the solution, K and η decrease slightly, while at higher degrees of carbonation these values fall sharply. The deterioration of absorption with increasing carbonation of the solution is due to the decrease of the chemical capacity of the solution and also to increase of the diffusion resistance in the liquid phase owing to the appearance in the liquid phase of a carbonate layer, in which CO_2 is considerably less soluble than in the main bulk of NaOH. This is confirmed by the results of experiments on absorption of CO_2 by solutions containing equal amounts of NaOH and different amounts of Na_2CO_3 (Fig. 4).

It follows from Fig. 3 that, after the degree of bicarbonation of the soda liquor has reached 20-25%, absorption of CO_2 improves, probably because of precipitation of bicarbonate and increased solubility of carbon dioxide in the system [4].

Variations of K and η with temperature are plotted in Fig. 5. Absorption of CO_2 improves with increase of temperature from 20 to 45-50°. This is

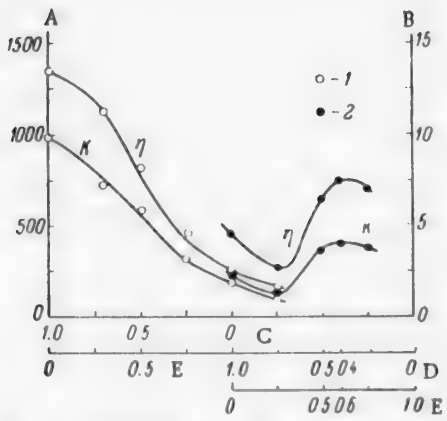

Fig. 3. Variations of K and η with the degree of carbonation of the solution: A) absorption coefficient K (in kg/m^2 · hour · kg/m^3), B) degree of absorption (efficiency) η (%), C) NaOH content of solution (in g-equiv/liter), D) Na_2CO_3 content of solution (in g-equiv/liter), E) $NaHCO_3$ content of solution (in g-equiv/liter); initial concentration C_{in} of CO_2 in gas (vol.%): 1) 6, 2) 30; 5/2 grid, w = 2.0 m/second, i = 5 m^3/m · hour, h_b = 100 mm, t = 18°.

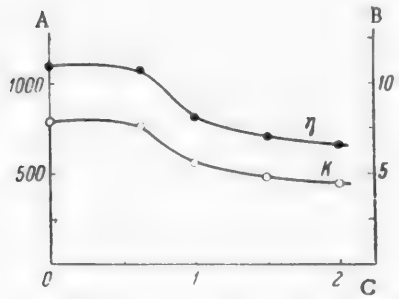

Fig. 4. Variations of K and η with the amount of Na_2CO_3 present in the NaOH solution: A) absorption coefficient K (in kg/m^2 · hour · kg/m^3), B) degree of absorption (efficiency) η (%), C) Na_2CO_3 content of NaOH solution (in g-equiv/liter); 5/2 grid, w = 2.0 m/second, H = 220 mm, 3 N NaOH solution, C_{in} = 6%, t = 18°.

because of the favorable influence of temperature on the rates of chemical reactions and somewhat improved foaming conditions. On further increase of temperature, K and η remain almost constant, and even begin to decrease a little at 70-80°. Thus, there are optimum temperatures (50-70°) for absorption of CO_2 by alkali at which the degree and rate of absorption are at their highest.

Fig. 6 shows variations of K and η with the liquid flow rate i calculated on the width of the overflow orifice of the tray (m^3/m · hour). The increases of K and η with increase of i are due to increase of the height H of the foam layer, which improves absorption characteristics.

The effects of linear gas velocity on K and η are more important and complex (Fig. 7). The height of the foam layer increases with w, and this leads to a corresponding increase of K. However, at w > 2.5-3 m/second the rate of increase of K diminishes somewhat. This is because of a considerable reduction in the time of phase contact, which is no longer balanced by an increase of the interfacial area, and a decrease of the efficiency [3]. Over a definite range of w (up to 2.5 m/second), fairly wide for practical purposes, the absorption coefficient increases symbatically with the height of the foam layer.

The data plotted in Fig. 7 were obtained at constant flow rate i and weir height h_b, i.e., at constant height h_0 of the initial liquid layer and variable foam height. From the theoretical viewpoint, in order to elucidate the physical influence of the gas velocity on absorption characteristics, it is of interest to study variations of K and η with w at constant foam height. These variations are plotted in Fig. 8 and 9; they were found by calculation from empirical relationships: K = f (H) and $\eta = \varphi(H)$ [1].

These results show that at a given foam height the absorption coefficient is proportional to the gas velocity in the apparatus (Fig. 8). This is to some extent a characteristic of the true dependence of K on w, since it is valid to assume that the influence of all other factors which also affect K and vary with the gas velocity is eliminated at constant H. It should be noted, however, that a constant value of H is achieved by variation of h_0 and therefore by variations of the structure of the gas–liquid system at different w.

The degree of absorption of CO_2 from the gas, or the tray efficiency η, decreases sharply with increase of w (Fig. 9), as the time of contact between the gas and liquid phases decreases at constant foam height (and approximately the same phase-contact area).

Investigations of the absorption of CO_2 by NaOH solution reveal the complexity of the mechanism of the process, and the dependence of its rate on the diffusion conditions in the gas and liquid phases, the rates of chemical reactions, contents of carbonate ions in solution, and temperature conditions.

The experimental results also show that the process (and therefore its separate stages) is considerably intensified when it is effected under high-turbulence foam conditions.

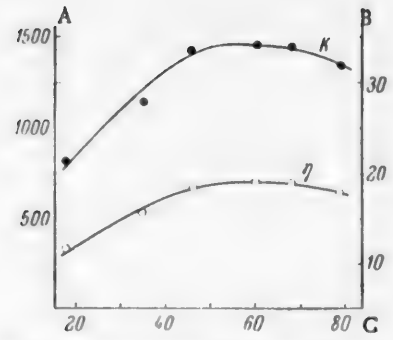

Fig. 5. Variations of K and η with temperature: A) absorption coefficient K (in kg/m^2 · hour · kg/m^3), B) degree of absorption (efficiency) η (%), C) temperature (°C); 5/2 grid, w = 2.0 m/second, i = 5 m^3/m · hour, h_b = 100 mm, 1 N NaOH solution, C_{in} = 6%

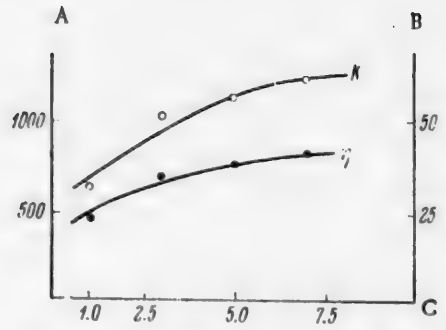

Fig. 6. Variations of K and η with the liquid flow rate: A) absorption coefficient K (in kg/m^2 · hour · kg/m^3), B) degree of absorption (efficiency) η (%), C) liquid flow rate $\underline{i}$ (m^3/m · hour); 5/2 grid, w = = 0.75 m/second, h_b = 200 mm, 1 N NaOH solution, C_{in} = 6%, t = 18°.

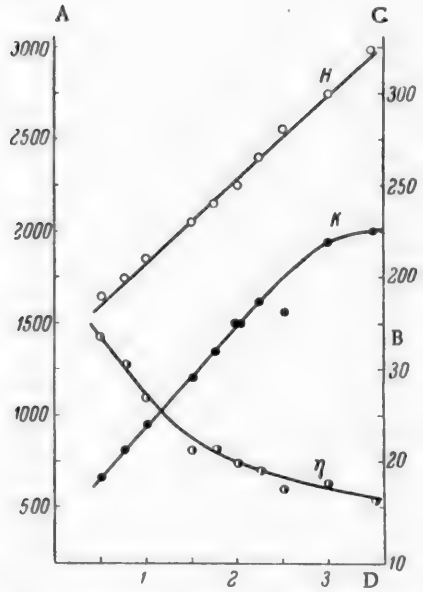

Fig. 7. Variations of K, η, and H with gas velocity in the full section of the apparatus: A) absorption coefficient K (in kg/m^2 · · hour · kg/m^3), B) degree of absorption (efficiency) η (%), C) foam height H(mm) D) gas velocity $\underline{w}$ in apparatus (m/second); 5/2 grid, i = 5 m^3/m · hour, h_b = 100 mm, 3 N NaOH solution, C_{in} = 6%, t = 60°.

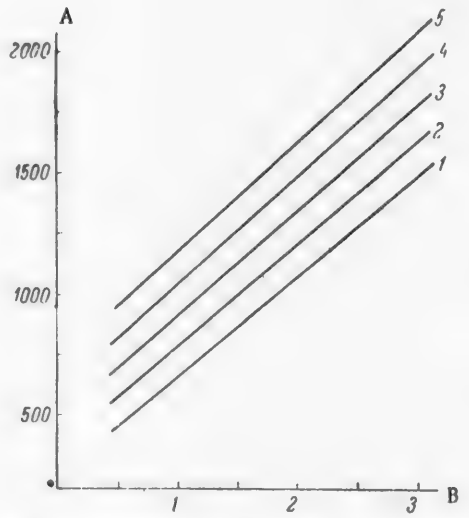

Fig. 8. Variation of the coefficient of absorption of carbon dioxide with the gas velocity in the full section of the apparatus (at constant foam height): A) absorption coefficient K (in kg/m^2 · hour · kg/m^3), B) gas velocity $\underline{w}$ in apparatus (m/second); foam height H (mm): 1) 100, 2) 150, 3) 200, 4) 250, 5) 300; 5/2 grid, 3 N NaOH solution, C_{in} = 6%, t = 60°.

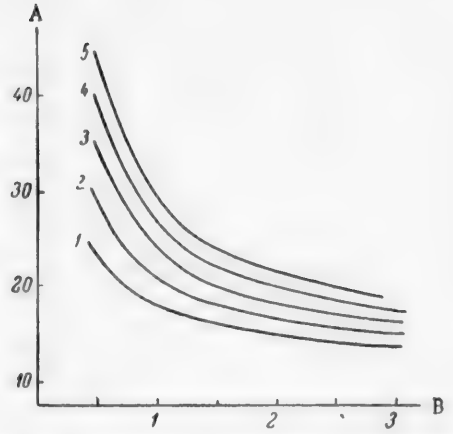

Fig. 9. Variation of the degree of absorption of carbon dioxide (efficiency) η with gas velocity in the full section of the apparatus at constant foam height: A) degree of absorption (efficiency) η (%), B) gas velocity $\underline{w}$ in apparatus (in m/second); foam height H (in mm): 1) 100, 2) 150, 3) 200, 4) 250, 5) 300; 5/2 grid, 3 N NaOH solution, C_{in} = = 6%, t = 60°.

According to available literature data [8, 13] the coefficient of absorption of CO_2 by NaOH solution in a packed tower operating under the normal film conditions does not exceed 1000-1250 kg/m^3 · hour · atmos.

At a linear gas velocity of 2-2.5 m/second in the full section of the foam apparatus, the absorption coefficient (with the intertray distance of 0.5 m taken into account) is 4-5 times that in packed scrubbers operated at full capacity.

SUMMARY

1. The effects of gas velocity, CO_2 concentration in the gas, NaOH concentration in solution, degree of carbonation of the alkaline solution, and temperature on the extent and rate of absorption of carbon dioxide by caustic soda under foam conditions have been studied.

2. The coefficient of absorption K of carbon dioxide by 3 N NaOH solution at 60° is almost independent of the CO_2 concentration in the gas between 2 and 15%.

3. The values of K and efficiency η as functions of the NaOH concentration in solution reach a maximum at approximately 2 N NaOH.

4. The values of K and η fall sharply with increasing carbonation of caustic soda; these values are approximately 4 times as high in the absorption of CO_2 by NaOH solution as in absorption by a completely carbonated solution. It was shown experimentally that the rate of absorption of carbon dioxide by caustic soda solution of constant NaOH concentration decreases with increase of the amount of Na_2CO_3 present in solution.

5. The variations of K and η with temperature are characterized by a maximum at 45-50°.

6. In the range of linear gas velocities from 0.5 to 3.5 m/second in the absorption of carbon dioxide by 3 N NaOH solution at 60°, K increases approximately from 700 to 2000 m/hour, while η decreases approximately from 34 to 16%.

7. These results can be used in the selection of optimum conditions for removal of carbon dioxide from various gases or for carbonation of alkaline solutions in the foam apparatus.

8. By use of the foam regime it is possible to accelerate the absorption of carbon dioxide by caustic soda solutions 4 to 5-fold in comparison with absorption in scrubbers working to full capacity.

LITERATURE CITED

[1] M. E. Pozin, B. A. Kopylev and É. Ya. Tarat, J. Appl. Chem. 32, No. 5, 1012 (1959).*

[2] M. E. Pozin, I. P. Mukhlenov, E. S. Tumarkina and É. Ya. Tarat, The Foam Method for Treatment of Gases and Liquids [in Russian] (Goskhimizdat, 1955).

[3] M. E. Pozin and B. A. Kopylev, J. Appl. Chem. 30, No. 3, 362 (1957).*

[4] M. E. Pozin, B. A. Kopylev and É. Ya. Tarat, J. Appl. Chem. 30, No. 5, 674 (1957).*

[5] M. E. Pozin, B. A. Kopylev and G. V. Bel'chenko, Trans. Lensoviet Technol. Inst. Leningrad, No. 36 (Goskhimizdat, 1956).

[6] M. E. Pozin, B. A. Kopylev and N. A. Petrova, J. Appl. Chem. 31, 849 (1958).*

*Original Russian pagination. See C. B. Translation.

[7] M. E. Pozin and É. Ya. Tarat, J. Appl. Chem. 31, 1332 (1958).*

[8] M. E. Pozin, J. Appl. Chem. 29, No. 10-11,12 (1946); 20, 3 (1947).

[9] J. W. Payne, B. F. Dodge, Ind. Eng. Ch. 24, 6, 630 (1932).

[10] S. Hatta, Techn. Reports Tohoku Imp. Univ. 8, 1 (1928).

[11] M. E. Pozin, J. Appl. Chem. 20, No. 4, 145 (1947).

[12] É. Ya. Turkhan, J. Appl. Chem. 21, No. 9, 927 (1948)

[13] J. B. Tepe, B. F. Dodge, Trans. Am. Inst. chem. Eng. 2, 255 (1943).

[14] M. Kh. Kishinevskii and M. A. Kerdivarenko, J. Appl. Chem. 24, No. 5, 42 (1951).*

Received October 3, 1957.

*Original Russian pagination. See C. B. Translation.

SURFACE RESISTANCE IN ABSORPTION PROCESSES

M. Kh. Kishinevskii and L. A. Mochalova

The State University, Kishinev

The absorption of gases by liquids consists of three stages: 1) transfer of substance from the gas volume to the interface; 2) transition of molecules of the absorbed gas from the gas phase to the liquid phase, or the dissolution stage; 3) transfer of substance from the interface into the liquid phase

In most papers dealing with analysis of the mechanism of absorption of gases by liquids it is assumed that the dissolution process at the interface – the second stage – proceeds at a considerably higher rate than the first and third stages, which determine the kinetics of the process as a whole. These assumptions are made, for example, in Whitman's two-film theory [1] and in our publications, with the consequent use of the Henry equation for determination of a quantitative relationship between the partial pressure of the absorbed gas and the concentration of the corresponding molecules in the liquid at the interface.

There must be at least some deviation from equilibrium at the interface to ensure a continuous flow of substance from the gas to the liquid phase. However, in the above-cited investigations this deviation is assumed to be so small that the Henry equation can be used without appreciable error. Some authors do not share this view. For example, Emmert and Pigford [2] consider it necessary to take surface resistance into account in analysis of absorption processes. In their opinion, the rate of transfer at the interface is given by the following expression:

$$q = \frac{1}{\sqrt{6\pi}}\left(A_G \bar{u}\alpha_1 - A_G^{*}\bar{u}\alpha_2\right), \tag{1}$$

where A is the concentration of the component in the gas phase (in $\frac{\text{kg-moles}}{\text{m}^3}$); $\bar{u}$ is the root mean square velocity of the gas molecules; α_1 is the accommodation coefficient for molecules penetrating from the gas to the liquid phase; A_G^{*} is the fictive concentration of the gas phase in equilibrium with the liquid concentration A_l at the interface; α_2 is the accommodation coefficient for molecules leaving the liquid phase.

When $\alpha_1 = \alpha_2 = \alpha$, the transfer equation assumes the form

$$q = \frac{\alpha \bar{u}}{\sqrt{6\pi}}\left(A_G - A_G^{*}\right). \tag{2}$$

In recent years a considerable number of papers have been published on the kinetics of absorption complicated by chemical reaction, and on the kinetics of simple absorption. Analysis of the available data shows that the concepts of the process kinetics based on two resistances – of the gas and liquid phases – are inadequate to account, from a single standpoint, for experimental data for different systems under a variety of hydrodynamic conditions. It is necessary to take into account the resistance associated with the dissolution process itself at the interface, i.e., the surface resistance. As is shown below, this does not involve a revision of the analysis of experimental data presented in our earlier papers and of our theory of diffusion from a free surface, which are merely supplemented by considerations of surface resistance.

The necessity to take surface resistance into account is demonstrated especially clearly by analysis of the experimental data of Pozin and Kopylev [3]. They studied, on a sieve plate, the influence of gas velocity on the coefficient of mass transfer for two systems: NH_3 – cuprammonium solution, and CO_2 – 1 N NaOH solution. In the

former case the height of the overflow weir was 10 mm, and in the second 200-240 mm, but despite this the coefficient of mass transfer per 1 m^2 of plate surface (in m/hour) was approximately one order of magnitude higher in the ammonia experiments than in the experiments with carbon dioxide. The authors classify the first system with absorption of readily soluble gases, and the second, with absorption of moderately soluble gases. In the former case the rate of the process is controlled by the resistance of the gas phase, and in the second, by the resistance of the liquid phase in addition to that of the gas phase.

However, it would be incorrect to explain in this way the large difference between the mass-transfer coefficients in the experiments with the two systems. In absorption of carbon dioxide from a gaseous mixture containing about 10% CO_2 by caustic soda solutions on a sieve plate, the liquid-phase resistance has no practical influence. This follows from the fact that the absorption rate does not change with increase of the caustic soda concentration above 1 N. Consequently, the low rates of absorption of CO_2 at these alkali concentrations cannot be attributed to resistance of the liquid phase. Evidently in the absorption of CO_2 at NaOH concentrations above 1 N, the rate of absorption is determined not by the resistances of the gas and liquid phases, but by surface resistance.

In analysis of the mechanism of absorption processes, surface resistance can be taken into account on the basis of more general although less formal considerations than those used by Emmert and Pigford. In particular, we do not think it is necessary to assume that the accommodation coefficients α_1 and α_2 are equal.

The rate of solution of the gas molecules at the interface is given by the equation

$$q = k_1 P_i - k_2 C_i, \tag{3}$$

where $k_1 P_i$ is the rate of the forward process and $k_2 C_i$ is the rate of the reverse process; P_i is the partial pressure (in atmos) of the absorbed gas at the interface; C_i is the concentration of the gas molecules in the liquid phase at the interface (in moles/liter).

By the Henry equation, the concentration C_i corresponds to a certain fictive partial pressure

$$C_i = HP_i^*. \tag{4}$$

Substitution of Equation (4) into Equation (3) gives

$$q = k_1 P_i - k_2 H P_i^*. \tag{5}$$

If a state close to equilibrium is established at the interface, for example as the result of retarded removal of the molecules from the surface into the volume, two relationships hold:

$$P_i \approx P_i^* \text{ and } k_1 P_i \approx k_2 H P^*.$$

It follows that

$$H = \frac{k_1}{k_2} \tag{6}$$

and the rate of the process is

$$q = k_1 (P_i - P_i^*). \tag{7}$$

An example of relatively rapid establishment of a state close to equilibrium is the solution of gas molecules in a liquid the surface of which is not renewed.

We shall now attempt, in the light of the foregoing considerations, to provide an explanation of the experimental data according to which the mass-transfer coefficient found from the limiting rate of absorption of CO_2 in NaOH solutions is considerably less than the coefficient found in experiments with ammonia or with humidification of the air.

The concentration of carbon dioxide C_i at the interface decreases with increase of the caustic soda concentration, and P_i^* decreases in accordance with Equation (4). There is also some decrease of P_i, but the

difference $P_i - P_i^*$ increases as the rate of absorption (Equation (7)) becomes higher. Since on further increase of NaOH concentration the limiting value of the absorption rate is ultimately reached, it is evident that P_i^* and the value of C_i corresponding to it approach zero.

In a series of papers [4, 5], for determination of the gas-phase transfer coefficient k_G we divided the limiting rate q_{lim} by the average partial pressure in the gas phase, P. In reality, as can now be seen, this method did not give k_G. In the general case this procedure corresponds to the expression

$$\frac{k_1 P_{i\,lim}}{P},$$

where $p_{i\,lim}$ is the partial pressure of the gas at the interface corresponding to the limiting rate.

It can be shown, however, that for the system CO_2 – aqueous NaOH solution the value of P_i is close to P, and therefore the above method gives a value close to the coefficient k_1.

The figure shows the dependence of the gas-phase transfer coefficient per 1 m^2 of plate area on the gas velocity in the full section of the column, based on the results of various workers. Some design details of the plates used in their investigations are given in the table.

It is seen that the mass-transfer coefficient found from data on air humidification is many times greater than the coefficient found from data on CO_2. Since the absorption rate may also be expressed in terms of mass flow through the gas phase

$$q = k_G(P - P_i), \tag{8}$$

it follows that the large difference between the rates for these systems under equal hydrodynamic conditions (equal k_G) and equal P (in the case of humidification, P is the water-vapor pressure) may be attributed to the low value of the driving force $P - P_i$ in the absorption of CO_2.

Design Details of Plates

Cross-sectional area of plate (m^2)	Number of openings	Diameter of openings (cm)	Distance between openings (cm)	Open section of plate (%)	Number of bubble caps	Diameter of bubble caps (cm)	Initial liquid level on plate (cm)	Level of overflow weir (cm)	Notes
$0.715 \cdot 10^{-2}$	83	0.318	—	—	—	—	1.27	—	Data of West, Gilbert, and Shimizu on air humidification [6]
			—	—	—	—	2.54	—	
			—	—	—	—	5.08	—	
0.067	—	—	—	—	13	3.8	9.15	—	Data of Gerster, Colburn, Bonnet, and Carmody on air humidification [7].
$2.28 \cdot 10^{-2}$	—	0.6	—	6.07	—	—	—	2.5	Data of Kuz'minykh, Aksel'rod, Koval', and Rodionov on air humidification [8].
	—	0.3	—						
	—	0.9	—						
—	—	0.2	0.5	—	—	—	—	1.0	Data of Pozin and Kopylev: on absorption of ammonia by cuprammonium solutions
—	—	0.2	0.5	—	—	—	—	20—24	on absorption of carbon dioxide by 1 N NaOH solution.

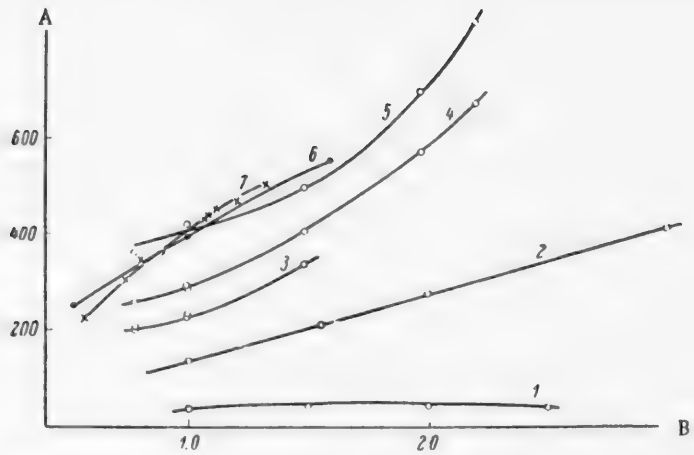

Dependence of the gas-phase transfer coefficient per 1 m^2 of plate area on the gas velocity in the full section of the column: A) gas-phase transfer coefficient per unit plate area (in kg-moles/hr · m^2), B) gas velocity (m/second); 1) system CO_2 – 1 N NaOH [3]; 2) system NH_3 – cuprammonium solution [3]; original level (in cm) [6]: 3) 1.27, 4) 2.54, 5) 508; 6) literature data [8], 7) literature data [7].

Thus, in the above-mentioned papers, a value close to k_1 rather than the transfer coefficient k_G was found from the limiting rate of absorption of carbon dioxide by NaOH solutions. Determination of the partial pressure at the interface (P*) at equilibrium with concentration (C*) of CO_2 molecules in the liquid phase (P* and C* are symbols used in these papers) was performed correctly, as Equation (7) was used for these calculations. Therefore our earlier conclusions concerning the mechanism of the processes in the liquid phase do not require revision if the surface resistance is taken into account.

It can now be explained why Pozin and Kopylev [3] found that the mass-transfer coefficient calculated from data on NH_3 increases continuously with increase of the gas velocity, whereas in the experiments with CO_2 it decreases after passing through a maximum. In the former case, because of the very high solubility of NH_3, they found a value close to k_G, which increases continuously with increase of the gas velocity owing to increasing turbulence in the gas phase. In the second case they found the coefficient k_1, the magnitude of which is determined by the average velocity of thermal motion of the molecules, the accommodation coefficient, and the extent of the interface (if the process is carried out on sieve plates the area of the interface is not known, and therefore it enters as a factor into k_1 and into the mass-transfer coefficients). The interfacial area decreases at high gas velocities, so that the curve for k_1 as a function of the gas velocity passes through a maximum.

The relationship between the over-all transfer coefficient $\underline{k}$, the partial coefficients k_G and k_L, and the coefficient of the rate of solution $k_p = (k_1)$, if the driving force is expressed as the difference of partial pressures, can be represented as follows:

$$\frac{1}{k} = \frac{1}{k_G} + \frac{1}{k_p} + \frac{1}{k_L H} \cdot \qquad (9)$$

It has been shown [6] that the solution rate coefficient k_p is proportional to the Henry coefficient. Therefore in absorption of easily soluble gases, and in evaporation and condensation processes, the expression

$$\frac{1}{k_p} + \frac{1}{k_L H}$$

may be disregarded in comparison with $\frac{1}{k_G}$. With sparingly soluble gases, the gas-phase resistance may be disregarded. It is not the gas-phase resistance but the surface resistance which determines the attainment of the so-called critical concentration of the chemically active part of the absorbent in absorption.

In conclusion, we wish to point out that this paper is not claimed to proved complete elucidation of the question of surface resistance. Our main object was to draw attention to the possible explanation of certain experimental facts which appear contradictory at first sight, and so to stimulate interest in this problem.

SUMMARY

1. Mass-transfer coefficients determined from data on air humidification, absorption of ammonia by cuprammonium solutions, and absorption of carbon dioxide by caustic soda solutions on sieve plates are compared.

2. It is shown that the low value of the mass-transfer coefficient in experiments on absorption of CO_2 by 1 N NaOH solution may be attributed to surface resistance.

3. It is suggested that, in the absorption of a sparingly soluble gas by a chemically active absorbent, surface resistance determines the rate of the process as the concentration of the absorbent increases.

LITERATURE CITED

[1] W. G. Whitman, Chem. Metall. Eng. 4, 18 (1928).

[2] R. E. Emmert and R. L. Pigford, Chem. Eng. Progr. 87, 50 (1954).

[3] M. E. Pozin and B. A. Kopylev, J. Appl. Chem. 31, 387 (1958).*

[4] M. Kh. Kishinevskii, J. Appl. Chem. 30, 185 (1957).*

[5] L. A. Mochalova and M. Kh. Kishinevskii, J. Appl. Chem. 31, 533 (1958).*

[6] F. B. West, W. D. Gilbert and T. Shimizu, Ind. Eng. Chem.44, 2470 (1952).

[7] J. A. Gerster, A. P. Colburn, W. E. Bonnet and T. Carmody, Chem.Eng.Progr.45, 716 (1949).

[8] I. N. Kuz'minykh, L. S. Aksel'rod, Zh. A. Koval', and A. I. Rodionov, J. Chem. Ind. 2, 86 (1954).

Received May 12, 1958.

*Original Russian pagination. See C. B. Translation.

SOME QUESTIONS OF THE ANALOGY BETWEEN DIFFUSIONAL AND THERMAL PROCESSES•

A. A. Medvedev and P. G. Romankov

The Technological Institute, Leningrad

The analogy between diffusional effects and heat conduction is widely used in investigations of diffusional processes. Thus, Fick [1] applied Fourier's method (1822) to unidimensional flow of matter in a stationary isotropic medium and formulated his equations for concentrated diffusion [1]:

$$i_x = -D \frac{\partial c}{\partial x} , \tag{1}$$

$$\frac{\partial c}{\partial \tau} = D \frac{\partial^2 c}{\partial x^2} . \tag{2}$$

The corresponding equations for heat conduction are:

$$q = -\lambda \frac{\partial t}{\partial x} , \tag{3}$$

$$\frac{\partial t}{\partial \tau} = a \frac{\partial^2 t}{\partial x^2} . \tag{4}$$

It was pointed out by Duclaux [2] that Fick's paper [1] dealing with the fundamental principles of the diffusion theory is cited very frequently and very inaccurately. Therefore the following quotation is not without interest: "To express Fick's basic idea it is sufficient to replace, in Fourier's law, the words quantity of heat by the words quantity of solute, and the word temperature by the words solution concentration" [2a]. It is also pointed out in the same book [2a] that Fick regarded Equation (1) as the mathematical form of his hypothesis which was used for derivation of Equation (2), and that Equation (2) is the only true Fick's equation.

In the original source [1] we find a paragraph which fully confirms the validity of the first comment by Duclaux with regard to the expression of the fundamental idea of this paper. His second comment, in our opinion, should be modified in the sense that both diffusion equations were derived by Fick by the Fourier method, and both equations are given in the paper [1] without their derivation. Fick actually wrote: "Exactly in the form of Fourier's equation for heat conduction we derive . . . the differential equation for diffusional flow" [1]. The diffusional equation is written only in its final form by the author.

Equation (1) as a statement of the hypothesis that the rate of diffusional flow is proportional to the concentration gradient, as well as Equation (2), has been confirmed by numerous experiments and has the force of an empirical law, valid under definite conditions.

In the theory of chemical engineering processes, it is usually assumed that Equations (1) and (2) are the complete analogs of Equations (3) and (4). For example, if we consider Equations (1) and (3) in the light of the

•Communication I in the series on diffusional processes.

foregoing, we might assume that the rate of diffusional flow i_x is the analog of the rate of heat flow q, the driving force $\frac{\partial C}{\partial t}$ is the analog of $\frac{\partial t}{\partial x}$, and D is the analog of λ.

Comparison of Equations (1) - (4) leads to a somewhat different conclusion: on the one hand, the coefficient D is the analog of thermal conductivity λ, and on the other, of temperature conductivity $\frac{\lambda}{\rho c_p}$. It is obvious that the same quantity cannot characterize equally different physical properties of substances.

Let us attempt to elucidate this difference by analysis of the diffusion equations. As an example, we consider molecular mass transfer in a binary solution. This kind of transfer is very characteristic of typical processes in chemical engineering, and in particular of extraction in solid – liquid systems.

The basis of our analysis is the complete analogy between the physicomathematical descriptions of diffusion and heat conduction, and the applicability of the methods of thermodynamics of irreversible processes [3, 4] to these phenomena.

A. V. Lykov [5] described moisture transfer phenomena in capillary-porous bodies with the assumption of a complete analogy in the light of classical thermodynamics. For this he introduced the concept of a single mass-transfer potential θ as the analog of the heat-transfer potential t, i.e., the temperature, and then defined the terms mass capacity, mass conductivity, and potential conductivity. For quantitative evaluation of the results, he proposed an experimental scale of mass (moisture) transfer.

From the general linearity equation [3,4]

$$I_i = \sum_{k=1}^{n} L_{ik} X_k \, (i = 1, 2, \ldots n) \tag{5}$$

we have for this instance (grad T = 0)

$$I_1 = -L_{11} \operatorname{grad} (\mu_1 - \mu_2), \tag{6}$$

where I_i is any flow rate; X_k is the driving force of the process; L_{ik} are kinetic coefficients characterizing conductivity (here the term "conductivity" also includes "conductance"); I_1 is the rate of diffusional flow, μ_1 and μ_2 are the chemical potentials of the solution components; L_{11} is a kinetic coefficient characterizing the diffusional properties of the solution.

Equation (6) is an expression for the rate of isothermal diffusion in a binary solution regarded as a single phenomenon of interpenetration of two components [4,6] without a superposition effect. With the aid of the Gibbs – Duhem equation.

$$c_1 d\mu_1 + c_2 d\mu_2 = 0, \tag{7}$$

where c_1 and c_2 are the concentrations of the components in fractions of the total mass, Equation (6) can be put into the form.

$$I_1 = -L_\mu \operatorname{grad} \mu_1, \tag{8}$$

where $L_\mu = \frac{L_{11}}{c_2}$.

By the law of conservation of mass, the flow rate of a component i corresponds to a continuity equation of the form

$$\frac{dc_1}{d\tau} + \operatorname{div} I_i = 0. \tag{9}$$

In this instance (V = 0, i = 1)

$$\frac{\partial c_1}{\partial \tau} = -\operatorname{div} I_1. \tag{10}$$

Substituting the flow density I_1, from Equation (8) into Equation (10) we have, after transformation

$$\frac{\partial \mu_1}{\partial \tau} = \frac{\partial \mu_1}{\partial C_1} \operatorname{div} (L_\mu \operatorname{grad} \mu_1). \tag{11}$$

Passing to concentrations per unit mass, and assuming that L_μ is a physical constant (which is quite admissible with small changes of chemical potential) we obtain Equation (11) in the following form:

$$\frac{\partial \mu_1}{\partial \tau} = \frac{L_\mu}{\rho \dfrac{\partial c_1}{\partial \mu_1}} \nabla^2 \mu_1. \tag{12}$$

The physical meaning of the kinetic coefficients L and $\dfrac{L_\mu}{\rho \dfrac{\partial c_1}{\partial \mu_1}}$ is defined by Equations (8) and (12). According to Equation (8), L_μ is the density of mass flow (quantity of mass passing across unit area in unit time) under unit driving force in isothermal conditions, i.e., when $\mu_1 = 1$ and when $t = 0$. Consequently L_μ is the coefficient of mass conductivity.

The complex ratio $\dfrac{L_\mu}{\rho \dfrac{\partial c_1}{\partial \mu_1}}$, as Equation (12) shows, characterizes the rate of change of the chemical potential field of the component, and can therefore be named the coefficient of conductivity of chemical potential.

It may be seen that the conductivity of chemical potential takes into account the diffusional properties of the system from two aspects.

First, it includes L_μ, the conductivity of mass flow, i.e., it characterizes the mass - transfer properties, and second, it includes $\dfrac{\partial c_1}{\partial \mu_1}$, the ability of the given system to change its concentrational field with change of the chemical potential field of the component, i.e., the inertia properties of the system.

In this sense $\dfrac{\partial c_1}{\partial \mu_1}$ may be named the coefficient of diffusional inertia of the system. Quantitatively it is defined by the increment of the concentration of component mass with unit change of its specific partial energy (chemical potential). It should be noted that the concepts of diffusional (concentrational) inertia of the system and inertia of the chemical potential field (in its propagation) are not identical. The latter concept is determined by the coefficient of conductivity of chemical potential.

Equations (8) and (12), which represent the process of isothermal diffusion in a two – component system, lead to the same result as the classical equations for concentrational diffusion. However, Equations (8) and (12) have the merit of being completely analogous to the corresponding equations for heat conduction. For a unidimensional field these equations are of the form

$$I_{1x} = -L_\mu \frac{\partial \mu_1}{\partial x}, \tag{8a}$$

$$\frac{\partial \mu_1}{\partial \tau} = \frac{L_\mu}{\rho \dfrac{\partial c_1}{\partial \mu_1}} \cdot \frac{\partial^2 \mu_1}{\partial x^2}. \tag{12a}$$

If we compare Equation (8a) with Equation (3), and Equation (12a) with Equation (4) we see that all the corresponding terms are completely analogous. Thus, in Equations (8a) and (3) the density of mass flow $I_x = i_x$ is the complete analog of the heat current density $\underline{q}$, the chemical – potential gradient $\dfrac{\partial \mu_1}{\partial x}$ is the complete analog of the temperature gradient $\dfrac{\partial t}{\partial x}$, and the mass conductivity L_μ is the complete analog of heat conductivity λ.

We now compare Equations (8a) and (1). Here the left-hand sides of the equations are the same, i.e., $I_{i\,x} = i_x$, so that

$$-D\frac{\partial C}{\partial x} = -L_\mu \frac{\partial \mu_1}{\partial x}. \tag{13}$$

Hence, taking into account that $C = \rho c_1$, we have

$$D = \frac{L_\mu}{\rho \dfrac{\partial c_1}{\partial \mu_1}}, \tag{14}$$

where ρ is the density of the system; c_1 is the concentration of the component per unit mass.

Therefore for isobasic and isothermal conditions the coefficient of concentrational diffusion D is equal to the conductivity of chemical potential $\dfrac{L}{\rho \dfrac{\partial c_1}{\partial \mu_1}}$.

Since the course of a real process does not depend on the method of its mathematical description, while diffusional and heat conduction processes are analogous in nature, then, in general, Equations (1), (3) and (2), (4) may be formally regarded as reciprocal analogs. However, this can apply only to analogy in the form of description, i.e., in complete analogy the conventional character of which is revealed by Equation (14).

In illustration, we present below the values of the kinetic coefficients in question, and certain relationships calculated in investigations of extraction processes for aqueous sucrose solution.

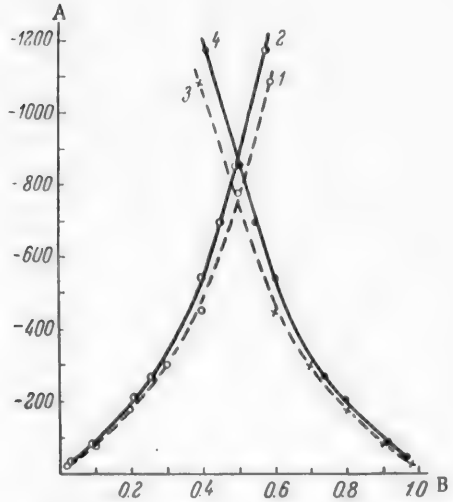

Fig. 1. Variation of the chemical potential of the component with concentration in aqueous sucrose solution; A) chemical potential of solvent (kg·m/kg), B) component concentrations in fractions of total mass (kg/kg); 1) $\mu_1 = f_1(c_2)$, t = 20°; 2) $\mu_1 = f_2(c_2)$, t = 60°; 3) $\mu_1 = f_3(c_1)$, t = 20°; 4) $\mu_1 = f_4(c_1)$, t = 60°.

Variations of the chemical potential of the solvent with the component concentrations c_1 and c_2 are plotted in Fig. 1. The values of chemical potential were calculated from osmotic pressure data and verified against activities [7, 8]. Experimental data of a number of workers on osmotic pressure [9-12], density [13] and partial vapor pressure [14] were used. The data covered both the region of low concentrations characterized by the van't Hoff [14] and Einstein [15] equations and the region of high concentrations, where deviations from these equations are observed. It follows from Fig. 1 that the absolute value of the chemical potential of the solvent increases with increase of sucrose concentration.

Variations of the coefficient of inertia of the solution with the concentrations of the components are represented by the curves in Fig. 2. This relationship was derived by graphical differentiation of the curves for variation of chemical potential (Fig. 1).

Fig. 3 represents the dependence of the coefficient of diffusion on sucrose concentration based on Oholm's experimental data [16]. This relationship can be assumed linear with sufficient accuracy. Thus, at 20° a solution with sucrose concentration $c_2 = 0.16$ kg/kg has diffusion coefficient $D = 0.411 \cdot 10^{-5}$ cm²/second, and a solution with concentration $c_2 = 0.544$ kg/kg has $D = 0.318 \cdot 10^{-5}$ cm²/second.

Variations of the coefficient of mass conductance (mass conductivity) with solvent concentration are plotted in Fig. 4. It is noteworthy that the coefficient of mass conductance changes more steeply than the coefficient of diffusion with increasing concentration of sucrose solutions. Thus, at t = 20°, for a change of sucrose concentration

Fig. 2. Variation of inertia coefficient with concentration in aqueous sucrose solutions: A) inertia coefficient (abs. value) $\frac{\partial c_1}{\partial \mu_1} \cdot 10^3$ (in kg/kg·m); B) component concentrations, fractions of total mass (kg/kg); 1) $\frac{\partial c_2}{\partial \mu_1} = \varphi_1(c_2)$, $t = 20°$; 2) $\frac{\partial c_2}{\partial \mu_1} = \varphi_2(c_2)$, $t = 60°$; 3) $\frac{\partial c_1}{\partial \mu_1} = \varphi_3(c_1)$, $t = 20°$; 4) $\frac{\partial c_1}{\partial \mu_1} = \varphi_4(c_1)$, $t = 60°$.

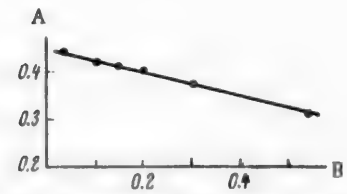

Fig. 3. Variation of diffusion coefficient with concentration in aqueous sucrose solution at $t = 20°$: A) diffusion coefficient $D \cdot 10^5$ (cm^2/second), B) sucrose concentration in fractions of total mass (kg/kg).

in the range of 0.1 - 0.5 kg/kg, changes in the range of $1.85 \cdot 10^{-6} - 0.402 \cdot 10^{-6}$ $\frac{kg}{m \cdot hr \cdot kg \cdot m/kg}$ whereas the diffusion coefficient decreases only from $0.42 \cdot 10^{-5}$ to $0.325 \cdot 10^{-5}$ cm^2/second. The inertia properties of the system evidently have an appreciable influence here.

The results of experimental investigations of chemical engineering processes are often represented in the form of criterial equations [17-20], as this has a number of considerable advantages over other methods. The similarity theory, as a method for analysis of experimental data was developed primarily in its applications to hydrodynamical and thermal processes. The principal criteria of diffusional similarity were derived mainly by analogy with criteria of thermal similarity. For example, simultaneous consideration of equations of concentrational diffusion in liquids and mass transfer at solid boundaries led to derivation of the diffusional criteria Nu', Bi', Ki', Pe', Pr' (Sc), Fo' and others, which are regarded as the complete analogs of the corresponding thermal criteria.

This viewpoint arose from an acceptance of the complete analogy between the concentrational diffusion and heat conduction equations. It was shown above that such a complete analogy is not valid [21]. This can be illustrated by means of similarity criteria.

The Nusselt and Prandtl criteria for thermal similarity are:

$$Nu = \frac{\alpha l}{\lambda}, \tag{15}$$

$$Pr = \frac{\nu}{a}. \tag{16}$$

The Nusselt and Prandtl criteria for diffusional similarity are of the form:

$$Nu' = \frac{\beta l}{D}, \tag{17}$$

$$Pr' = \frac{\nu}{D}. \tag{18}$$

If we compare Equation (15) with (17), and (16) with (18), we see in the first case an analogy in the denominator between the coefficient of heat conductivity λ and the diffusion coefficient D; and in the second, between the coefficient of temperature conductivity a and the same diffusion coefficient D. The imperfection of this analogy was already discussed earlier. Since, in the Nu' criterion, D is not the complete analogy of λ, here B cannot be the complete analogy of α. This which follows from dimensional analysis, is in good agreement with the physical meaning of α and β.

To obtain criteria of diffusional similarity as the complete analogs of the corresponding criteria of thermal similarity, the corresponding differential equations must be considered simultaneously. For example, by such transformation of the boundary – condition equation

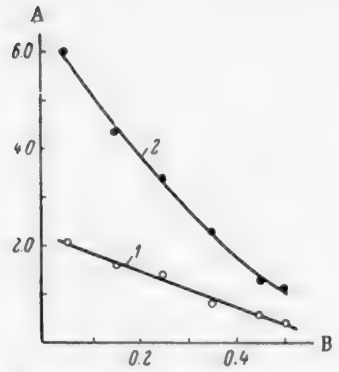

Fig. 4. Variation of the coefficient of mass conductivity (mass conductance) with concentration in aqueous sucrose solutions: A) coefficient of mass conductivity $L_\mu \cdot 10^6 \left(\frac{kg}{m \cdot hour \cdot kg \cdot m/kg}\right)$, B) sucrose concentration (in kg/kg): 1) at t = 20°, 2) at t = 60°.

$$-L_\mu \operatorname{grad} \mu_1 = \alpha_D \Delta\mu_1 \tag{19}$$

and the differential equation

$$\frac{d\mu_1}{d\tau} = a_D \nabla^2 \mu_1 \tag{12b}$$

the following criteria may be obtained:

$$Nu_D = \frac{\alpha_D l}{L_\mu}, \tag{20}$$

$$Bi_D = \frac{\alpha_D l}{L_\mu^*}. \tag{21}$$

$$Pe_D = \frac{wl}{a_D}, \tag{22}$$

$$Fo_D = \frac{a_D \tau}{l^2}, \tag{23}$$

Combining the criteria Re and Pe_D, we have:

$$Pr_D = \frac{Pe_D}{Re} = \frac{\nu}{a_D}, \tag{24}$$

where α_D is the mass-transfer coefficient, L_μ is the coefficient of mass conductivity, and $a = \frac{L}{\rho \frac{dc_1}{d\mu_1}}$ is the coefficient of conductivity of chemical potential.

The resulting diffusional criteria Nu_D, Bi_D, Pe_D and others are the true (complete) analogs of the corresponding criteria of thermal similarity. The quantities contained in them are reciprocally analogous; for example, the mass-transfer coefficient α_D is analogous to the heat-transfer coefficient α, the coefficient of mass conductivity L_μ to the coefficient of thermal conductivity λ, and the coefficient of conductivity of chemical potential a_D to the coefficient of temperature conductivity a.

In conclusion we must point out that the kinetic coefficients discussed above are directly connected with the phenomenological coefficients of the thermodynamics theory of irreversible processes. It is therefore permissible to use the Onsager reciprocity equations in investigations of interconnected processes of heat and mass transfer.

SUMMARY

1. The classical equations for concentrational diffusion cannot be regarded as the complete analogs of the corresponding equations for heat conduction. This result in no way invalidates the diffusion equations.

2. The coefficient of diffusion represents the rate of propagation of concentration in space (material medium). By its physical meaning it may be termed the coefficient of concentration conductivity of the system. In isothermal diffusion, this coefficient is numerically equal to the coefficient of conductivity of chemical potential.

3. The diffusion coefficient D takes into account both the inertia and the mass-transfer properties of a system; it can with sufficient accuracy be regarded as reduced analog of the coefficient of temperature conductivity a but not of heat conductivity λ. This result quantitatively confirms the corresponding point in Lykov's theory [5].

4. Numerical values of the coefficients of mass conductivity and inertia have been found for aqueous solutions of sucrose and certain other substances; these coefficients are shown to be dependent on concentration.

5. The criteria of diffusional similarity derived from the concentrational diffusion equation are not the true (complete) analogs of the corresponding criteria of thermal similarity, but the former may be regarded as the reduced analogs of the latter. A special position is occupied by criteria derived from boundary conditions, of the type of Nu', Bi', Ki'. It is shown why, for example, in the criterion $Bi' = \frac{\beta l}{D}$ the coefficient β is not the complete analog of α, and the coefficient D is not the analog of λ.

Quantitatively this conclusion is consistent with the results of dimensional analysis.

6. In most calculations such criteria as Nu' and Ki' are the determined criteria and therefore the values of the reduced and true similarity criteria are equal. In the general case, the incomplete analogs may differ numerically from true analogs. This difference is determined by the dependence of the chemical potential of a component on its concentration.

As the methods of thermodynamics of irreversible processes were used, the foregoing results have a strict scientific basis and fairly general significance.

LITERATURE CITED

[1] A. Fick, Ann. d. Ph., XCIV, 59 (1855).

[2] J. Duclaux, Diffusion dans les liquides, Paris (1936); (also Russian translation, Leningrad – Moscow, 1939).

[3] L. Onsager, Phys. Rev. 37, 405 (1931).

[4] S. R. de Groot, Thermodynamics of Irreversible Processes, Amsterdam (1952).

[5] A. V. Lykov, Transfer Phenomena in Capillary Porous Bodies [in Russian] (State Tech. Press, Moscow, 1954).

[6] W. Jost, Diffusion (Darmstadt, 1957).

[7] R. Haase, Thermodynamik der Mischphasen (Berlin, 1956).

[8] I. Prigogine, The Molecular Theory of Solutions (Amsterdam, 1957).

[9] H. N. Morse, W. W. Holland, C. N Myers, G. Cash and J B. Zinn, Am. Chem. J. 48, 29 (1912).

[10] E. Berkeley and E G Hartley, Proc. Royal Soc. 92, 477 (1916)

[11] J. C. Frazer and R. T. Myrick, J. Am Chem. Soc. 38, 1907 (1916).

[12] F. Plato, Wiss. Abh. d. Kaiserl. Norm. – Eich. – Kom. 2,153 (1900).

[13] E. Berkeley, E. G. Hartley and C. V. Burton, Phil. Trans. Royal Soc. of London, Ser. A, 218, 295 (1919).

[14] J. H. van't Hoff, Z. phys. Ch. 1, 481 (1887).

[15] A. Einstein, Ann. d. Ph., XIX, 481 (1906).

[16] L. Öholm, Z. Phys. Ch., LXX, 378 (1910).

[17] J. M. Coulson and J. F. Richardson, Chemical Engineering (London, 1955).

[18] A. G. Kasatkin, Processes and Equipment of Chemical Technology [in Russian]. (Goskhimizdat, Moscow, 1955).

[19] P. G. Romankov, Hydraulic Processes of Chemical Technology [in Russian] (Goskhimizdat, Leningrad, 1948).

[20] Ya. Tsiborovskii, Processes of Chemical Technology [in Russian] (Goskhimizdat, Leningrad, 1958).

Received December 24, 1958.

BUBBLING OF AIR THROUGH A LAYER OF VISCOUS LIQUID

I. P. Levsh and O. B. Balandina

Chair of Chemical Engineering Processes and Equipment, the Polytechnic Institute of Central Asia

Determinations of hydraulic resistances during bubbling are a necessary stage in hydraulic calculations relating to fractionating columns, bubbling absorbers, gas scrubbers, stills, and other equipment in the chemical and food industries.

The hydrodynamics of bubbling equipment has been studied by Stabnikov [1,2], Ramm [3], Zhavoronkov and Furmer [4], Usyukin and Aksel'rod [5], Aksel'rod and Dil'man, [6-9], Pozin, Mukhlenov, Tumarkina, and Tarat [10], Aerov and Darovskikh [11], and other workers. Their experiments were concerned with the operation of rectification columns or foam apparatus, generally with liquid layers not more than 5 cm high. Bubbling was studied in the systems water–steam [1,2], dilute salt solutions–air [10], water–air [10,7], ethyl alcohol–air [7], water–nitrogen [9], liquid air–air [5], organic solvents–air [9], and other systems, usually with liquid phases of low viscosity. Because of this, the due significance was not attached to the influence of viscosity on hydraulic resistance in bubbling, and a number of workers disregarded viscosity entirely in hydrodynamic calculations of the bubbling process. Hardly any information is available on bubbling in viscous liquids in layers of large height.

In this paper we consider the bubbling of air through aqueous glycerol solutions of viscosity from 1 to 80 centipoises, in layers from 0.3 to 70 cm high in a laboratory column, and derive equations for calculation of hydraulic resistance in bubbling with liquid viscosity taken into account.

Glycerol solutions were chosen for the experiments because their viscosities vary over a wide range with slight differences of surfaces tension σ and density γ_L.

Scheme of the Process

When the gas is fed at a sufficient velocity into a bubbler within the liquid, a gaseous emulsion consisting of ascending gas bubbles in the liquid is formed. The hydraulic resistance which the gas layer must then overcome depends on the hydrostatic pressure of the column of gaseous emulsion and the hydrodynamic resistances which arise when the gas moves through the layer.

The hydrostatic pressure is determined by the density of the emulsion, which depends on the extent of saturation of the liquid by the gas. Saturation of the liquid with gas lowers the density of the emulsion and so reduces the hydrostatic pressure. However, for greater saturation it is necessary to increase the gas feed rate, and this inevitably leads to increase of the hydrodynamic resistance. Thus, the hydrostatic pressure and hydrodynamic resistance in bubbling are interconnected: increase of hydrostatic pressure must lead to decrease of hydrodynamic resistance. Both factors are functions of the liquid viscosity μ (kg/ second·m^2) and gas rate V (m^3/ second), provided that the height H of the liquid layer (m), density of the liquid (kg/ m^3), density of the gas γ_L(kg/ m^3), diameter of the bubbler column $\underline{d}$ (m), liquid volume V_L in the column (m^3), and surface tension σ(kg/ m) are all constant.

Consideration of the effect of viscosity on the bubbling process at constant gas rate shows that increase of the liquid viscosity leads to increase of hydrodynamic resistance, decrease of the density of the gaseous emulsion, and changes in the bubbling conditions. The increase of hydrodynamic resistance with viscosity follows from the hydrodynamic equation.

$$\Delta p_g = \lambda \cdot \frac{l}{d} \cdot \frac{w^2}{2g} \gamma, \tag{1}$$

where $\Delta \rho_g$ is the hydrodynamic resistance (kg/m^2), λ is the coefficient of friction, l is the path of the gas (m), d is the diameter of a bubble or gas stream (m), w is the velocity of the gas (m/second), and g is the gravitational acceleration (m/sec^2). It is known that $\lambda = \varphi(\mathrm{Re})$, where Re is the Reynolds number. Consequently, provided that all the other quantities are constant, $\lambda = \varphi(\mu)$ and $\Delta \rho_g = \varphi(\mu)$. The change in the density of the gaseous emulsion with the viscosity of the liquid is associated with an increase in the diameter of the ascending bubbles. For determination of bubble diameter as a function of viscosity we assume that bubbling occurs under transitional conditions, and perform the calculations by means of the generalized equation derived by Zrelov [12]

$$w = \sqrt[n]{\frac{\pi \cdot d^{3-n} \cdot (\rho_1 - \rho) \cdot g}{6 \cdot k_n \cdot \nu^{2-n} \cdot \rho}}, \tag{2}$$

where d is the bubble diameter (m), ρ_1 and ρ are the densities of the liquid and gas respectively $\left(\frac{\text{kg} \cdot \text{sec}^2}{\text{m}^4}\right)$, k_n and n are coefficients which depend on the regime of bubble motion, and ν is the coefficient of kinematic viscosity (m^2/second).

For the transitional regime at Re = 25-350, according to Zrelov's data [12], $\mathrm{Kn} = \frac{10 \cdot \pi}{8} = 3.92$, n = 1.5. Equation (2) then becomes

$$w = \sqrt[1.5]{\frac{\pi \cdot d^{1.5} \cdot (\rho_1 - \rho) \cdot g}{6 \cdot 3.92 \cdot \nu^{0.5} \cdot \rho}}. \tag{3}$$

It follows from the experimental data of a number of workers, cited by Ramm [3], that the rate of ascent of gas bubbles of $d > 6$ mm increases only slightly with increase of diameter, and is about 0.25 m/second. Therefore it may be assumed approximately that w is constant. From the foregoing, it follows that ρ_1 = const and ρ = const, and then

$$d = K \cdot \sqrt[3]{\nu}, \tag{4}$$

where K is a numerical coefficient which incorporates all the constant quantities: π, ρ_1, ρ, g, and others. For different diameters d_1, d_2 and different viscosities μ_1, μ_2 we can write

$$d_1 = K_1 \cdot \sqrt[3]{\mu_1}, \tag{5}$$

$$d_2 = K_2 \cdot \sqrt[3]{\mu_2}. \tag{6}$$

But if follows from the foregoing that $K_1 \cong K_2$, and then

$$\frac{d_2}{d_1} = \sqrt[3]{\frac{\mu_2}{\mu_1}}. \tag{7}$$

With a fixed value d = 1 cm at μ_1 = 1 centipoise, we find the bubble diameters at μ_2 = 10 centipoises, μ_3 = 20 centipoises, etc. Bubble diameters at different viscosities, calculated from Equation (7), are given below.

Viscosity (centipoises)	1	10	20	30	40	50	60	70
Bubble diameter (cm)	1	2.16	2.72	3.11	3.43	3.69	3.91	4.13

The Reynolds number in motion of bubbles of the above diameters is in the range of 150-250, which corresponds to stage III of the transitional flow regime.

The above calculation is approximate, since in bubbling even in the most viscous of liquids it is not single bubbles that move, but a whole series of bubbles ascend at definite distances apart. However, the calculation demonstrates the increase of bubble diameter with increase of the liquid viscosity, which can be easily observed

experimentally; the actual increase of bubble size is greater than indicated by calculations with the aid of Equation (7).

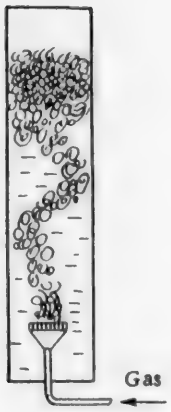

Fig. 1. Bubbling of gas in liquid of low viscosity.

Alteration of the bubbling regime with increase of viscosity is associated with expenditure of the kinetic energy of the gas stream in overcoming hydrodynamic resistance. Suppose that in the original liquid of low viscosity we have streaming motion of the gas, with a well-defined bubble stream as shown in Fig. 1. The hydrodynamic resistance in this case depends on the liquid viscosity, and therefore with increase of the latter, at constant gas rate, the gas velocity decreases, the cross section of the gas stream increases, individual small streams in it coalesce, and the whole stream begins to disintegrate into gas bubbles.

The higher the liquid viscosity, the smaller the stream becomes, and at a sufficiently high viscosity it should disappear entirely, and become converted into large bubbles (Fig 2). Therefore, the flow of gas should pass from streaming to bubbling with increase of liquid viscosity; this is fully confirmed by our experiments.

Alterations of the gas rate cause changes in the hydrodynamic resistance, density of the gaseous emulsion, and the bubbling regime. The density of the emulsion depends on the degree of saturation of the liquid by the gas; this increases with increase of gas rate. The increase of hydrodynamic resistance is the consequence of the increased velocity of the gas stream in the medium. At constant viscosity the gas flow passes from streaming to bubbling with decrease of gas rate, and conversely. It follows that changes of the gas rate should have an appreciable influence on the hydrodynamics of the process.

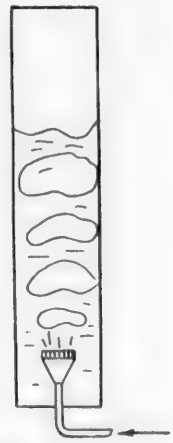

Fig. 2. Bubbling of gas in a liquid of high viscosity.

This bubbling scheme is characterized by two extreme cases: bubbling in a liquid of low viscosity, with a well-defined gas stream, and bubbling in a liquid of high viscosity, with almost complete breakdown of the stream and formation of separate large bubbles of gas.

It follows from the foregoing that increase of liquid viscosity leads to two opposing effects: the hydraulic resistance to the motion of the gas through the liquid increases, and the hydrostatic pressure of the column of gaseous emulsion on the bubbler decreases because of the decrease in the density of the emulsion. The total hydraulic resistance in bubbling may either increase or decrease with increase of viscosity; this depends on which of the above factors is predominant. The influence of viscosity becomes more pronounced with increasing thickness of the liquid layer; this follows from the very nature of these forces, the absolute value of which increases with increase of the surface area and path along which they act. At small depths of the liquid layer the influence of viscosity is inappreciable.

The suggested bubbling scheme gives an indication of some methods for deriving equations for calculating hydraulic resistance in bubbling devices.

We take as the general formula

$$\Delta p = \Delta p_1 + \Delta p_2 + \Delta p_3, \tag{8}$$

where: Δp is the hydraulic resistance of the bubbling device (kg/m^2); Δp_1 is the hydraulic resistance of the dry bubbler grid (kg/m^2); Δp_2 is the resistance due to forces of surface tension (kg/m^2); Δp_3 is the resistance of the liquid layer (kg/m^2).

The value of Δp_1 is found from the usual equation for calculating any kind of local resistance [10, 13].

From the nature of the surface tension forces it follows that

$$\Delta p_2 = \varphi(\sigma, \Pi), \tag{9}$$

where σ is the surface tension (kg/m); Π is the wetted perimeter of the grid (m).

With the aid of the theory of dimensions we have for the functional relationship of Equation (9)

$$\Delta p_2 = A \cdot \frac{\sigma}{H} . \tag{10}$$

where A is a dimensionless coefficient.

Equation (10) has been confirmed by a number of authors [6,10].

For determination of Δp_3 we use the equation

$$\Delta p_3 = H \cdot \gamma_L \cdot (k + c), \tag{11}$$

where k is a dimensionless coefficient which takes into account the influence of viscosity on the hydrodynamic resistance of the layer of medium, and c is a dimensionless quantity which accounts for the influence of saturation of the liquid with gas.

As a measure of the quantity n of the bubbled gas we take

$$n = \frac{V_L}{V_{sec}} \quad \left(\frac{sec \cdot m^3}{m^3}\right), \tag{12}$$

where V_L is the volume of liquid on the surface F of the bubbler grid

$$V_L = H \cdot F. \tag{13}$$

It may be assumed that

$$c = B \cdot \left(\frac{n}{n_0}\right)^{k_1}, \tag{14}$$

where n is the quantity of the bubbled gas, n_0 is the initial quantity of gas, B is a proportionality factor, and k_1 is an experimental coefficient.

In determination of the value of the coefficient k, it must be taken into account that, in bubbling, the influence of viscosity on the value of Δp_3 is continuously interrelated with the quantity of the bubbled gas n.

On the basis of the physical nature of the bubbling process we may write the funtional relationship

$$k = \varphi(n, \nu, g, D, d), \tag{15}$$

where ν is the coefficient of kinematic viscosity of the liquid (m^2/second).

Equation (15) is written in the form of a power equation

$$k = A \cdot n^a \cdot \nu^b \cdot g^c \cdot D^e \cdot d^m. \tag{16}$$

Substitution of dimensions gives

$$0 = [sec]^a \cdot \left[\frac{m^2}{sec}\right]^b \cdot \left[\frac{m}{sec^2}\right]^c \cdot [m]^e \cdot [m]^m, \tag{17}$$

and hence

$$0 = sec^{a-b-2c} \cdot m^{2b+c+e+m}. \tag{18}$$

We assume that e = 0 and m = 0. Then $a = \frac{3}{2}c$; $b = -\frac{c}{2}$. To determine the relationship between e and m we take a = 0; b = 0; c = 0, then e = −m.

Finally we have

$$k = A \cdot \left(\frac{n^{1.5} \cdot g}{\nu^{0.5}}\right)^c \cdot \left(\frac{D}{d}\right)^e .$$

We now introduce the quantity

$$m = \frac{1}{n} = \frac{V_{sec}}{V_L} \left[\frac{1}{sec} \right]$$

which we term the specific gas rate. Equation (19) is rewritten in the form

$$k = A \cdot \left(\frac{g}{m^{1.5} \cdot \nu^{0.5}} \right)^{e} \cdot \left(\frac{D}{d} \right)^{s}, \tag{20}$$

where $\frac{g}{m^{1.5} \cdot \nu^{0.5}} = \frac{g^{0.5} \cdot \gamma^{0.5}}{m^{1.5} \cdot \mu^{0.5}} = Re_b$, a dimensionless quantity which we term the Reynolds bubbling number. $\frac{D}{d} = \Gamma$ is the criterion of geometrical similarity.

To prove that Re_b is analogous to Re in respect of the physical quantities represented in it, we find the value of $\underline{m}$

$$m = \frac{V_{sec.}}{V_L} = \frac{w_G \cdot F}{H \cdot F} = \frac{w_G}{H}, \tag{21}$$

where w_G is the velocity of the gas calculated for the total area of the bubbler grid (in m/second).

Substituion of this value of $\underline{m}$ gives

$$Re_b = \frac{g \cdot H^{1.5}}{w^{1.5} \cdot \nu^{0.5}}, \tag{22}$$

comparing the expression for Re_b with the usual $Re = \frac{w \cdot l}{\nu}$, where l is the determined dimension of flow, we note that H is the determining dimension in bubbling, and the presence of $\underline{g}$ in the expression is the consequence of free ascent of the gas bubbles. Therefore Re_b is to some extent analogous to Re.

Substitution of the value found for $\underline{k}$ and $\underline{c}$ into Equation (11) and simple rearrangement gives

$$\frac{\Delta p_3}{H \cdot \gamma_L} = A \cdot (Re_b)^{e} \cdot \Gamma^{s} + B \cdot \left(\frac{m}{m_0} \right)^{k_1}, \tag{23}$$

where $\frac{\Delta p_3}{H \cdot \gamma_L} = E$, a dimensionless quantity which is a peculiar measure of hydrodynamic disturbance in bubbling.

Finally we obtain an equation in criterial form

$$E = A \cdot Re_L^{e} \cdot \Gamma^{s} + B \cdot \left(\frac{m}{m_0} \right)^{k_1}, \tag{24}$$

which is valid when increase of liquid viscosity lowers the hydraulic resistance Δp_3 of the layer.

We now find an equation which is valid when increase of the liquid viscosity increases hydraulic resistance in bubbling. Here we note that $b = -\frac{c}{2}$, $a = \frac{3}{2}c$, and hence $c = -2b$, $a = -3b$.

Substitution of these coefficients into Equation (16) gives

$$k = A \cdot \left(\frac{\nu \cdot m^3}{g^2} \right)^{b} \cdot \left(\frac{D}{d} \right)^{s}. \tag{25}$$

In Equation (25)

$$\frac{\nu \cdot m^3}{g^2} = \frac{1}{Re^2_b}.$$

Hence the general form of Equation (11) is

$$E = A_1 \cdot (Re^{-2}_b)^{b} \cdot \Gamma^{s} + B_1 \cdot \left(\frac{n}{n_0} \right)^{k_1}. \tag{26}$$

Equation (26) is valid when increase of the liquid viscosity increases hydraulic resistance of the layer in bubbling.

EXPERIMENTAL

The objects of the experimental part of this work were to eludicate the physical picture of the bubbling process and to verify the derived equations.

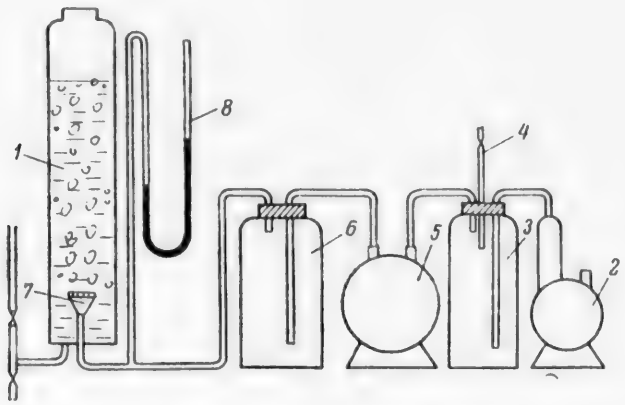

Fig. 3. Diagram of bubbling column.

Air was bubbled through the glycerol layer in a glass column 1, 6 cm in diameter and 110 cm high (Fig.3). Air was fed into the column from a rotary blower 2 through a buffer vessel 3, 15 liters in capacity, fitted with an exhaust valve 4 for regulation of the air supply. From the buffer vessel,the air passed through a gas meter 5 into another buffer vessel 6, and then entered the liquid layer through the flat bubbler grid 7. The hydraulic resistance Δp of the bubbler device was measured by means of the manometer 8.

The bubbler grid was made from a flat nickel plate 2.1 cm in diameter and 0.14 cm thick. 19 orifices, 0.13 cm in diameter, were arranged in concentric circles. The experiments were performed with glycerol solutions of volume concentrations 100, 90, 80, 60, 40, 20%, and corresponding viscosities of 80, 30, 10, 5, 2.5, 1.7 centipoises, with pure water, and with aqueous thiosulfate solution. The height of the liquid layer in the bubbling column was 0.3, 5, 15, 20, 50 and 70 cm. The air velocity $\underline{w}$ in the openings of the bubbler grid was varied from 2 to 16 m/second. The density of the glycerol solutions was determined pycnometrically. Solution viscosity was determined with the Ostwald viscosimeter. The values for the surface tension σ of the glycerol solutions, found by measurement of the maximum bubble pressure in the Rebinder apparatus, are given below.

Concentration of glycerol solutions (vol. %)	Water	20	40	60	80	90	100
Surface tension (dynes/cm).	73.05	70.50	68.91	68.01	67.41	69.32	70.03

The experiments were performed in the following sequence: first the hydraulic resistance of the bubbler with a wetted grid was found, then the resistance of a liquid layer 0.3 cm was determined, followed by determinations at 5, 10 cm up to the maximum depth of 70 cm. The resistances of layers of different heights were determined for each solution viscosity at air velocities of 2, 4, 6, 8, 10, 12, 14, 16 m/second. A series of experiments was then performed with glycerol of a higher concentration.

The experimental results were used for plotting curves for the pressure drop in the whole bubbling apparatus (Δp) as a function of viscosity, a few of which are shown in Fig. 4, and curves for the variation of the hydraulic resistance of the liquid layer during bubbling (Δp_3) with the air velocity (w) in the openings of the bubbler grid, given in Fig. 5 and 6. The calculated values of the hydraulic resistance of the liquid layer Δp_3 are given in Tables 1 and 2.

TABLE 1

Hydraulic Resistance of Liquid Layers of Viscosity μ = 1-10 Centipoises Calculated from Equation (28) and Found Experimentally. At μ = 1 centipoise γ_L = 1000 kg/m³, at μ = 10 centipoises γ_L = 1200 kg/m³

μ (centipoises)	w (m/sec)	H (m)	m(sec^{-1})	Re_b	$Re_b^{0.25}$	$\frac{0.3}{m^{0.33}}$	Δp_3 calculated (kg/m²)	Δp_3 experimental (kg/m²)	Relative error (%)	E
1	4	0.7	0.40	36500	0.073	0.40	760	690	+11	0.98
1	6	0.7	0.62	19850	0.084	0.35	695	680	+ 1	0.98
1	10	0.7	1.04	9250	0.104	0.29	640	620	+ 3	0.89
10	4	0.7	0.42	12700	0.093	0.40	950	840	+13	1.00
10	6	0.7	0.62	6870	0.110	0.96	890	860	+ 4	1.02
10	10	0.7	1.04	3220	0.134	0.29	795	870	− 7	1.04
1	4	0.5	0.59	21100	0.082	0.36	505	500	+ 0.5	1.00
1	8	0.5	1.18	7670	0.108	0.28	449	520	−14	1.04
1	12	0.5	1.77	4210	0.123	0.25	426	455	− 6	0.91
10	4	0.5	0.59	7340	0.108	0.25	426	455	− 6	0.91
10	8	0.5	1.18	2660	0.139	0.36	645	610	+ 7	1.02
10	12	0.5	1.77	1450	0.164	0.28	584	600	− 3	1.00
1	4	0.2	1.45	5560	0.116	0.26	174	180	− 3	0.90
1	6	0.2	2.20	3020	0.135	0.23	168	190	−11	0.95
1	12	0.2	4.40	1070	0.175	0.18	164	170	− 3	0.85
10	4	0.2	1.45	1940	0.151	0.26	229	230	− 0.5	0.96
10	6	0.2	2.20	1040	0.176	0.23	225	240	− 6	1.00
10	12	0.2	4.40	368	0.228	0.18	226	210	+ 8	0.87
1	4	0.05	5.90	687	0.127	0.17	45	58	−12	1.15
1	8	0.05	11.30	242	0.260	0.13	45	50	−10	1.00
10	4	0.05	5.90	236	0.254	0.17	58	75	−22	1.25
10	8	0.05	11.80	84	0.329	0.13	64	70	− 9	1.17
1	8.1	0.04	37.50	42	0.390	0.09	44	40	+10	1.10

TABLE 2

Hydraulic Resistance of Liquid Layers of Viscosity μ = 10-70 Centipoises Calculated from Equation (27) and Found Experimentally

μ (centipoises)	w(m/second)	H(m)	m(sec^{-1})	Re_b	$Re_b^{0.25}$	$1.2m^{0.5}$	Δp_3 calculated (kg/m²)	Δp_3 experimental (kg/m²)	Relative error(%)
70	4	0.7	0.42	4920	8.37	0.77	792	740	+ 7
70	6	0.7	0.62	2640	7.20	0.84	700	710	− 1
70	10	0.7	1.04	1230	5.92	1.21	624	580	+ 8
10	4	0.7	0.42	12710	10.62	0.77	965	840	+15
10	6	0.7	0.62	6870	9.10	0.95	887	860	+ 1
10	8	0.7	0.93	3820	7.86	1.16	760	860	−12
70	4	0.5	0.59	2720	7.21	0.93	510	490	+ 4
70	8	0.5	1.18	1020	5.65	1.32	435	400	+ 9
70	10	0.5	1.45	750	5.21	1.45	415	360	+15
70	12	0.5	1.77	560	4.87	1.59	403	340	+17
10	4	0.5	0.59	7350	9.30	0.93	611	610	0
10	8	0.5	1.18	2660	7.20	1.32	516	600	−14
10	10	0.5	1.45	1940	6.65	1.45	490	540	− 9
10	12	0.5	1.77	1520	6.25	1.59	474	540	−13
70	4	0.2	1.45	750	5.21	1.44	166	140	+18
70	6	0.2	2.20	402	4.50	1.78	159	160:	− 6

TABLE 2 (Cont'd)

μ (centipoise)	w(m/sec)	H (m)	m(sec^{-1})	Re_b	$Re_b^{0.25}$	$1.2\,m^{0.5}$	Δp_3 calculated (kg/m^2)	Δp_3 experimental (kg/m^2)	Relative error (%)
70*	12	0.2	4.40	141	3.41	2.52	148	110	+34
10	4	0.2	1.45	1940	6.61	1.44	193	220	−12
10	6	0.2	2.20	1040	5.70	1.78	179	210	−15
10	12	0.2	4.40	370	4.40	2.53	166	195	−15
70*	4	0.05	5.90	91	4.50	1.55	37	30	+23
70*	8	0.05	11.80	32	3.18	1.85	31	30	+ 3
70*	12	0.05	17.70	18	2.62	2.06	28	22	+28
10*	4	0.05	5.90	240	6.21	1.55	46	70	−33
10*	8	0.05	11.80	84	4.37	1.85	37	50	−26
10*	12	0.05	17.70	46	3.60	2.06	33	25	+31

*Calculated with A = 0.1, B = 1.0, k_1 = 0.25, c = 0.33.

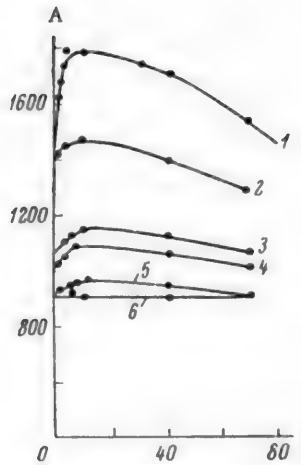

Fig. 4. Variations of the hydraulic resistance of the whole bubbling apparatus with glycerol viscosity at w = 10 m/second: A) hydraulic resistance Δp (mm H_2O), B) viscosity of glycerol (centipoises); height of liquid layer (cm): 1) 70, 2) 50, 3) 20, 4) 15, 5) 5, 6) 0.3.

The experimental results were used for plotting curves for the pressure drop in the whole bubbling apparatus (Δp) as a function of viscosity, a few of which are shown in Fig. 4, and curves for the variation of the hydraulic resistance of the liquid layer during bubbling (Δp_3) with the air velocity (w) in the openings of the bubbler grid, given in Fig. 5 and 6. The calculated values of the hydraulic resistance of the liquid layer Δp_3 are given in Tables 1 and 2.

For the calculations Equation (24) was reduced to the form

$$\Delta p_3 = A \cdot H \cdot \gamma_L \cdot \left[\left(\frac{g^{0.5} \cdot \gamma_L^{0.5}}{m^{1.5} \cdot \mu^{0.5}} \right)^c + B \cdot \left(\frac{m}{m_0} \right)^{k_1} \right], \qquad (27)$$

where $m_0 = 1\ m^3 \cdot sec \cdot m^3$. The experimental values of the coefficients in Equation (27) are: A = 0.1, B = 1.2, c = 0.25, k_1 = 0.5.

Equation (26) was transformed into the equation

$$\Delta p_3 = A_1 \cdot H \cdot \gamma_L \cdot \left[\left(\frac{m^{1.5} \cdot \mu^{0.5}}{g^{0.5} \cdot \gamma_L^{0.5}} \right)^{2b} + B_1 \left(\frac{m}{m_0} \right)^{k_1} \right], \qquad (28)$$

where the values of the coefficients, found from our experimental results are: A_1 = 2.30, b = 1/8, B_1 = 0.3, k_1 = − 1/3.

DISCUSSION OF RESULTS

The bubbling process presented the following picture. The passage of air through the bubbler was not uniform at the different openings; air did not pass at all through some, and there was pulsating air flow through others. The distribution of the working openings over the bubbler grid area was random, and varied with time. The nature of the bubbling at a constant air rate depended on the viscosity of the liquid. With liquids of viscosities from 1 to 10 centipoises, if the gas rate was sufficient, the gas penetrated into the liquid layer in a swirling stream, its subsequent course followed a spiral, and a layer of foam was formed in the upper part of the bubbling column. With decrease of gas rate in a liquid of given viscosity the spiral became more distinct and its pitch increased.

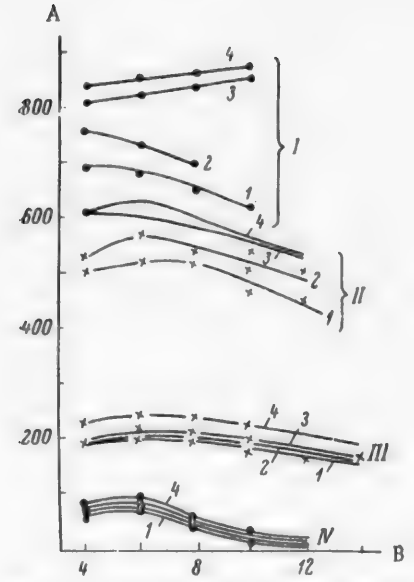

Fig. 5. Variations of hydraulic resistance of glycerol solutions with viscosities μ = = 1-10 centipoises with the air velocity in the grid openings: A) hydraulic resistance Δp_3 (in mmH_2O), B) air velocity $\underline{w}$ in the bubbler grid openings (m/second); height of liquid layer (cm): I) 70, II) 50, III) 20, IV) 5; viscosity of glycerol solutions (centipoises): 1) 1, 2) 2.5, 3) 5, 4) 10.

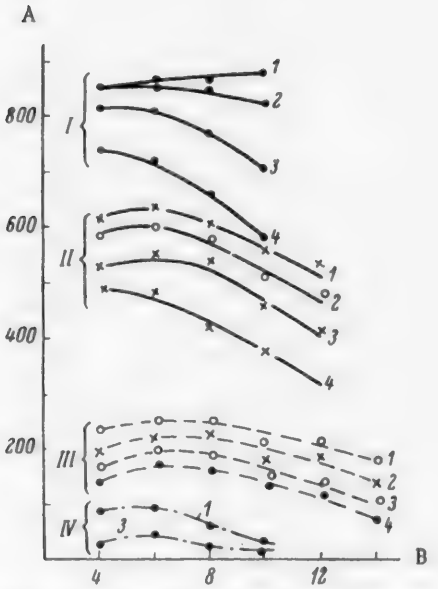

Fig. 6. Variations of hydraulic resistance of glycerol solutions with viscosities μ = = 10-70 centipoises with the air velocity in the grid openings: A) hydraulic resistance of layer (mm H_2O), B) air velocity w in the bubbler grid openings (m/second); height of liquid layer H (cm): I) 70, II) 50, III) 20, IV) 5; viscosity μ of the glycerol solutions (centipoises): 1) 10, 2) 30, 3) 50, 4) 70.

With high-viscosity liquids of μ = 60-80 centipoises, the streaming form of the gas outflow broke down; near the exit plane of the gas the separate streams coalesced into large bubbles which increased in size with increasing viscosity and reached 6 cm and over in diameter at the highest viscosities.

Thus, the visual picture of the bubbling process (Figs. 1 and 2) itself demonstrates the considerable influence of viscosity on the process, as the other factors – surface tension σ and liquid density γ_L – varied little in our experiments.

The quantitative influence of viscosity on hydraulic resistance in bubbling is shown by Fig. 4, where the $\Delta p - \mu$ curves have well-defined maxima at μ = 5-10 centipoises. This maximum is appreciable for thick layers and almost vanishes for layers 5 cm and less in thickness. The influence of viscosity is especially clear from Fig. 5 and 6, where it is also seen that this influence becomes increasingly pronounced with increasing depth of liquid. Increase of viscosity from 1 to 10 centipoises produces a 1.2 to 1.3 fold increase in the hydraulic resistance of the layer (Δp_3) (Fig. 5). Further increase of viscosity from 10 to 70-80 centipoises, on the contrary, reduces the hydraulic resistance 1.3 to 1.5-fold (Fig. 6). At viscosities from 60 to 70 centipoises, the value of Δp_3 is considerably lower than the hydrostatic pressure of a column of the pure liquid.

These effects in viscous media may be attributed to high saturation of the liquid with gas, which leads to a decrease in the density of the system which prevails over the hydrodynamic resistance in the layer. In liquids of low viscosity, where μ = 1-10 centipoises, the degree of saturation of the liquid with gas is lower, hydrodynamic resistance due to the larger gas stream prevails, and this causes increase of the hydraulic resistance of the layer (Δp_3) with increase of viscosity.

Comparison of values of Δp_3 calculated from Equation (28) and found experimentally shows (Table 1)

that for glycerol solutions with viscosities from 1 to 10 centipoises, the calculated values of Δp_3 deviate from the experimental data within a range of ± 15%. In most of our experiments at H > 5 cm, these deviations did not exceed ± 7%. With liquid layers of H ≥ 5 cm and specific air rates m > 6 the relative error in the calculations is considerably greater. At the same time, analysis of Pozin's experimental results [10] for m = 25-100 and H = 1-5 cm showed that values of Δp_3 calculated from Equation (28) deviate by 10-15% from the experimental values. It follows that Equation (28) may be used for calculations of Δp_3 over a fairly wide range.

Comparison of the calculated values of Δp_3 for glycerol solutions of μ = 10-70 centipoises shows (Table 2) that the relative error with the use of Equation (27) is within ±15%. Here the relative errors were determined for solutions of μ = 20-70 centipoises and H = 15-70 cm. Deviations from the experimental values increase appreciably with decrease of viscosity to μ = 10 centipoises. Larger deviations between the calculated and experimental values of Δp_3 are observed at $Re_b > 400$; this leads to the tentative conclusion that the bubbling regime changes at this value of Re_b. Under this new regime more satisfactory agreement between experimental and calculated values of Δp_3 is obtained when the coefficients in Equation (27) have the values: A = 0.1, B = 0.1, k = 0.25, c = 0.33, but even here, with small absolute deviations in the value of Δp_3, the relative error is in the range of ±30%; this may be due to the influence of the criterion of geometrical similarity (Γ). In most cases the influence of the criterion of geometrical similarity is not great; this is confirmed, in particular, by the results of Aksel'rod [9], who noted that the geometrical dimensions of an absorber have no appreciable influence on the hydrodynamics of bubbling.

It must also be taken into account that with liquid layers of H < 5-10 cm and at high gas rates the hydrodynamic resistance in bubbling is appreciably influenced by the foam, the resistance of which must be correlated with the surface tension σ. It seems likely that under such conditions, i.e., in presence of a relatively high resistance of the foam itself, as shown by Aksel'rod [9], it is necessary to introduce the ratio $\frac{\mu}{\sigma}$ into the equation for calculation of Δp_3. Our calculated and experimental data show that for layers of H > 10 cm the influence of σ may be disregarded, especially as it is taken into account in determination of the total hydraulic resistance of the entire bubbling device in the form of the quantity Δp_2; the equations (27) and (28) are suitable for such calculations.

SUMMARY

1. Bubbling mechanism in liquids of viscosity μ = 1-80 centipoises with layer heights H > 10 cm is discussed. It is shown that the viscosity must be one of the most important factors determining the hydrodynamics of bubbling, especially in layers of considerable thickness.

2. An equation for determination of hydraulic resistance in bubbling is derived from an experimental fuctional relationship with the aid of the theory of dimensions.

3. It is shown experimentally that the bubbling process in liquids of low and high viscosity differs sharply; the hydraulic resistance of the liquid layer ($1\Delta p_3$) has been determined for different viscosities and specific air rates.

4. Experimental and calculated values of Δp_3 are compared; they are in satisfactory agreement under the conditions of our experiments at H > 10-15 cm, and for the experimental data of certain other workers. The calculation error does not exceed ±15% in most cases.

LITERATURE CITED

[1] V. N. Stabnikov, Trans. Voronezh Chem. Tech. Inst. 3-4 (1939).

[2] V. N. Stabnikov, Chem. Equipment Construction 1, 6 (1938).

[3] V. M. Ramm, Absorption Processes in Chemical Industry [in Russian] (Moscow — Leningrad, 1951).

[4] N. M. Zhavoronkov and I. E. Furmer, Oxygen 5 (1947).

[5] N. P. Usyukin and L. S. Aksel'rod, Oxygen 1 (1952).

[6] L. S. Aksel'rod and V. V. Dil'man, Oxygen 5 (1952); 1 (1954).

[7] L. S. Aksel'rod and V. V. Dil'man, Chem. Ind. 1 (1954).

[8] L. S. Aksel'rod and V. V. Dil'man, J. Appl. Chem. 27, No. 5 (1954). *

[9] L. S. Aksel'rod and V. V. Dil'man, J. Appl, Chem. 29, No. 12 (1956).*

[10] M. E. Pozin, I. P. Mukhlenov, E. S. Tumarkina, and E. Ya. Tarat, The Foam Method for Treatment of Gases and Liquids [in Russian] (Leningrad, 1955).

[11] M. É. Aérov and E. P. Darovskikh, Chem. Ind. 2 (1957).

[12] N. P. Zrelov, Trans. Hydraulics Lab. All-Union Sci. Res. Inst. Water Supplies and Hydrogeology, 4 (Moscow, 1955).

[13] A. G. Kasatkin, Principal Processes and Equipment of Chemical Technology [in Russian] (Moscow,1955).

Received August 13, 1957.

*See C. B. Translation.

INTERFACIAL TENSION IN CERTAIN SULFIDE–SILICATE SYSTEMS AT A HIGH TEMPERATURE

V. L. Kheifets and A. B. Sheinin

Planning and Scientific Research Institute of the Nickel, Cobalt, and Tin Industry

Investigations of surface properties of fused systems are of great theoretical and applied significance, but they involve serious experimental difficulties. This is especially true for measurements of interfacial tension at the boundary between two liquid phases.

The sessile-drop method generally used for measurement of interfacial tension between two liquid phases has a number of defects [1]. Moreover, the applicability of this method is limited by difficulties in the choice of a material stable with respect to both liquid phases at high temperatures.

In the present investigation a new method, based on measurement of the angle of contact between the two phases, was used for determination of the interfacial tension σ at the boundary between two liquid phases (Curves 1 and 2; Fig. 1).

It is evident that

$$\sigma_{12} = \frac{\sigma_{13} - \sigma_{23}\cos\varphi_1}{\cos\varphi_2}\,. \quad (1)$$

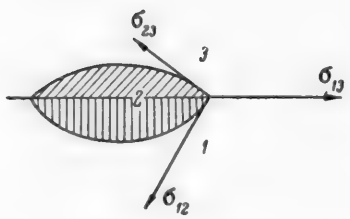

Fig. 1. Method for determination of interfacial tension between two liquids: 1, 2) liquid phases, 3) gas phase.

The values of the surface tension at the liquid–gas interfaces (σ_{13} and σ_{23}) can be found experimentally. The angle φ_1 can also be measured directly. If the drop is small enough, both its parts (the part projecting from the heavier liquid, and the part immersed in it) are close to spherical segments in shape. Taking this fact and the law of Archimedes into account, we can calculate the angle from the equation

$$\frac{\tan\frac{\varphi_1}{2}\left(3+\tan^2\frac{\varphi_1}{2}\right)}{\tan\frac{\varphi_2}{2}\left(3+\tan^2\frac{\varphi_2}{2}\right)} = \frac{D}{d} - 1, \quad (2)$$

where d and D are the densities of the light and heavy liquid respectively.

If the values of σ_{13}, φ_{23}, σ_1 and φ_2 are known, the interfacial tension σ_{12} at the boundary between the two liquids can be calculated from Equation (1).

A similar idea formed the principle of the method used by Mikiashvili, Samarin, and Tsylev [2, 3] for determination of interfacial tension between liquid iron and slag. However, they considered only the visible part of the contact angle (Fig. 1), and this must influence the calculated results.

---

* φ_1 and φ_2 are angles formed with the horizontal plane by the vectors σ_{23} and σ_{12} respectively.

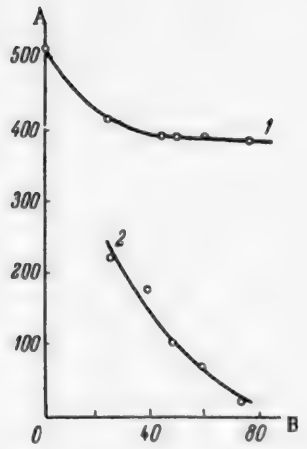

Fig. 2. Surface tension of fused sulfides (σ_{13}) and interfacial tension at the fused sulfide–iron orthosilicate boundary (σ_{12}): A) σ, B) iron sulfide content of melt; 1) σ_{13}, 2) σ_{12}.

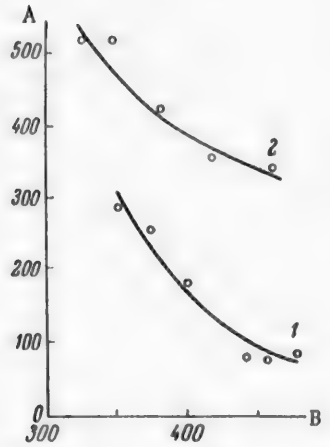

Fig. 3. Dependence of interfacial tension at the matte – slag boundary (σ_{12}) on the surface tension of the slag (σ_{13}). A) σ_{12}, B) σ_{23}; 1) slags with ratio $\frac{FeO}{CaO} < 1$, 2) slags with ratio $\frac{FeO}{CaO} > 1$.

In the present investigation we studied fused systems of the matte–slag type, significant in nonferrous metallurgy. Surface tension at slag–gas and matte–gas boundaries was measured by the maximum gas-bubble pressure method [4,5]. Nickel capillaries 0.5-1.0 mm in diameter and iron crucibles were used in experiments on slags, and quartz capillaries 1-2 mm in diameter and Alundum (or sometimes porcelain) crucibles in experiments on mattes. The gas was oxygen-free nitrogen in both cases. For surface tension at slag–gas boundaries literature data [6,7] determined by the ring method, and confirmed by us by the maximum bubble pressure method, were also used. All the determinations were carried out at 1300°.

The angle φ_1 was measured as follows. A weighed sample of matte in a graphite boat was melted in a Silit tubular furnace through which thoroughly purified nitrogen was blown; a small briquet of slag weighing 0.2-0.5 g was then placed on the matte surface, and melted instantly. The system was kept in a stream of nitrogen for about 30 minutes at 1300°; an image of the slag drop on the matte surface was then projected by means of a long-focus lens onto a screen, and drawn. The image was approximately 10 times the size of the drop.

The densities of the slags and mattes were calculated from the densities of the pure components at room temperature, on the principle of additivity of specific volumes. In the case of SiO_2, the density of tridymite was taken, as this is the silica modification stable at the experimental temperature. Comparison with the experimental values available for some slags showed that the error in this method of calculation does not exceed 3%.

The error in determinations of interfacial tension in duplicate experiments was usually 5-10%.

Fig. 2 shows experimental data for the influence of the composition of the sulfide phase on its surface tension and on interfacial tension at the boundary between a melt of iron and nickel sulfides and iron orthosilicate. Both values decrease with increase of iron sulfide content in the melt, and the interfacial tension decreases considerably more rapidly. This variation is quite consistent with the fact that iron sulfide is more soluble than nickel sulfide in the slag.

Quite similar relationships, in the quantitative sense, were found by Sryvalin, Esin and Nikitin [8,9] for the systems Cu_2S–FeS and Cu_2S–Ni_3S_2 at the boundary with slag.

In Fig. 3, values of interfacial tension at the sulfide melt–slag boundary are compared with the surface tension of slag. The interfacial tensions were calculated from our data on the surface tension of mattes and slags, and values of φ_1 determined by Vanyukov and Ivanov [10]. The matte was of the same composition in all experiments: 20.3% Ni, 53.4% Fe, 25% S. The surface tension of slags, as numerous experimental data [6,7] show, depends mainly on their silica content; the higher the silica content, the lower is the surface tension of the slag. Therefore the data in Fig. 3 give an indication of the influence of slag composition on the interfacial tension at the slag–sulfide melt boundary. The more silica in the slag (i.e., the more acid it is), the lower is the surface tension. Replacement of CaO in the slag by FeO increases interfacial tension.

These results can be used in an examination of the losses of nickel with slags during smelting. These losses

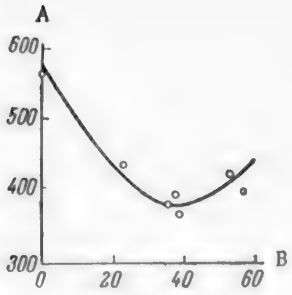

Fig. 4. Surface tension of iron–nickel mattes of constant sulfur content; A) σ_{12}, B) iron content (atomic %).

are mainly due to two causes: chemical interaction between matte and slag, and mechanical loss of matte beads trapped in the slag. The extent of the "mechanical" losses depends considerably on interfacial tension at the matte–slag boundary. * A high interfacial tension favors aggregation of matte beads and therefore tends to reduce losses. By increasing the interfacial tension at the matte–slag boundary in some way, the losses of nickel with slag can be reduced.

It follows from Fig. 3 that losses of nickel with slag increase with increasing acidity of the slag. This result is quite consistent with smelting practice.

It was noted above that the surface tension of matte varies symbatically with interfacial tension at the matte–slag boundary (Fig. 2). Therefore data on the surface tension of mattes can be used for considering the question of nickel losses. Fig. 4 shows our data for one section of the Ni–Fe–S ternary diagram corresponding to a constant sulfur content (18%). This sulfur concentration is usual in industrial nickel mattes.

It is clear from Fig. 4 that in the composition range typical for nickel mattes (50-60% atomic % Fe) the surface tension increases with decrease of nickel content in the matte. The interfacial tension at the matte–slag boundary should increase, and therefore "mechanical" losses with slag should decrease with decrease of the nickel content of the matte. This result is also fully confirmed by experience in nickel smelting.

LITERATURE CITED

[1] R. E. Boni and G. Derge, J. of Metals, 8, 53 (1956).

[2] Sh. M. Mikiashvili, A. M. Samarin, and L. M. Tsylev, Bull. Acad. Sci. USSR, Div. Chem. Sci. 4, 54 (1957).

[3] Sh. M. Mikiashvili, L. M. Tsylev, and A. M. Samarin, Physicochemical Principles of Steel Production [in Russian] (Izd. AN SSSR, Moscow, 1955). p. 423.

[4] F. Jaeger, Z. anorg. allg. Chem. 101, 1 (1957).

[5] N. K. Adam, Physics and Chemistry of Surfaces (State Tech. Press, 1947) [Russian translation].

[6] P. P. Kozakevich and A. F. Kononenko, J. Phys. Chem. 14, 1118 (1940).

[7] T. B. King, J. Soc. Glass Techn. 35, 241 (1951).

[8] I. T. Sryvalin, O. A. Esin, and Yu. P. Nikitin, Trans. Ural Polytech. Inst. 49, 95 (1954).

[9] I. T. Sryvalin, Yu. P. Nikitin, and V. V. Khlynov, Trans. Ural Polytech. Inst. 67, 64 (1957).

[10] A. V. Vanyukov and G. F. Ivanov, Coll. Sci. Trans. Ministry Nonferrous Metals and Gold 25, 90 (1955).

Received February 18, 1958.

* The mechanical losses are also influenced by the viscosity of the slag, but this influence is less important, as it can be diminished by an appropriate change of furnace temperature.

PREPARATION AND CERTAIN PROPERTIES OF THIN SILICA DIELECTRIC FILMS

N. N. Tvorogov

Thin layers of various substances are extensively used in modern science and technology. They are used in beneficiation of minerals, in metallography; in modern radio engineering and electronics for production of photocells, rectifiers, capacitors, high resistances; in optics for preparation of new types of lenses and filters; in modern electron microscopy, etc. The uses and methods of preparation of thin layers and measurement of their thickness, are described in adequate detail in a book [1].

In connection with a study of the autoemission of dielectrics we had the problem of preparing metal points coated with thin, dense, and uniform layers of silica. The production of thin silica films by vacuum dispersion is a fairly difficult task, as this process involves the use of high temperatures (of the order of 1800°). The purity of the films so obtained depends on the purity of the quartz, which does not always conform to the experimental requirements.

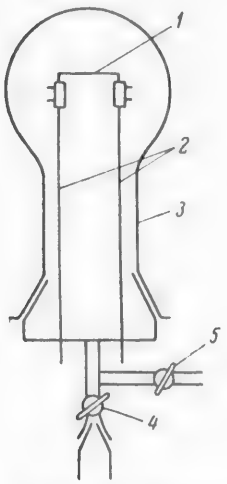

Fig. 1. Reaction vessel for coating metal surfaces with films of SiO_2 formed by decomposition of ethyl orthosilicate: 1) wire for coating; 2) molybdenum leads; 3) quartz flask; 4) stopcock for trap with ethyl orthosilicate; 5) stopcock between flask and pump.

A short paper [2] was published in 1949, in which it was reported that thin silica films can be prepared by dissociation of ethyl orthosilicate $(OC_2H_5)_4Si$ on metal supports heated to a definite temperature. The author studied the formation of silica films on nickel supports only. Up to 800° silica was not formed. SiO_2 was formed fairly rapidly only at 900-1100°. The paper contains a curve for the effect of temperature on the growth rate of a SiO_2 layer on a nickel support.

We studied the conditions of formation of silica by the decomposition of ethyl orthosilicate at heated tungsten and molybdenum wires (d = 100 μ) and at Nichrome and tungsten plates, in the apparatus shown in Fig. 1. The wire 1 was first etched electrochemically in an alkaline solution and then fixed between the molybdenum leads 2. The quartz bulb 3 was evacuated down to 10^{-4} mm, and the wire was heated at a temperature of the order of 1200-1300°. The stopcock 4 was then opened and the stopcock 5 closed, and tetraethyl silicate vapor was admitted into the bulb 3. The wire was kept for some time in the vapor at a definite temperature. The temperature was measured by means of the OPIR-9 pyrometer, and the thickness of the layer by the IKV optimeter fitted with an additional device (specimen inserter) whereby the wire thickness could be measured both before and after application of the SiO_2 layer. With this device, the measurements could be made to within 1% with wires 100 μ thick. The wire thickness was measured 5-8 times at points one millimeter apart over a length of 7 mm. The average thickness was found from all these results. The course of coating of a molybdenum wire as a function of time was studied at 920, 1000, 1150, and 1200°. Up to 850° there was almost no SiO_2 formation. In the 900-1200° range a silica film is formed rapidly (Table 1).

The data in Table 1 were used to plot curves for the thickness of the

SiO_2 layer as a function of the support heating time at different temperatures (Fig. 2). The probable cause of the scattering of the points is errors in measurements of the support temperatures as the formation of SiO_2 greatly depends on the temperature.

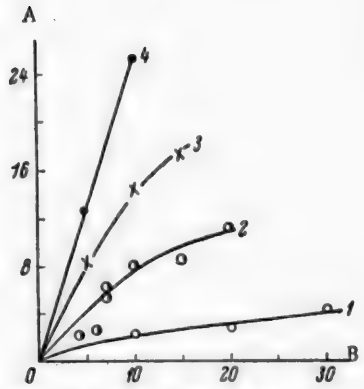

Fig. 2. Curves for variation of the thickness of SiO_2 layers with the heating time of molybdenum wire at different temperatures: A) layer thickness (μ), B) time (minutes); temperature (°C): 1) 920, 2) 1000, 3) 1150, 4) 1200.

It is seen in Fig. 2 that the slope of the curve for the layer thickness as a function of time shows an appreciable progressive decrease at each temperature. As the measurements of the support temperature were unreliable, it cannot be definitely decided whether this is due to decrease of temperature with increasing thickness of the silica layer or to decrease of the catalytic effect of the support.

Table 2 contains the results of consecutive measurements of the thickness of the SiO_2 layer, performed by means of the optimeter, at the same point on a molybdenum wire coated with silica.

These results show that with thicker films there are greater variations between the results of consecutive measurements of layer thickness at the same point. This indicates that the layer becomes more loose as it grows in thickness.

In some instances (more often with molybdenum) undesirable transparent SiO_2 dendrites were formed.

The results of spectrum analysis showed that the films were free from impurities. Absence of crystalline silica was demonstrated by x-ray analysis with the URS-55 unit (CuK α-radiation; $\underline{d}$ of camera 57 mm; thickness of SiO_2 layer 1μ on copper and 10μ on molybdenum wire).

Silica films were also made on Nichrome and tungsten plates (60× 15× 0.1 mm). The results are given in Table 3.

TABLE 1*

Effects of Heating Time and Temperature of the Support on the Thickness of SiO_2 Films Formed on Molybdenum Wire.

920°		1000°		1150°		1200°	
Support heating time (min)	Layer thickness (μ)	Support heating time (min)	Layer thickness μ	Support heating time(min)	Layer thickness μ	Support heating time(min)	Layer thickness μ
10	2.4	4	2.3	5	8.3	5	12.5
20	3.0	6	2.8	10	14.5	10	25.4
30	4.6	7	6.4 5.9	15	17.5	—	—
—	—	10	8.4	—	—	—	—
—	—	15	8.6	—	—	—	—
—	—	20	11.5	—	—	—	—

*Microscopic observations showed that the silica layer is more uniform on tungsten than on molybdenum wire. Quantitative data on film thickness distribution on tungsten surfaces are not given, as the layer thickness could not be measured with the optimeter owing to the brittleness of tungsten wire.

The layer thickness was calculated from the formula

$$h = \frac{\Delta P}{S \cdot d},$$

where ΔP is the weight of silica on the support, S is the surface area of the coating, and d is the density of silica.

Comparison of the data in Tables 1 and 3 shows that the decomposition rate is much lower on Nichrome than on molybdenum or tungsten supports.

TABLE 2

Results of Consecutive Measurements at One Point of a Wire Coated with SiO_2

Consecutive measurements	Film thickness (μ)				
	10 minutes			20 minutes	
	920°	1000°	1150°	920°	1000°
1	2.4	8.5	15.2	3.0	12.5
2	2.4	8.4	14.7	3.0	11.1
3	2.4	8.0	14.5	3.2	10.7
4	—	8.0	—	—	—

TABLE 3

Effects of Heating Time and Temperature of the Support on the Thickness of Layers on Nichrome and Tungsten Plates

Support material	Coating temperature (°C)	Coating time (min)	Layer thickness (μ)
Nichrome	980	15	0.13
	1050	30	0.39
	1050	40	0.47
	1100	15	0.39
	1100	30	0.65
	1100	35	0.60
Tungsten	1050	15	0.63
	1050	30	1.6

SUMMARY

1. Appreciable formation of silica by decomposition of ethyl orthosilicate vapor on heated molybdenum, tungsten, and Nichrome supports occurs only at temperatures of the order of 900° and over.

2. Data on variations of the thickness of SiO_2 layers with heating time at different temperatures are presented. The formation rate of SiO_2 greatly depends on the temperature and the support material. It is lower with Nichrome than with molybdenum or tungsten.

3. The density of the layer and the uniformity of its thickness over the surface decrease with increasing thickness.

In conclusion, I thank Ya. S. Savitskaya for her interest and help in presentation of this paper.

LITERATURE CITED

[1] S. Methfessel, Dunne Schichten, Halle (Saale) Knapp (1953).

[2] H. B. Law, Rev. Sci. Inst. 20, 5, 958 (1949).

Received January 8, 1958.

STABILITY OF ELECTROLYTE FOAMS

V. G. Gleim, I. K. Shelomov, and B. R. Shidlovskii

Chair of Chemistry, Rostov-on-Don Institute of Railroad Transport Engineers

Problems relating to the stability of electrolyte foams can be examined in the light of the theoretical concepts developed in our earlier papers [1, 2].

Investigations of foam stability in the surface-active region of the $\sigma - C$ diagram lead to the conclusion that the increase of the average bubble life (as compared with distilled water) observed in this region is due to a peculiar energy "skewness" between the surface and volume of the solution. At the solution–gas (vapor) interface there is a sharp decrease in the energy of intermolecular action as the result of adsorption processes. At the same time the potential energy of fixation of the molecules within the volume of the liquid changes very little. The same considerations are applicable to solutions of surface-inactive substances. Here the energy of intermolecular action changes more rapidly within the solution than at the liquid surface. Since the volume of the solution is many times as great as the volume of the surface layer, the energy of intermolecular action must alter little with small concentrational changes, and therefore the influence of concentration on film strength must be considerably less with surface-inactive substances (electrolytes) than with surface-active substances.

For the range of solutions with which we are concerned, and in particular for dilute electrolyte solutions, adsorption can be calculated with the aid of the Gibbs equation in the form proposed by Semenchenko [3]:

$$\Gamma_1 = \frac{V_2(1 - V_1C_1)C_1}{V_2 + V_1(V_1 - V_2)C_1} \cdot \frac{G}{RT}, \tag{1}$$

where C is the concentration, V is the molar volume, and G is the surface activity; the subscript 1 corresponds to the solvent (water) and the subscript 2 to the solute (salt).

For dilute electrolyte solutions evidently $C_1 \gg C_2$.

Disregarding C_2, we may assume $C_1 \approx \frac{1}{V_1}$ or $V_1 \approx \frac{1}{C_1}$.

Substitution of this value of V_1 into Equation (1) gives

$$\Gamma_1 \approx 0. \tag{2}$$

It was shown earlier [2] than the work of adsorption can be expressed in the form

$$\varphi = RT\Gamma \ln\left(\frac{\Gamma \cdot 1000}{\beta \cdot C} + 1\right). \tag{3}$$

With the previous notation [2] $\Psi = \frac{\sigma + \varphi}{3\sigma + 2\varphi}$ which gives $\varphi = 0$ and $\Psi = \frac{1}{3}$.

Then the ratio of the energy of rupture of a film of the solution W_{cr}^{s} to the corresponding value for water $W_{cr}^{H_2O}$, established by us earlier [2], becomes

$$\frac{W_{cr}^{s}}{W_{cr}^{H_2O}} = \frac{\sigma_s}{\sigma_{H_2O}} . \qquad (4)$$

Thus, in the surface-inactive region, film strength is directly proportional to the coefficient of surface tension.

It was necessary to develop a special method of investigation for experimental verification of Equation (4) as film strength or bubble life at the interface are very small for electrolyte solutions.

The method proposed by Shidlovskii for investigation of film strength in these liquids is as follows.

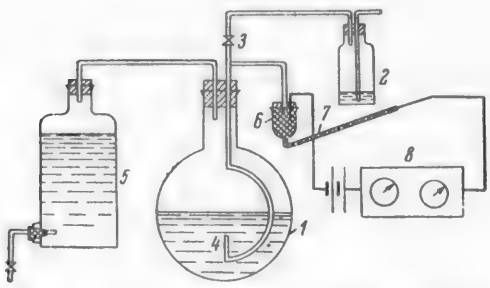

Fig. 1. Apparatus for determination of average bubble life.

Bubbles of gas (air, vapor) are generated at the liquid–gas interface in such a manner that there is only one bubble at the surface at any given instant. If n bubbles are generated in t seconds, then the average life of a bubble is

$$\tau_{av} = \frac{t}{n} \text{ sec.}$$

The apparatus designed for these determinations is shown in Fig. 1. The experimental procedure is as follows.

The test solution is contained in the vessel 1. Air is washed in the flask 2 and passes through the valve 3, which controls the air rate, into the capillary 4 and then

TABLE 1

C (meq/liter)	Average life of bubble τ_{av} at solution surface (seconds)				
	$MgSO_4$	NaCl	Na_2SO_4	NaOH	Na_2CO_3
0	0.20	0.20	0.20	0.20	0.20
100	0.28	0.33	0.37	0.77	0.50
200	0.35	0.63	0.59	0.90	0.80
300	0.44	0.87	0.84	1.00	0.96
500	0.50	1.27	1.24	1.51	1.45
750	—	1.42	1.50	1.43	1.50
1000	—	1.48	1.48	1.60	1.54

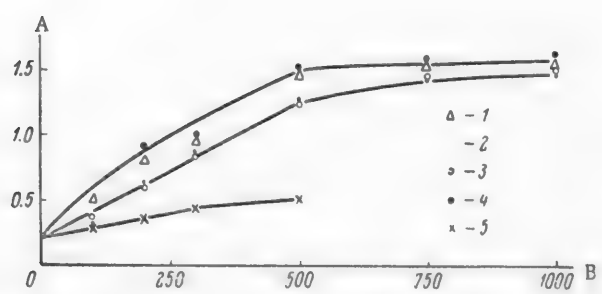

Fig. 2. Bubble stability in solutions of different electrolytes: A) average bubble life τ_{av} (seconds), B) solution concentration (meq/liter); 1) Na_2CO_3, 2) NaCl, 3) Na_2SO_4, 4) NaOH, 5) $MgSO_4$.

TABLE 2

Solution	C (meq liter)	$\frac{w^s_{cr}}{w^{H_2O}_{cr}}$	τ_{av} (sec)	log τ_{av}
$MgSO_4$	0	1.000	0.20	—0.70
	100	1.001	0.28	—0.55
	200	1.004	0.35	—0.46
	300	1.005	0.44	—0.36
	400	1.006	0.48	—0.32
	500	1.007	0.50	—0.30
NaCl	0	1.000	0.20	—0.70
	100	1.002	0.38	—0.42
	200	1.005	0.60	—0.22
	300	1.007	0.85	—0.07
	400	1.009	1.08	0.03
	500	1.012	1.27	0.10
NaOH	0	1.000	0.20	—0.70
	100	1.002	0.60	—0.22
	200	1.005	0.84	—0.07
	300	1.007	1.04	0.02
	400	1.009	1.24	0.09
	500	1.012	1.45	0.16

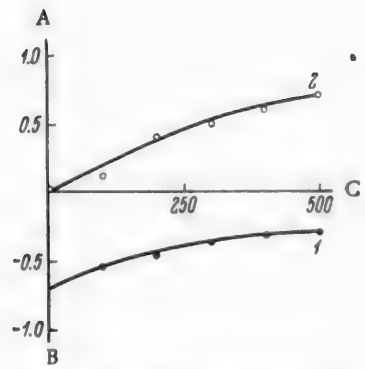

Fig. 3. Film strength (theoretical) and bubble stability (experimental) in $MgSO_4$ solutions: A) log of bubble life (log τ_{av}), B) film strength $\left(\frac{w^s_{cr}}{w^{H_2O}_{cr}}\right)$; C) solution concentration (meq/liter); curves: 1) log τ_{av}, 2) film strength.

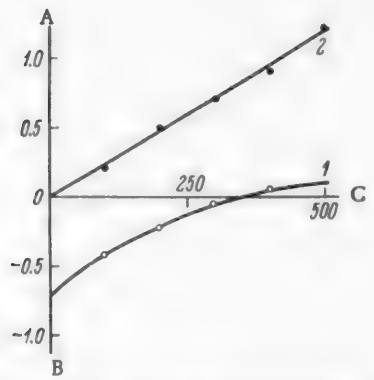

Fig.4.Film strength (theoretical) and bubble stability (experimental) in NaCl solutions: A) log of bubble life (log τ_{av}), B) film strength, C) solution concentration (meq/ liter); curves: 1) log τ_{av}, 2) film strength.

in the form of bubbles to the surface of the solution. (Air is drawn out of the vessel 1 by means of the aspirator 5.) The capillary 4 is connected to the contact manometer 6. A rack (not shown in the diagram)serves to regulate the mercury level in the inclined capillary 7 of the manometer. The circuit is broken during the formation of each bubble. After the bubble has become detached, the circuit is closed owing to increase of pressure in the capillary 4. The electric pulse is recorded by means of the pulse counter 8. The vessel 1 is contained in a thermostat.

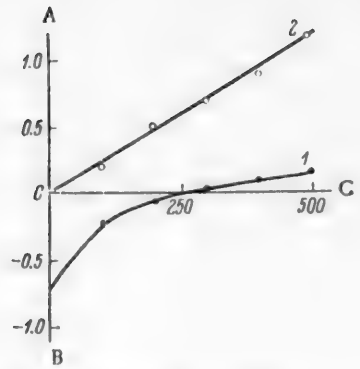

Fig.5. Film strength (theoretical) and bubble stability (experimental) in NaOH solutions: A) log of bubble life (log τ_{av}), B) film strength, C) solution concentration (meq/liter); curves 1) log τ_{av}, 2) film strength.

The average bubble life τ_{av} was determined for the following compounds: NaCl, Na_2SO_4, NaOH, Na_2CO_3 and $MgSO_4$. The solution concentrations were varied from 0 to 1000 meq/liter. The determinations were performed at 20°. It should be noted that complete reproducibility of the results was attained only after the most throrough measures had been taken to prevent contamination of the solution by traces of surface-active substances and colloids.

The results are given in Table 1 and Fig. 2.

It follows from these data that bubble stability, which remains small in absolute magnitude, increase with concentration. At a concentration of about 500 meq/liter, breaks are found on the τ_{av}–C curves for most of the solutions, beyond which the rate of increase of τ_{av} is less.

It may be assumed that in this concentration region the decrease of film thickness, demonstrated by Deryagin [4], begins have an influence. Our results show that at concentrations up to 500 meq/liter this effect may be ignored.

These results also demonstrate the influence of solution pH on the average bubble life (i.e., film strength). The greatest film strength is found with substances which make the solution alkaline (NaOH and Na_2CO_3). This should probably be attributed to interaction of hydroxyl ions with water molecules. For verification of Equation (4) the calculated values of $\frac{W^{s}_{cr}}{W^{H_2O}_{cr}}$ were compared with experimental values of log τ_{av} (t = 20°).

The results for solutions of $MgSO_4$, NaCl and NaOH are presented in Table 2 and Fig. 3-5.

SUMMARY

Experimental results show that film stability increases with increase of pH of the medium.

Consideration of the data leads to the conclusion that Equation (4) correctly represents variations of film strength (bubble life) with concentration of electrolyte solutions.

The above theoretical and experimental data therefore show that the stabilization mechanism of gas (vapor) bubbles is the same in the surface-active as in the surface-inactive region, and is determined by adsorption effects which give rise to an energy "skewness" or change in the energy of intermolecular action in the surface layer for solutions of surface-active substances, and in the volume of the liquid for solutions of surface-inactive substances. This change is considerably greater in the former case than in the latter.

The foregoing considerations are in good agreement with Durov's extensive experimental data [5].

LITERATURE CITED

[1] V. G. Gleim, B. R. Shidlovskii, and I. K. Shelomov, J. Appl. Chem. 32, No.1, 218 (1959).*

[2] V. G. Gleim and I. K. Shelomov, J. Appl. Chem. 32, No. 4, 770 (1959).*

[3] V. K. Semenchenko, Surface Phenomena in Metals and Alloys [in Russian] (GITTL, 1957).

[4] B. V. Deryagin, Bull. Acad. Sci. USSR 5, 1119 (1938).

[5] S. A. Durov, Physicochemical Principles of Foam Priming of Boiler Water [in Russian] (1948).

Received October 7, 1957.

*Original Russian pagination. See C. B. translation.

A STUDY OF THE OXIDATION OF ALUMINUM POWDER IN AQUEOUS ALCOHOLIC SOLUTIONS

L. I. Virin

The surface of metallic aluminum is always coated with a dense oxide layer, which confers high corrosion resistance to aluminum.

To increase the resistance of aluminum to various corrosive media, thicker and stronger films are produced artificially on its surface. These films may consist of amorphous aluminum hydroxide, crystalline modifications of $Al_2O_3 \cdot H_2O$ – bayerite or boehmite – or anhydrous aluminum oxide. Such films are made by chemical or electrochemical treatment (anodizing). The production and properties of these films have been extensively studied and have been described, for example, in Akimov's book [1], in Altenpohl's review article [2], etc. Nevertheless, when we were faced with the task of surface oxidation of fine aluminum powder we found that the great majority of the known methods are inapplicable for this purpose. In general, the thickness of the films obtained by these methods was greater than the thickness of the powder sales (0.6 μ for PAK-3).

The problem of surface oxidation of aluminum powder arose in connection with the production of colored aluminum powders for decorative and other purposes. The problem was solved by oxidation of aluminum powder in boiling aqueous alcohol solutions. This method gives thin and strong oxide films on the surface of aluminum powder.

The oxide film is formed in this process as the result of interaction between aluminum and water, which may be represented by the equation:

$$2Al + (3 + n)\,H_2O = Al_2O_3 \cdot nH_2O + 3H_2. \qquad (1)$$

The role of alcohol is to retard this reaction. Thus, in boiling pure water almost all the aluminum powder is converted into hydroxide in a few minutes; by varying the alcohol concentration we can influence the rate of the oxidation reaction and control very accurately the thickness of the film formed.

EXPERIMENTAL

Mixtures of water and ethyl alcohol, containing from 20 to 35% of water by weight, were used.

Aluminum powder of PAK-3 grade (GOST 5491-50), containing about 3.5% of stearic acid, was degreased by boiling in acetone before the experiments, to a final grease content of 0.9-1%. Usually 100 g of water–alcohol mixture was taken per 5 g of aluminum powder in each experiment. The experiments were conducted at the boiling point in a vessel under a reflux.

The rate of Reaction (1) was estimated from the volume of hydrogen collected in a gas buret.

Fig. 1 shows curves for the variation of gas volume with time for four different initial concentrations of water in the water–alcohol mixture. The curves are characteristically S-shaped. This form of the curve shows that the process can be tentatively divided into 3 stages: the induction stage, with very slow liberation of hydrogen at an almost constant rate; the kinetic stage, with turbulent liberation of hydrogen at a continuously-increasing rate; and the diffusion stage, in which the reaction dies down, with its rate decreasing continuously. These three stages are revealed especially clearly in a plot of the reaction rate against time (Fig. 2).

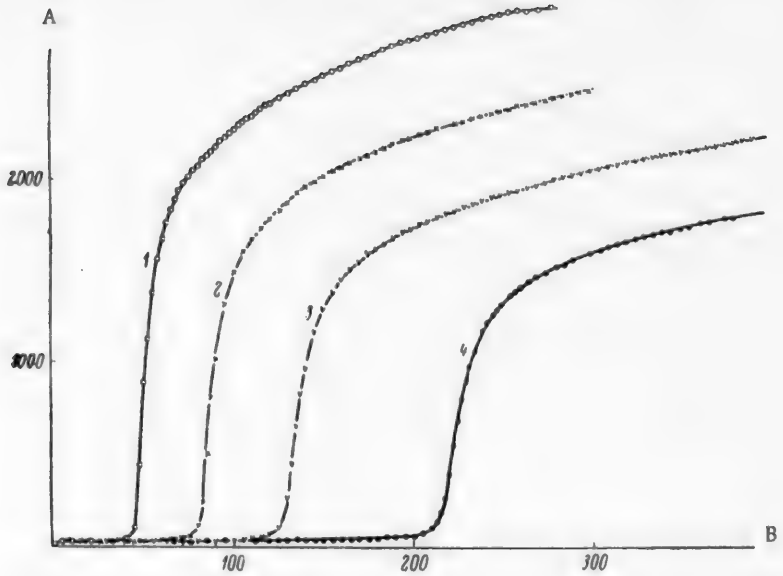

Fig. 1. Course of the oxidation reaction in aqueous alcohol solutions with different initial concentrations of water: A) volume of liberated hydrogen, reduced to standard conditions (in ml), B) time (minutes); water contents (%): 1) 35, 2) 30, 3) 25, 4) 20.

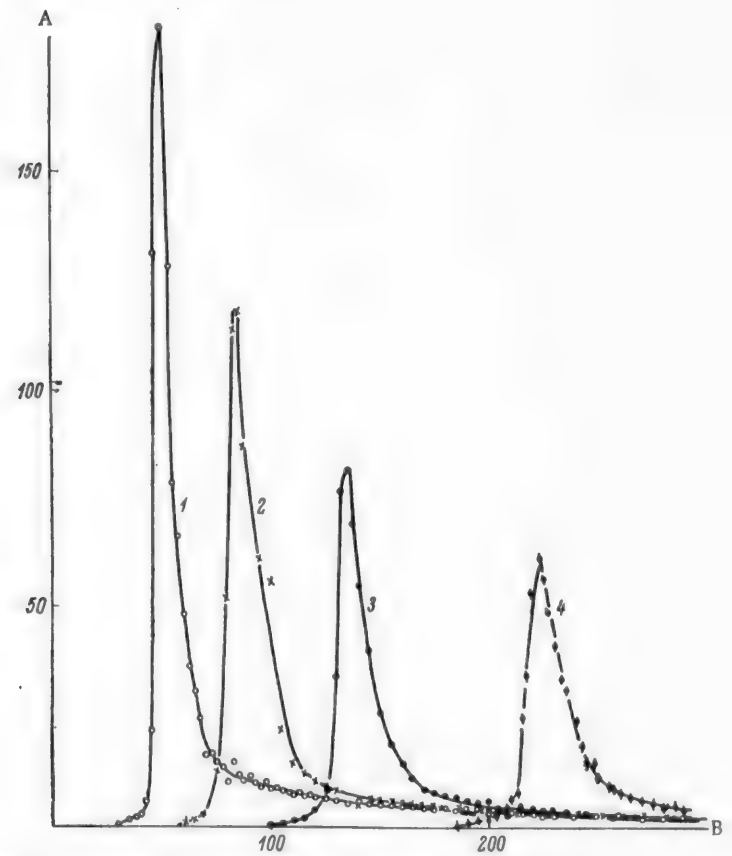

Fig. 2. Variation of oxidation rate with time: A) oxidation rate, calculated from the volume of liberated hydrogen under standard conditions (ml/min); B) time (minutes); water contents (%): 1) 35, 2) 30, 3), 25, 4) 20.

This course of the process may be explained as follows.

The aluminum powder is covered with a layer of stearic acid (3.5%). This layer cannot be removed completely by the usual methods. As reported by Trillat [5], an aluminum stearate film which is not washed away by solvents is formed on the metal surface. After threefold boiling (2 hours each time) in acetone, about 1% of stearic acid remains on the powder. This corresponds to roughly a trimolecular layer on the very extensive surface of the powder (12,200 cm^2/g). It is probable that a thicker multilayer exists on some regions of the surface, and a monolayer on others. Possibly there are also regions entirely free from the grease film.

Oxidation of the metal can be affected only by water molecules which have diffused through this hydrophobic film, and therefore the reaction rate is determined by the rate of diffusion, which is very low and almost constant under these conditions.

Dissolution of the metal leads to appreciable anodic polarization of its surface; this lowers the contact angle and assists degreasing, as has been demonstrated [4,5]. The liberated hydrogen bubbles detach the grease molecules from the metal and "float" them. When the surface has been degreased in this manner, oxidation becomes more rapid. When a considerable proportion of the surface has been freed from the stearic acid film by the liberated hydrogen, the process passes from the induction to the kinetic stage.

Oxidation of aluminum is accompanied by considerable evolution of heat, which increases the reaction rate.

However, as oxidation proceeds, the surface becomes coated with a dense film of more or less hydrated aluminum oxide. This film (of thickness 0.05μ and over) retards the reaction and the process passes into the slower diffusional stage.

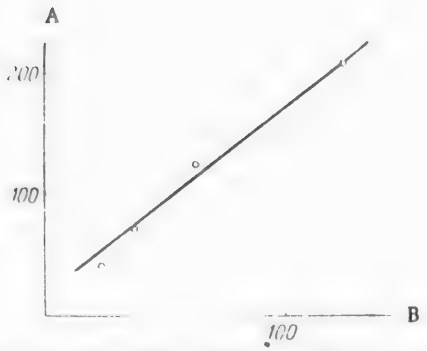

Fig. 3. Variation of the length of the induction period (τ) with the initial concentration: A) τ (minutes), B) values of $\frac{1}{C^3_{H_2O}}$.

At this stage the rate of the process is determined by the the rate of diffusion of the reacting substances through the oxide film.

It follows from Fig. 1 that the amount of oxidized aluminum, i.e., the film thickness, depends on the concentration of water—the higher the concentration of water, the more active and deeper is the reaction.

The rate of the reaction

$$2Al + 3H_2O = Al_2O_3 + 3H_2 \qquad (2)$$

must be proportional to the cube of the water concentration:

$$W \cong K \cdot C^3_{H_2O}. \qquad (I)$$

The duration τ of the induction period is inversely proportional to the reaction rate

$$\tau = \frac{1}{W} \cong K_1 \cdot \frac{1}{C^3_{H_2O}}. \qquad II)$$

The data in Fig. 3 fully confirm this relationship.

The formation of a dense oxide film in our experimental conditions occurs considerably before any appreciable decrease of the water concentration. Therefore increase of the volume of the water—alcohol mixture per unit weight of aluminum should not influence appreciably the course of the reaction.

This was confirmed by the experiments; two- and fivefold increases of the solution volume decreased the length of the induction period somewhat, probably because of partial dissolution of the grease film.

The experiments were performed with boiling solutions, but the difference between the boiling points for the extreme concentrations (35 and 20%) of water is 2.4°. To eliminate any possible influence of this temperature difference, a series of experiments was carried out at 79° in a thermostat. The results were not significantly different. The relative positions and form of the curves remained the same; decrease of temperature led to some increase of the induction period and decrease of the maximum rate. Therefore the differences in the course of oxidation in mixtures with different water concentrations do not depend on differences of boiling point.

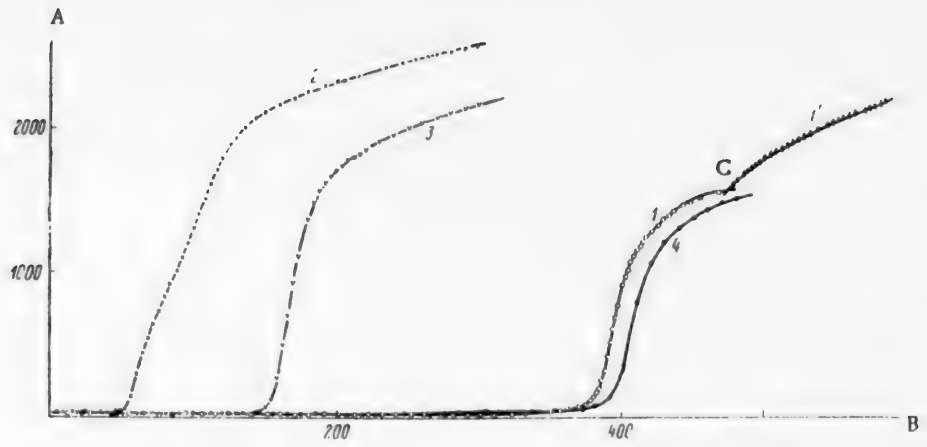

Fig. 4. Effect of addition of water after formation of a film in 20% solution: A) volume of liberated hydrogen, reduced to standard conditions (ml), B) time (minutes); water contents (%): 1) film in solution with 20% water; 1') after addition of water to 35%; C represents the point of addition; 2) 35; 3) 30; 4) 20.

During prolonged storage of degreased powder its surface is oxidized by air, and the resultant oxide layer causes an appreciable lengthening of the induction period. The amount of hydrogen liberated during oxidation decreases, as the aluminum is oxidized under an existing film. This was found in experiments on oxidation of samples of aluminum powder stored for 10 and 37 days respectively.

The following experiment was carried out to investigate the role of the formed film on the subsequent course of the reaction (Fig. 4). 5 g of aluminum powder was treated with a mixture containing 20% water until a film was formed, i.e., until the reaction slowed down; water was then added to the reaction vessel to raise the water concentration to 35%. It is clear from Fig. 4 that the reaction is accelerated appreciably at the instant when water is added, but the course of the reaction is closer to the experiment with 30% rather than with 35% water. This confirmed once again that the water concentration in solution is the main determining factor in the process. The influence of the formed film on the course of the process, demonstrated by this experiment, suggests that the film formed in a solution containing 20% water differs qualitatively from the film formed in a solution with 35% water.

Oxidation of aluminum by water under our experimental conditions, i.e., at temperatures above 78°, may yield either anhydrous aluminum oxide Al_2O_3, or boehmite γ-AlOOH, or amorphous aluminum hydroxide $Al(OH)_3$.

The heats of formation of Al_2O_3, γ-AlOOH and $Al(OH)_3$ are similar (206-203 kcal/mole). Therefore all these reactions are equally probable, but at higher temperatures formation of anhydrous aluminum oxide on the metal surface is to be expected.

A series of experiments was carried out in order to determine the composition of the films formed at different initial water concentrations. The water contents of the initial and final water–alcohol mixtures were determined from the densities to an accuracy of some hundredths of 1%. The amount of water consumed in oxidation of the metal was calculated from the final volume of hydrogen, reduced to standard conditions. Water of constitution was found by difference, and was calculated per mole of aluminum oxide formed.

Increase of the initial water concentration leads to a higher reaction temperature at the metal surface and, as expected, to formation of a film of higher Al_2O_3 content, whereas when the initial concentration of water is 20% a film of almost pure boehmite is formed. In addition to experiments with ethyl alcohol–water mixtures we carried out experiments on oxidation of aluminum powder in isopropyl alcohol–water and acetone–water mixtures (Fig. 5).

Replacement of ethyl alcohol by an equimolar amount of isopropyl alcohol has almost no influence on the course of the reaction. Mixtures with isopropyl alcohol are somewhat more active; for example, a mixture with isopropyl alcohol containing 20.9% of water by weight (Curve 2) acts similarly to a mixture with ethyl alcohol containing 30% of water by weight (Curve 3).

The experiment with acetone–water mixture was not carried out under comparable conditions (the temperature was 61°), but the fact that oxidation took place confirms the hypothesis that alcohol and acetone merely serve to retard the process.

Composition of Oxide Films for Different Initial Water Concentrations in Mixtures with Alcohol

Water concentration (%)		Final volume of hydrogen (ml) under standard conditions	Number of moles of water of constitution per mole of Al_2O_3
initial	final		
19.57	17.98	1440	1.11
20.9	19.26	1460	0.954
20.9	19.57	1385	0.94
30.52	28.54	1990	0.66
34.52	32.37	2385	0.37
34.62	32.39	2285	0.65
35.77	32.02	2360	0.11
35.77	33.62	2340	0.28

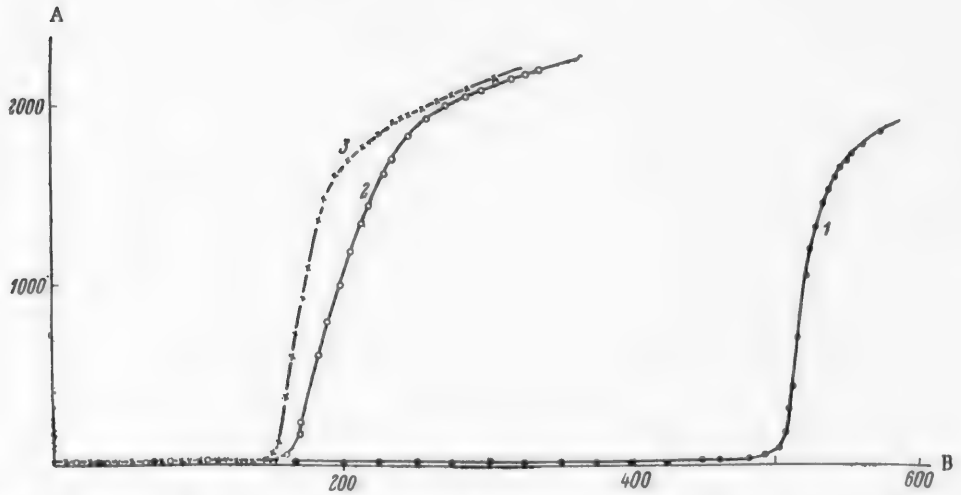

Fig. 5. Results of experiments on oxidation of aluminum powder in water–isopropyl alcohol and water–acetone mixtures: A) volume of liberated hydrogen under standard conditions (ml), B) time (minutes); solution composition (%): 1) water 30, acetone 70; 2) water 20.9, isopropyl alcohol 79.1; 3) water 30, ethyl alcohol 70.

SUMMARY

1. Surface oxidation of aluminum powder in aqueous alcohol solutions proceeds in three stages: electrochemical degreasing of the powder (induction period), active oxidation of aluminum (kinetic period), and retardation of the reaction by the formed oxide film (diffusional period).

2. The reaction rate and the thickness and composition of the oxide film formed are determined by the concentration of water in the mixture, while the alcohol acts only as a diluent and retarding agent.

3. In a mixture containing 35 wt. % of water, a film of anhydrous aluminum oxide is formed. Decrease of the water concentration in the solution leads to an increase of the water content in the film. With 20% water in the solution the film corresponds to boehmite in composition.

4. The effects of temperature, volume of solution, and time of storage of the degreased powder on the course of the process were studied.

5. Experiments on oxidation of aluminum powder in mixtures of water and isopropyl alcohol and water and acetone showed that the organic component of the mixture retards the reaction in all cases.

LITERATURE CITED

[1] G. V. Akimov, Theory and Methods of Investigation of Metal Corrosion [in Russian] (Izd. AN SSSR, 1945).

[2] D. Altenpohl, Metall. 9, 5/6, 164 (1955).

[3] J. J. Trillat, Peintures, pigments, vernis 23, 328 (1947).

[4] B. N. Kabanov, J. Phys. Chem. 4, 5, 549 (1933).

[5] A. N. Frumkin, V. S. Bagotskii, Z. A. Ioffa, and B. N. Kabanov, Kinetics of Electrode Processes [in Russian] (Izd. MGU, 1952).

Received March 28, 1958.

EFFECT OF SULFUR COMPOUNDS ON THE CURRENT EFFICIENCY FOR MAGNESIUM IN THE ELECTROLYSIS OF CARNALLITE

S. A. Pushkareva

It has long been known that magnesium sulfates present as impurities in carnallite lower the current efficiency in electrolysis [1]. This problem was studied quantitatively by Strokan [2], Vasil'ev and Popov [3], and Rudnitskii and Tverdovskii [4]. All these authors state that the possible occurrence of a reaction of the type

$$3MgO + MgSO_4 = 4MgO + S, \quad (1)$$

is the main cause of the decrease of current efficiency. However, until now the question of the behavior of sulfates and other sulfur compounds in the electrolytic production of magnesium from fused salts has not been studied sufficiently.

We studied current efficiency for magnesium in electrolysis of $MgCl_2$ + KCl melts in relation to the concentrations of added $MgSO_4$ and MgS. The experiments were performed in a laboratory cell which consisted of a quartz beaker about 800 ml in capacity, with rod electrodes (Fig. 1). The anode material was graphite, and the cathode was carbonaceous iron. The distance between the electrodes was about 2.5 cm. The cathode area s_c was 8.8 cm^2, and the anode area s_a was 9.6 cm^2. The current densities were: cathode, i_c = 0.57 amp/cm^2; anode, i_a = 0.52 amp/cm^2. The volume current density in the electrolyte i_v = 0.02 amp/cm^2. The anode and cathode spaces were separated by means of a porcelain tube around the anode. The tube was 75 cm long and 4 cm in diameter. About 2% by weight of calcium fluoride was added to the electrolyte. The magnesium chloride content of the melts was in the 27-30% range. The electrolyte temperature was maintained at 700 ± 5°.

All the salts were dehydrated by the usual method before fusion. Before the start of electrolysis the electrolyte was conditioned by the action of direct current at i_c = 0.1 amp/cm^2 for 30 minutes. The additive to be tested was introduced into the electrolyte after this treatment. Each experiment on determination of current efficiency lasted 2-3 hours. Gas was evacuated from the anode and cathode spaces by means of a water-jet pump.

In absence of impurities the current efficiency was stable at about 83.5%. Large drops of magnesium up to 1.5 cm in diameter, which wetted the iron well, were formed on the cathode surface.

The magnesium sulfate concentration, calculated as sulfur, was varied from 0.01 to 0.825 wt.%; the sulfide concentration, from 0.01 to 2.0%. Good reproducibility of current efficiencies was found for each of the impurities investigated. The experimental data are plotted in Fig. 2 in the form of $A = f(C_{SO_4^{-2}})$ and $A = f(C_{S^{-2}})$, where A is the current efficiency; the concentrations C are calculated as percentages by weight of atomic sulfur.

When magnesium sulfide was introduced into the melt a large amount of sludge was formed. The sludge in this case contained MgS in addition to magnesium oxide and elemental sulfur.

At high contents of sulfur compounds, the cathode became coated with a dark loose film which enveloped fine droplets of magnesium.

If the electrolyte contained 1.5 – 2.0% SO_4^{-2} and the temperature of the melt before immersion of the electrodes was low (700°), and the electrodes were cold when immersed, a solid "pear" formed rapidly on the cathode. This "pear" was a gray mass permeated with minute droplets of magnesium. It consisted of the

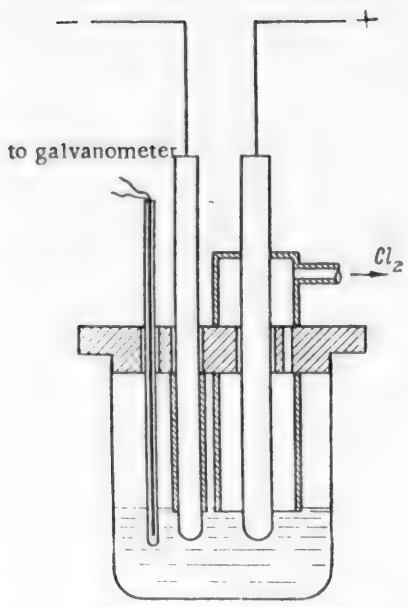

Fig. 1. Electrolytic cell for investigation of the effect of additions of sulfur on current efficiency for magnesium in electrolysis of carnallite.

electrolyte and magnesium sulfide. After its formation, the cell voltage rose sharply while the current fell. Under the "pear" the cathode was covered with a layer of metallic magnesium. The current efficiency for magnesium fell to zero. This "pear" could not be melted even if the electrolyte temperature was raised to 800-820°.

In the course of electrolysis in presence of magnesium sulfates and sulfides the electrolyte acquired an azure or blue color. The color intensity increased with increase of the SO_4^{-2} content up to 0.9-1.0 wt.%. On further increase of the sulfate concentration the color became somewhat weaker. It should also be noted that the color was not always uniformly distributed through the melt. When the electrolyte cooled, its blue color changed to gray, but reappeared on remelting. The blue color became noticeable when the SO_4^{-2} content reached 0.05-0.1 wt.%. The blue color generally reduced the transparency of the melt, but in some cases the melt remained transparent and a sludge with a bluish tinge formed at the bottom of the cell. This happened when the melt had a high content (0.5-0.6%) of magnesium oxide.

A series of experiments was carried out to determine the cause of coloration of the melts during electrolysis. These experiments were performed with fused chlorides in quartz tubes without application of direct current. Several experiments were carried out in an atmosphere of argon or carbon dioxide.

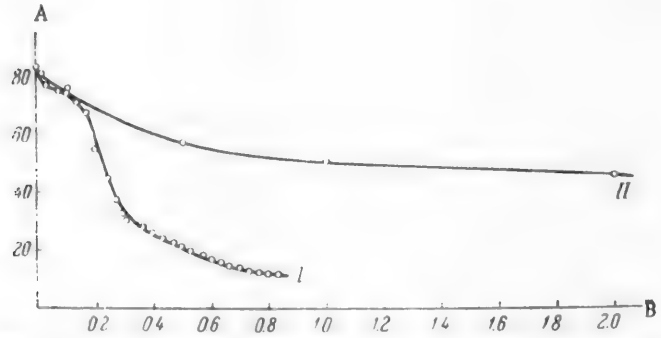

Fig. 2. Variation of current efficiency with sulfur concentration: A) current efficiency (%), B) sulfur concentration (wt.%); additions: I) $MgSO_4$, II) MgS.

The chlorides were subjected to qualitative chemical analysis for SO_4^{-2}, SO_3^{-2}, $S_2O_3^{-2}$, S^{-2} ions [5] during the investigations.

The results may be summarized as follows.

1. Addition of magnesium sulfate to a melt of $MgCl_2 + KCl$, free from metallic magnesium, or in presence of magnesium at temperatures below 650°, did not produce a blue color. The color appeared only in presence of melted magnesium, i.e., at temperatures above 650°.

2. Addition of magnesium sulfites or thiosulfates to a melt of $MgCl_2 + KCl$, free from magnesium at 700° in an atmosphere of air, argon, or CO_2 resulted in rapid appearance (within a few minutes) of a blue color.

The color was more intense in an inert atmosphere. Qualitative analysis of the salt after the experiment showed absence of SO_3^{-2}, SO_4^{-2} and S^{-2} ions. Elemental sulfur was deposited on the walls of the quartz tubes in the experiments in an inert atmosphere. In air, sulfur was not liberated, but the formation of sulfur dioxide was detected (by smell).

3. If elemental sulfur was added to the melt a blue color appeared, which gradually weakened, even if the melt did not contain metallic magnesium.

4. On addition of a small amount of finely divided magnesium oxide to a colored melt, the color disappeared, but a colored sludge formed on the bottom of the tube.

All these experiments were easily reproducible.

These results lead to quite definite conclusions concerning the behavior of sulfur compounds in chloride melts during electrolysis.

First, the results of qualitative chemical analysis show that in presence of liquid magnesium in the electrolyte no appreciable amounts of SO_3^{-2}, SO_4^{-2} and $S_2O_3^{-2}$ ions can be detected after introduction of sulfate into the melt. This suggests that all these compounds yield elemental sulfur in the melt. This may occur by the reaction

$$Mg^{+2} + 3Mg + SO_4^{-2} \rightleftarrows 4MgO + S, \qquad (a)$$

where the reducing agent is probably dissolved magnesium, as this reaction does not occur in presence of the solid metal. The standard free energy change in this reaction at 700° [6] is $\Delta F_a^{\circ} = -267169$ kcal/mole. In other words, Equilibrium (a) must be shifted completely to the right.

When sulfites and thiosulfates are added to chloride melts they probably also decompose thermally with liberation of elemental sulfur.

Magnesium sulfide may react at 700° with atmospheric oxygen and with chlorine liberated by electrolysis:

$$MgS + Cl_2 \rightleftarrows MgCl_2 + S \qquad (b)$$

$$MgS + 1\,1/2O_2 \rightleftarrows MgO + SO_2 \qquad (c)$$

$$SO_2 + 2Mg \rightleftarrows 2MgO + S. \qquad (d)$$

The standard free energy changes in these reactions (from left to right) are respectively:

$$\Delta F_b^0 = -35918 \text{ kcal/mole}$$

$$\Delta F_c^0 = -113\,300 \text{ kcal/mole}$$

$$\Delta F_d^0 = -172\,000 \text{ kcal/mole}$$

All this indicates that when sulfates and sulfides are introduced into the melt they decompose under the action of metallic magnesium, chlorine, and air with liberation of elemental sulfur. Because of the poor solubility of MgS in the chloride melt, some of the sulfide passes into the sludge. The data below give some indication of the distribution of magnesium sulfide during electrolysis.

Magnesium Sulfide Balance in the Cell

Intake		Yield		
Put into cell before the experiment		Passed into sludge	2.81 g	70.2%
4.000 g	100%	Remained in electrolyte as sulfur	0.12 g	3.0%
		Passed to cathode and decomposed during electrolysis owing to combustion of sulfur	0.70 g*	26.8%
		Total	4.00	100%

*As in original – Publisher's note.

Apparently it is the elemental sulfur that colors the electrolyte. Despite the high temperature (the boiling point of sulfur is 441°) sulfur volatilizes slowly from the melt, probably owing to the molecular structure of the melted sulfur. It should be assumed that the sulfur does not remain in the melt in the form of individual atoms, but forms polymers of the S_n type, with high surface activity. Such polymers can apparently be adsorbed by magnesium oxide and taken with it into the sludge, as was found in several experiments. It is still not clear whether the sulfur in chlorides is in the form of a true or a colloidal solution.

The weaker influence of sulfide as compared with sulfate on the current efficiency is probably attributable to the low solubility of magnesium sulfide, which limits the concentration of the harmful impurity in the melt.

LITERATURE CITED

[1] Dr. F. Oettel, Z. Elektroch. 2, 394 (1895).

[2] B. V. Strokan, Trans. Sci. Res. Inst. Light Metals 10, 22 (1934).

[3] Z. V. Vasil'ev and B. V. Popov, Trans. All-Union Aluminum and Magnesium Inst. 11-12, 169 (1935).

[4] I. P. Tverdovskii and A. A. Rudnitskii, J. Appl. Chem. 9, 1, 26 (1936).

[5] V. N. Alekseev, Qualitative Analysis [in Russian] (Goskhimizdat, 1953).

[6] O. Kubaschewski and E. Evans, Metallurgical Thermochemistry (IL, Moscow, 1954) [Russian translation].

Received June 2, 1958.

ELECTROLYTES FOR ELECTROCHEMICAL POLISHING OF STEEL

G. P. Maitak and G. S. Tret'yakova

Institute of General and Inorganic Chemistry, Academy of Sciences,
Ukrainian SSR

A fairly large number of electrolytes for electrochemical polishing of steel has been proposed, but most of them are not used in practice. The most widely used in industry are electrolytes containing phosphoric and sulfuric acids and chromic anhydride [1-2]. However, these electrolytes also have a number of serious disadvantages which restrict the use of electrochemical polishing in industry.

One disadvantage of these electrolytes is the high content of the costly and scarce orthophosphoric acid. For electrochemical polishing of carbon steel, an electrolyte of the following composition has been recommended [4] (in wt.%): H_3PO_4 65, H_2SO_4 15, CrO_3 6, H_2O 14; this contains 4.3 times as much orthophosphoric as sulfuric acid.

Another important disadvantage of such electrolytes is the need to operate at high temperatures. This causes changes in the concentration (owing to evaporation of water) and polishing properties of the solution, and leads to corrosion of the lead cathode and the cell lining. All this has an adverse effect on the polishing properties of the electrolyte [2]. The use of hot solutions is inconvenient, involves the use of heat-resisting equipment, and is accompanied by additional expenditure of power and evaporation of solution components harmful to health.

The main disadvantage of these electrolytes, which is the chief obstacle to the extensive use of electrochemical polishing of steel in industry, is their short service life. They become unserviceable and require renewal [2,3,5] after the passage of 50-120 amp-hr per liter. Therefore a number of investigations have been concerned with further studies and improvement of sulfuric–phosphoric–chromic acid electrolytes with the aim of increasing their service life, but no results of practical value have been obtained as yet. Moreover, increase of their service life does not remove the other serious defects of these electrolytes. Therefore such investigations are accompanied by searches for new electrolytes for electrochemical polishing of steel.

The favorable effects of inhibitors on electrochemical polishing of metals are generally known and have been noted by us earlier [6]. The inhibitor "Unikol" was recommended by Balezin, Barannik, and Putilova [7] as an additive to pickling liquors containing sulfuric and hydrochloric acid, which hinders dissolution of the metal in them but does not prevent dissolution of rust. Unikol has not been previously suggested as an additive to solutions for electrochemical polishing of metals. However, pickling liquors containing this inhibitor can be used for removing rust even from polished objects, not strongly rusted, without detriment to the polish [7]. It was therefore reasonable to test the effectiveness of this inhibitor in electrochemical polishing. Preliminary tests showed that additions of Unikol to mixtures of sulfuric and phosphoric acids have a very favorable effect on electrochemical polishing of steel in such solutions; it extends the range of acid mixture compositions suitable for electrochemical polishing of steel, and it lowers the necessary and optimum current density and solution temperature needed for electrochemical polishing of steel in such solutions.

The present work was concerned with a study of the conditions of electrochemical polishing of steel at room temperature in mixtures of sulfuric and phosphoric acids of different compositions, with and without added Unikol MN-10.

EXPERIMENTAL

The first of these experiments were performed on ShKh-15 high-carbon steel. The experimental conditions, apparatus, amount of electrolyte in the beaker used as the cell, steel specimens, their structure, dimensions, and preparation were all the same as before [6]. The only difference was that instead of a copper cathode a lead cathode of the same size and shape was used.

In mixtures of sulfuric and phosphoric acid without inhibitor, high-carbon steel is not electropolished to a mirror-bright surface at 18-25°. Under these conditions, high-carbon steel is electropolished only when treated in an acid mixture containing (wt.%): H_3PO_4 – 70, H_2SO_4 – 20, H_2O – 10. In electrolytes consisting of the same acids with added Unikol, high-carbon steel is electropolished under the same conditions, at acid mixture compositions comprising a whole region of the $H_3PO_4 - H_2SO_4 - H_2O$ ternary diagram. The optimum addition of Unikol is about 2.5% by volume on the acid mixture.

We tested electrolytes consisting of sulfuric and phosphoric acid mixtures of different compositions and concentrations, with additions of Unikol MN-10 (2.5% on the volume of the acid mixture). The steel was treated at 18-25° in unstirred and stirred electrolytes at current densities of 10, 25, 50, 75, and 100 amp/dm^2 for 5 or 10 minutes. The results are plotted in a triangular diagram and summarized in Table 1. The region of acid mixtures corresponding to electrolytes in which high-carbon steel is electropolished under the stated conditions is crosshatched on the triangular diagram. Double crosshatching indicates the region of optimum compositions of acid mixtures, corresponding to electrolytes with the best polishing power.

TABLE 1

Optimum Compositions of Acid Mixtures and Current Densities Tested for Electropolishing of High-Carbon Steel (ShKh-15) in Electrolytes Consisting of These Mixtures with Added Unikol MN-10 (2.5% by Volume on the Acid Mixture Taken)

Composition of acid mixture (wt. %)			Current density D_a (amp/dm^2)	
H_3PO_4	H_2SO_4	H_2O	polishing*	nonpolishing
70	20	10	25, **50**	10, 75, 100
60	30	10	25, **50**, 75, 100	10
50	40	10	50, **75**, 100	10, 25
75	10	15	**50**, 75	10, 25, 100
65	20	15	**50**, 75	10, 25, 100
55	30	15	50, **75**, **100**	10, 25
45	40	15	75, **100**	10, 25, 50
35	50	15	75, **100**	10, 25, 50
30	50	20	75, **100**	10, 25, 50

*The optimum current density for electropolishing in a given electrolyte is shown in heavy type.

It follows from these results that the best electrolytes for electropolishing of high-carbon steel at 18-25° contain 30-75 wt. % H_3PO_4, 10-50 wt. % H_2SO_4, 10-15 wt. % H_2O, and 2.5% (volume/volume) of Unikol.

The current densities at which high-carbon steel is electropolished in the electrolytes of optimum composition are given in Table 1. It follows from this table that the polishing and optimum polishing current densities vary with the electrolyte composition. Comparison of the diagram and Table 1 reveals a regularity in these variations.

As we pass in the triangular diagram from left to right along the horizontal lines corresponding to constant H_2SO_4 contents from solutions containing 10% water to solutions containing 15% water, the optimum current density increases. This is caused by the increase of water content, although the phosphoric acid content also changes. For an electrolyte of the composition 10% H_2O, 70% H_3PO_4 and 20% H_2SO_4, the polishing current

densities are 25 and 50 amp/dm^2, and for an electrolyte of the composition 15% H_2O, 65% H_3PO_4 and 20% H_2SO_4 (toward the right along the same horizontal line in the diagram) the polishing current densities are 50 and 75 amp/dm^2. This cannot be attributed to a lower content of phosphoric acid in the electrolyte, as in the transition, in the same region of the diagram, from the first solution named above, containing 70% H_3PO_4, to a solution containing the same amount of water (10%) and less H_3PO_4 (60%) the range of polishing current densities extends, owing to the increase of H_2SO_4 content, to higher current densities but the optimum current density remains the same – 50 amp/dm^2. As we pass from this last solution to a solution containing 50% H_2O and 55% H_3PO_4 (toward the right along the same horizontal line in the diagram), both the polishing and the optimum current densities, as Table 1 shows, are displaced toward higher values (the optimum values are 75 and 100 amp/dm^2). The same is found for the next horizontal line, corresponding to solutions containing 40% H_2SO_4, in the transition from a solution containing 10% H_2O and 50% H_3PO_4, for which the polishing current densities are 50, 75, and 100 amp/dm^2 and the optimum is 75 amp/dm^2, to a solution containing 15% H_2O and 45% H_3PO_4, for which the polishing current densities are 75 and 100 amp/dm^2, and the optimum is 100 amp/dm^2.

These observations were confirmed by an experiment with direct dilution of the electrolyte, when the relative proportions of the acids were unchanged. The optimum current density for electropolishing in an electrolyte of the composition (wt. %): H_3PO_4 – 70, H_2SO_4 – 20, H_2O – 10 and 2.5% (volume/volume) of Unikol MN-10 was 50 amp/dm^2. When 15% of water (volume/volume) was added to this electrolyte, so that the total water content in the electrolyte apart from the water introduced with the Unikol, became 19 wt.%, the optimum current density rose to 75 amp/dm^2. It follows that for solutions of optimum composition, the optimum current density for electropolishing increases with increase of water content.

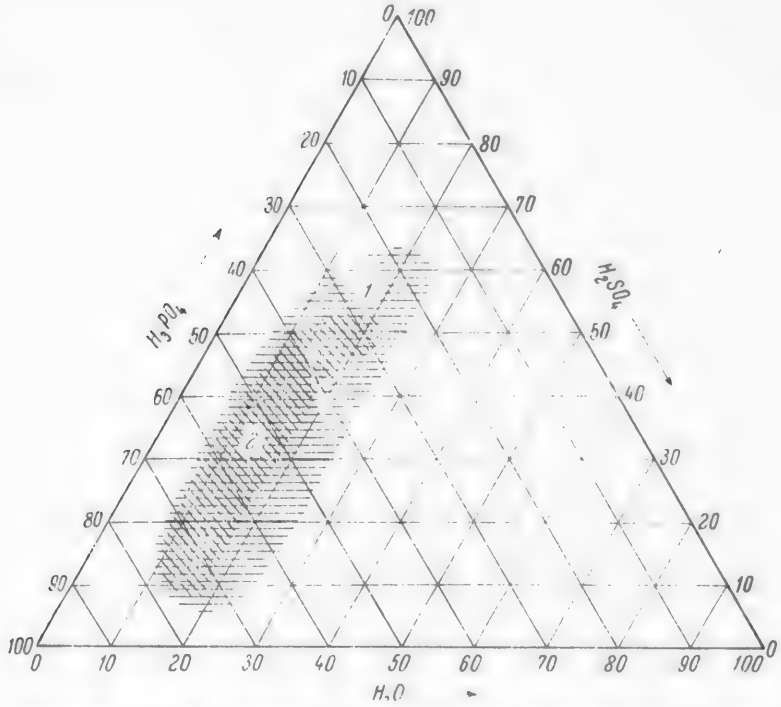

Composition of acid mixtures in electrolytes for electropolishing of high-carbon ShKh-15 steel at 18-25°, with addition of Unikol MN-10 (2.5% volume/volume): 1) acid mixtures for electrolytes suitable for electropolishing, 2) acid mixtures for electrolytes of the best polishing power.

As we pass in the region of solutions of optimum composition (see diagram) along lines of constant water content (10 and 15%), there is also a regularity in the variation of the polishing and optimum electropolishing current densities . Electrolytes containing 60-70 wt. % phosphoric acid and 10-15 wt. % water are the best with regard to current density, i.e., they have the lowest current densities for best electropolishing. It follows from Table 1 that the optimum current density for electropolishing in these solutions is 50 amp/dm^2, whereas for solutions with higher and lower contents of phosphoric acid the optimum current densities are higher.

Investigations performed specially with solutions of the optimum composition with regard to current density showed that with them the optimum current densities are less than 50 amp/dm^2, and are close to 35 amp/dm^2, but,as in the mass trials performed with all the other solutions, polishing power was tested only at current densities of 10, 25, 50, 75 and 100 amp/dm^2, only these values are given in Table 1 for the current densities tested for electropolishing. It must also be pointed out that these data refer to freshly prepared solutions which had been used little. With increasing use of the solutions the optimum polishing current densities decrease somewhat, but not as much as was noted [2] with sulfuric—phosphoric—chromic acid electrolytes. The polishing power of used electrolytes is better than that of freshly prepared.

A film is visible on the polished surfaces in electropolishing in hot electrolytes, but this is not observed if the electrolyte is warmed gently to 30-35°. Therefore at high current densities the electrolyte must be cooled and stirred. However, since the polish is somewhat less good in stirred electrolytes and a longer treatment is needed, stirring may be performed at intervals or only at the start of the treatment. For example, with a total electropolishing time of 5 minutes, the electrolyte may be stirred continuously or intermittently during the first 3-4 minutes, and left unstirred during the last 1-2 minutes. All the investigated electrolytes are stable on keeping, and their service life is considerably longer than that of sulfuric—phosphoric—chromic acid electrolytes.

In addition to ShKh-15 high-carbon steel used in these investigations,other carbon and stainless steels can be electropolished in electrolytes consisting of sulfuric and phosphoric acids with added Unikol at 18-25°. The conditions of electropolishing of stainless steel in these electrolytes were studied in greater detail with specimens of 1Kh18N9T chromium—nickel steel. Specimens in the form of rods 5 mm in diameter were immersed vertically in the electrolyte to a depth of 18 mm, so that their treated surface, as for the high-carbon steel specimens, was 0.03 dm^2. All the other conditions were as before. The results of these tests are given in Table 2.

TABLE 2

Compositions of Acid Mixtures and Current Densities Tested in Electropolishing of Stainless Steel at 18-25° in Electrolytes Consisting of These Mixtures without Additives and with Addition of Unikol MN-10 (2.5% Volume/Volume)

Composition of acid mixture (wt. %)			Acid mixture without addition		Acid mixture with added Unikol MN-10	
			Current density D_a (amp/dm^2)			
H_3PO_4	H_2SO_4	H_2O	polishing*	nonpolishing	polishing*	nonpolishing
70	20	10	**50, 75, 100**	10, 25	20, **25**, 50, 75, 100	10
60	30	10	75, **100**	10, 25, 50	25, **50**, 75, 100	10
50	40	10	75, 100	10, 25, 50	50, 75, 100	10, 25
40	50	10	—	10, 25, 50, 75, 100	50, 75, **100**	10, 25
75	10	15	50, 75, **100**	10, 25	25, 50	10, 75, 100
65	20	15	50, **75**, 100	10, 25	25, **50**, **75**, **100**	10
55	30	15	75, **100**	10, 25, 50	50, **75**, **100**	10, 25
45	40	15	—	10, 25, 50, 75, 100	50, **75**, **100**	10, 25
35	50	15	—	10, 25, 50, 75, 100	50, 75, **100**	10, 25
25	60	15	—	10, 25, 50, 75, 100	50, 75, **100**	10, 25
60	20	20	25, 50, 75, **100**	10	25, **50**, 75, 100	10
50	30	20	25, 50, 75, **100**	10	25, **50**, 75, 100	10
40	40	20	—	10, 25, 50, 75, 100	75, **100**	10, 25, 50

*The optimum current density for electropolishing in a given electrolyte is shown in heavy type.

It is clear from these data that Unikol also has a favorable effect in the electropolishing of stainless steel, which can be polished at lower current densities than high-carbon steel in electrolytes containing sulfuric and phosphoric acids and Unikol. The electrolytes of optimum composition with regard to current density (25 amp/dm^2) for electropolishing of stainless steel are contained in the triangular diagram (see figure) within the triangle formed by solutions with 60-75% phosphoric acid and 10% water and the solution containing 60% phosphoric acid and 20% water.

The inhibitor Unikol PB-5, a condensation product of aniline and urotropine [8], is now being produced industrially and is used for retardation of dissolution of steel in hydrochloric acid. Instead of Unikol MN-10, the same amounts of Unikol PB-5, may be added to our recommended electrolytes. The measured quantity of Unikol PB-5 is first dissolved in a small amount of dilute sulfuric acid (to prevent overheating the solution must be cooled in the process), and this amount of acid must be taken into account in the composition of the acid mixture; or it may be dissolved in the acid mixture (warmed to not over 60°) taken for preparation of the electrolyte.

SUMMARY

1. Carbon, high-carbon, and stainless steels can be electropolished at 18-25° in electrolytes consisting of mixtures of sulfuric and phosphoric acids with added inhibitor — Unikol MN-10 or PB-5.

Addition of Unikol extends the range of acid mixtures suitable for electropolishing of steel and lowers the necessary and optimum current densities and solution temperature. The optimum amount of Unikol is 2.5% by volume on the acid mixture.

2. For the best electrolytes for electropolishing of high-carbon steel the composition of the acid mixtures corresponds to 50-75 wt.% of phosphoric acid (with correspondingly 40-15% sulfuric acid) and 10 wt. % water, and 35-75 wt. % phosphoric acid (with correspondingly 50-10% sulfuric acid) and 15% water. Of these electrolytes the best with regard to current density are those in which the composition of the acid mixtures is limited by 60-70 wt. % phosphoric acid with 10-15 wt. % water. The optimum current density for electropolishing of high-carbon steel in these electrolytes is 35-50 amp/dm^2.

3. The composition of electrolytes for electropolishing of stainless steel may be varied over a wider range. For electropolishing of stainless steel the best electrolytes with regard to current density are those in which the composition of the acid mixtures is limited by 60-75% phosphoric acid with 10% water, and 60% phosphoric acid with 20% water. The optimum current density for electropolishing of stainless steel in these electrolytes is 25 amp/dm^2.

4. The electrolytes described in this paper have a number of advantages over sulfuric-phosphoric—chromic acid electrolytes: a much longer service life, the use of room temperatures for polishing, and lower corrosiveness, so that cheap and available metals and nonmetallic materials may be used for cathodes and tank linings.

LITERATURE CITED

[1] C. L. Faust, and H. A. Pray, Steel 109, 20, 30 (1941); C. L. Faust, U.S. Patent 2,338,321 (1944); A. I. Pankratov, Bull. Machine Constr. 9-10, 48 (1944); K. A. Nesmeyanova, in the book: Corrosion, Corrosion Protection, and Electrolysis [in Russian] (Mashgiz, Moscow, 1948) p. 139.

[2] K. P. Batashev, Trans. Leningrad Polytech. Inst. 6, 121 (Metallurgy Press, Moscow, 1953).

[3] N. P. Fedot'ev, E. G. Kruglova, and S. Ya. Grilikhes, J. Appl. Chem. 27, 157 (1954).*

[4] L. Ya. Bogorad, S. Ya. Grilikhes, and R. S. Arson, Electrochemical Polishing of Steel [in Russian] (Leningrad Press, 1951) p.29.

[5] L. Ya. Popilov, Technology of Metal Electropolishing [in Russian] (Mashgiz, Moscow — Leningrad, 1953) p. 120.

[6] G. P. Maitak, Ukrain. Chem. J. 25, 3 (1959).

*Original Russian pagination. See C. B. translation.

[7] S. A. Balezin, V. P. Barannik, and I. N. Putilova, Utilization of Acid-Corrosion Inhibitors [in Russian] (Goskhimizdat, Moscow – Leningrad, 1948)

[8] Chemical Products, Vol. 1 [in Russian] (Goskhimizdat, Moscow – Leningrad, 1954) p. 246.

Received October 10, 1957.

THE CAUSE OF LUSTER IN ELECTROLYTIC NICKEL DEPOSITS

A. V. Pamfilov and R. M. Morgart

Laboratory of Physical Chemistry, Chernovits University

Many authors consider that the cause of luster in electrolytic deposits is their orientation texture [1-5]. However, very often no direct relationship between luster and orientation texture of deposits can be detected [2]. According to Gorbunova [3], in presence of the [100] texture axis, when (with metals crystallizing in the cubic system) cube faces project onto the surface of the deposit, a much higher luster is probable than in presence of other texture axes, especially [111], when three-sided corners should project onto the surface. However, Arkharov [4] found that chromium deposits have higher luster with this last texture axis.

Most of the cited investigations were concerned with the texture of deposits formed under various definite electrolysis conditions. We used the x-ray method for studying a large number of nickel deposits of greatly varying degrees of luster, deposited from baths without additives, with different sulfur-containing additives, with changes in the direction of the current in the cell, and with variations of the electrolysis conditions. The electrolyte used had the following composition (in g/liter): $NiSO_4 \cdot 7H_2O$ 200, $NiCl_2 \cdot 6H_2O$ 15, H_3BO_3 30.

The direction of the preferred orientation was determined by the Polanyi method, modified by Palatnikov [5]. The x-ray patterns were taken by the "polished section" method in a Debye camera 57 mm in diameter and 60 mm high. The degree of perfection of the texture was estimated on a four-point scale by comparison of the breadth and intensity of the interference spots on the x-ray patterns.

The texture was studied in deposits formed in presence of various sulfur-containing brighteners [6]. In the case of thiamine hydrobromide as additive, the texture of deposits formed under a great variety of electrolysis conditions was studied. The texture of deposits formed from the same bath without additives under analogous electrolysis conditions was studied for comparison. The texture was studied in deposits of two different thicknesses – 10 μ and 60 μ – formed at three different electrolysis temperatures – 20, 40, and 60° – and at different pH values. In addition, x-ray patterns of deposits formed with changes in the direction of the current were obtained. Luster was estimated by comparison of the specimens with standards on a 10-point scale [7]. The specimens were placed in such a manner that the x-ray beam fell in the center of the specimen. Accordingly, if the luster distribution was irregular over the surface, data on the luster are also given for the center of the specimen.

Table 1 contains data on luster, texture axes, and extent of orientation of deposits formed in presence of various sulfur-containing additives.

It follows from Table 1 that the texture axes [100], [112], [112], [120] and [112], [120], [100] were found for all deposits with luster in the range of 7-10, with a great variety in the extent of orientation, and also with total disorientation.

For deposits 10μ thick, formed from a bath without additives at 20° and D_c = 1 amp/dm^2, the mixed texture axis [120], [112] is characteristic at low pH values, and also the [120] and [110] directions at lower acidities. At the greatest current density D_c = 4 amp/dm^2 the [110] texture axis predominates, supplemented in some instances by the [120] direction. At pH = 3.0 the [120] texture axis is characteristic, supplemented at low current densities by the [112] axis. At pH = 5.0 the [120] texture axis generally predominates, and the [100] axis is found only at a low current density – 0.5 amp/dm^2. The extent of orientation in general diminishes

TABLE 1

Luster, Type and Degree of Perfection of Texture of Specimens Formed in Presence of Additives at t = 20° and pH = 5.0

Additive	Concentration (g/liter)	D_c (amp/dm²)	Luster	Texture axis	Perfection of texture
Sodium 2-(p-aminobenzenesulfonamido)thiazole	0.2	2	9—10	[112]	1
Thiourea	0.2	4	9	[100]	3
Butylthiouronium bromide	0.1	3	9—10	[100] [112]	1
2-Methyl-N-ethylbenzothiazole-p-toluenesulfonate	0.2	4	9	[120] [100]	4
Sodium thiosulfanate	0.05	0.5	7	—	0
Potassium thiocyanate	0.025	4	10	[112] [120]	3
Thioindigo Red S	Suspension	2	8—9	—	0
Thioindigo bright rose J		2	10	—	0
Sulfur black		1	8	[112] [120]	3
Sulfur sky blue		1	9	—	0
Sulfur blue		1	8	[100]	1
Sulfur brown		1	8	—	0
Etazol		3	10	[112]	2
Thiosalicylic acid		4	10	—	0
Dithiooxamide		4	9	[112] [120] [100]	2
Nickel sulfide		3	10	[112] [120] [100]	2

with increase of current density. However this is only true for a definite and unchanging texture axis. In the transition to a new type of texture with increase of current density the extent of orientation may be less than with the preceding type. The texture becomes simplified on increase on thickness of the deposit to 60 μ, i.e., mixed texture axes are less common. The [100] texture axis is met more frequently, especially at relatively low current densities and at higher electrolyte acidities. On increase of temperature to 40° the [100] texture direction becomes predominant in deposits both to 10μ and 60 μ thick; at relatively high current density the [110] texture axis appears, and with electrolytes at low acidity (pH = 6.0), also the [112] texture axis. At 60° the mixed [120], [112] direction appears in addition to the [100], [110], and [112] texture axes. With increase of current density and pH, the [100] direction passes into [112], often by way of the mixed [120], [112] texture axis. The [110] texture axis is characteristic at high current densities — 15-18 amp/dm². The extent of orientation at 40 and 60°, as at 20°, usually increases with current density.

For specimens 10 μ thick, formed at 20° in a bath containing 0.05 g of thiamine hydrobromide per liter, the [120], [112] and [120], [112], [100] mixed texture axes are characteristic in most cases. The extent of orientation passes through a maximum with increase of current density at low electrolyte acidities. The extent of orientation first falls and then rises with decrease of acidity. In deposits 60μ thick there was either total disorientation, or orientation exclusively along the [120], [112] axes, of a very high degree of perfection. At 40° the [100] and [112] texture axes are characteristic. The latter is more frequent in deposits 60μ thick. The extent of orientation as a rule increases with current density. It is significant that with increase of temperature from 20 to 40° the extent of orientation diminishes, and the texture axes approach those found in deposits formed in dull baths. At 60° the [100] texture axis becomes predominant in deposits 10μ thick, and the extent of orientation passes through a maximum with increase of current density. In deposits 60μ thick the [112] texture axis is characteristic at relatively low electrolyte acidities, while at high acidity the [100] texture axis predominates. The [100], [110], [112], [120] texture axes are found in deposits formed with changes in the direction of the current.

Data on the texture of deposits formed from baths without additives and with added thiamine hydrobromide reveal a distinct difference between their texture axes. Deposits with the following texture axes: [120], [112], [110], [120], [120], [100], [110], were obtained from the electrolyte without additives at 20°, in accordance with the electrolysis conditions and thickness of the deposits. Deposits formed from a bath with added thiamine hydrobromide are as a rule oriented in the [120], [112] direction, and in some instances in the [120], [112], [100] directions. The [110] texture axis was found in only one instance. It is evident that the texture axis is changed in presence of the additive. However, deposits of a given degree of luster may have the most diverse texture axes with a wide range of orientation – from total disorientation to high degrees of orientation. On increase of temperature the texture axes characteristic for 20° gradually disappear, especially in the case of deposits 10μ thick, and are replaced by the [100] and [112] axes. Here again no definite connection can be detected between the luster and extent of orientation.

TABLE 2

Distribution of Specimens According to Luster and Extent of Orientation

Luster	Extent of orientation					Luster	Extent of orientation				
	0	1	2	3	4		0	1	2	3	4
1	—	15	24	31	12	6	1	3	2	1	2
1—2	—	—	3	7	—	6—7	1	—	—	1	—
2	—	4	4	2	4	7	2	1	2	3	1
2—3	—	—	—	—	—	7—8	—	—	—	1	1
3	—	2	3	2	1	8	2	4	2	4	3
3—4	—	—	—	—	—	8—9	1	—	—	1	1
4	—	1	4	4	1	9	3	3	1	5	2
4—5	—	1	—	2	1	9—10	1	4	2	—	—
5	1	—	3	—	2	10	8	1	4	4	6
5—6	—	—	1	—	—						

Table 2 contains data on luster and extent of orientation for all the 219 specimens studied; it is seen that there is no definite correlation between luster and extent of orientation.

Of the 44 mirror-bright specimens (luster 9-10), 12 (27%) were without orientation, 8 (18%) had very weak orientation, 16 (36%) had moderate orientation, and only 8 specimens (18%) had a high degree of texture. At the same time, of 82 completely dull specimens none was completely without orientation, 15 (18%) were weakly oriented, 55 (67%) had moderate orientation, and 12 specimens (15%) had perfect texture. Among the specimens of moderate luster there were relatively many without orientation and with low and moderate orientation, and few with perfect orientation.

Data on luster and type of texture for all the specimens studied are presented in Table 3.

Of the 44 very bright specimens (luster 9-10) only 6 (14) had the [100] texture axis, 2 (5%) had the [110] and [120] texture axes, 8 (18%) had the [112] texture axis, 14 (32%) had mixed [120] [112] and [120], [112],[100] texture axes, while 12 deposits (27%), as already noted, were completely disoriented. At the same time, of the 82 dull deposits 47 (57%) had the [100] texture axis, while the remaining 43% also had the [110], [120], [112] texture axes and mixed [110], [120] and [120], [112] axes.

These results lead to the conclusion that the [100], [110], [120], [112] texture axes and some combinations of them may be found in bright, semibright, and dull deposits. The results indicate that the luster of electrolytic nickel deposits does not depend on the type or degree of perfection of their texture. As already noted, deposits formed in presence of thiamine hydrobromide brightener are characterized by a mixed type of texture along the [120], [112] and also the [120], [112], [100] axes, especially if formed at low temperatures. If the luster of deposits is regarded as dependent on texture, the [100] texture axis should be found in bright deposits; according to Gorbunova [3] this should favor regular, specular reflection of light. The [120] and [112] texture axes, and especially the two present simultaneously, can hardly cause luster, as in this case three-sided corners

of the cubic crystals should project onto the surface. It is probable that even a relatively perfect texture along the [100] axis cannot always tend to improve the reflectance of the deposits. This follows from the fact that most of our dull deposits had this type of texture. In all probability, despite the apparently favorable type of texture, these deposits have surface irregularities which arise during growth of the deposit, in the form of various steps or imperfect layers which prevent regular reflection of light from the surface. It follows that neither the presence of texture nor the extent of orientation are determining factors favoring luster of electrolytic deposits.

Some authors attribute luster of electrolytic deposits to microcrystallinity [8]. However, in many publications the correlation between luster and grain size is not based on experimental data, but is assumed as self-evident. Nevertheless, it has been shown experimentally in some instances that luster does not depend on grain size [9].

It is not always possible to determine the dimensions of metal crystals exactly by the x-ray method. There are two regions of grain size in which very different x-ray patterns are obtained. With crystals larger than 1-2μ the lines on the x-ray patterns are discontinuous. As the grain size decreases, the lines in the x-ray patterns become diffuse if relatively thin metal layers are used. In our experiments the lines in the x-ray patterns were continuous and not diffuse for all the specimens; this indicates that there is probably no difference in grain size between dull and bright deposits.

TABLE 3

Distribution of Specimens According to Luster and Type of Texture

Luster	Texture axes								
	[100]	[110]	[120]	[112]	[110] [120]	[120] [112]	[100] [120] [112]	[100] [110]	no orientation
1	47	11	5	6	6	7	—	—	—
1—2	6	3	—	—	1	—	—	—	—
2	4	1		5	1	2		1	
2—3	—	—	—	—	—	—	—	—	—
3	3	3	—	1	—	1	—	—	—
3—4	—	—	—	—	—	—	—	—	—
4	5	1	2	2	—	—	—	—	—
4—5	2	—	1	—	—	1	—	—	—
5	2	2	—	—	—	1	—	—	1
5—6	—	—	—	—	—	1	—	—	—
6	2	—	—	3	—	2	1	—	1
6—7	—	—	—	1	—	—	—	—	1
7	2	—	—	2	—	3	—	—	2
7—8	1	—	—	—	—	1	—	—	—
8	3	1	—	1	—	5	3	—	2
8—9	—	1	—	—	—	1	—	—	1
9	3	—	—	3	—	3	2	—	3
9—10	2	1	—	3	—	—	—	—	1
10	1	1	2	2	—	8	1	—	8

It follows from the foregoing that the luster of electrolytic nickel deposits cannot be ascribed either to texture and extent of orientation, or to microcrystallinity.

Stratification of bright deposits must be considered briefly. Many workers [10, 11] have observed a definite stratified structure in studies of polished cross sections of bright deposits. We also observed such stratification in a number of bright deposits. It is known that in very thin layers a deposit reproduces the structure of the underlying layer, and therefore attempts have been made to attribute luster to stratification. However, some brighteners give rise to deposits which are brighter than the basis metal, and their action cannot be attributed to stratification. Moreover, a stratified deposit is not necessarily bright. Stratification is most likely not the cause of luster but an effect accompanying it, which arises as the result of a definite mechanism of action of the brightener.

Most probably, luster of deposits is determined by the degree of leveling of various submicroscopic projections on their surfaces, as was suggested by Gorbunova et al. [11].

We thank G. P. Kushtu, Head of the Department of Metal Physics, for the opportunity of taking the x-ray photographs and for advice.

SUMMARY

1. The [100], [110], [112], [120] texture axes and certain combinations of them are met equally often both in bright and in dull electrolytic nickel deposits.

2. Dull and specular nickel deposits do not differ in grain size.

3. Neither texture nor microcrystallinity are the causes of luster in electrolytic deposits. Luster is most probably determined by leveling of submicroscopic surface irregularities during electrolysis.

LITERATURE CITED

[1] W. A. Wood. Phil. Mag. 20, 964 (1935); Trans. Faraday Soc., 31, 1248 (1935); G. F. Kosolapov, B. Yu. Mett, J. Tech. Phys. 9, 1421 (1939); H. Fischer, H. Barmann, Z. Metalkunde 32, 376 (1940); E.Raub, and B. Wullhorst, Z. Elektroch. 48, 342 (1942); A. K. Shevelev, J. Tech. Phys. 16, 1299 (1946); S. P. Makar'eva, Bull. Acad. Sci. USSR, Div. Math. Nat. Sci., Chem. Ser., 1211 (1938); Bull. Acad. Sci. USSR, Div. Chem.Sci. 573 (1941); N. T. Kudryavtsev and G. V. Érshler, Proc. Acad. Sci. USSR 72, 363 (1950).

[2] A. T. Vagramyan and Z. A. Solov'eva, J. Phys. Chem. 26, 910 (1952); A. W. Hothersall, G. E. Gardam, J. Electrodepositor's Techn. Soc. 15, 127 (1939); W. Smith, J. H. Keeler, H. J. Read, Plating 36, 355 (1949); G. L. Clark, S. H. Simonsen, J. Electroch. Soc. 98, 110 (1951); F. Denise, H. Leidheiser, J. Electroch. Soc. 100, 490 (1953).

[3] K. M. Gorbunova, Bull. Acad. Sci. USSR, Div. Math. Nat. Sci., Chem. Ser. 1175 (1938).

[4] V. I. Arkharov, J. Tech. Phys. 6, 1777 (1936).

[5] L. Palatnik, J. Tech. Phys. 6, 1624 (1936).

[6] A. V. Pamfilov and R. M. Morgart, Ukrain. Chem. J. 23, 684 (1957).

[7] A. V. Pamfilov and O. E. Panchuk, Ukrain. Chem. J. 24, 266 (1958).

[8] W. Blum, Trans. Electroch. Soc. 36, 213 (1919); E. J. Alexander, Colloid Chemistry 4, 527 (1932); D. J. Nacnaughtan, A. W. Hothersall, Trans. Faraday Soc. 24, 387 (1928); D. J. Macnaughtan, R. A. F. Hammond, Trans. Faraday Soc. 27, 633 (1931); G. E. Gardam, D. J. Macnaughton, Trans. Faraday Soc. 29, 755 (1933); D. J. Macnaughtan, A. W. Hothersall, Trans. Faraday Soc. 31, 1168 (1935); J. B. O'Sullivan. Trans. Faraday Soc. 26, 80 (1930); E. Liebreich, Trans. Faraday Soc. 31, 1188 (1935); R. Springer, Oberflachentechn. 14, 49 (1937); Metalloberfl. 5, A 101 (1951); S. M. Kochergin, J. Tech. Phys. 16, 1325 (1946); Trans. Kazan' Chem. Tech. Inst. 10, 25 (1947); J. Atanasiu, L. A. Blum, and A. Calusaru, Bul. Stint. Acad. R. P. R., Sect. Stinte Mat. Fiz., 5, 305 (1953).

[9] W. R. Meyer and A. Phillips, Trans. Electroch. Soc. 73, 377 (1938); H. J. Read and R. Weil, Plating 37, 1257 (1950); Metalloberfl. 5, A97 (1951).

[10] J. A. Henricks, Trans. Electroch. Soc. 82, 113 (1942); Met. Ind. 61, 378 (1942); H. Fischer. Elektrolytische Abscheidung und Electrokristallisation von Metallen. Springer Verlag, 514, 546 (1954); A. F. Brockington Met. Ind. 69, 468, 513 (1946).

[11] K. M. Gorbunova, T. V. Ivanovskaya, and N. A. Shishakov, J. Phys. Chem. 25, 981 (1951); K. M. Gorbunova, T. V. Ivanovskaya, and O. S. Popova, Proc. Conference on Electrochemistry [in Russian] (Moscow, 1953) p. 396.

Received March 10, 1958.

SODIUM SALICYLATE AS INHIBITOR OF STEEL CORROSION IN NEUTRAL MEDIA

E. V. Bogatyreva and S. A. Balezin

During recent years the benzoates of alkali and alkaline-earth metals have become widely known as inhibitors of steel corrosion in neutral media; they belong to the class of "mild" inhibitors which do not cause pitting corrosion at concentrations insufficient for complete protection of steel in water, and they ensure complete protection of steel specimens at the water line in incomplete immersion [1-4]. These substances are nontoxic and therefore harmless to people in the vicinity.

Benzoic acid, the salts of which are inhibitors of corrosion in water, belongs to the series of aromatic acids, which suggests that salts of other aromatic acids may also serve as inhibitors of steel corrosion in neutral media. For example, we found that sodium phenylacetate in the form of a buffer solution of pH 7 prevents corrosion, in distilled and tap water, of steel and steel articles in contact with certain metals (steel – copper, steel – aluminum), and of nickel-plated and chromium-plated articles.

A method has been patented for protection of metal articles from metallic corrosion by the use of wrapping paper impregnated with organic amines in conjunction with ammonium phthalate [5].

In 1921 Friend suggested that sodium salicylate may protect steel from corrosion in water [6], and Stroud and Vernon [1] suggested the addition of sodium salicylate to latexes to protect steel from atmospheric corrosion. Apart from these brief communications, the literature contains little detailed information on the anticorrosion properties of salicylates.

This paper contains the results of a study of changes in the protective properties of salts of benzoic acid as the result of introduction of a hydroxyl group (OH) into the benzene ring. The sodium salt of salicylic acid, with the hydroxyl group in the ortho position was used for this purpose:

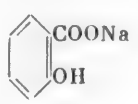

EXPERIMENTAL

The properties of sodium salicylate as inhibitor of steel corrosion were tested in distilled and tap water, in conditions of natural and intensified aeration and in an oxygen-free medium, in relation to the temperature, pH, and presence of Cl', SO_4'', and NO_3' ions in the water. Experiments with sodium benzoate were performed simultaneously for comparison.

Experiments performed at 18-20° with different steels in distilled and tap water with additions of sodium benzoate or salicylate showed that sodium salicylate, like sodium benzoate, inhibits the corrosion of steel in water.

Steel specimens do not change in external appearance in aqueous solutions of these inhibitors (if the protection is complete), because the protective film formed on the steel is invisible.

TABLE 1

Minimum Protective Concentrations of Sodium Salicylate and Benzoate for Certain Steels in Tap and Distilled Water at 18-20° in Experiments Lasting 2 Months

Steel type	Minimum Protective Concentrations (moles/liter)			
	sodium benzoate		sodium salicylate	
	in distilled water	in tap water	in distilled water	in tap water
10 steel	$4 \cdot 10^{-4}$	$4 \cdot 10^{-3}$	$8 \cdot 10^{-4}$	$5 \cdot 10^{-2}$
20 steel	$8 \cdot 10^{-4}$	$8 \cdot 10^{-3}$	$1 \cdot 10^{-3}$	$8 \cdot 10^{-2}$
U-8 steel	$5 \cdot 10^{-3}$	$1 \cdot 10^{-2}$	$8 \cdot 10^{-3}$	$8 \cdot 10^{-1}$

TABLE 2

Minimum Protective Concentrations of Sodium Salicylate and Benzoate for 10 Steel in Distilled Water at Various Temperatures in 24-Hour Experiments

Temperature (°C)	Minimum protective concentration (moles/liter)	
	sodium benzoate	sodium salicylate
20	$6 \cdot 10^{-4}$	$1 \cdot 10^{-3}$
40	$2 \cdot 10^{-3}$	$5 \cdot 10^{-3}$
60	$2 \cdot 10^{-3}$	$7 \cdot 10^{-3}$
80	$2 \cdot 10^{-3}$	1
100	$2 \cdot 10^{-2}$	–

TABLE 3

Minimum Protective Concentrations of Sodium Salicylate and Benzoate in Solutions of NaCl, Na_2SO_4 and $NaNO_3$ of Various Concentrations for 10 Steel at 18-20° in Experiments Lasting 2 Months

Corrosive medium	Minimum protective concentrations (moles/liter)	
	sodium benzoate	sodium salicylate
Distilled H_2O	$4 \cdot 10^{-4}$	$8 \cdot 10^{-4}$
NaCl:		
0.1 m	$4 \cdot 10^{-1}$	1
0.01 m	$4 \cdot 10^{-2}$	$5 \cdot 10^{-2}$
0.001 m	$1 \cdot 10^{-2}$	$3 \cdot 10^{-2}$
Na_2SO_4:		
0.1 m	$4 \cdot 10^{-1}$	1
0.01 m	$1 \cdot 10^{-1}$	$3 \cdot 10^{-1}$
0.001 m	$4 \cdot 10^{-2}$	$1 \cdot 10^{-1}$
$NaNO_3$:		
0.1 m	$8 \cdot 10^{-2}$	$1 \cdot 10^{-2}$
0.01 m	$8 \cdot 10^{-3}$	$5 \cdot 10^{-3}$
0.001 m	$4 \cdot 10^{-3}$	$4 \cdot 10^{-3}$

TABLE 4

Effect of Concentrations of Sodium Salicylate and Benzoate in Distilled Water on Corrosion of 20 Steel with Natural and Intensified Aeration (Air Blown through Solution at 100 ml/minute) at 18-20° in 5-Day Experiments

Inhibitor concentration (moles/liter)	Sodium salicylate				Sodium benzoate			
	normal aeration of solution		intensified aeration of solution		normal aeration of solution		intensified aeration of solution	
	corrosion of 20 steel (g)	proportion of specimen surface attacked (%)	corrosion of 20 steel (g)	proportion of specimen surface attacked (%)	corrosion of 20 steel (g)	proportion of specimen attacked (%)	corrosion of 20 steel (g)	proportion of specimen attacked (%)
0	0.0092	100	0.0358	100	0.0094	100	0.0362	100
$5 \cdot 10^{-5}$	0.0087	100	0.0334	97.5	0.0092	100	0.0137	23.8
$1 \cdot 10^{-5}$	0.0091	100	0.0081	9.3	0.0096	100	0.0127	15.6
$5 \cdot 10^{-5}$	0.0098	100	0.0048	4.2	0.0093	100	0.0056	8.2
$1 \cdot 10^{-4}$	0.0098	100	0.0029	1.23	0.0093	100	0.0040	1.29
$3 \cdot 10^{-4}$	0.0088	100	0.0022	1.3	0.0094	100	0.0026	0.3
$5 \cdot 10^{-4}$	0.0083	100	0.0025	1.7	0.0092	100	0	0
$8 \cdot 10^{-4}$	0.0079	100	0	0	0	0	0	0
$1 \cdot 10^{-3}$	0	0	0	0	0	0	0	0

Both substances are mild inhibitors of steel corrosion in water; they do not cause pitting corrosion of steel with natural aeration of the solution, and provide complete protection of steel specimens at the water line in incomplete immersion.

Sodium salicylate is less effective than sodium benzoate, as the minimum protective concentration for steel in water is higher for sodium salicylate than for sodium benzoate. The protective effects of both inhibitors diminish with increase of the carbon content in steel (Table 1), because of increased structural heterogeneity of the steel surface and the appearance of numerous galvanic microcouples, the complete suppression of which requires a higher concentration of inhibitor than is needed for protection of low-carbon steel under the same conditions.

The protective action of sodium salicylate and benzoate on steel decreases with increase of temperature, probably because the protective films formed on steel in solutions of these inhibitors crack or partially dissolve with increase of temperature, so that the inhibitor concentration must be raised with increase of temperature to ensure complete protection of steel (Table 2).

In 24-hour tests on 10 steel in distilled water in presence of these inhibitors at temperatures from 20 to 100° it was found that sodium benzoate is effective at temperatures from 20 to 100° (inclusive), whereas sodium salicylate protects 10 steel in distilled water only in the temperature range from 20 to 60°. At temperatures above 80° it does not protect steel completely, but merely retards its rate of corrosion slightly.

In presence of Cl', SO_4'', or NO_3' ions in distilled water (Table 3) the protective properties of sodium benzoate and salicylate deteriorate, as Cl', SO_4'', and NO_3' ions can easily destroy the protective films formed by many inhibitors on the metal. For most rapid repair of the defects formed in films by the action of these ions, the concentrations of sodium benzoate and salicylate must be increased considerably. Complete protection of steel can be achieved under these conditions; the protective action of sodium salicylate on steel in aqueous solutions of NaCl, Na_2SO_4 and $NaNO_3$ is less than that of sodium benzoate under the same conditions.

Investigation of the effects of intensified aeration on the protective properties of sodium salicylate and benzoate showed that intensified aeration of the solutions has a twofold influence on their inhibitor action: on the one hand, it lowers the minimum protective concentrations of these inhibitors for 20 steel in distilled water as compared with a control experiment with normal aeration, owing to more rapid supply of the inhibitor to the steel surface; on the other hand, it places these inhibitors in the class of "dangerous" inhibitors which cause pitting

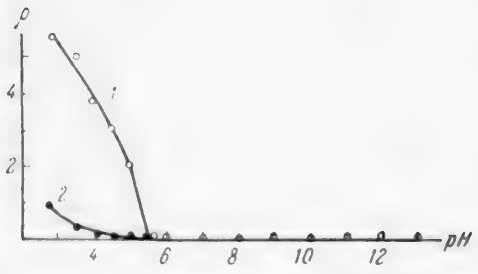

Variation of corrosion rate ρ (in $g/m^2 \cdot$ day) of 20 steel with pH of salicylic and benzoic acid solutions: 1) salicylic acid, 2) benzoic acid.

corrosion at concentrations insufficient for complete protection of steel in distilled water, because owing to the rapid supply of inhibitor to the steel surface most of the latter becomes protected, while the most vulnerable regions of the surface are rapidly attacked because of the rapid supply of oxygen owing to intensified aeration of the solution. Corrosion of these regions could be prevented only by increase of the inhibitor concentration in the solution.

With normal aeration, these inhibitors in amounts insufficient for complete protection of steel in water neither retard nor stimulate corrosion, which is continuous and uniform (Table 4).

With intensified aeration of the solution, sodium benzoate is more effective than sodium salicylate in protecting steel under the same conditons.

It was also necessary to determine the pH range in which sodium salicylate and benzoate have a protective effect. For these experiments 0.0125 M solutions of salicylic and benzoic acids were prepared and titrated with 0.98 N caustic soda solution to give buffer solutions of pH 2.7 to 13 in the case of salicylic acid, and 2.9 to 13 in the case of benzoic acid.

The results showed that sodium salicylate exerts a protective action at pH ≥ 6, and sodium benzoate at pH ≥ 5.5; at these pH values the corrosion of 20 steel in water ceases completely (see figure). Experiments in an oxygen-free medium (in a nitrogen atmosphere) with 0.1 M sodium salicylate and benzoate solutions showed that these substances lose their protective properties in absence of oxygen. On the assumption that the protective action of these substances is due to the formation of insoluble complex compounds containing ferric ions on the steel surface [7], the function of oxygen in the solution is to oxidize ferrous to ferric ions, which then enter the insoluble complex compounds on the steel surface.

SUMMARY

1. Sodium salicylate retards the corrosion of steel in distilled and tap water. The minimum protective concentrations of sodium salicylate and benzoate in tap and distilled water for 10, 20, and U-8 steels have been determined.

2. The optimum temperatures for the protective action of sodium salicylate are 20-60°, and for sodium benzoate, 20-100°.

3. Cl', SO_4'' and NO_3' ions decrease the protective action of sodium salicylate. The minimum protective concentrations of sodium salicylate and benzoate in 0.1, 0.01, and 0.001 M solutions of NaCl, Na_2SO_4 and $NaNO_3$ for 10 steel have been determined.

4. Intensified aeration in solution has a dual effect on the protective properties of these inhibitors: on the one hand, it reduces the minimum protective concentrations of these inhibitors for steel in water, and on the other hand it brings them into the class of "dangerous" inhibitors which cause pitting corrosion at concentrations insufficient for complete protection of steel in distilled water.

5. Sodium salicylate protects 10 steel in the pH range of 6-13.

6. Presence of oxygen is a necessary condition for sodium salicylate to act as an inhibitor of steel corrosion in distilled water.

7. Investigation of the influence of the above-mentioned factors on the protective properties of the two inhibitors showed that the protective action of the salts is diminished by the presence of a hydroxyl group in the benzene nucleus.

LITERATURE CITED

[1] E. G. Stroud and W. H. Vernon, J. Appl. Chem. 2, 4, 166 (1952).

[2] E. G. Stroud and W. H. Vernon, J. Appl. Chem. 2, 4, 173 (1952).

[3] F. C. S. Williams, Eng. Boiler House Rev. 68, 10, 312 (1953).

[4] F. Wormwell and A. D. Mercer, J. Appl. Chem. 2, 3, 150 (1952).

[5] British Patent No. 728634 (1955).

[6] J. A. N. Friend, J. Chem. Soc , 115, 932 (1921).

[7] V. P. Barannik et al., Sci. Mem. OZPI 1, 1, 157 (1955).

Received November 30, 1957.

THE ROLE OF DIFFUSION IN HYDROLYSIS OF POLYSACCHARIDES IN A HETEROGENEOUS MEDIUM*

A. A. Konkin and E. A. Shukalova

The All-Union Scientific Research Institute of Artificial Fibers

Determination of the role of diffusional processes in heterogeneous hydrolysis of polysaccharides by dilute acid solutions is of great significance. In analysis of diffusional processes accompanying hydrolysis it is necessary to take into account changes of acid concentration within the polysaccharide being hydrolyzed, diffusion of the hydrolytic agent toward the inner regions of polysaccharides, and removal of water-soluble products of low molecular weight formed as the result of hydrolysis.

It is known that at the low liquor ratios used in industrial wood hydrolysis, diffusional processes play an important part. In research practice, in studies of cellulose hydrolysis the reaction is usually carried out with large excess of the hydrolytic agent. Various views are held by research workers concerning the role of internal diffusion under such conditions. The relationship between the rate of the hydrolysis reaction and the rate of internal diffusion is still unknown.

It is known that two different mechanisms are possible in heterogeneous reactions. If the rate of diffusion (D) is considerably greater than the rate of chemical reaction, the process takes place in the kinetic region and, conversely, if the rate of chemical reaction exceeds the diffusion rate the process is determined by diffusion. According to Frank-Kamenetskii [1] the following equations are the criteria for determination of the type of reaction: a) if the rate of the process is determined by internal diffusion,

$$\text{then} \quad \frac{NuD_1}{d} \gg \sqrt{D_2 K} \text{ and } H \gg L \gg h;$$

b) if the rate of the process does not depend on diffusion into the solid phase,

$$\text{then} \quad \frac{NuD_1}{d} \gg \sqrt{D_2 K} \text{ and } L \gg H.$$

Many workers consider that heterogeneous hydrolysis of cellulose takes place in the diffusional region and therefore the rate of the process as a whole is determined by diffusion. However, this conclusion is based not on experimental data but on logical reasoning arising from the need to explain certain laws governing the hydrolysis of cellulose. The following arguments are usually advanced as proof. It is known that the heterogeneous hydrolysis of cellulose proceeds at a variable rate. In the opinion of many investigators [2], this is due to differences in the accessibility of different regions of cellulose to the action of the hydrolytic agent or, in other words, it is because the agent penetrates easily and rapidly into some regions and slowly into others, so that the hydrolysis rate varies with time. It follows from this reasoning that variations of the hydrolysis rate, and therefore the process as a whole, are determined by the rate of diffusion of the hydrolytic agent. This viewpoint is currently being developed by E. A. Pakshver and A. B. Pakshver [3]. However, it is based on assumptions which require experimental verification and confirmation.

*Communication 13 in the series on polysaccharide hydrolysis.

Some workers consider that heterogeneous hydrolysis occurs in the kinetic region. Sharkov, Korol'kov, and others [4] have recently supported this view.

Because of the lack of definite data in the literature, we performed an investigation in order to determine the role of diffusion of the hydrolytic agent in heterogeneous hydrolysis of polysaccharides. The criterion for determination of the course of reaction was the value of the activation energy of polysaccharide hydrolysis determined under different reaction conditions. In addition the activation energy for diffusion of water into cellulose was determined. The results obtained are discussed below.

According to our results, the activation energy of polysaccaride hydrolysis in a heterogeneous medium is 26-30 kcal/mole, which is a value characteristic of chemical processes (Table 1).

TABLE 1

Activation Energies of Hydrolysis of Polysaccharides, Monosides, and Disaccharides

Compound	Values of activation energy (cal/mole) in:	
	homogeneous hydrolysis	heterogeneous hydrolysis
Cellulose	27400	27600
Amylose	28400	30600
Galactan	25150	25500
Laminarin	26500	26100
Chitin	25200	27200
Xylan	26200	25400
Cellobiose	29000	—
Maltose	28200	—
Lactose	26150	—
β-Isopropyl glucoside	27400	—
β-Isopropyl galactoside	28100	—
β-Propyl glucoside	27600	—

Similar values for the activation energy of cellulose hydrolysis have been obtained by numerous workers. With increase of temperature, the rate of chemical reaction increases much more rapidly than the rate of diffusion, and therefore at low temperatures heterogeneous reactions very often occur in the kinetic, and at high temperatures in the diffusional region. The transition is usually indicated by a break in the linear plot of the $\log K = f(\frac{1}{T})$ relationship. In the case of cellulose [5], the activation energy of the hydrolysis reaction remains approximately constant over a wide temperature range, up to 200°.

The values of the activation energy of polysaccharide hydrolysis in homogeneous and heterogeneous media, and of homogeneous hydrolysis of monosides and disaccharides, are approximately equal (within the limits of experimental error) (Table 1). This indicates that the activation energy of hydrolysis of the acetal linkage is almost independent of the molecular weight, composition, structure of the monomer unit, and structure of the macromolecules. Since hydrolysis of polysaccharides in a homogeneous medium is not associated with diffusional effects, in such cases the value of the activation energy characterizes the energy aspects of the breakdown of the acetal linkage. Equal values of the activation energy were obtained for hydrolysis of each of the polysaccharides in homogeneous and heterogeneous media. It follows that the activation energy of polysaccharide hydrolysis in a heterogeneous medium relates to breakdown of the acetal linkage. Consequently, diffusion is not the retarding factor in heterogeneous hydrolysis of polysaccharides, and the reaction proceeds in the kinetic region. The above criterion for determination of the nature of a reaction is inadequate only if the activation energy of diffusion of the hydrolytic agent is close to the activation energy of the hydrolysis reaction. Diffusion of gases and liquids through compounds of high molecular weight is a peculiar form of activated diffusion of the molecular type. Migration of substances of low molecular weight (gases and liquids) through polymers is possible after breakdown of intermolecular action. Accordingly, the activation energy of diffusion into polymers may be considerably greater than it is for diffusion in gases and liquids. For many gas–polymer systems the activation energy of diffusion [6] is 7-14 kcal/mole, and for liquids it is much greater (up to 25-30 kcal/mole).

There are no data in the literature on the value of the activation energy (E) of diffusion of water into cellulose, and investigation of this problem was therefore necessary. This investigation involves certain difficulties. The value of E can be found from the relationship between the coefficient of diffusion or the diffusion rate constant and the temperature. The cause of the difficulties is that water diffuses into cellulose at a high rate, and therefore kinetic determinations are rather difficult to carry out. The swelling of cellulose is usually complete in 5-7 minutes. For estimation of E, we consider that it is possible to use water instead of the hydrolytic agent – dilute sulfuric acid solution. The experimental results presented below must be regarded as tentative, as high accuracy is not claimed for the method used for determination of the diffusion rate, but they make it possible to determine the order of magnitude of E.

Viscose monofils 400-800 μ in diameter were used as the starting material. The fibers were previously extracted with dichloroethane to remove fats which might hinder wetting. To diminish the effect of shrinkage, the fibers were soaked in hot water, squeezed out, and dried first in air to the natural moisture regain and then to constant weight over phosphoric anhydride.

The diffusion of water into the fiber was determined from changes in the degree of swelling. Several methods were tested for studying the course of swelling; optical determination of changes in the fiber diameter was chosen as the most suitable method. Determination of only one diameter leads to errors, as changes of fiber volume are determined not only by increase of diameter but also by change of length. However, the error due to this is not large, as the change of fiber length is relatively small whereas the diameter increases by 20-50%.

The coefficient of diffusion was determined from the following equations:

$$x = K\sqrt{\tau}, \tag{1}$$

$$D = \frac{K^2 r_0^2 \pi}{16}, \tag{2}$$

where x is the degree of swelling of the fiber for time τ; τ is the time; K is a constant; r_0 is the fiber radius; D is the coefficient of diffusion.

The degree of swelling was found from the equation

$$x = \frac{d_\infty^2 - d_0^2}{d_\infty^2 - d_\tau},$$

where d_0 is the initial diameter of the fiber; d_τ is the diameter after time τ; d_∞ is the diameter of the fiber at the end of the swelling process.

For determination of K, a graph was plotted in $x - f(\sqrt{\tau})$ coordinates. The value of K was found from the slope of the plot. Graphs for different temperatures are shown in the figure.

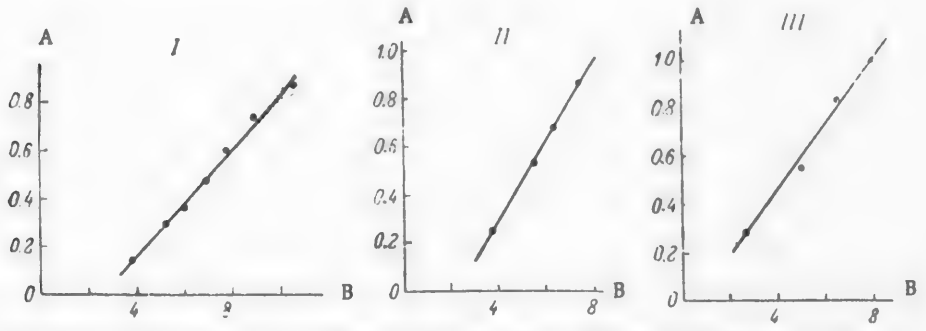

Variations of the degree of swelling of viscose fibers with time at different temperatures: A) degree of swelling (x), B) values of $\sqrt{\tau}$ (seconds); temperature (°C). I) 17, II) 27, III) 37.

TABLE 2

Values of K at 17°

d_0	d_T	K (in $sec^{-1/2}$)
16.4	24	0.142
18.6	26	0.138
17.0	22	0.129
16.6	24	0.138
17.4	23	0.143
	Mean. . . .	0.138

TABLE 3

Values of K at 27°

d_0	d_T	K(in $sec^{-1/2}$)
12.5	20	0.173
15.0	19.5	0.170
16.0	22	0.178
16.0	22	0.163
17.0	24	0.163
21.0	27	0.165
	Mean. . . .	0.169

TABLE 4

Values of K at 37°

d_0	d_T	K(in $sec^{-1/2}$)
11.6	18	0.200
15.0	21	0.186
15.4	19	0.199
16.4	16.8	0.191
18.0	21.5	0.205
23.0	27	0.188
24.0	29	0.195
	Mean. . . .	0.194

TABLE 5

Values of the Coefficient of Diffusion at Various Temperatures

Temperature (°C)	K(in $sec^{-1/2}$)	$D \cdot 10^6$ (cm^2/sec)
17	0.138	3.65
27	0.169	5.48
37	0.194	7.23

The swelling of cellulose was studied at 17, 27, and 37°. It is clear from the data in Tables 2-4* that the value of K remains roughly constant in the different experiments.

The coefficients of diffusion, values of which are given in Table 5, were calculated from these values of K by means of Equation (2).

The activation energy was found graphically from the relationship between the coefficient of diffusion and temperature; the value was 7800 cal/mole.

Direct determination of the coefficient of diffusion of water into cellulose showed that the activation energy of this process is relatively low, and in any event lower than the activation energy of hydrolysis of the acetal linkage in polysaccharides.

Determinations of the activation energy of polysaccharide hydrolysis in homogeneous and heterogeneous media and of the activation energy of diffusion of the hydrolytic agent into cellulose yielded quite convincing results which confirm that the heterogeneous hydrolysis of cellulose, and therefore of other polysaccharides, takes place in the kinetic region. It follows that diffusion of the hydrolytic agent does not influence the rate of polysaccharide hydrolysis in a heterogeneous medium. There is a number of other observations which confirm this conclusion. Sharkov has shown that the rate of cellulose hydrolysis is independent of the duration of its preliminary impregnation with dilute acid for up to 1000 hours. Bone-dry hydrate cellulose, and hydrate cellulose kept in water for a long time are hydrolyzed at the same rate. It must be remembered that our results refer to mild experimental conditions such as are commonly used in research practice. It has been shown by several workers [7] that in the hydrolysis of wood under industrial conditions diffusion effects may play a significant role.

Thus, when the mechanism of polysaccharide hydrolysis in a heterogeneous medium is considered, diffusion of the hydrolytic agent may be disregarded, as it does not control the rate of the process. Variations of the rates of polysaccharide hydrolysis, the influence of polysaccharide structure on hydrolysis rate, and the difficult hydrolyzability of cellulose are due to causes other than diffusion.

SUMMARY

1. The activation energies of hydrolysis of a number of polysaccharides in homogeneous and heterogeneous media, of disaccharides and monosides in a homogeneous medium, and the activation energy of diffusion of water in cellulose have been determined.

*The diameters in Tables 2-4 are given in arbitrary units.

2. It is shown that heterogeneous hydrolysis of polysaccharides takes place in the kinetic region.

LITERATURE CITED

[1] Frank-Kamenetskii, Diffusion and Heat Transfer in Chemical Kinetics [in Russian] (Izd. AN SSSR,1947) p. 110.

[2] N. Nickerson, Ind. Eng. Ch. 34, 85, 1482 (1942); H. Phillipp, Nelson Ziifle, Text. Res. 17, 585 (1947); G. Gibbons, J. Text. Inst. 43, 38 (1952); G. Davidson, J. Text. Inst. 34, 187 (1943).

[3] E. A. Pakshver and A. B. Pakshver, Hydrolysis Ind. USSR 5, 4 (1952).

[4] V. I. Sharkov, Hydrolysis Ind. USSR 4, 4 (1952); V. I. Sharkov, in the book: Chemistry and Physical Chemistry of High Polymers [in Russian] (Izd. AN SSSR, 1952) p. 132.

[5] V. I. Sharkov, Hydrolysis Ind. 1 (1954).

[6] S. A. Reitlinger, Progr. Chem. 10, 213 (1951).

[7] A. P. Zakoshchikov, Z. M. Potyagailo, and O. F. Suvorova, Hydrolysis and Wood Chem. Ind. 8, 4 (1955); I. I. Korol'kov, V. I. Sharkov, E. N. Garmanova, and A. V. Krupnova, Hydrolysis and Wood Chem. Ind. 6, 14 (1955).

Received December 31, 1957.

EFFECT OF ACID CONCENTRATION ON THE HYDROLYSIS RATE OF POLYSACCHARIDES*

L. I. Novikova and A. A. Konkin

Acetal linkages in compounds of low and high molecular weight are resistant to the action of water. Rupture of the acetal linkage is sharply accelerated in presence of catalysts. The reaction is catalyzed by enzymes, acids, salts of weak bases and strong acids, and acid salts. Among these catalysts, acids are the most widely used. The effect of the nature and concentration of the acid on the rate of hydrolysis of the acetal linkage has been the subject of numerous investigations. In the modern view, the mechanism of action of acid catalysts consists of formation of an unstable intermediate compound between the acetal linkage and the hydronium ion. This unstable compound decomposes with formation of the final reaction products. According to this theory the catalytic activity of an acid should be determined by its degree of dissociation. This relationship holds, as a first approximation, at low acid concentrations. The rate of hydrolysis of simple acetals and monosides at low acid concentrations increases in proportion to the acid concentration as has been shown in [1]. This fact was used as the basis for determinations of pH of buffer solutions and hydrogen-ion concentrations in acid solutions from the hydrolysis rates of simple acetals [2]. Arrhenius [3] had shown that the rate of polysaccharide hydrolysis increases in proportion to the acid concentration. Subsequently this was confirmed by a number of workers for the hydrolysis of cellulose by dilute sulfuric acid solutions. According to the data of Zheltukhin, Korol'kov, and Sharkov [4], in the range of sulfuric acid concentrations between 0.1 and 1 N the rate of hydrolysis increases in proportion to the acid concentration over a wide range of temperatures (130-200°). At higher acid concentrations the relationship between hydrolysis rate and concentration becomes more complex. As a rule, the rate of hydrolysis of the acetal linkage increases more rapidly than the concentration and the activity of the acid, especially in the case of concentrated acids. For example, on increase of the concentration of hydrochloric acid from 2.5 to 6 N the hydrolysis rate constant is increased 11-fold. Recently a number of investigators have shown that the relationship between the hydrolysis rates of simple acetals and sucrose and the acid concentration is represented more accurately by the Hammett function [5]. The logarithm of the hydrolysis rate constant (log K) is proportional to the acidity function (H_0). It should be remembered, however, that only a few investigations have been concerned with the influence of concentrated acids on the hydrolysis rates of polysaccharides. The rate of breakdown of the acetal linkage depends not only on the hydrogen-ion concentration but also on the nature of the acid. Different acids have different catalytic activities at the same normality [6]. To account for this, Arrhenius [3] advanced a dualistic theory which took into account the influence of hydrogen ions and undissociated acid molecules on the reaction rate. The mechanism of catalytic action of undissociated acid molecules is still unknown. Direct proportionality between the Hammett acidity function and the logarithm of the hydrolysis rate constant holds fairly accurately not only for any one acid at different concentrations, but also for a number of different acids. This was convincingly demonstrated by Hammett [7] in the inversion of sucrose.

The aim of the present investigation was to study the influence of moderate and high acid concentrations on the rate of polysaccharide hydrolysis, and to establish the relationship between the hydrolysis rate constant and the Hammett acidity function. This question is considered in detail in the literature in relation to simple

* Communication 14 in the series on polysaccharide hydrolysis.

acetals and disaccharides, especially sucrose. No investigations have been reported on this subject in relation to polysaccharides.

EXPERIMENTAL AND DISCUSSION OF RESULTS

The substances chosen for the investigation were cellobiose, cellulose, laminarin, and xylan. Xylan was isolated from straw by the method described by Konkin and Rogovin [8]. The laminarin used in the investigations was isolated from the White Sea alga Laminaria Saccharina by the method described by Black et al. [9]. Cellulose was used in the form of viscose fibers which, in contrast to high-molecular cellulose, dissolve in sulfuric acid of moderate concentration. The hydrolytic agents were sulfuric and hydrochloric acids. The concentration of sulfuric acid was varied in the range of 15.77-50.98%, and of hydrochloric acid, in the range of 7.04-22.4%.

Laminarin and cellulose were hydrolyzed at 30°, and cellobiose and xylan at 40°. The course of the reaction was followed by determinations of iodine number at different stages. The hydrolysis rate constant was calculated from the equation for a first-order reaction. The hydrolysis rate constants calculated for different stages of the reaction vary little. As an example, values of the hydrolysis rate constant for cellulose are given in Table 1. Variations of the hydrolysis rate constants were 0.6-15% of the mean values for the investigated compounds.

TABLE 1

Values of the Hydrolysis Rate Constant for Cellulose at Different Concentrations of Sulfuric Acid

H_2SO_4 concentration (%)					
41.9		46.55		50	
duration of hydrolysis (hours)	hydrolysis rate constant $K \cdot 10^2$ in hr^{-1}	duration of hydrolysis (hours	hydrolysis rate constant $K \cdot 10^2$ in hr^{-1}	duration of hydrolysis (hours)	hydrolysis rate constant $K \cdot 10$ in hr^{-1}
4	0.66	4	0.84	4	2.98
8	0.55	8	0.99	8	3.50
16	0.62	13	1.08	12	3.46
20	0.64	—	—	16	3.59
—	—	—	—	20	3.59
—	—	—	—	24	3.75

TABLE 2

Values of Hydrolysis Rate Constant and Acidity Function at Different Concentrations of Sulfuric Acid

Compound	H_2SO_4 concentration (%)													
	15.77		23.97		35.55		41.9		46.55		50		50.98	
	hydrolysis rate const. $K \cdot 10^2$ in hr^{-1}	acidity function H_0	hydrolysis rate const. $K \cdot 10^2$ in hr^{-1}	acidity function H_0	hydrolysis rate const. $K \cdot 10^2$ in hr^{-1}	acidity function H_0	hydrolysis rate const. $K \cdot 10^2$ in hr^{-1}	acidity function H_0	hydrolysis rate const. $K \cdot 10^2$ in hr^{-1}	acidity function H_0	hydrolysis rate const. $K \cdot 10^2$ in hr^{-1}	acidity function H_0	hydrolysis rate const. $K \cdot 10^2$ in hr^{-1}	acidity function H_0
Cellobiose	0.20	—0.33	—	—	2.03	—1.68	—	—	—	—	—	—	12.54	—3.04
Laminarin	—	—	0.165	—0.86	—	—	1.36	—2.13	2.50	—2.47	10.45	—2.99	—	—
Cellulose	—	—	—	—	—	—	0.62	—2.13	0.97	—2.47	3.48	—2.99	—	—

TABLE 3

Values of Hydrolysis Rate Constant and Acidity Function at Different Concentrations of Hydrochloric Acid

Compound	HCl concentration (%)					
	7.04		16.2		22.4	
	hydrolysis rate constant $K \cdot 10^2$ in hr^{-1}	acidity function H_0	hydrolysis rate constant $K \cdot 10^2$ in hr^{-1}	acidity function H_0	hydrolysis rate constant $K \cdot 10^2$ in hr^{-1}	acidity function H_0
Xylan	1.05	−0.58	9.06	−1.42	41.5	−2.0
Cellobiose	0.30	−0.58	1.87	−1.42	7.35	−2.0

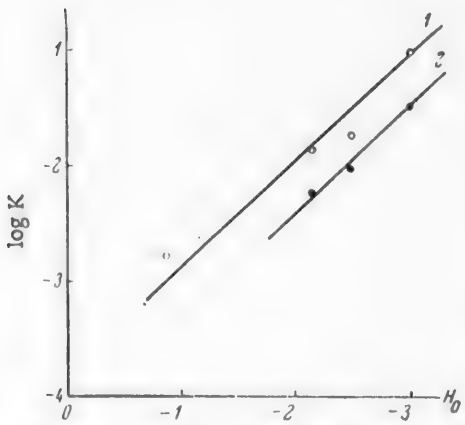

Fig. 1. Variation of the logarithm of the hydrolysis rate constant log K with the acidity function (H_0): 1) laminarin (23.97 − 50% H_2SO_4), 2) cellulose (41.9− 50% H_2SO_4).

Values of the acidity function were taken from Hammett's papers [7,10].

Our results are summarized in Tables 2 and 3 and in Fig.1 and 2.

It follows from these data that the hydrolysis rate constants for cellobiose and polysaccharides increase much more rapidly than the concentrations of sulfuric and hydrochloric acids. When the concentration of sulfuric acid is approximately doubled (from 15.77 to 35.55%), the rate of hydrolysis of cellobiose increases 10-fold. A similar relationship holds for the hydrolysis of cellobiose in hydrochloric acid. Polysaccharides show an even more rapid increase of reaction rate with increase of sulfuric acid concentration. For example,when the concentration of sulfuric acid is doubled (from 23.97 to 46.55%),the rate of hydrolysis of laminarin increases 15-fold.

The hydrolysis rates of cellulose and laminarin increase to roughly the same extent with increase of sulfuric acid concentration. Thus, when the ratio of sulfuric acid concentrations is about 1.2 (from 41.9 to 50%), the ratio of the hydrolysis rates is 6 for cellulose and 7 for laminarin. These results indicate that all polysaccharides conform to a similar relationship with regard to variations of the hydrolysis rate with the sulfuric acid concentration.

The rate of hydrolysis of xylan in hydrochloric acid also increases much more rapidly than the concentration of the acid. A threefold increase of the hydrochloric acid concentration (from 7.04 to 22.4%) results in a 40-fold increase of the rate of xylan hydrolysis.

Fig. 1 and 2 show that there is direct proportionality between the logarithm of the hydrolysis rate constant and Hammett's acidity function. All the points on the plot of $\log K = f(H_0)$ lie on a straight line inclined at 45°. This applies to cellulose, laminarin, and xylan hydrolyzed both in sulfuric and in hydrochloric acid. A similar relationship should apply to all polysaccharides. Thus the acidity function is a quantity which represents most fully and completely variations of the hydrolysis rate in acids of moderate and high concentrations. The lines for different polysaccharides in Fig. 1 and 2 do not coincide, although they lie parallel to each other. This is because of differences in the stability of the acetal linkage and its breakdown rate in acid media. However, the differences between the positions of the lines are not large, as the rates of hydrolysis of different polysaccharides differ little [11].

On the basis of the foregoing results, the hydrolysis rate constants of polysaccharides can be determined graphically for any values of the acidity function. For each value of the Hammett function the corresponding

acid concentration is found from tables or graphs. With the aid of this function it is possible to determine very simply and rapidly the hydrolysis rates of polysaccharides in a homogeneous medium at different acid concentrations.

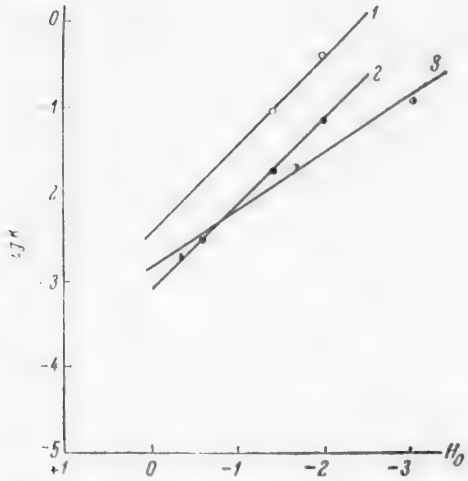

Fig. 2. Variation of the logarithm of the hydrolysis rate constant log K with the acidity function (H_0): 1) xylan (7.04–22.4% HCl), 2) cellobiose (7.04–22.4% HCl), 3) cellobiose (15.77–50.98% H_2SO_4).

For hydrolysis of cellobiose in sulfuric acid, although all the points on the plot of log K = $f(H_0)$ lie on a straight line, the slope of this line is considerably less than 45°. At the same time, if the reaction is carried out in hydrochloric acid, the logarithm of the rate constant is proportional to the Hammett function. The cause of this is not clear.

The direct proportionality between the hydrolysis rate and the acidity function makes it possible to determine the mechanism of the catalytic action of hydronium ions. The acidity function (H_0) is defined by the equation

$$H_0 = -\lg \frac{K_a^B \cdot C_{BH^+}}{C_B},$$

where K_a^B is the dissociation constant of the base, and C_{BH^+} and C_B are the concentrations of the ionized and nonionized forms of the base.

Hammett derived the equation on the assumption that the neutral base interacts with a proton. At the same time, this function is a measure of the ability of a proton to interact with the neutral base. Since the hydrolysis of polysaccharides takes place in accordance with the acidity function, the fundamental assumptions on which the derivation of the equation is based extend to the hydrolysis reaction.

The oxygen in the acetal linkage contains an unshared electron pair and is a typical base. A proton, or, more accurately, a hydronium ion reacts with the oxygen of the acetal linkage, forming an unstable intermediate compound. This intermediate compound – an active complex – decomposes with scission of the acetal linkage between the first (acetal) carbon and oxygen. This reaction mechanism has recently been elucidated by Bunton et al. [12] in the hydrolysis of methyl glucoside by water containing an admixture of heavy water with the O^{18} isotope. This reaction results in the formation of a hydroxyl group at the fourth carbon atom of the glucose residue, and of an unstable complex which decomposes instantaneously under the action of water. An aldehyde group is formed in latent form at the first carbon atom, and this is accompanied by liberation of a proton.

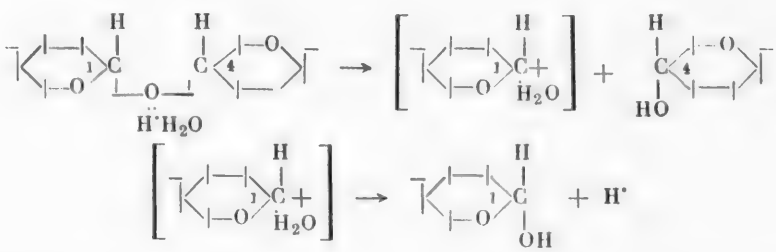

The reaction rate is determined by the stability of the active complex, and, in particular, by the stability of the bond between the acetal oxygen and the first carbon atom. It is known that the rate of hydrolysis of polysaccharides in a homogeneous medium depends, if only slightly, on the structural characteristics of the polysaccharides. The above schemes for the breakdown on the acetal linkage do not explain the specific behavior of acetal linkages in individual polysaccharides. Additional investigations are needed to clarify this problem.

SUMMARY

1. It was shown in a study of the dependence of the rates of homogeneous hydrolysis of cellobiose, cellulose, laminarin, and xylan on the concentrations of sulfuric and hydrochloric acids that the logarithm of the hydrolysis rate constant for cellulose, xylan, and laminarin is directly proportional to the Hammett acidity function. The hydrolysis of cellobiose in sulfuric acid is an exception.

2. The relationship between the hydrolysis rate and the Hammett function is evidence of the formation of an intermediate compound between the acetal linkage and the hydronium ion.

LITERATURE CITED

[1] A. Skrabal and K. Mirtl, Z. Phys. Chem. 111, 98 (1924); H. Hibbert and E. G. Percival, J. Am.Chem. Soc. 52, 3995 (1930).

[2] L. Riesen, and M. Kilpatrick, J. Phys. Chem. 39, 561 (1935); J. Bronsted and G. Grove, J. Am. Chem. Soc. 52, 1394 (1930).

[3] Rideal and Taylor, Catalysis in Theory and Practice (Goskhimizdat, 1933) p. 255 [Russian translation].

[4] D. V. Zheltukhin, I. M. Korol'kov, and V. I. Sharkov, Hydrolysis Ind. USSR 1, 8 (1952).

[5] McIntyre, and F. A. Long, J. Am. Chem. Soc. 76, 3240 (1954); A. I. Shatenshtein, Theory of Acids and Bases [in Russian] (Goskhimizdat, 1949) p. 102.

[6] Ostwald, J. Prakt. Chem. 27, 1 (1883).

[7] L. Hammett and M. A. Paul, J. Am. Chem. Soc. 56, 827 (1934).

[8] A. A. Konkin and Z. A. Rogovin, J. Appl. Chem. 23, 536 (1950).*

[9] A. Black, W. Cornhill, E. Dewar and F. Woodward, J. Appl. Chem. 1, 505 (1951).

[10] L. P. Hammett and A. J. Deyrup, J. Am. Chem. Soc. 54, 2721 (1932).

[11] A. A. Konkin and Z. A. Rogovin, J. Appl. Chem. 32, No.4, 852 (1959).*

[12] G. A. Bunton, T. A. Lewis, D. R. Llewellyn, H. Tristram and C. A. Vernon, Nature 174, 560 (1954).

Received January 16, 1958.

*Original Russian pagination. See C.B. Translation.

POLYMERIZATION OF STYRENE IN PRESENCE OF 1,1'-BIS-HYDROPEROXODICYCLOHEXYL PEROXIDE AND COBALT NAPHTHENATE

R. K. Gavurina, P. A. Medvedeva, Sh. G. Yanovskaya, and L. O. Visleneva

The preceding paper [1] reported results obtained in a study of the polymerization of styrene in presence of 1-hydroxy-1'-hydroperoxodicyclohexyl peroxide (HPC-1) and cobalt naphthenate (CN).

The present paper deals with the continuation of these studies of the polymerization of styrene in presence of 1-hydroxy-1'-hydroperoxodicyclohexyl peroxide (HPC-1) and cobalt naphthenate (CN).

The present paper deals with the continuation of these studies, and is concerned with the polymerization of styrene in presence of CN and 1,1'-bishydroperoxodicyclohexyl peroxide (HPC-1,1').

The results can also be used for estimating the relative activities of HPC-1 and HPC-1,1' in conjunction with CN in oxidation – reduction systems.

RESULTS AND DISCUSSION

The kinetics of polymerization was studied by the dilatometric method and also (at higher conversions) by polymerization in ampoules.

In all the experiments the concentration of HPC-1, 1' was constant at 0.8 mole/liter, while the amount of CN was varied in the range of $0.058 \cdot 10^{-3}$ to $5.8 \cdot 10^{-3}$ mole of Co per liter.

Polymerization in dilatometers. The experiments were performed at three different temperatures: 25, 38.4, and 56.4°.

The corresponding kinetic curves are presented in Fig. 1-3.

Fig. 1(a)-3 (a) show the most interesting initial regions of the curves on an enlarged scale. It is clear from Fig. 3 that addition of CN results in an appreciable increase of the initial rate of polymerization (R_0) at all three temperatures. The concentration of CN is significant – the higher it is, the greater is R_0 (Table 1).

In Fig. 4, R_0 is plotted as a function of the square root of the cobalt concentration.

It is clear from Fig. 4 that R_0 is a linear function of $[Co]^{1/2}$.

As the degree of conversion increases, the polymerization rate begins to a fall somewhat, but still remains fairly high (Fig. 1-3). The higher the CN concentration, the more sharply does the rate change.

Despite the decrease of the polymerization rate, the total duration of the process (for 19% conversion) in all the experiments is decreased considerably on addition of CN, as is clear from the data in Table 2.

The shortest duration of the process was observed in experiments with the highest CN concentration. The samples obtained in these experiments were characterized by the values of $[\eta]$ of their benzene solutions. The values of $[\eta]$ for samples obtained in experiments with and without CN differed little from each other, i.e., up to 19% conversion, addition of CN did not produce any significant change of $[\eta]$.

Polymerization in ampoules was carried out at 38.4°, at HPC-1,1' concentration of 0.8 mole/liter, and CN concentrations in the range of $0.058 \cdot 10^{-3}$ to $0.58 \cdot 10^{-3}$ mole Co/liter.

The results of this series of experiments are given in Fig. 5 and 6.

It follows from Fig. 5 that the polymerization rates remain high in presence of CN even at high conversions up to 80-85 wt. %, and in some experiments almost up to 100% conversion. In this respect the system in question differs favorably from the oxidation–reduction system consisting of Bz_2O_2 and dimethylaniline. According to Imoto et al. [2], in the latter case the initial high polymerization rates subsequently decrease so much that the polymerization process is completely arrested at not very high conversions (in some experiments at 15-20 wt. %).

The influence of this system on the values of $[\eta]$ is clearly seen in Fig. 6.

During the first 20 hours, i.e., at low conversions, additions of CN have no effect on $[\eta]$. These results are in good agreement with the results of determinations of $[\eta]$ for samples obtained by polymerization in dilatometers. However, with increasing conversion, addition of CN results in a considerable increase of $[\eta]$. The increase of $[\eta]$ is greater at higher CN concentrations (compare Curves 2 and 3).

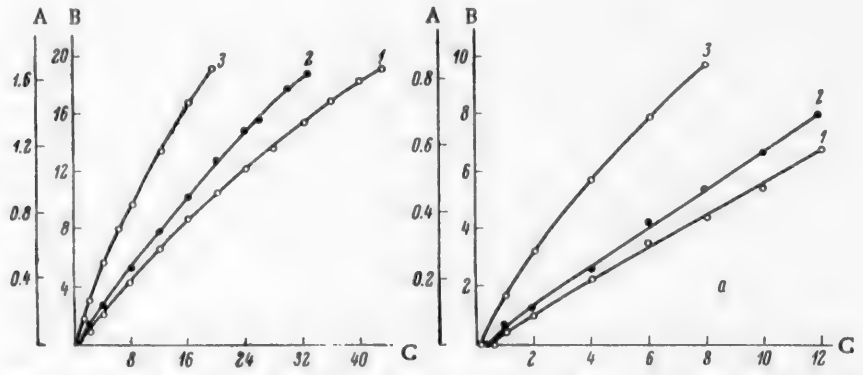

Fig. 1. Kinetic curves for polymerization of styrene at 25° in presence of CN and HPC-1,1': A) conversion (moles/liter), B) conversion (wt.%), C) time (hours); concentration of CN (moles Co/liter): 1) 0, 2) $0.058 \cdot 10^{-3}$, 3) $0.58 \cdot 10^{-3}$.

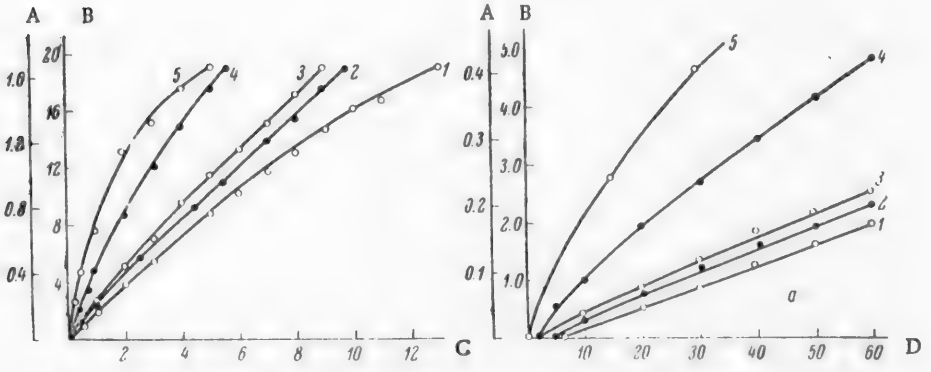

Fig. 2. Kinetic curves for polymerization of styrene at 38.4° in presence of CN and HPC-1,1': A) conversion (moles/liter), B) conversion (wt. %), C) time (hours), D) time (minutes); concentration of CN (moles Co/liter): 1) 0, 2) $0.058 \cdot 10^{-3}$, 3) $0.116 \cdot 10^{-3}$, 4) $0.58 \cdot 10^{-3}$, 5) $5.8 \cdot 10^{-3}$.

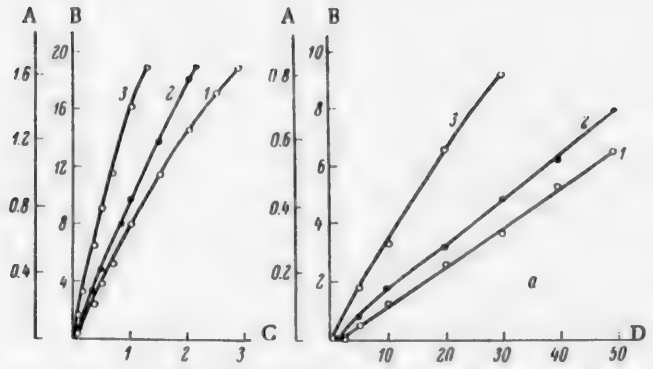

Fig. 3. Kinetic curves for polymerization of styrene at 56.4° in presence of CN and HPC-1,1': A) conversion (moles/liter), B) conversion (wt.%), C) time (hours), D) time (minutes); concentration of CN (in moles Co/liter): 1) 0, 2) $0.058 \cdot 10^{-3}$, 3) $0.58 \cdot 10^{-3}$.

TABLE 1

Effect of Cobalt Naphthenate Concentration on the Initial Polymerization Rate

CN concentration $\left(\frac{\text{moles Co}}{\text{liter}} \cdot 10^3\right)$	$\left(R_0 \frac{\text{moles}}{\text{liter·sec}} \cdot 10^3\right)$		
	25°	38.4°	56.4°
0	0.016	0.054	0.20
0.058	0.019	0.080	0.33
0.116	–	0.082	–
0.58	0.070	0.19	0.62
5.8	–	0.42	–

TABLE 2

Total Duration of Polymerization for 19% Conversion

CN concentration $\left(\frac{\text{moles Co}}{\text{liter}} \cdot 10^3\right)$	Duration of polymerization (hours)		
	25°	38.4°	56.4°
0	42	13	2.8
0.058	32.5	9.7	2.5
0.116	–	9	–
0.58	19	5	1.3
5.8	–	5	–

Comparison of the oxidation–reduction systems HPC-1 + CN and HPC-1,1' + CN. The difference in the course of the kinetic curves with the use of HPC-1 and HPC-1,1' respectively is illustrated by Fig. 7. These curves were determined in the polymerization of styrene in dilatometers at 38.4° at catalyst concentration of 0.8 mole/liter.

Comparison of Curves 1 shows that in absence of accelerator, HPC-1,1' is the more active catalyst. On addition of CN, the curves for HPC-1 and HPC-1,1' differ considerably in their course.

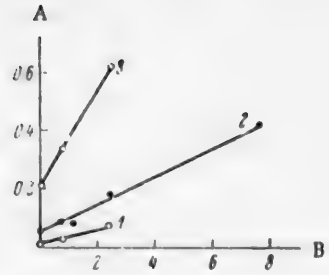

Fig. 4. Effect of accelerator concentration on the initial rate of polymerization: A) initial rate of polymerization $R_0 \cdot 10^3$ (moles/liter.second), B) $[Co]^{1/2} \cdot 10^2$, where [Co] is the CN concentration (moles Co per liter); temperature (°C): 1) 25, 2) 38.4, 3) 56.4.

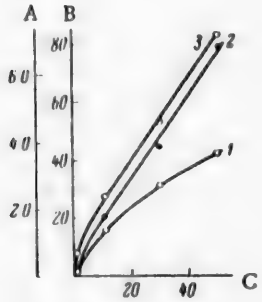

Fig. 5. Kinetic curves for polymerization of styrene in ampoules at 38.4° in presence of CN and HPC-1,1': A) conversion (moles/liter), B) conversion (wt.%), C) time (hours); concentration of CN (in moles Co/liter): 1) 0, 2) $0.058 \cdot 10^{-3}$, 3) $0.58 \cdot 10^{-3}$.

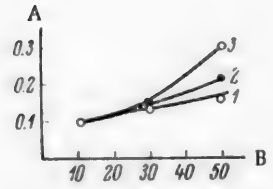

Fig. 6. Variation of intrinsic viscosity $[\eta]$ with time of polymerization in ampoules at 38.4°: A) values of $[\eta]$, B) time (hours); concentration of CN (moles of Co/liter): 1) 0, 2) $0.058 \cdot 10^{-3}$, 3) $0.58 \cdot 10^{-3}$.

In the case of HPC-1 the rate of the process decreases much more sharply with increasing conversion. This effect is especially pronounced at higher CN concentrations, as can be seen from a comparison of Curves 3. Although the initial rates of polymerization for these curves differ little, in the subsequent experiment with HPC-1 the process slows down very sharply whereas with HPC-1,1' the rate alters relatively little. As a result, 19% conversion by weight is reached after 29 hours with HPC-1, and after only 4 hours with HPC-1,1'. On decrease of the CN concentration, the kinetic curves for HPC-1 and HPC-1,1' come closer together (compare Curves 2).

Similar results are obtained on comparison of the kinetic curves for the two systems at other temperatures: 25 and 56.4°.

The difference between of the two systems is also seen clearly on comparison of the relationship between R_0 and $[Co]^{1/2}$ for each (Fig. 8).

At all temperatures, R_0 is higher for HPC-1,1' in absence of CN. However, the change of R_0 on addition of CN is much more pronounced in the case of HPC-1. The straight lines for HPC-1 have a considerably greater slope at all three temperatures (compare 1,2, and 3 respectively).

It is of considerable interest, especially from the practical standpoint, to compare the systems when the polymerization is taken to relatively high conversions. The relevant data for polymerization of styrene in ampoules are given in Tables 3 and 4.

It follows from Table 3 that under equal conditions HPC-1,1' gives higher conversions. The difference is especially large at high conversions; for example, after 50 hours the conversion with HPC-1 was 48-56%, whereas with HPC-1,1' it reached 80-83%. In practice, in experiments with HPC-1,1' quite hard glassy polystyrene samples with low volatile contents can be obtained after 50-55 hours (t = 38.4°). The polymers so formed are completely soluble. In a control experiment with 2% Bz_2O_2 at the same temperature the conversion of styrene after 41 hours reached only 19 wt.%. Comparison of the values of $[\eta]$ given in Table 4 suggests that polymers formed in presence of HPC-1,1' have somewhat lower molecular weights.

To summarize, we may note that the oxidation–reduction systems HPC-1 + CN and HPC-1,1' + CN differ considerably from each other.

EXPERIMENTAL PROCEDURE

The preparation of the styrene and the experimental conditions of polymerization in dilatometers were the same as before, [1].

The synthesis of HPC-1,1', which is stated to have the structure:

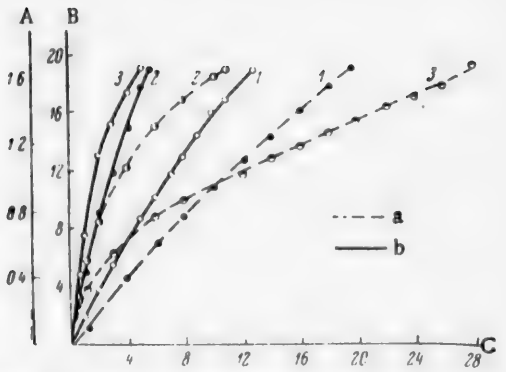

Fig. 7. Kinetic curves for polymerization with different CN concentrations in presence of HPC-1 (a) and HPC-1,1' (b): A) conversion (moles/liter), B) conversion (wt.%), C) time (hours); concentration of CN (moles Co/liter): 1) 0, 2) $0.058 \cdot 10^{-3}$, 3) $5.8 \cdot 10^{-3}$.

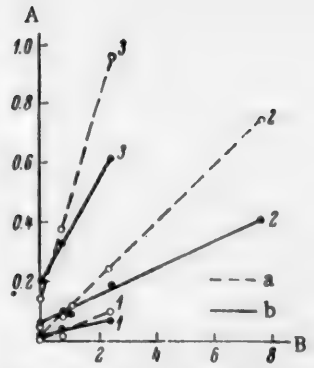

Fig. 8. Effect of accelerator concentration on the initial rate of polymerization R_0: A) initial rate of polymerization $R_0 \cdot 10^3$ (moles/liter · second), B) $[Co]^{1/2} \cdot 10^2$, where [Co] is the CN concentration (in moles Co/liter); a) HPC-1, b) HPC-1,1'; temperature (°C): 1)25, 2) 38.4, 3) 56.4.

TABLE 3

Variation of Conversion with Time; t = 38.4°, catalyst concentration 0.8 mole/liter

Duration of polymerization (hours)	Conversion (wt.%)					
	concentration of CN (moles Co/liter)					
	0		$0.058 \cdot 10^{-3}$		$0.58 \cdot 10^{-3}$	
	HPC-1	HPC-1,1'	HPC-1	HPC-1,1'	HPC-1	HPC-1,1'
1	1	1.9	4.8	—	5.7	7.7
11	12.2	15.8	26	20.3	19.3	27.2
30	24.9	31.8	39.8	44.5	30.8	50.0
50	36	41.9	56	80.0	48.3	83

TABLE 4

Variation of $[\eta]$ with Polymerization Time; t = 38.4°, catalyst concentration 0.8 mole/liter

Duration of polymerization (hours)	Intrinsic viscosity $[\eta]$					
	concentration of CN (moles Co/liter)					
	0		$0.058 \cdot 10^{-3}$		$0.58 \cdot 10^{-3}$	
	HPC-1	HPC-1,1'	HPC-1	HPC-1,1'	HPC-1	HPC-1,1'
1	0.17	0.07	0.1	—	0.16	—
11	0.2	0.10	0.18	0.10	0.28	0.1
30	0.25	0.15	0.27	0.15	0.4	0.15
50	0.28	0.17	0.39	0.22	0.5	0.31

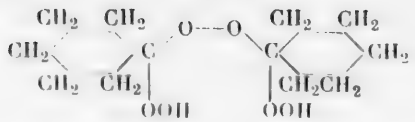

was effected by the Milas method [2,3], by the reaction of concentrated H_2O_2 solutions (80-90%) with cyclohexanone.

The components were taken in the proportions of 2 moles of H_2O_2 (as 2.7 M solution in diethyl ether) to 1 mole of cyclohexanone. The reaction was carried out at room temperature without stirring. After 20 hours of standing, the ether was evaporated off under vacuum and the residual oil was kept under vacuum for 2 hours at 30°, and then under atmospheric pressure at 20°. After 5-10 hours the product began to crystallize. After 15-20 hours the crystalline substance was separated off on a Schott filter and recrystallized twice from methanol. 0.75 g of methanol was taken per 1 g of substance; the treatment temperature was 40-45°. The recrystallized substance was dried under vacuum at 40°.

The same batch of HPC-1, 1' was used for all the polymerization experiments. The substance melted at 82.5-83.5° and contained 17.5% active oxygen.

SUMMARY

1. The action of an oxidation–reduction system consisting of 1,1'-bis-hydroperoxodicyclohexyl peroxide (HPC-1,1') and cobalt naphthenate was studied in the block polymerization of styrene; it was found that the system is active at low temperatures (25-56°).

2. The initial rate of polymerization (R_0) increases with the Co concentration. The relationship between R_0 and $[Co]^{1/2}$ is linear.

3. In the region of low conversion, $[\eta]$ of the polymers is almost unaffected by addition of CN, but it increases appreciably at high conversions. The value of $[\eta]$ increases with the CN concentration.

4. Comparison of the oxidation – reduction systems 1-hydroxy-1'-hydroperoxodicyclohexyl peroxide (HPC-1) + CN and 1,1'-bis-hydroperoxodicyclohexyl peroxide (HPC-1,1') + CN revealed a considerable difference between the effects of the two systems: a) in absence of CN, HPC-1,1' is the more active catalyst, but addition of CN produces a smaller increase of R_0 with this catalyst; b) with HPC-1,1' the polymerization rate changes much less with increasing conversion and remains high at high conversions, so that the total time required to reach high conversions (80-100% by weight) is much less with HPC-1,1'; c) the molecular weight of the polymers is lower with HPC-1,1'.

LITERATURE CITED

[1] R. K. Gavurina, P. A. Medvedeva, Sh. G. Yanovskaya, and Z. A. Granova, J. Appl. Chem. 32, No. 4, 857 (1959).*

[2] M. Imoto, T. Otsu, K. Kimura, Polym. Sci, XV, 80, 475 (1955).

[3] N. A. Milas, S. A. Harris and P. C. Panagiotakos, J. Am. Chem. Soc. 61, 2430 (1939).

[4] R. Criegee, W. Schnorrenberg and J. Becke, Lieb. Ann. 565, 1, 7 (1949).

Received March 24, 1958.

*Original Russian pagination. See C. B. translation.

STUDY OF THE CHEMICAL STRUCTURE OF EMULSION-POLYMERIZED DIVINYL RUBBERS MADE AT + 50 AND − 35°

A. I. Yakubchik, S. K. Zykova, and V. M. Vlasova

The purpose of the present investigation was to carry out a comparative study of the chemical structure of divinyl (butadiene) rubbers made by emulsion polymerization in an acid medium at −35 and +50° .*

Most investigations of the chemical structure of divinyl rubbers have been concerned with determinations of the percentage contents of 1,2 units and of the cis and trans forms of 1,4 units [1-3].

It has been found that the polymerization temperature has little effect on the percentage content of 1,2 units in emulsion-polymerized divinyl, but has a significant influence on the contents of cis and trans 1,4 units. These results were obtained by means of ozonolysis and infrared spectroscopy [1-3].

We used the ozonolysis method, which gives not only the relative amounts of 1,2 and 1,4 units but also their relative arrangement.

The structure of emulsion-polymerized divinyl rubber was studied by the ozonolysis method by Hill et al. [4]. The ozonides were decomposed by the action of hot water and the volatile decomposition products were distilled off under vacuum. The remaining ozonolysis products were oxidized by 1% aqueous potassium permanganate solution. The resultant mixture of acids was separated by distillation of their methyl esters.

In our investigation the emulsion-polymerized rubber ozonides were decomposed by means of acetyl hydroperoxide in acetic acid [5, 6], and the acid mixtures were separated and identified by the method of partition chromatography [5], which had been used earlier by Marvel [7-9] for the same purpose. The methods for separation and analysis of the acid mixtures were described by us earlier [5].

The individual acids in the mixtures were identified by comparison of chromatograms of the mixtures with chromatograms of individual known acids, described as standard acids (the peaks for the standard acids are indicated by dash lines in Fig. 1,2).

The qualitative and quantitative compositions of the acid mixtures formed by ozonolysis of +50 and −35° rubber are given in Table 1. The regions of the macromolecules from which these acids originated are indicated in Table 2.

Apart from the acids which have been presumed and already found in the ozonolysis products of emulsion-polymerized divinyl rubbers [4, 10-12], we found 1, 2, 3-propanetricarboxylic and levulinic acids, which had already been identified in emulsion-polymerized rubbers by Marvel [8,9] and Shikheeva [11].

*For brevity, these are termed +50° rubber and −35° rubber.

TABLE 1

Quantitative and Qualitative Composition of Mixtures Formed by Oxidative Decomposition of the Ozonides of +50 and −35° Rubbers

Peak No.	Acid	+50° rubber: amount of acids in sample, meq	+50° rubber: amount of acids in sample, g	+50° rubber: amount of acids total (g)	+50° rubber: contents of C in acid (g)	+50° rubber: contents of carbon skeleton of rubber in acid (%)	−35° rubber: amount of acids in sample, meq	−35° rubber: amount of acids in sample, g	−35° rubber: amount of acids total (g)	−35° rubber: contents of C in acid (g)	−35° rubber: contents of carbon skeleton of rubber in acid (%)
	Viscous acids										
II	Levulinic	0.0372	0.0043	0.1072	0.0554	1.02	0.024	0.0027	0.0766	0.039	0.74
IV	Formic	0.0425	0.0019	0.0474	0.0123	0.227	0.0137	0.0006	0.017	0.0004	0.008
VI	Succinic	0.5217	0.0308	0.7683	0.312	5.75	0.2976	0.0175	0.4963	0.2015	3.83
VII	1,2,4-Butanetricarboxylic	1.4762	0.0934	2.33	1.03	19.00	1.118	0.0707	2.006	0.8866	16.90
VIII	1,2,3-Propanetricarboxylic	0.2538	0.0148	0.369	0.151	2.78	0.1713	0.0099	0.2805	0.1147	2.18
IX	1,2,4,6-Hexanetetracarboxylic	0.0558	0.0036	0.0898	0.0411	0.75	0.0271	0.0016	0.0454	0.0208	0.40
	Crystals I										
VI	Succinic	0.1888	0.0111	0.902	0.366	6.75	0.2152	0.0127	2.21	0.8972	17.08
	Crystals II										
VI	Succinic	0.226	0.0133	3.51	1.42	26.2	0.1966	0.0116	3.88	1.28	24.42
VII	1,2,4-Butanetricarboxylic	0.0058	0.0003	0.08	0.035	0.6	—	—	—	—	—
	Total					63.08					65.56

TABLE 2

Contents of the Carbon Skeleton of +50 and −35° Rubbers Found in Definite Regions of the Macromolecules

Peak No.	Acid	content of carbon skeleton of rubber in acid (%) +50°	content of carbon skeleton of rubber in acid (%) −35°	Region from which acid originated	Contents of carbon skeleton of rubber in units +5°	Contents of carbon skeleton of rubber in units −35°	Contents of carbon skeleton of rubber in units: 1,2 +50°	1,2 −35°	1,4 +50°	1,4 −35°
II	Levulinic	1.02	0.74	1,4—1,2—1,4*	1.36	0.98	0.68	0.37	0.68	0.37
IV	Formic	0.23	0.008	1,2 units						
VI	Succinic	38.70	45.33	1,4—1,4	38.70	45.33	—	—	38.70	45.33
VII	1,2,4-Butanetricarboxylic	19.60	16.90	1,4—1,2—1,4	22.40	19.28	11.20	9.64	11.20	9.64
VIII	1,2,3-Propanetricarboxylic	2.78	2.18	1,4—1,2—1,4*	3.17	2.48	1.58	1.24	1.58	1.24
IX	1,2,3-Propanetricarboxylic	0.75	0.40	1,4—$(1,2)_2$—1,4	0.90	0.48	0.60	0.26	0.30	0.13
	CO_2 liberated during decomposition of ozonide	0.33	0.82	—	—	—	—	—	—	—
		63.41	66.38		66.53	68.55	14.06	11.51	52.46	56.71

*Abnormal ozonolysis products from 1,4-1,2-1,4 region.

The formation of 1,2,3-propanetricarboxylic acid may be accounted for in two ways: first, 1,2,3-propanetricarboxylic acid may have been formed from the 1,4-1,4 region as the result of chain transfer by the growing radical at the α-methylene group [8, 11]:

$$-CH_2-CH=CH-CH_2-CH_2-CH=CH-CH_2-\ldots + R^{\cdot} \rightarrow$$
$$-CH_2-CH=CH-\underset{|}{CH}-CH_2-CH=CH-CH_2- + RH;$$

second, addition of monomer molecules to a new radical gives a branched region (I):

$$-CH_2-CH=CH-\underset{\displaystyle CH_2}{\underset{|}{CH}}-CH_2-CH=CH-CH_2- \qquad (I)$$
$$\begin{array}{l} | \\ CH \\ \| \\ CH \\ | \\ CH_2 \\ | \end{array}$$

Ozonolysis of region (I) should yield 1,2,3-propanetricarboxylic acid.

The formation of region (I) may lead not only to branching but also to cross linking of the molecules. However, Drysdale and Marvel [13] showed that this kind of branching of divinyl molecules at the α-methylene carbon in radical polymerization is unlikely. Second, it may be supposed that 1,2,3-propanetricarboxylic acid may be formed as the result of secondary reactions during ozonolysis of rubbers from the 1,4–1,2–1,4 regions [8, 9].

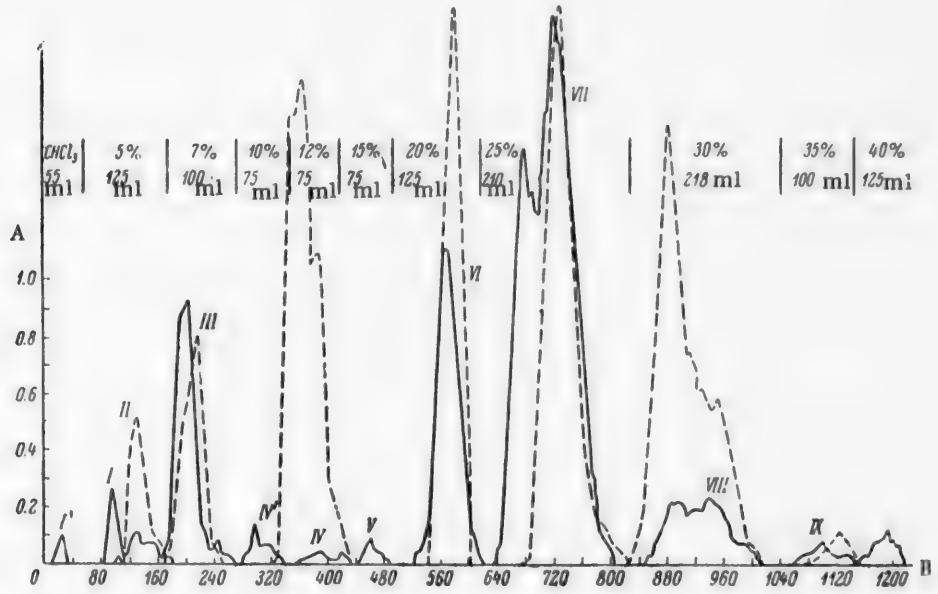

Fig. 1. Chromatogram (medium column) of the acids formed by ozonolysis of −35° rubber (viscous acids): A) amount of 0.028 N alkali (ml) for titration of the eluate, B) volume of eluate (ml); peaks: II) levulinic; III) acetic; IV) formic; VI) succinic; VII) 1,2,4-butanetricarboxylic; VIII) 1,2,3-propanetricarboxylic; IX) 1,2,4,6-hexanetetracarboxylic acid; the numbers above represent the development system, the percentage content of butanol in chloroform and the amount of motile solvent (ml).

Evidence in support of this hypothesis is the presence of propanetricarboxylic acid in the ozonolysis products of vinylcyclohexene [8,9,14,15], which is a model of the 1,4–1,2–1,4, region.

The ozonolysis products of our rubbers were found to contain a small amount (~3 % of the carbon skeleton of the rubber) of 1,2,3-propanetricarboxylic acid, which is the abnormal product of ozonolysis of 1,4–1,2–1,4 regions in these rubbers. Levulinic acid could have been formed from an isomerized 1,4–1,2–1,4 region [9]. In addition, this acid may have been the product of abnormal decomposition of ozonides [16]. Ziegler [16] considers that levulinic acid is formed as the result of peroxide – formate regrouping from the 1,4–1,2–1,4, region, where the 1,2 link contains a tertiary carbon atom in the α-position with respect to the carbon linked by a double bond.

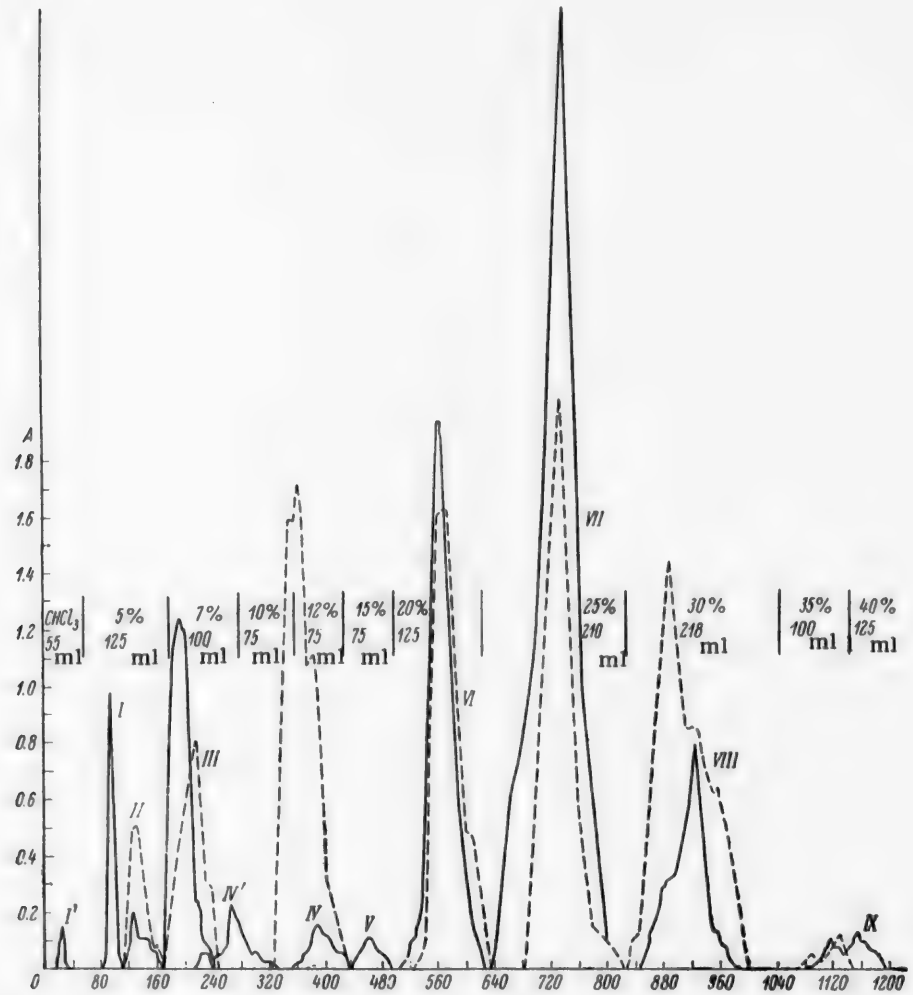

Fig. 2. Chromatogram (medium column) of acids from +50° rubber (viscous acids); caption as in Fig. 1.

Levulinic acid was found in the oxidative-decomposition products of vinylcyclohexene ozonide [14-16]; this confirms that the acid can be formed from the 1,4–1,2–1,4 region as the result of abnormal decomposition of ozonides.

Succinic, 1,2,4-butanetricarboxylic, and 1,2,4,6-hexanetetracarboxylic acids are the normal ozonolysis products of the 1,4–1,4; 1,4–1,2–1,4; 1,4–$(1,2)_2$–1,4 regions respectively.

In the acids which we identified – ozonolysis products of the two rubbers – we found 63-65% of the carbon skeleton of the rubbers. The remaining 35% of the carbon skeleton includes, first, the three unidentified acids which corresponds to the peaks I^1, I, IV^1, V in the chromatograms (Fig. 1 and 2) and second, losses which might have occurred in the oxidative decomposition of ozonides and as the result of partial breakdown of the acids by the action of acetyl hydroperoxide [6].

The chromatograms of the mixed acid ozonolysis products of the two rubbers were used to calculate the amount of each acid in the mixtures and the proportion of the carbon skeleton of the rubber present in each acid. The percentage of the carbon skeleton corresponding to the region of the macromolecule from which a given acid was formed was calculated from the amount of acid.

The results are given in Tables 1 and 2.

Acetic acid was not taken into account, as it was used as the medium for oxidative decomposition of the ozonides.

It follows from Table 2 that +50 and −35° rubbers are very similar in chemical structure (within the limits of the carbon skeleton accounted for); neither are there large differences in the distribution of the different units.

EXPERIMENTAL

Divinyl rubbers made by emulsion polymerization in an acid medium at −35 and +50° were taken for the experiments.

The rubber made at −35° was purified by 3-fold precipitation by ethyl alcohol from 2% solution in benzene. Neozone D (0.2%) was added to the alcohol in the precipitation. The rubbers were precipitated and dissolved in an atmosphere of purified nitrogen. The + 50° rubber was purified by extraction with an azeotropic mixture (70 parts of ethyl alcohol and 30 parts of toluene) in a Soxhlet apparatus.

The rubbers were dried under 2-3 mm vacuum at 34°.

Results of Combustion of Rubbers with Copper Oxide

Found %: C 88.49, H 11.23 for −35° rubber;
C 88.58, H 11.01 for +50° rubber.

$(C_4H_6)_n$. Calculated %: C 88.88, H 11.11.

The degree of unsaturation was determined only for the −35° rubber, as the +50° rubber was insoluble. Unsaturation of the −35° rubber was determined by Vasil'ev's method for divinyl rubbers [17]. The unsaturation of −35° rubber found by this method was 89.85%. The content of external double bonds in the −35° rubber was 26.7% (by the method with formic acid and aldehyde [1]).

Ozonized oxygen (containing 6-7% ozone) was used for ozonation of the −35 and +50° rubbers. Ozonized oxygen was passed at a rate of 20 liters/hour through a suspension of rubber in methyl acetate. The ozonation was performed at −20, −25°.

The course of ozonation was followed by determinations of the ozone concentrations in the incoming and outgoing gas by iodometric titration. The oxidative decomposition of rubber ozonides was effected by the action of acetyl hydroperoxide in acetic acid [6]. Acetyl hydroperoxide was prepared by the action of acetic anhydride (b.p. 136°) on concentrated hydrogen peroxide in presence of concentrated sulfuric acid. The acetyl hydroperoxide so prepared was usually of 56-57% concentration. All the operations in the oxidative decomposition of rubber ozonides were performed in the same sequence as in the earlier investigation [14].

It is possible that secondary processes occur during oxidative decomposition of ozonides, and some of them may be accompanied by liberation of gaseous products; we therefore attempted to collect such gaseous products in all the experiments on oxidative decomposition. The gas was collected in gas holders filled with a saturated solution of common salt.

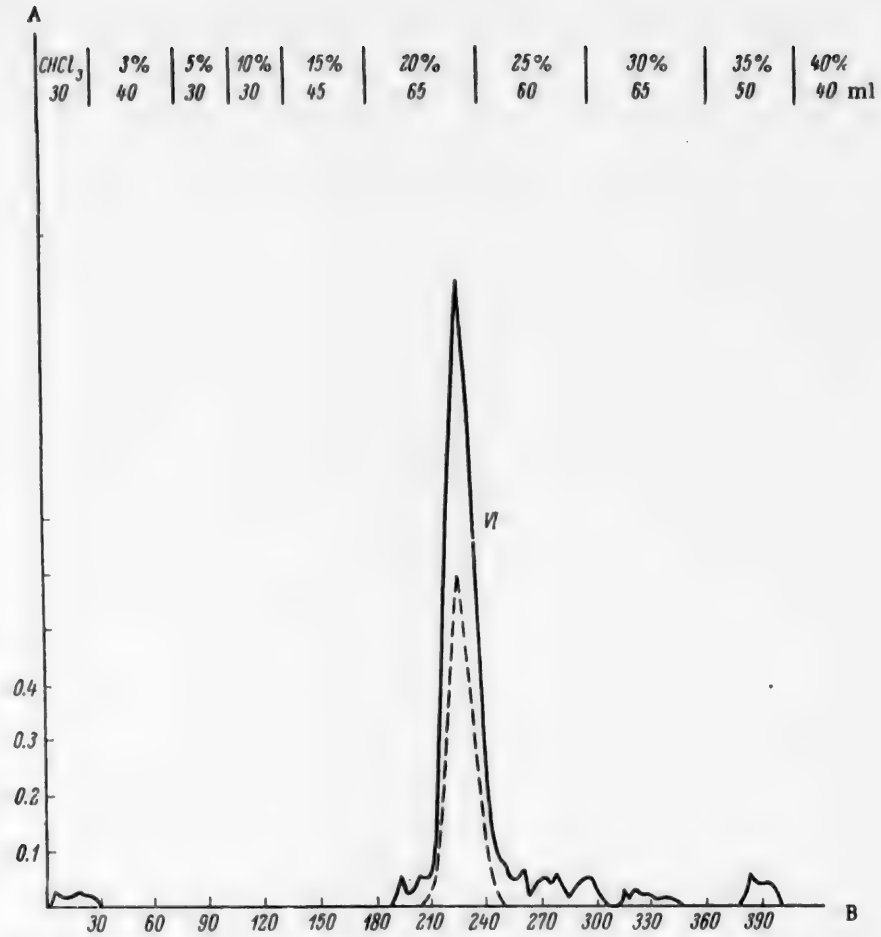

Fig. 3. Chromatogram (medium column) of acids from −35° rubber (crystals I); caption as in Fig. 1.

A control experiment was carried out for comparison: acetyl hydroperoxide and acetic acid, in the quantity necessary for decomposition of rubber ozonide (calculated for 3 g of rubber) were subjected to the same procedure as in the experiments with rubber. The liberated gas was collected and analyzed. Analysis showed that the gases consisted mainly of oxygen and carbon dioxide. The same components were found in the gas in the control experiment. The amounts of the gases liberated in the oxidative decomposition of both rubber ozonides were found from the amounts of gases liberated in the control experiment and in the oxidative decomposition of the ozonides respectively. The proportion of the carbon skeleton of the rubber present in the liberated carbon dioxide was calculated; it was found to be 0.33% for +50° rubber, and 0.82% for the −35° rubber.

At the end of the oxidative decomposition of ozonides the excess acetyl hydroperoxide in the mixture of products was decomposed by means of platinum black. Complete disappearance of peroxide was indicated by the potassium iodide test. A qualitative test for aldehydes was negative.

The crystals deposited in the ozonolysis products were filtered off and dried (crystals I). Acetic acid was distilled off from the solutions of the ozonolysis products of both rubbers at 10-13 mm and bath temperature 35-40°, with a system of traps with water in order to collect any acids which might distil over with the acetic acid; the yellowish viscous mass, permeated with crystals, which remained after removal of acetic acid was separated into two portions – crystals II as "viscous acids" – by treatment with ethyl ether.

The acid products of rubber ozonolysis were separated and analyzed by partition chromatography [5]. Levulinic, formic, acetic, and succinic acids were used for preparation of the artificial mixtures. In addition, the following acids were synthesized for this purpose: 1,2,4-butanetricarboxylic, 1,2,3-propanetricarboxylic,

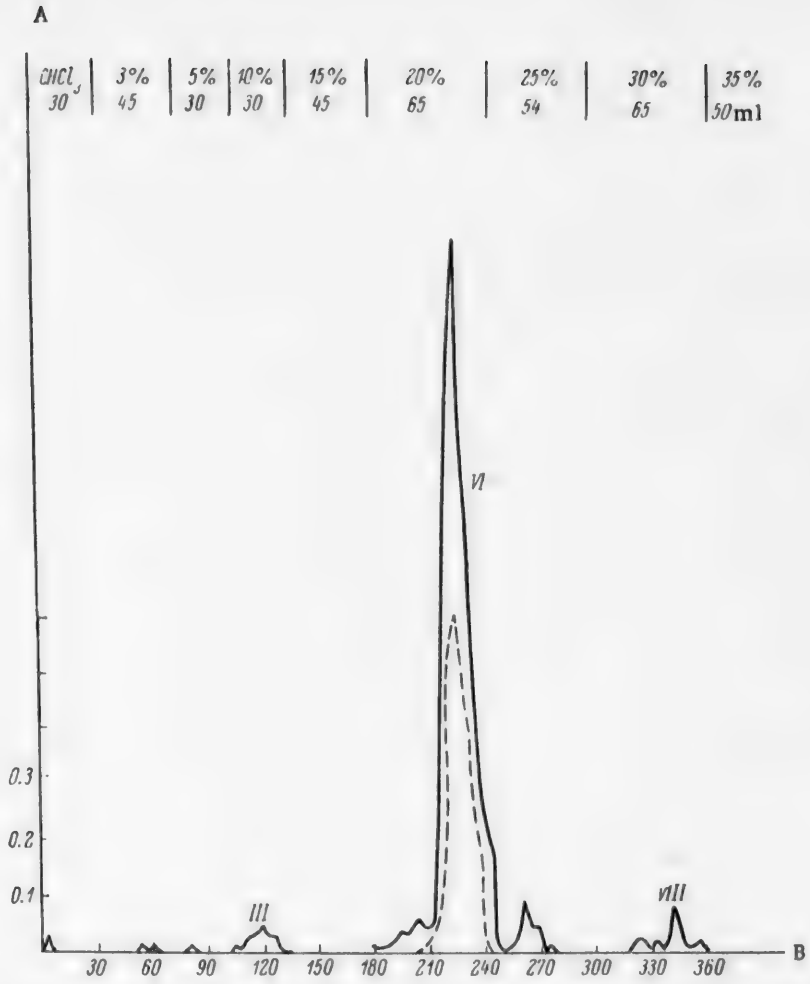

Fig. 4. Chromatogram (small column) of acids from −35° rubber (crystals II); caption as in Fig.1.

and 1,2,4,6-hexanetricarboxylic. Small columns (internal diameter 16 mm, 7 g of silica gel) and medium columns (internal diameter 18 mm, 22 g of silica gel) were used for the chromatographic separations. The columns were packed, the solvents prepared, and the acids eluted as described previously [5, 14]. Chromatograms were obtained for solutions of acid products of ozonolysis of +50 and −35° rubbers ("viscous acids"), in a 50% mixture of tertiary amyl alcohol and chloroform in a small column, and in water in a medium column (the latter are shown in Fig. 1, 2). With the medium column, samples weighing 0.1226 g were taken in 1.2 ml of water (+50° rubber), and the eluate was titrated by 0.028 N NaOH solution (Fig.1,2). Solutions of crystals I and II in 50% mixture of isoamyl alcohol and chloroform were passed through small columns under the same conditions as those used for viscous acids (Fig. 3-6). The weights taken were: crystals I, 0.0137 g; II, 0.0134 g (−35° rubber); I, 0.0123 g; II, 0.0137 g (+50° rubber).

The same conditions (efflux rate, developing system, volume of solution) were used for passing solutions of standard acids for chromatographic identification of the acids in the unknown mixtures (results are shown by dash lines in the chromatograms in Fig. 1-4).

Acetic acid distilled off from the ozonolysis products of the two rubbers, and water from the traps used in the distillation of the acetic acid, were passed through a small chromatographic column.

The chromatograms showed that only small amounts of acids are carried over with the acetic acid, and no acids were detected in the water traps.

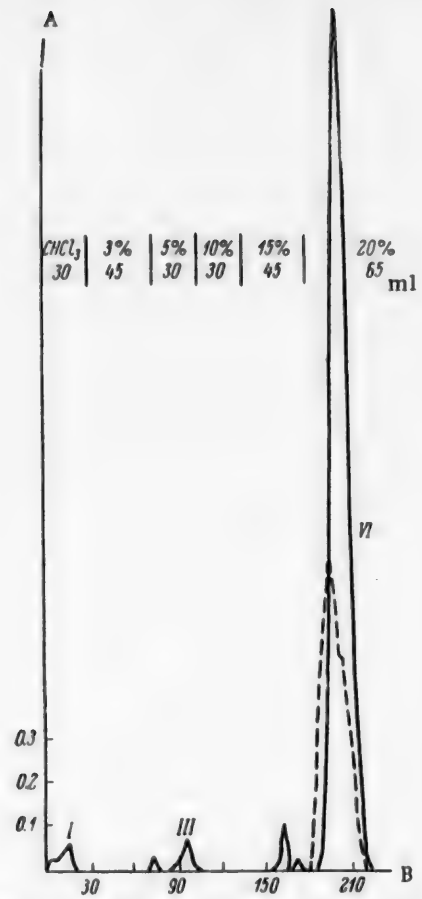

Fig. 5. Chromatogram (small column) of acids from +50° rubber (crystals I); caption as in Fig. 1.

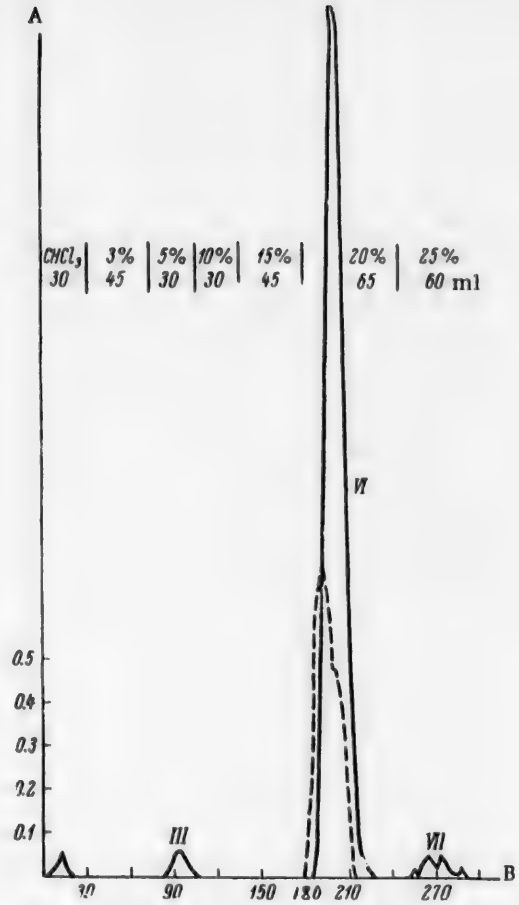

Fig. 6. Chromatogram (small column) of acids from +50° rubber (crystals I); caption as in Fig. 1.

SUMMARY

1. The ozonolysis products of +50 and −35° rubbers were found to contain 1,2,3-propanetricarboxylic acid and levulinic acid, which are the products of abnormal decomposition of ozonides of 1,4–1,2–1,4 regions.

2. The chemical structures of the two rubbers (within the limits of the carbon skeleton accounted for) are similar.

LITERATURE CITED

[1] A. I. Yakubchik, A. A. Vasil'ev, and V. M. Zhabina, J. Appl. Chem. 17, 63, 107 (1944).

[2] E. I. Hart, and A. W. Meyer, J. Am. Chem.Soc. 71, 6, 1980 (1949).

[3] A. W. Meyer, Ind. Eng. Chem. 41, 8, 1570 (1949).

[4] R. Hill, I. R. Lewis and J. L. Simonsen, Trans. Faraday Soc. 35, 8, 1067 (1939).

[5] A. I. Yakubchik and S. K. Zykova, J. Appl. Chem. 29, No.10, 1591 (1956). *

[6] H. Wilms, L. Ann. 567, 1, 3, 96 (1950).

[7] C. S. Marvel, E. Rupert and R.Light, J. Am. Chem. Soc. 72, 9 (1950).

[8] C. S. Marvel and W. Schilling et al., J. Org. Chem. 16, 6, 838 (1951).

[9] C. S. Marvel and C. Bluestein, J. Org. Chem. 16, 6, 854 (1951).

[10] E. N. Alekseeva, J. Gen. Chem. 9, 15, 1426 (1939); J. Gen. Chem. 11, 4, 353 (1941).

[11] A. I. Yakubchik, in the book: Academician S. V. Lebedev [in Russian] (Izd. AN SSSR, Moscow, 1954).

[12] W. Rabjohn and C.E. Bryan, J. Am. Chem. Soc. 69, 314 (1947).

[13] J. J. Drysdale and C. S. Marvel, J. Polym. Sci. 13, 72, 513 (1954).

[14] A. I. Yakubchik, S. K. Zykova, and S. P. Goncharuk, J. Appl. Chem. 30, 1657 (1958).*

[15] A. I. Yakubchik, A. I. Spasskova,and B. I. Tikhomirov, J. Gen. Chem. 28, 916 (1958).*

[16] K. Ziegler, and W. Hechelhammer, L. Ann. 567, 99 (1950).

[17] A. A. Vasil'ev, J. Gen. Chem. 17, 5, 923 (1947).

Received December 30, 1957.

*Original Russian pagination. See C. B. translation.

EPOXY RESINS BASED ON DIPHENYLOLETHANE (4,4'-DIHYDROXY-DIPHENYLMETHYLMETHANE) AND PHENOL–ACETALDEHYDE RESINS

G. L. Yukhnovskii and Zu Khva-den

Epoxy resins are condensation products of epichlorohydrin (ECH) with di- or polyhydric phenols, usually diphenylolpropane [1]. Resorcinol, hydroquinone, and other polyhydric phenols are also used [2]. The use of a low-molecular alkylphenol novolac resin as the polyhydric phenol is described in a patent [3].

The present investigation was concerned with the use of diphenylolethane (DPE) and phenol–acetaldehyde resins as polyhydric phenols instead of diphenylolpropane (DPP). This work was carried out in connection with the raw materials available in Korea. As is known, diphenylolpropane is synthesized from phenol and acetone, while diphenylolethane, like phenol–acetaldehyde resins, is made from phenol and acetaldehyde.

In Korea, acetone and acetaldehyde are produced from acetylene. In consequence, the cost of acetaldehyde is considerably lower than the cost of acetone. Therefore replacement of acetone by acetaldehyde in the production of epoxy resins is of great practical importance.

We found no publications on this subject in the literature.

At the start of this investigation we used DPE obtained from the works, previously distilled with steam to remove free phenol, for synthesis of epoxy resins.

With the molar proportions of 1-2 moles of ECH to 1 mole of DPE, cross-linked polymers were always obtained; these were insoluble in all solvents.

It was of great interest to find why cross-linked polymers were formed.

The formation of a space polymer in the reaction of DPE with ECH indicates that DPE contains more more than two functional groups in the molecule.

A cross-linked polymer may have been formed if, apart from pure DPE, its polymer homologs also took part in the reaction according to the following scheme:

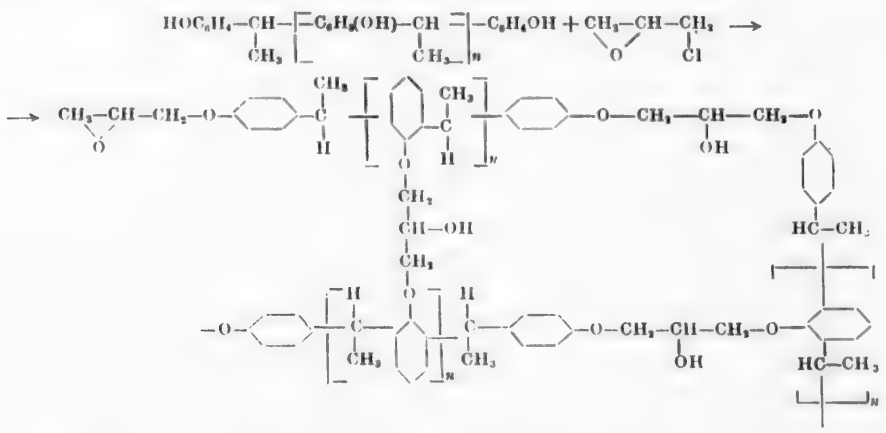

It was therefore necessary to prepare an epoxy resin from pure DPE free from homologs. Pure DPE and phenol–acetaldehyde resins were synthesized for this purpose.

Synthesis of diphenylolethane and phenol–acetaldehyde resins. Bayer [4] found as long ago as 1872 that resinous substances are formed when acetaldehyde is added to a mixture of phenol and sulfuric acid. Later Fabinyi [5] isolated a small quantity of a white crystalline substance of m.p. 122°, with the composition $C_{14}H_{14}O_2$, from the resin formed by condensation of phenol with paraldehyde in presence of stannic chloride; analytical data indicated that this substance was diphenylolethane. However, it was not until 1904 that Lun'yak showed [6] that to obtain crystalline diphenylolethane in good yields mixtures containing a large excess of phenol should be used; for example, 4 moles of phenol per mole of aldehyde. Vansheidt, Itenberg, and Shifrina [7] described phenol–acetaldehyde resins obtained with various molar proportions of phenol to acetaldehyde (1 to 4 moles of phenol per mole of acetaldehyde). They reported that pure DPE is obtained only at molar ratios of over 4 moles of phenol to 1 mole of acetaldehyde. With lower phenol contents phenol–acetaldehyde resins of the novolac type are formed. They also described a method for synthesis of DPE. It has also been reported [8,9], when phenol reacts with acetylene in presence of $H_3PO_4 \cdot BF_3$ and HgO as catalysts, DPE is formed in yields of up to 50% of the theoretical.

We synthesized DPE by the method of Vansheidt et al. (with 4:1 molar ratio of phenol to acetaldehyde). After removal of free phenol by steam distillation, the melting point of the product (which was lower and less sharp than that of DPE) and its molecular weight did not correspond to pure DPE. For purification, it was recrystallized from solutions in benzene, toluene, xylene, ligroine, and ethanol. Benzene proved to be the most suitable solvent. Benzene dissolves DPE quite well on heating, and homologs are also partially dissolved. When the benzene solution is cooled, the DPE homologs are first deposited in the form of a resinous mass. The benzene solution of DPE is separated by decantation from DPE homologs and left to crystallize. On standing, the solution gradually deposits DPE in the form of crystals. After twofold recrystallization from benzene, DPE forms snow-white crystals melting at 121°.

We synthesized DPE with different proportions of phenol to acetaldehyde, in the range of 4 to 1.75 moles of phenol to 1 mole of acetaldehyde. In each experiment pure DPE could be isolated by extraction in benzene followed by recrystallization. The residue after extraction of DPE was a phenol–acetaldehyde resin of the novolac type.

TABLE 1

Characteristics of the Products of DPE Synthesis

Resin code mark	Molar ratio of phenol to acetaldehyde	Amount (g)		Yield (g)			Amount of DPE as % of total yield	Softening temp. of resin after separation of DPE (°C)	Molecular weight of resins after separation of DPE
		phenol	aldehyde	phenol	DPE	resin			
F-1	4 : 1	201.0	23.5	98.1	51.0	47.1	52.0	52	340
F-2	3.5 : 1	176.0	23.5	93.6	29.2	64.4	31.2	56	360
F-3	3 : 1	151.0	23.5	90.5	13.5	77.0	14.9	58	362
F-4	2.5 : 1	126.5	23.5	89.1	10.0	79.1	11.2	59	372
F-5	2 : 1	100.5	23.5	84.1	7.1	77.0	8.45	66	414
F-6	1.75 : 1	116.0	31.35	103.0	4.6	98.4	4.46	74	430

Table 1 gives details of the products formed and the percentage contents of pure DPE in the products at different initial molar ratios of phenol to acetaldehyde. The synthesis was carried out at room temperature, with a reaction time of two days.

It follows from Table 1 that even with a 4:1 molar ratio of phenol to acetaldehyde, an approximately equal amount of phenol–acetaldehyde resin is formed together with DPE. In other cases DPE is also formed in addition to the resin, although the yield of DPE falls sharply with decrease of the molar content of phenol.

TABLE 2

Characteristics of the Products of Synthesis of Phenol–Acetaldehyde Resins

Resin code mark	Molar ratio of phenol to acetaldehyde	Amount (g)		Yield of resin (g)	Softening temperature (°C)	Molecular weight of resins	Reaction conditions
		phenol	aldehyde				
F-7	4 : 1	1000	117.0	480	–	264	At room temperature (20-24°) for 2 days
F-8	3 : 1	302	47.0	184	35	295	
F-9	2 : 1	201	47.0	164	54	330	
F-10	1.75 : 1	174	47.0	151	65	402	
F-11	1.75 : 1	116	31.35	108	77	460	Overnight at room temperature, then heated at 60-65° for 3 hours
F-12	1.5 : 1	100	31.35	93	84	640	
F-13	1.5 : 1	200	62.7	193	84	800	Overnight at room temperature, then heated at 85-105° for 3.5 hours
F-14	1.25 : 1	166	62.7	168	91	1075	
F-15	1 : 1	133	62.7	139	96	1400	

As starting materials for subsequent synthesis of epoxy resins we required, in addition to DPE, phenol–acetaldehyde resins of different molecular weights. For this purpose we specially synthesized a series of resins of different molecular weights (without isolation of DPE).

The characteristics of these resins and the reaction conditions are given in Table 2.

Investigation of works DPE. To find the causes of formation of the cross-linked polymer, we synthesized epoxy resins with the use of pure DPE of m.p. 121°.

The characteristics of epoxy resins made from pure DPE are given below.

Resin code mark	Molar ratio of DPE to ECH	Softening temperature of resin (°C)	Epoxy equivalent	Mol. wt.
No. 1	1 : 2.5	liquid	272	380
No. 2	1 : 2.25	liquid	295	475
No. 3	1 : 2.0	32	310	540
No. 4	1 : 1.7	48	387	582
No. 5	1 : 1.5	64	495	750
No. 6	1 : 1.2	82	755	945
No. 7	1 : 1.0	93	1520	1280

It follows from the above data that space polymers are not formed when epoxy resins are made with pure DPE at any molar ratios of DPE to ECH. This shows that works DPE is not an individual product, but contains polyfunctional DPE homologs, which are the cause of formation of the cross-linked polymer.

To determine the contents of pure DPE in works DPE we attempted to isolate pure DPE by benzene extraction as described above for the synthesis of pure DPE. Pure DPE could not be isolated by this method. After removal of free phenol the works DPE had a softening temperature of 76° and a molecular weight of 448.

The works procedure for synthesis of DPE is as follows. Phenol is put into a stainless steel reactor fitted with a stirrer and condenser. The phenol is melted at 40-50°, the stirrer is switched on, and hydrochloric acid is added. Paraldehyde is fed during one hour at 50°, and condensation then proceeds at 65 ± 2°, for 6 hours.

The formulation used in the works production of DPE is given below.

Raw material	Amount (%)	Molar ratio
Phenol	77.70	1.66
Paraldehyde	21.85	1
Hydrochloric acid sp.gr. 1.19	0.45	–

We repeated the synthesis of DPE by the works procedure. The resinous product was free from phenol by steam distillation and then treated with benzene. Only 1.5% of pure DPE was isolated. The rest was a phenol–acetaldehyde resin of the novolac type.

The results of Vansheidt et al. [7] and the experimental data in Table 1 show that DPE cannot be obtained as the main product by the works procedure at the molar ratio of phenol to acetaldehyde used (1.66:1).

The main product obtained by the works procedure is phenol–acetaldehyde resin, while DPE itself is obtained as an impurity in very small amounts, or may be entirely absent.

Thus, the works product described as DPE is not DPE but a phenol–acetaldehyde resin, and the formation of a cross-linked polymer in the synthesis of epoxy resins from works DPE is due to the presence of polyfunctional phenol–acetaldehyde resin.

EXPERIMENTAL

Starting materials. Acetaldehyde (in ampoules), produced by the Khar'kov Reagent Factory, 99% pure, b.p. 20-22°, acidity (CH_3COOH) 0.8%.

Phenol, chemically pure (purity over 99%), solidification point 40.6°, nonvolatile content 0.006%.

Epichlorohydrin had the following characteristics: ECH content 98%, b.p. 115-119°, sp.gr. 1.183.

Synthesis of epoxy resins from works DPE. Works DPE was used after removal of phenol in steam and subsequent drying under vacuum. The absence of phenol in the product was confirmed by the qualitative reaction with $FeCl_3$ solution.

The calculated amount (in the correct molar proportions) of works DPE in ECH was put in a 3-necked flask fitted with a mechanical stirrer and a mercury seal, a reflux condenser, and a thermometer. The flask was warmed, with the stirrer working, to 60° on a water bath. After the DPE and ECH had dissolved completely, 15% NaOH solution in an amount equimolecular with respect to the ECH was added gradually during 30 minutes from a dropping funnel. The temperature of the reaction mixture was maintained in the 60-65° range. As the reaction is exothermic, the flask has to be cooled in cold water at intervals to maintain the required temperature. After all the alkali had been added, the reaction mixture was heated to 70-80° and the reaction was continued at that temperature. In all these experiments the reaction mass was converted into a cross-linked polymer.

Synthesis of DPE and phenol–acetaldehyde resins. The correct molar amounts of phenol and acetaldehyde were put into the flask. The flask was firmly stoppered to avoid evaporation of acetaldehyde. After the phenol had completely dissolved in the acetaldehyde, the liquid was cooled in an ice bath. Hydrochloric acid (sp.gr. 1.19) in the proportion of 0.5% on the total amount of reaction mixture was then added.

Cooling of the reaction mixture, with intermittent shaking, was continued until the exothermic reaction stopped, and the flask was then left at room temperature (20-24°).

For synthesis of resins F-1 to F-6, the reaction mixture was left for 48 hours, washed, first with cold and then warm water, until free from chloride ions. The washed mixture was then distilled in live steam to remove free phenol. The steam distillation was continued until the condensate was free from phenol (tested qualitatively with ferric chloride). The mixture was then treated 3-6 times with benzene; for this, the contents were boiled each time under reflux with a 3-fold quantity of benzene. When the benzene solution was cooled, the partially dissolved DPE homologs were first precipitated as resinous masses. The benzene solution of DPE was decanted off,

and the residue was added to the main bulk of resin. After 3-6 extractions, all the DPE benzene extracts were combined and left overnight. The DPE was deposited in the form of crystals. It was then dried in a vacuum drying oven at 70-80°.

The benzene solutions remaining after separation of DPE crystals were combined, benzene was distilled off, and the DPE residues were added to the main mass of DPE. The resinous residue after removal of benzene was dried under vacuum.

Resins F-7 to F-10, after 48 hours of exposure at room temperature and removal of phenol by steam distillation, were dried under vacuum without separation of DPE.

Resins F-11 to F-15 were left to stand overnight, additionally warmed (Table 2), and then dried under vacuum after removal of phenol.

Synthesis of epoxy resin from pure DPE. The correct molar proportions of DPE and ECH were put into the flask. After all the DPE had dissolved in ECH, the flask was cooled and the calculated amount (equivalent to the ECH present) of 15% NaOH was added from a dropping funnel. The temperature in the flask was maintained below 25° by means of cold water. The contents of the flask were stirred for 5-10 minutes. The temperature then gradually rose to 50°. A strongly exothermic reaction then started.

The mixture was cooled intermittently to keep its temperature in the 52-55° range for 30 minutes. The mass was then heated to between 70 and 100°, according to the resin viscosity required (higher temperatures correspond to higher viscosities). The mixture was kept 1.5 hours at the required temperature. The resin was washed with hot water (until neutral to litmus paper) and dissolved in a solvent mixture (50% ethyl acetate, 25% toluene, 25% acetone). The solution was filtered under vacuum and the solvents were removed by straight distillation. The resin was then dried under vacuum to remove residual solvents.

Epoxy groups were determined by the pyridine hydrochloride method [2].

Molecular weight was determined cryoscopically in dioxane solution. Freshly-purified and redistilled dioxane was used. The dioxane was purified as follows: it was shaken in a liter flask with mercury on an electric shaker for a day. It was then left to stand overnight, filtered, and distilled over alkali in a nitrogen atmosphere.

SUMMARY

1. It was shown that when phenol reacts with acetaldehyde in 4:1 molar ratio, DPE is not the only reaction product, but phenol–acetaldehyde resins are also formed.

2. Conditions have been worked out for isolation of DPE in pure form from phenol–acetaldehyde resins by extraction in benzene and subsequent crystallization.

3. DPE was isolated quantitatively from phenol–acetaldehyde resins made with phenol and acetaldehyde taken in molar ratios of 4 : 1, 3.5 : 1, 3: 1, 2.5 : 1, 2 : 1, 1.75 : 1. It was shown that decrease of the molar proportion of phenol leads to a sharp decrease of the DPE content in the resin.

4. The causes of formation of a cross-linked polymer in the synthesis of epoxy resins from works DPE have been found. The formation of a cross-linked polymer is caused by the presence of polyfunctional DPE homologs. Pure DPE does not form cross-linked polymers with ECH in any molar proportions.

5. It was shown that the product issued by the works under the name of DPE is not DPE but a phenol–acetaldehyde resin, and that by the technological procedure used, DPE can be formed only as a minor impurity.

LITERATURE CITED

[1] S. O. Greenlee, U. S. Patent 2582985 (1952).

[2] E. C. Dearborn et al., Ind. Eng. Chem. 45, 2715 (1953).

[3] T. F. Bradley, U. S. Patent 2716099 (1955).

[4] A. Bayer, Ber. 5, 25 (1872).

[5] R. Fabinyi, Ber. 11, 283 (1878).

[6] A. I. Lun'yak, J. Russ. Chem. Soc. 36, 301 (1904).

[7] A. A. Vansheidt, A. G. Itenberg, and V. S. Shifrina, J. Gen. Chem. 12, 500 (1942).

[8] V. L. Vaiser and V. D. Ryabov, Proc. Acad. Sci. USSR 100, 2, 271 (1955).

[9] V. L. Vaiser, Proc. Acad. Sci. USSR 74, 2, 57 (1950).

Received January 6, 1958.

WATERPROOFING OF PAPER BY ALKYL ACETOXYSILANES AND SILOXANES*

M. G. Voronkov, V. P. Davydova, and N. P. Grishanina

Institute of Silicate Chemistry, Academy of Sciences USSR

This paper describes some results of our studies on the waterproofing of paper by organic acetoxysilanes $R_nSi(OCOCH_3)_{4-n}$ and acetoxysiloxanes. For comparison, we also present data on the use of polyalkyl hydrosiloxanes $(RSiHO)_n$, where R is CH_3 or C_2H_5, polymethylsilazane $[CH_3Si(NH)_{1.5}]_n$ and methyltrichlorosilane.

EXPERIMENTAL

The acetoxysilanes listed in Tables 1 and 2 were used for waterproofing of paper.

Paper. The following types of sized and unsized paper were used for the tests: 1) laboratory filter paper (TUMM and TP RSFSR, No. 304-53); 2) sulfite-pulp wrapping paper, made on the cylinder machine, smooth on one side; 3) cylinder-machine kraft paper, machine-smooth.

Waterproofing method. The compounds were dissolved in dry toluene to give the waterproofing solutions of required concentrations. The paper samples were put for a definite time in these solutions, contained in covered beakers. The samples were removed from the solution, dried in air until all the solvent had evaporated, and warmed in a thermostat at 105-110° for a definite time.

Methods of testing waterproofed paper. Water resistance and water absorption were determined by the methods described earlier [1,2].

DISCUSSION

For determination of the optimum concentration of the waterproofing solution and treatment time we used methyltriacetoxysilane (A-1) as the specimen substance in studies of the variation of water resistance of paper with the concentration of A-1 in the treatment solution.

The results are given in Table 3; they show that the water resistance of filter paper increases continuously with increase of the treatment time in 2.5-10% solutions of methyltriacetoxysilane, reaching a maximum value of 62-69 cm.

Solutions containing less than 1% of methyltriacetoxysilane are not effective in the treatment of filter paper.

The optimum practical treatment conditions are the use of 2.5-5% solutions and exposure of the paper to these solutions for at least 10 minutes. It is interesting to note that in the case of wrapping paper, weaker solutions of methyltriacetoxysilane are effective, and even 0.01% solutions increase water resistance considerably. Therefore in the case of wrapping paper, 0.5-1% solutions of A-1 with the same exposure time can be recommended for practical purposes.

Table 3 also contains analogous data for ethyltriacetoxysilane (A-8). These results show that ethyltriacetoxysilane is absorbed more slowly by paper fibers, and the water resistance of the paper after treatment

*Communication V in the series on waterproofing of materials by organosilicon compounds.

is therefore somewhat lower. The use of A-8 solutions below 5% concentration for waterproofing is ineffective, and the exposure time in solution should exceed 10 minutes.

The results of tests on filter paper waterproofed by 3% solutions of different acetoxysilanes in toluene are summarized in Table 1. These results show that ethyltriacetoxysilane (A-8) is less effective, while phenyltri - acetoxysilane (A-13) and n-butyltriacetoxysilane (A-30) are more effective than methyltriacetoxysilane (A-1). The difunctional dialkyl diacetoxysilanes hardly raise the water resistance of paper at all. They are therefore unsuitable for waterproofing. The explanation is that when they are hydrolyzed they form linear polymer chains or cyclic $(R_2SiO)_n$, molecules, incapable of combining with paper or with each other.

The good waterproofing properties of di-n-butoxydiacetoxysilane (A-33) and n-butoxy-tert-butoxydiacet - oxysilane (A-34) can probably be attributed to the ability of one n-butoxy group to split off by hydrolysis; these substances can therefore be classed with trifunctional monomers.

After treatment by methylalkoxydiacetoxysilanes with difficultly saponifiable alkoxy groups, such as methyl-sec-octoxydiacetoxysilane (A-5) and methylisoamoxydiacetoxysilane (A-36), the paper acquired some degree of water resistance, but its water absorption remained high.

Paper treated by 5% tetraacetoxysilane solution (A-21) had the highest water resistance (Table 1). However, as expected, this high water resistance was not sufficiently permanent. After exposure to water for only 1 hour the water resistance of the paper fell sharply (Table 4).

TABLE 1

Water Resistance and Water Absorption of Filter Paper Waterproofed by 3% Solutions of Various Acetoxysilanes in Toluene (heat treatment for 6 hours at 105-110°)

Code mark	Formula	Filter paper		Wrapping paper
		water resistance (cm H_2O	water absorption (%)	water resistance (cm H_2O
—	Untreated paper	0	96.4	150
A-1	$CH_3Si(OCOCH_3)_3$	59.5	34.6	52.0
A-8	$C_2H_5Si(OCOCH_3)_3$	33.5	36.5	58.0
A-13	$C_6H_5Si(OCOCH_3)_3$	65.0	23.5	—
A-30	$n\text{-}C_4H_9Si(OCOCH_3)_3$	69.0	20.8	—
A-31	$iso\text{-}C_4H_9Si(OCOCH_3)_3$	41.0	56.3	—
A-32	$tert\text{-}C_4H_9OSi(OCOCH_3)_3$	86.0	17.2	—
A-33	$(n\text{-}C_4H_9O)_2Si(OCOCH_3)_2$	90.0	21.5	—
A-34	$(tert\text{-}C_4H_9O)(n\text{-}C_4H_9O)Si(OCOCH_3)_2$	73.0	86.9	—
A-35	$(tert\text{-}C_4H_9O)_2Si(OCOCH_3)_2$	3.0	112	—
A-7	$CH_3(tert\text{-}C_4H_9O)Si(OCOCH_3)_2$ . . .	8.0	105.6	—
A-36	$CH_3(iso\text{-}C_5H_{11}O)Si(OCOCH_3)_2$ . . .	14.5	100.8	—
A-5	$CH_3(sec\text{-}C_8H_{17}O)Si(OCOCH_3)_2$ . .	49.5	82.2	—
A-4	$CH_3Si(OCOC_{16}H_{33})(OCOCH_3)_2$	78.0	—	66.0
A-2	$(CH_3)_2Si(OCOCH_3)_2$	7.0	91.0	48.0
A-9	$(C_2H_5)_2Si(OCOCH_3)_2$	0	106.3	36.0
A-21	$Si(OCOCH_3)_4$	99.0	—	84.0

TABLE 2

Water Resistance of Paper Waterproofed by 5% Solutions of the Agents in Toluene (immersed in solution for 1 hour, heated for 3 hours at 105-110°)

Paper	Water resistance (cm H_2O) of papers: filter	wrapping	kraft
Untreated	2	15	132
Treated with:			
A-11	76	73	—
A-12	96	108	188
A-16	93	100	236
A-17	85	75	246
A-18	87	96	161
A-19	73	79	189
A-20	64	77	116
EH-4 $(C_2H_5SiHO)_n$	73	75	95
Methazane $[CH_3Si(NH)_{1.5}]_n$	76	57	144
Vapor CH_3SiCl_3	71	64	143

TABLE 3

Effects of Concentration of Waterproofing Solution and Exposure Time on Water Resistance of Paper (Heat treatment for 3 hours at 105-110°)

Time	Water resistance (cm H_2O) for solution concentration (%) 10		5		2.5		1		0.5		0.1		0.01	
	filter paper	wrapping paper	filter paper	wrapping paper	filter paper	wrapping paper	filter paper	wrapping paper	filter paper	wrapping paper	filter paper	wrapping paper	filter paper	wrapping paper
Treatment by solutions of $CH_3Si(OCOCH_3)_3$ (A-1) in toluene														
1 second	41	43	5	43	5	40	3	31	3	57	3	57	2	55
10 minutes	45	47	49	46	53	39	7	40	3	46	3	58	3	64
1 hour	55	47	57	52	64	43	35	45	10	45	3	49	2	62
3 hours	57	47	62	57	59	47	13	52	5	54	3	47	2	45
6 hours	62	64	69	58	60	60	23	50	3	62	3	55	2	65
Treatment by solutions of $C_2H_5Si(OCOCH_3)_3$ (A-8)														
1 second	43	64	10	41	8	49	1	38	1	51	1	50	1	47
10 minutes	47	71	43	57	26	39	12	36	2	35	2	41	2	57
1 hour	64	49	41	58	29	57	8	62	2	48	2	53	2	49
Untreated paper	2	15	—	—	—	—	—	—	—	—	—	—	—	—

The probable explanation is that in waterproofing by tetraacetoxysilane, the hydroxyl groups in the paper fibers are esterified to form cellulose orthosilicate esters. On prolonged contact with water these esters are saponified, and as a result the OH groups are regenerated, SiO_2 is formed, and waterproofness is lost. However, the possibility of acetylation of cellulose by tetraacetoxysilane cannot be excluded. It should be noted that paper waterproofed by methyltriacetoxysilane becomes harder to the touch. In order to soften it, experiments were carried out in which it was impregnated with 3% solutions of mixtures of alkyl triacetoxysilanes with dialkyl diacetoxysilanes (Fig. 1 and 2). Investigation of the effect of the proportions of the components in these mixtures showed that materials treated with 3% solutions of mixtures consisting of 80% alkyl triacetoxysilane and 20%

TABLE 4

Water Absorption of Paper Waterproofed by 5% Solutions of Agents, and Water Resistance After Exposure for 1 Hour and 24 Hours to Water at Room Temperature or for 6 Hours to Boiling Water

Paper type	Filter						Wrapping						Kraft					
	water absorption (%)		water resistance ($cm H_2O$) after				water absorption (%)		water resistance ($cm H_2O$) after				water absorption (%)		water resistance ($cm H_2O$) after			
	1 hour	24 hours	0	1 hour	24 hours	6 hours of boiling	1 hour	24 hours	0	1 hour	24 hours	6 hours of boiling	1 hour	24 hours	0	1 hour	24 hours	6 hours of boiling
Untreated	64.7	98.8	2	—	—	—	19.5	45.3	15	—	—	—	31.9	42.8	132	—	—	—
Treated by:																		
EH-1	4.9	32.2	73	40	15	5	6.9	35.7	75	69	52	30	21.5	22.3	95	152	94	42
A-11	4.2	14.0	76	88	65	44	8.5	36.0	73	110	91	55	10.7	22.6	—	179	118	120
A-12	4.6	17.0	96	86	56	36	4.5	34.7	108	73	50	43	8.6	26.4	188	172	115	89
A-16	5.5	23.0	93	111	79	58	8.6	25.8	100	126	71	31	8.6	27.8	236	214	189	134
A-17	9.5	24.9	85	86	80	80	14.2	27.6	75	96	80	93	15.5	32.8	246	207	175	159
A-18	12.8	36.8	87	65	63	40	10.9	28.0	96	86	67	83	13.2	37.9	161	151	146	125
A-19	11.4	28.6	73	75	75	75	13.2	37.9	79	89	77	73	18.0	24.4	189	163	152	116
A-20	12.8	35.6	64	67	42	49	21.1	40.4	77	72	55	69	18.2	39.2	116	140	115	99
A-21	5.7	7.5	99	17	10	9	9.8	18.8	84	26	41	9	13.3	20.7	228	131	132	61

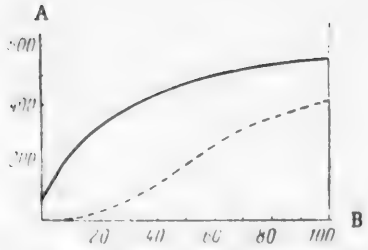

Fig. 1. Effect of the relative proportions of dialkyl diacetoxysilane and alkyl triacetoxysilane in solution on the water resistance of paper: A) water resistance (MM), B) contents of $RSi(OCOCH_3)_3$ (%).*

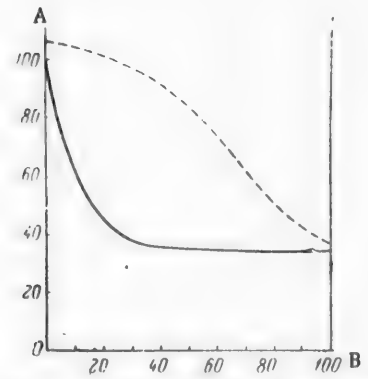

Fig. 2. Effect of the relative proportions of dialkyldiacetoxysilane and alkyl triacetoxysilane in solution on water absorption of paper: A) water absorption (%), B) contents of $RSi(OCOCH_3)_3$ (%).*

dialkyl diacetoxysilane have almost the same water absorption as materials treated with alkyl triacetoxysilanes only. The hardness of the treated materials decreased considerably as a result.

The water absorption and water resistance decrease appreciably with increase of the relative proportion of dialkyl diacetoxysilane in the mixture. Therefore mixtures consisting of 20% methylalkoxy diacetoxysilanes or dialkoxy diacetoxysilanes with 80% methyltriacetoxysilane were used for the treatment. The results (Table 5) showed that with the use of such mixtures the waterproofness and quality of the treated material are improved.

Much better results than those obtained in waterproofing by alkyl triacetoxysilanes were obtained in waterproofing of paper by mixtures of dialkyl diacetoxysilanes with tetraacetoxysilane, in which polymers of the following types are probably formed:

$$—O—SiR_2—[O—Si(OCOCH_3)_2—O—SiR_2]_n—O—Si(OCOCH_3)_2—$$

or

$$—O—Si$$

$$(OCOCH_3)_2—[O—SiR_2—O—Si(OCOCH_3)_2]_n—O—SiR_2—O—SiR_2—.$$

The paper was treated either by mixtures of tetraacetoxysilane with dimethyl- and diethylacetoxysilane in 1 : 1.2 molar ratio (agents A-16 and A-11), or by polydialkyl diacetoxysiloxanes of the type indicated above, made by joint pyrolysis of dialkyl diacetoxysilanes and tetraacetoxysilane (agents A-17, A-18, A-19, A-20), and also by A-12, which is the reaction product of a mixture of silicon tetrachloride and trimethylchlorosilane with acetic anhydride.

The results are given in Table 2.

The best results with all types of paper are given by 5% solutions of A-12 and A-16.

TABLE 5

Effect of the Relative Proportions of Components in Mixtures on Water Absorption and Water Resistance of Paper

Composition of mixture (%)			Water resistance (cm H_2O)	Water absorption (%)
78	A-1, 22	A-2	64.0	27.9
77	A-8, 23	A-9	33.5	55.1
80	A-1, 20	A-9	68.0	26.1
78	A-1, 22	A-33	67.0	29.4
80	A-1, 20	A-34	53.0	29.8
80.5	A-1, 19.5	A-36	69.0	26.1
77	A-1, 23	A-5	68.0	21.5

* R: Continuous line represents CH_3, dash line represents C_2H_5.

Waterproofing by A-12 and A-16 increases the water resistance of filter paper from 2 to 100-110 cm,or more than 50-fold; of wrapping paper, from 15 to 108-119 cm, or more than 7-fold of wrapping paper, from 15 to 108-119 cm, or more than 7-fold; and of kraft paper, from 132 to 190-220 cm, or 1.6-fold.

These results are considerably better than those given by earlier known methods for waterproofing of paper, such as the use of methazane or alkyl hydrosiloxane solutions (MN-1, EN-1, GKZh-94) or treatment with methyltrichlorosilane vapor and then with ammonia (Table 2).

Data on water absorption of waterproofed paper after exposure to water for 1 hour and for 24 hours are presented in Table 4.

The best results with regard both to water absorption and water resistance are given by A-12, A-16, and A-11.

The considerable decrease of water absorption in paper treated with 5% tetraacetoxysilane solution (A-21) should also be noted. This effect is probably caused by acetylation of the OH groups in cellulose and by clogging of its pores by the SiO_2 formed by hydrolysis of A-21.

Tests of the mechanical properties of paper waterproofed by A-11 and A-16 show that the properties remain almost unchanged, and are even improved in some cases (Table 6).

Evidently the acetic acid and acetic anhydride formed during hydrolysis and pyrolysis of acetoxysilanes do not have adverse effects on paper.

In all our experiments on the waterproofing of paper by alkyl acetoxysilanes and siloxanes the paper was subjected to final heat treatment for 3 hours at 105-110°.

Since such long heat treatment of paper is difficult to carry out under production conditions, this raised the problem of the greatest shortening of this treatment time.

However, if paper treated with A-16 and A-12 was heated for less than 2-3 hours, the water resistance was inadequate. Increase of the drying temperature to 150° also failed to give the desired results.

A very effective catalyst for waterproofing of paper (and also textile fabrics) proved to be ethyl orthotitanate, $Ti(OC_2H_5)_4$. It was found that addition of 0.1% of this catalyst to a 2.5% waterproofing solution of A-16 makes it possible to reduce the heat treatment time to 10-30 minutes at 105-110°, or to 2 minutes at 150°. Similar results were obtained with A-12 and other acetoxysilanes.

TABLE 6

Mechanical Properties of Paper

Paper	Flex test	Breaking length (m)	Extensibility (%)	Bursting test
Filter:				
untreated	20.1	2391	1.3	0.8
A-11	26.0	2404	0.5	0.9
A-16	19.0	2034	0.45	1.1
Wrapping:				
untreated	147.5	3286	1.3	0.8
A-11	88.0	2326	1.4	1.1
A-16	146.5	2620	0.8	1.1
Kraft:				
untreated	604.0	4890	2.1	2.6
A-11	366.5	4816	2.7	3.0
A-16	551.5	4398	2.2	2.5

On the basis of these results the use of 2-5% solutions of A-12 and A-16 may be recommended for waterproofing of paper.

SUMMARY

It is shown that the water absorption of paper is considerably lowered and its water resistance increased as the result of treatment with organic acetoxysilanes and siloxanes.

The optimum treatment conditions, the most effective waterproofing agents, and a catalyst for the process (ethyl orthotitanate) are recommended.

LITERATURE CITED

[1] N. G. Belen'kaya, M. G. Voronkov, and B. N. Dolgov, J. Appl. Chem. 28, 886 (1955).*

[2] B. N. Dolgov and M. G. Voronkov, J. Leningrad State Univ. 5, 193 (1954).

Received November 27, 1957.

*Original Russian pagination. See C. B. translation.

DEHYDROGENATION OF HIGHER PARAFFIN HYDROCARBONS OVER CARBON CATALYSTS

I. B. Rapoport, B. K. Nefedov, and S. G. Grakhova

Olefins can be obtained from the lower paraffins by dehydrogenation, either without catalysts or in presence of suitable catalysts.

In the case of hydrocarbons with five or more carbon atoms in the molecule the dehydrogenation reaction hardly proceeds at all. At temperatures between 400 and 600° these hydrocarbons decompose with formation of saturated and unsaturated hydrocarbons [1].

It was therefore desired to study certain catalysts and to find process conditions such that the dehydrogenation of hydrocarbons with five or more carbon atoms in the molecule could be intensified during the decomposition.

Reports have recently appeared in the literature concerning the use of activated carbon as a reforming catalyst for kerosene–ligroine fractions.

The most detailed communications on the subject are those by Sanford and Friedman [2,3].

Later, Kel'tsev et al. [4] also studied the behavior of activated carbon as an aromatization catalyst for high-boiling gasoline fractions for improving their antiknock properties.

According to Sanford and Friedman, in presence of activated carbon aromatization is accompanied to a small extent by dehydrogenation of paraffins. Dehydrogenation accompanied by cyclization proceeds in presence of activated carbon under atmospheric pressure at 530-630°. Examination of the work of Sanford and Friedman suggested that it should be quite possible to find conditions under which the cracking process could be simultaneously directed toward dehydrogenation of paraffins with formation of unsaturated hydrocarbons.

As the result of our investigations it was shown that at 450-510° the cracking of paraffins over promoted activated carbon is accompanied to a considerable extent by dehydrogenation. Virtually no cyclization takes place under these conditions. The yield of liquid catalyzate was 82-95% in individual experiments. The gas yield varied from 3 to 15% in accordance with the composition of the catalyst and the process conditions. The gas contained from 50 to 79% hydrogen, from 2 to 30% unsaturated hydrocarbons, and from 5 to 25% hydrocarbons of the methane series. The liquid reaction products contained up to 20-30% of unsaturated compounds.

The catalyst could be used for a long time without loss of activity. As carbon is deposited on the catalyst surface the activity decreases, but the catalyst is easily regenerated by the action of steam, with restoration of its original activity.

EXPERIMENTAL

Raw material. The raw material for the experiments comprised individual fractions from synthine distillation, and paraffin hydrocarbons isolated from synthine.*

*Product synthesized from CO and H_2 in presence of Co–ThO_2–MgO catalyst.

TABLE 1

Characteristics of Raw Fractions

Details	Fraction No.1* 180–200°	Fraction No.2 180–210°	Fraction No.3 220–300°	Fraction No.3 Paraffin-oil
Engler distillation				
Start of boiling (°C)	180	175	223	300
20% boils out at	184	182	235.5	—
50% boils out at	187.5	188	251	—
70% boils out at	190	196	273	—
90% boils out at	192	206	295	—
97% boils out at	196	209	297	—
End of boiling (n °C)	200	210	300	380
Residue (%)	1.4	1.5	1.2	—
Losses (%)	0.6	0.5	0.8	—
ρ_4^{20}	0.7430	0.7427	—	—
n_D^{20}	1.4200	1.4236	1.4432	—
Iodine number	0.8	2.9	5.2	0.0

*Fraction previously hydrogenated over Ni catalyst.

TABLE 2

Characteristics of Activated Carbons

Carbon type	Activity for I_2 (%)	Bulk density (g/ml)	Analysis (%)			
			W^a	A^c	S^c	V^g
BAU No.1	79	0.236	2.8	2.85	0.15	9.6
BAU No.2	83	0.198	—	—	—	—
KAD*	68.5	0.521	—	—	—	—

*KAD activated carbon was kindly supplied by S. B. Vselyubskii, to whom the authors offer their thanks.

The details of the individual fractions, given in Table 1, show that they contained up to 95-99% saturated hydrocarbons. These fractions contained from 5 to 10% of hydrocarbons of iso structure.

Catalysts. The dehydrogenation catalyst for paraffins was activated carbon in which a salt of Na, Li, Rb, Cs, or other metal was previously deposited.

Characteristics of the activated carbons are given in Table 2.

Preparation of catalyst. The activated carbon was sifted to remove fines and dust. The residue on the sieve (1-4 mm fraction) was treated with hot dilute hydrochloric acid (1:10) for 1-2 hours. The carbon was then washed with hot distilled water to a neutral reaction. The washed activated carbon was heated in a current of nitrogen at 500-510° to remove traces of adsorbed hydrochloric acid. The carbon was then promoted with the appropriate salts by dropwise addition of an aqueous solution of the salt with continuous stirring. The carbon was kept for some time under vacuum, and the pressure was then raised to atmospheric; the impregnated carbon was transferred to a porcelain basin and dried in a drying oven at 102-105° for 8 hours. The dried catalyst was cooled in a desiccator and kept in a jar with a ground-glass stopper. Before each experiment the catalyst was slowly heated to 500-510° in a current of nitrogen.

TABLE 3

Comparative Results of Experiments without and with the Use of Activated Carbon

Experimental data	Without catalyst	BAU No.1, not promoted	BAU No. 1 + + 1% NaOH
Obtained (wt.%):			
liquid hydrocarbons	95.25	91.24	88.19
$C_3 + C_4 +>$	1.55	0.62	0.47
coke	3.20	8.14	0.40
gas + losses			10.94
	100.00	100.00	100.00
Distillation of liquid hydrocarbons (wt.%) *:			
fraction up to 180°C	5.0	19.2	23.5
180-200° fraction	93.0	78.8	74.8
losses	2.0	1.0	2.7
Formed (in moles/mole of raw feed):			
C_nH_{2n}	0.0715	0.110	0.230
H_2	0.0089	0.114	0.455
C_nH_{2n+2}	0.0995	0.315	0.336
Ratio $\frac{H_2}{C_nH_{2n+2}}$	0.0895	0.362	1.360
Iodine number:			
of liquid reaction products	18.35	25.9	33.5
of fraction up to 180°	—	74.5	80.3
of 180-200° fraction	5.98	13.47	16.7
$n^{20}D$ of liquid reaction products	1.4235	—	1.4246

*Distillation data for the catalyzate are given here and in the other tables.

Apparatus. The dehydrogenation experiments were conducted in the usual apparatus for carrying out reactions at high temperatures and atmospheric pressure. The reactor was a quartz tube 22 mm in internal diameter. The volume of the catalyst in the tube was always 30 ml. The tube was packed with broken glass as far as the catalyst layer. The tube was placed in an electric furnace fitted with a thermoregulator. The temperature inside the furnace was measured by means of a thermocouple. Raw material, nitrogen, hydrogen, and steam could be fed into the reaction tube. The raw material was supplied from a special graduated buret; steam was superheated before entry into the furnace. The liquid reaction products were collected in a graduated receiver cooled to 0°. Gasoline was collected partly in the ice-cooled receiver and partly together with the $C_3 + C_4$ fraction in a carbon adsorber cooled to 0°. The uncondensed gases were collected in a gas holder and analyzed in the VTI apparatus.

The density, refractive index, iodine number, and fractional composition were determined for the liquid reaction products and for the individual fractions obtained by distillation of the catalyzate from a Favorskii flask.

DISCUSSION OF RESULTS

Comparison of the results of experiments without catalyst and with unpromoted and promoted activated carbon, given in Table 3, shows that, in experiments without catalyst, dehydrogenation and cracking reactions proceed to only a slight extent at 500-510°. The extent of dehydrogenation and cracking increases considerably in presence of activated carbon.

Here the dehydrogenation reaction is accompanied by cracking, as shown by the increased yield of low-boiling fractions (boiling below 180°) and the considerable contents of unsaturated and saturated hydrocarbons. In presence of promoted activated carbon (with NaOH), the dehydrogenation reaction is more pronounced. The $\frac{H_2}{C_nH_{2n+2}}$ ratio increases to 1.35 as compared with 0.362 with the use of unpromoted carbon. The fact that

the refractive index remains almost unchanged indicates that no cyclization takes place. Absence of aromatic compounds in the reaction products was also proved by analysis of fractions boiling up to 180°.

The results of experiments on the effects of different sodium salts on activated carbon are summarized in Table 4.

It follows from these data that the best promoter is caustic soda. The results of experiments with activated carbon promoted by NaOH as catalyst show that, in comparison with other catalysts, the dehydrogenation reaction proceeds further (as shown by the highest hydrogen content in the gas, the highest $\frac{H}{C_nH_{2n+2}}$ ratio, a lower yield of fractions boiling up to 180°, and high contents of unsaturated hydrocarbons in individual fractions).

TABLE 4

Results of Test on Activated Carbon Promoted by Sodium Salts. Temperature 500-510°, atmospheric pressure, space velocity 2 vol./vol. catalyst·hour, Fraction No. 2, duration of experiment 2 hours

Experimental data	BAU № 1 + 0.2% NaOH	BAU № 1 + 0.2% Na_2CO_3	BAU № 1 + 0.2% NaCl	BAU № 1 + 0.2% Na_3PO_4
Obtained (wt.%):				
liquid hydrocarbons	89.00	87.6	86.50	89.00
$C_3 + C_4 +>$	2.94	2.7	1.52	5.70
coke + gas + losses	8.06	9.7	11.98	5.30
	100.00	100.00	100.00	100.00
Formed (in moles/mole of raw feed):				
C_nH_{2n}	0.175	0.132	0.231	0.0211
H_2	0.246	0.156	0.147	0.0680
C_nH_{2n+2}	0.242	0.372	0.433	0.1730
Ratio $\frac{H_2}{C_nH_{2n+2}}$	1.015	0.420	0.340	0.393
Analysis of reaction products				
Entire liquid product:				
ρ_4^{20}	0.7410	0.7415	—	—
n_D^{20}	1.4234	1.4231	1.4216	1.4220
unsaturated compounds (%) . .	15.0	18.1	17.25	9.85
Yield of fraction up to 180° (% on catalyzate by weight) .	25.3	34.1	35.0	27.0
n_D^{20}	1.4145	1.4151	1.4128	1.4168
unsaturated compounds (%) . .	32.0	33.8	21.5	12.2
Yield of 180-200° fraction (% on catalyzate by weight)	68.8	64.4	59.6	66.2
ρ_4^{20}	0.7435	0.7478	0.7494	—
n_D^{20}	1.4254	1.4286	1.4296	—
unsaturated compounds (%). . .	11.05	12.2	11.2	8.05

The next promoter of interest is Na_2CO_3.

Additions of NaCl and Na_3PO_4 have much lower dehydrogenation effects.

It was found in special experiments that the amount of promoter to be added to activated carbon depends on the chemical composition of the compound used. For example, 5% of Na_3PO_4 is required, whereas in the case of NaOH about 1-2% is sufficient, although it was found that increase of the NaOH content to 5% increases the dehydrogenation activity of the catalyst somewhat. In the subsequent investigations we used additions of 1% NaOH to the activated carbon.

Tests of catalysts made by impregnation of activated carbon with salts of Li, Rb, Cs, Mg, Cr, Al, Th, showed that only Li salts have a positive influence on the dehydrogenation reaction.

All the experiments described above were carried out with a catalyst made by impregnation of BAU No.1 activated carbon with various salts. It was necessary to test other types of activated carbon.

The results of tests on catalysts made with different carbons are given in Table 5. It follows from Table 5 that the best support for a dehydrogenation catalyst for the 180-200° fraction is KAD activated carbon.

For comparison, this table contains data on unpromoted and promoted active carbons.

Effect of fractional composition of the raw material. Experiments on dehydrogenation of paraffins of different fractional composition were performed with the catalysts BAU + 1% NaOH and KAD + 1% NaOH.

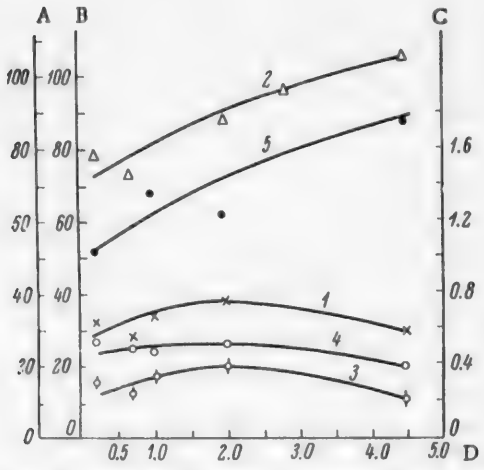

Fig. 1. Effects of different amounts of NaOH as promoter: A) iodine number, B) yield of fraction up to 180° (wt.%), C) H_2/C_nH_{2n+2} ratio, D) NaOH content (%); 1) iodine numbers of reaction products, 2) the same, of fraction up to 180°, 3) the same, of 180-200° fraction, 4) yield of fraction up to 180°, 5) H_2/C_nH_{2n+2} ratio.

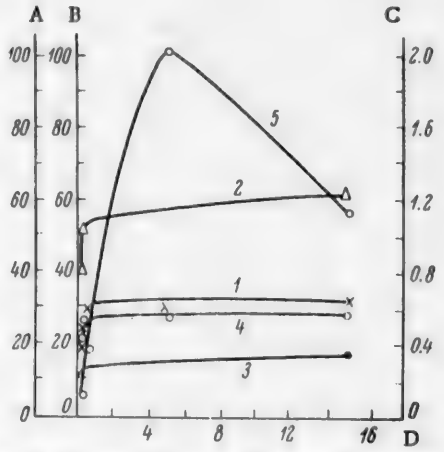

Fig.2. Effects of different amounts of Na_3PO_4 as promoter: A) iodine number, B) yield of fraction up to 180° (wt.%), C) H_2/C_nH_{2n+2} ratio, D) Na_3PO_4 content (%); designations of curves as in Fig.1.

The data in Table 6 show that with increase of the boiling point of the raw material there is considerable cracking in addition to dehydrogenation. The relative proportion of dehydrogenation in the cracking of paraffin hydrocarbons at 500-510° varies in accordance with the catalyst and the fractional composition of the raw material. As the fractional composition of the raw material becomes heavier, the yield of liquid hydrocarbons decreases, more coke and gas is formed, and the contents of unsaturated hydrocarbons and the $\frac{H_2}{C_nH_{2n+2}}$ ratio increase. The temperature of the process must be lowered to suppress the cracking reaction.

Effect of temperature. At 450° in presence of KAD + 1% NaOH catalyst, the cracking reaction proceeds to a much lesser extent than the dehydrogenation reaction (Fig. 3). At 470-480° the relative proportion of the cracking reaction increases, as indicated by the increase of gas yield, change of the gas composition, and the lighter fractional composition of the liquid reaction products. At 500-510° the cracking reaction predominates. Therefore in order to direct the process so that dehydrogenation of paraffins predominates, the temperature must be lowered to 470-480°

Effect of space velocity. Increase of space velocity results in a sharp decrease of the relative proportion of the cracking reaction (Fig. 4). At a space velocity of 3 vol./vol.catalyst·hour with KAD + 1% NaOH catalyst the dehydrogenation reaction predominates. The $\frac{H_2}{C_nH_{2n+2}}$ ratio is 6.75, and the hydrogen content of the gas reaches 77%. On further increase of space velocity both the cracking and the dehydrogenation reactions die down.

TABLE 5

Comparative Effects of Different Catalysts

Experimental data	BAU No.1, unpromoted	BAU + 1% NaOH	KAD, unpromoted	KAD + 1% NaOH
Obtained (wt.%):				
liquid hydrocarbons	91.24	88.19	87.00	83.60
$C_3 + C_4 +$	0.62	0.47	2.00	2.64
coke	8.14	0.40	11.00	1.25
gas + losses		10.94		13.51
	100.00	100.00	100.00	100.00
Formed (in moles/mole of raw feed):				
C_nH_{2n}	0.110	0.230	0.157	0.306
H_2	0.114	0.455	0.464	1.160
C_nH_{2n+2}	0.315	0.336	0.397	0.342
Ratio ... $\frac{H_2}{C_nH_{2n+2}}$	0.362	1.36	1.17	3.40
Analysis of reaction products				
Entire liquid product:				
ρ_4^{20}	—	—	0.7363	0.7456
n_D^{20}	—	1.4246	1.4241	1.4286
unsaturated compounds:	10.85	13.6	18.3	20.9
Yield of fraction up to 180°(wt.%)	19.2	23.5	38.2	27.7
n_D^{20}	—	—	1.4146	1.4212
unsaturated compounds:	29.8	32.2	32.6	33.3
Yield of 180-200° fraction(wt. %)	76.7	74.8	57.1	68.2
ρ_4^{20}	—	—	0.7532	0.7542
n_D^{20}	—	—	1.4314	1.4322
unsaturated compounds (%). . .	8.96	11.1	13.09	15.7

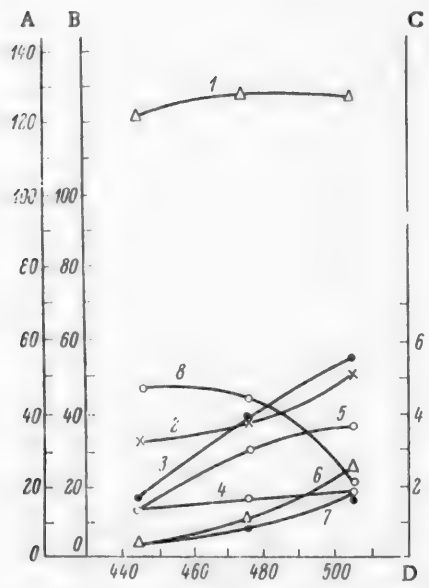

Fig. 3. Effect of temperature; catalyst KAD + 1% NaOH: A) iodine number, B) yield of reaction products (wt.%), C) $H_2/C_n H_{2n+2}$ ratio, D) temperature (°C); 1) iodine number of fraction up to 180°, 2) the same, of 180-300° fraction, 3) the same, of reaction products, 4) the same, of 300° fract., 5) yield of 180-300° fraction, 6) the same, up to 180°, 7) yield of gas, 8) $H_2/C_n H_{2n+2}$ ratio.

At a space velocity of 10 vol./vol. catalyst · hour both reactions stop completely; the yield of gas at this space velocity is only 1.1%, the yield of fraction boiling up to 300° is 13.85%, and the $\frac{H_2}{C_nH_{2n+2}}$ ratio is 0.123. The character of the process was similar with BAU 1 catalyst with Na_3PO_4.

Time of operation and regeneration of the catalyst. The KAD + 1% NaOH catalyst was in service for 24 hours. The raw material for the experiment was paraffin. After 10-12 hours of continuous operation the catalyst activity fell owing to deposition of coke on its surface. The catalyst was regenerated by the action of superheated steam. The duration of regeneration was about 10 hours. The activity of the catalyst was restored after regeneration. The regeneration gas had the following composition (vol.%): CO_2–29.45, CO–3.07, H_2–67.48.

Experiments with individual hydrocarbons. A series of experiments was conducted with individual hydrocarbons: n-heptane and cetane. The n-heptane used had b.p. 98-99°, $n^{20}D$ 0.6841, the cetane had b.p. 287° $n^{20}D$ 1.4352, ρ_4^{20} 0.7753. The literature data for these hydrocarbons are:

TABLE 6

Dehydrogenation of Paraffin Hydrocarbons of Different Fractional Compositions over KAD + 1% NaOH Catalyst. Temperature 500-510°, space velocity 2 vol./vol. catalyst·hour, atmospheric pressure, duration of experiment 2 hours

Experimental data	Raw material		
	№ 2	№ 3	№ 4
Obtained (wt.%):			
liquid hydrocarbons	83.60	81.10	80.67
$C_3 + C_4 +$ >	2.64	2.46	1.59
coke	1.25	0.65	1.14
gas + losses	13.51	15.79	16.60
	100.00	100.00	100.00
Formed (in moles/mole of raw feed):			
C_nH_{2n}	0.306	0.440	0.764
H_2	1.160	0.968	1.34
C_nH_{2n+2}	0.340	0.445	0.66
Ratio $\frac{H_2}{C_nH_{2n+2}}$	3.4	2.18	2.03
Distillation of catalyzate (wt.%) Fractions:			
to 180°	27.7	24.5	20.8
180—220°	—	16.2	—
180—300°	—	—	35.6
Unsaturated compounds (wt.%). .			
Liquid hydrocarbons	21.0	42.5	44.5
Fractions:			
to 180°	33.6	55.2	56.0
180—220°	—	36.4	—
180—300°	—	—	40.2
n_D^{20}			
Liquid hydrocarbons	1.4286	1.4396	1.4446
Fractions to 180°	1.4212	1.4196	1.4219

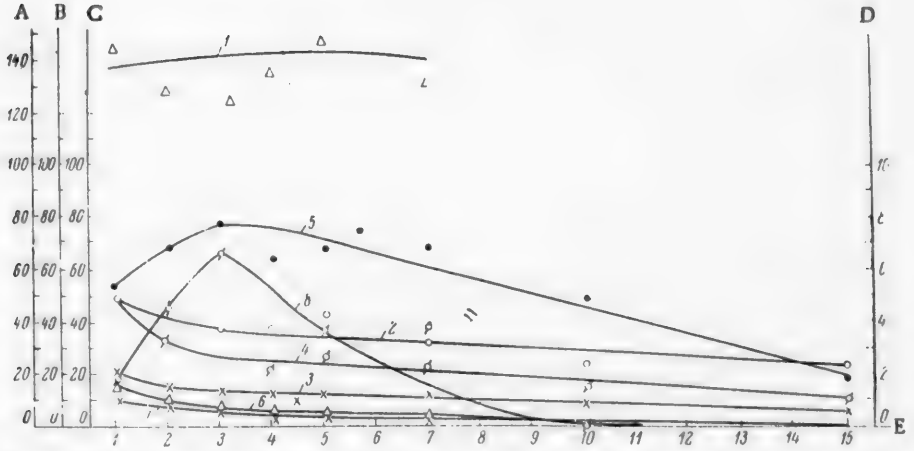

Fig. 4. Effect of space velocity; catalyst KAD + 1% NaOH, temperature 470-480°: A) iodine number, B) H_2 content (vol.%), C) yield of reaction products (wt.%), D) H_2/C_nH_{2n+2} ratio, E) space velocity (vol./vol. catalyst·hour); 1) iodine number of fraction up to 180°, 2) the same, of 180-300° fraction, 3) the same, of fraction > 300°, 4) the same, of reaction products, 5) H_2 content, 6) yield of fraction up to 180°, 7) yield of gas, 8) H_2/C_nH_{2n+2} ratio.

	n-Heptane	n-Cetane
Boiling point (°C)	98.43	287.1
$n^{20}D$	1.3877	1.4345
ρ_4^{20}	0.6837	0.7751

The experiments were performed with KAD + 1 % NaOH catalyst at a space velocity of 3 vol./ vol.catalyst·hour. Under these conditions,n-heptane only undergoes partial dehydrogenation without any appreciable cracking. The uncondensed gases contain 96% hydrogen.

When the length of the carbon chain in the molecule is increased (in experiments with cetane), the dehydrogenation reaction is accompanied by cracking. The hydrogen content of the gas falls to 83.5% (as compared with 96% in the dehydrogenation of n-heptane), and the content of saturated hydrocarbons rises to 10.8%; the gas contains unsaturated hydrocarbons in addition to hydrocarbons of the methane series.

The fact that the refractive indices of the catalyzates remain almost unchanged confirms that dehydrogenative cyclization does not occur.

Investigations by means of Raman spectroscopy showed that the resultant unsaturated hydrocarbons have the double bond in the α-position.

SUMMARY

1. It is shown that it is possible in principle to effect dehydrogenation of paraffin hydrocarbons, containing from 8 to 20 carbon atoms in the molecules, over catalysts based on activated carbons.

2. Of the two activated carbons, BAU and KAD, KAD carbon is the better.

3. The dehydrogenation is intensified considerably if the activated carbon is promoted by Na or Li salts. The optimum promoter concentration is in the range of 1-2%.

4. Different paraffinic fractions are dehydrogenated at 450-510°, under atmospheric pressure, and at a space velocity of 2-4 vol./ vol.catalyst.hour.

5. Dehydrogenation of paraffin hydrocarbons with 10-20 or more carbon atoms in the molecule is accompanied by cracking. The resultant low-boiling fractions, which boil in the ranges of 40-180° and 180-300°, are rich in unsaturated compounds and may be used as raw materials for production of high-quality lubricating oils and fine detergents respectively.

6. The unsaturated hydrocarbons formed as the result of dehydrogenation have the double bond in the α-position.

LITERATURE CITED

[1] M. D. Tilicheev, Chemistry of the Cracking Process [in Russian] (State Fuel Tech. Press, 1941).

[2] R. A. Sanford and B. S. Friedman, Ind. Eng. Chem.46, 12, 2568 (1954).

[3] R. A. Sanford and B. S. Friedman, U. S. Patent 2592603 (1952).

[4] N. V. Kel'tsev, G. N. Selyutina, and A. P. Khalif, Gas Ind. 3 (1956).

Received October 9, 1957.

DEHYDROGENATION OF PARAFFIN HYDROCARBONS OVER CHROMIUM OXIDE–ALUMINA CATALYSTS

I. B. Rapoport and B. K. Nefedov

It was shown in the preceding communication [1] that activated carbons impregnated with alkali catalyze the dehydrogenation of higher paraffins.

It was of interest also to test certain chromium oxide–alumina catalysts for this purpose.

Previously Z. I. Vozzhinskaya had carried out experiments on the dehydrogenation of paraffins over catalysts of this type. Later Shuikin and his associates [2] used chromium oxide – alumina catalysts for dehydrogenation of hydrocarbons containing five carbon atoms in the molecule.

According to Shuikin et al., n-pentane undergoes 31% conversion into pentene in presence of a catalyst of the composition $Al_2O_3 : Cr_2O_3 : K_2O = 90.7 : 5.6 : 3.7$ (in molar %) at 527° and space velocity 0.5 vol./vol. .catalyst·hour.

A later paper by Könnecke and Gawalek [3] also deals with dehydrogenation of paraffins over these catalysts.

Chromium oxide–alumina catalysts are used industrially for dehydrogenation of n-butane to butylene. Our results, presented below, show that under suitable conditions the dehydrogenation of higher paraffins over chromium oxide –alumina catalysts is very selective, with almost total absence of dehydrocyclization.

The catalysts are stable in operation and are easily regenerated.

According to Könnecke, the dehydrogenation process takes place at 450-530°, under atmospheric pressure, and at a space velocity of 0.5-2 vol./vol.catalyst.hour. Our results are in good agreement with these data, and confirms that chromium oxide– alumina catalysts can be used for dehydrogenation of paraffins containing from 8 to 20 carbon atoms in the molecules.

EXPERIMENTAL

Raw material. Individual 180-200° and 300-380° synthine fractions were used. The synthine was produced over $Co–ThO_2–MgO$ catalyst at 10 atmos pressure.

The fractions contained 98-99% of paraffin hydrocarbons. The first fraction contained 0.8% olefins, and the 300-380° fraction was free from olefins.

Apparatus. Experiments on dehydrogenation of paraffins over chromium oxide–alumina catalysts were carried out in the type of apparatus commonly used for reactions at high temperatures under atmospheric pressure. The reactor was a quartz tube of 22 mm internal diameter. The tube was heated in an electric furnace. The internal temperature was measured by means of a thermocouple. The raw material was fed from a special graduated buret. The reaction products were cooled to 0° and collected in receivers. The $C_3 + C_4$ fraction was collected in a carbon adsorber.

Catalysts. Of the available range of chromium oxide–alumina catalysts, three were tested, with the following Cr_2O_3 contents (%): Sample No.1, 8; Sample No.2, 16; Sample No.3, 20.

Cr_2O_3 was deposited on alumina in Samples No.1 and 3, and on clay in Sample No.2.

DISCUSSION OF RESULTS

The first series of experiments on dehydrogenation of paraffins was conducted with a catalyst containing 16% Cr_2O_3.

The results of experiments (Table 1) on dehydrogenation of the 180-210° paraffin fraction show that dehydrogenation is the main reaction. The hydrogen content of the gas reaches 65%. The liquid reaction products contain about 12% of unsaturated hydrocarbons, with a relatively low yield (10%) of fractions boiling up to 180°.

When the number of carbon atoms in the original paraffin chain is increased, as in the use of the 300-380° fraction, the dehydrogenation reaction is accompanied to a considerable extent by cracking.

TABLE 1

Dehydrogenation of Paraffin Hydrocarbons over a Chromium Oxide–Alumina Catalyst (Sample No.2). Temperature 500-510°, atmospheric pressure, space velocity 2 vol./vol.catalyst·hour, duration of experiment 2 hours

Experimental data	180–210° fraction	300–380° fraction
Obtained (wt.%): liquid hydrocarbons	92.50	86.00
$C_3 + C_4 +$	0.50	2.80
coke	0.44	0.93
gas + losses	6.56	10.27
	100.00	100.00
Composition of gas (vol%):		
CO_2	0.10	—
C_nH_{2n}	17.90	—
CO	0.62	—
H_2	65.25	—
C_nH_{2n+2}	16.13	—
Formed (in moles/mole of raw feed):		
C_nH_{2n}	0.173	0.602
H_2	0.632	1.27
C_nH_{2n+2}	0.155	0.475
Ratio ... $\frac{H_2}{C_nH_{2n+2}}$	4.07	2.68
Contents of liquid products (wt.%) ...		
fraction up to 180°	10.7	15.8
180-300° fraction	—	25.0
Unsaturated compounds (%)		
in liquid hydrocarbons	12.4	38.7
in fraction up to 180°	47.5	87.0
in 180-300° fraction	—	51.0
n_D^{20}:		
of liquid hydrocarbons	1.4208	—
of fraction up to 180°	—	1.4238
of 180-300° fraction	—	1.4497

TABLE 2

Tests of Chromium Oxide–Alumina Catalysts with Different Chromium Contents. Temperature 500-510°, atmospheric pressure, space velocity 2 vol./vol.catalyst·hour, 300-380° fraction used as raw feed, duration of experiment 2 hours

Experimental data	Catalyst	
	Sample No.1	Sample No.2 *
Obtained (wt.%): liquid hydrocarbons	81.50	72.50
$C_3 + C_4 +$	1.42	2.88
coke	2.01	24.62
gas + losses	15.07	
	100.00	100.00
Formed (in moles/mole of raw feed):		
H_2	4.15	2.56
C_nH_{2n}	0.576	0.695
C_nH_{2n+2}	0.50	0.692
Ratio ... $\frac{H_2}{C_nH_{2n+2}}$	8.30	3.71
Contents of liquid products (wt.%):		
fraction up to 180°	12.5	14.0
180-350° fraction	25.6	24.2
Unsaturated compounds (%):		
in liquid hydrocarbons	34.0	39.4
in fraction up to 180°	59.1	68.2
in 180-300° fraction	48.0	47.0
in 300-380° fraction	44.0	34.4
n_D^{20}:		
of fraction up to 180°	—	1.4376
of 180-300° fraction	—	1.4552

*Catalyst volume was 18 ml in this experiment, and 30 ml in the others.

It is clear from Table 1 that this results in a lower yield of liquid products, higher yields of gas, coke, and low-boiling fractions, and an increase in the contents of unsaturated compounds in the reaction products.

All three chromium oxide–alumina catalysts were tested with the 300-380° paraffin fraction. It was found (compare Tables 1 and 2) that the best catalyst for dehydrogenation of paraffin hydrocarbons of the 300-380° fraction is Sample No.1 (containing 8% Cr_2O_3). The $\frac{H_2}{C_nH_{2n+2}}$ ratio obtained with this catalyst is 8.3%, which is the highest, while all the other characteristics are almost the same. The somewhat higher refractive indices of the individual fractions suggest that dehydrogenation may be accompanied by dehydrocyclization in this case. However, this requires further confirmation.

Comparison of the data in Table 3 shows that chromium oxide–alumina catalysts are the best dehydrogenation catalysts for the 180-200° fraction. Thus, with a chromium oxide– alumina catalyst (Sample No.2) the $\frac{H_2}{C_nH_{2n+2}}$ ratio in the gas is 4.07 as compared with 3.4 with the catalyst consisting of KAD + 1% NaOH; the yield of liquid products is higher, and less coke and gas is formed. Moreover, the degree of cracking (yields of gas and gasoline) are lower with the chromium oxide–alumina catalyst.

TABLE 3

Comparative Data on Carbon and Chromium Oxide–Alumina Catalysts, Temperature 500-510°, atmospheric pressure, space velocity 2 vol./vol.catalyst·hour, 180-210° fraction used as raw feed, duration of experiment 2 hours

Experimental data	Catalysts		
	BAU + 1% NaOH	KAD + 1% NaOH	chrome-alumina catalyst (Sample No.2)
Obtained (wt.%):			
liquid hydrocarbons	88.19	83.60	92.50
$C_3 + C_4 +$	0.47	2.64	0.50
coke	0.40	1.25	0.44
gas + losses	10.94	13.51	6.56
	100.00	100.00	100.00
Composition of gas (vol.%):			
CO_2	0.61	0.00	0.10
C_nH_{2n}	21.90	16.85	17.90
CO	1.89	0.31	0.62
H_2	43.70	64.00	65.25
C_nH_{2n+2}	31.90	18.84	16.13
Formed (in moles/mole of raw feed)			
C_nH_{2n}	0.230	0.306	0.173
H_2	0.455	1.160	0.632
C_nH_{2n+2}	0.336	0.342	0.155
Ratio $\frac{H_2}{C_nH_{2n+2}}$	1.36	3.40	4.07
Contents of liquid products (wt. %):			
fraction up to 180°	23.5	27.7	10.7
180-210° fraction	74.8	68.2	85.6
Unsaturated compounds (%)			
in liquid hydrocarbons	13.6	20.9	12.3
in fraction up to 180°C	32.2	33.3	47.4
in 180-210° fraction	11.1	15.7	8.52
n_D^{20} of liquid reaction products	1.4216	1.4286	1.4263
n_D^{20} of fraction up to 180°C	—	1.4212	1.4208
n_D^{20} of 180-210° fraction	—	1.4322	1.4268

TABLE 4

Conversion with Recycling of Residues. Temperature 500-510°, space velocity 2 vol./ vol. .catalyst·hour

Experimental data	Fresh feed – 300-380° fraction (paraffin)	Fresh feed + recycled oil	Fresh feed + recycled oil
Yield (wt.%):			
liquid hydrocarbons	88.80	91.07	94.87
coke + gas + losses	11.20	8.93	5.13
	100.00	100.00	100.00
Iodine number of catalyzate.	52.0	48.0	47.0

TABLE 5

Tentative Data on Exhaustive Dehydrogenation of Paraffin Hydrocarbons (300-380° Fraction) over Carbon and Chromium Oxide–Alumina Catalysts

Experimental data	Catalyst	
	KAD + 1% NaOH	chrome-alumina (Sample No. 2)
Reaction products (wt.%):		
40-180° fraction	25.5	30.5
180-300° fraction . . .	42.2	47.5
coke	2.3	2.00
C_1, C_2, C_3, C_4 + gas + losses	30.0	20.50

Service life and regeneration of catalyst. Catalyst No.2 was used in these experiments. This catalyst was used continuously for 28 hours. During the first two or three hours the activity of the catalyst was somewhat higher, and then it fell and remained almost constant for 25-26 hours. The activity of such catalyst is completely restored by regeneration in a current of air at 600-650°.

The possibility of complete conversion of the raw feed was studied with the use of this catalyst (Sample No.2). It was found (Table 4) that if the residues are recycled the activity of the catalyst remains almost constant (the iodine numbers of the catalyzates remain constant in the 47-52 range).

Typical yields obtained by dehydrogenation of high-boiling paraffin hydrocarbons (300-380° fraction) over carbon and chromium oxide –alumina catalysts are given in Table 5.

SUMMARY

1. It is shown that it is possible in principal to effect dehydrogenation of paraffin hydrocarbons, containing from 8 to 20 carbon atoms in the molecule, over certain chromium oxide –alumina catalysts.

2. Dehydrogenation of different paraffin fractions proceeds at 450-530°, under atmospheric pressure, at a space velocity of 2-4 vol./ vol.catalyst·hour.

3. Dehydrogenation occurs selectively in presence of chromium oxide–alumina catalysts, but a low space velocities (1 vol./ vol.catalyst,hour) dehydrocyclization may occur.

4. The catalysts are stable in operation, are easily regenerated, and fully recover their activity.

LITERATURE CITED

[1] I. B. Rapoport, V. N. Nefedov, and S. G. Grakhova, J. Appl. Chem. 32, No.5, 1112 (1959).*

[2] E. A. Timofeeva, S. S. Novikov, and N. I. Shuikin, Proc. Acad. Sci. USSR 92, No.2, 345 (1953); N. I. Shuikin, E. A. Timofeeva, and V. M. Sladkikh, Bull. Acad. Sci. USSR Div. Chem. Sci. 567 (1955);* N. I. Shuikin, T. N. Dobrynin, E. A. Timofeeva, and Yu. P. Egorova, Bull. Acad. Sci. USSR, Div. Chem. Sci. 952 (1955);* N. I. Shuikin, E.A. Timofeeva, and V. M. Kleimenova, Bull. Acad. Sci. USSR, Div. Chem. Sci. 7, 875 (1957).*

*Original Russian pagination. See C. B. translation.

[3] H. G. Könnecke and G. Gawalek, Chem. Techn X, 8, 10, 603 (1956).

Received October 9, 1957.

OXIDATION OF ACENAPHTHENE TO NAPHTHALIC ANHYDRIDE

G. P. Petrenko and M. M. Dashevskii

Various methods are described in the literature for oxidation of acenaphthene to naphthalic anhydride; for example, by dichromate in presence of sulfuric [1] or acetic [2] acids, by hydrogen peroxide [3], and by oxygen under pressure in o-dichlorobenzene solution [4]. Good yields of naphthalic anhydride were obtained only in acetic acid solution. However, the consumption of the latter is 5 to 10 times the amount of acenaphthene oxidized, which is unacceptable economically.

According to an American patent, acenaphthene is smoothly oxidized to naphthalic anhydride by aqueous dichromate solution under pressure [5].

The patent literature on vapor-phase oxidation of acenaphthene is extensive. Thus, according to American patents of the Selden Company, acenaphthene is oxidized by oxygen-containing gases mixed with steam at 400°. Oxides of Group V and VI elements and of alkaline-earth metals are recommended as catalysts. In accordance with the conditions, oxidation of acenaphthene (I) yields different products: acenaphthylene (II), acenaphtene quinone (III), naphthalic anhydride (IV), and others [6, 7].

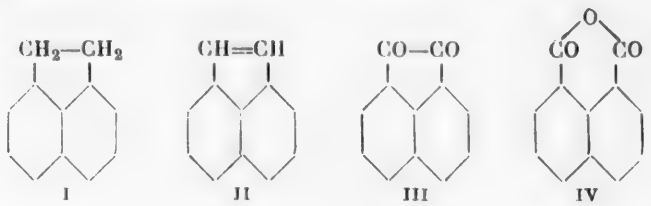

I II III IV

According to other patents, acenaphthene may first be oxidized to acenaphthylene, and the latter is then oxidized at a higher temperature over a less active catalyst [8-11]. According to certain British patents, acenaphthene is oxidized by air (1 : 20—30) mixed with steam at 350-400° over iron vanadate on pumice. Almost pure naphthalic anhydride is obtained under these conditions. If the oxidation is performed at 380-420° over lead vanadate on quartz, acenaphthylene is predominantly formed [12,13]. Naphthalic anhydride is also formed in the oxidation of acenaphthene by air (1:40) over a catalyst consisting of silver vanadate stabilized by 3-5% of sodium or potassium carbonate [6].

Among the oxidation products of acenaphthene the most interest attaches to acenaphthylene, acenaphthene quinone, and naphthalic anhydride. Evidently vapor-phase oxidation cannot be stopped at the quinone stage whereas, according to the literature, acenaphthylene and naphthalic anhydride are formed in good yields.Both these compounds are now used in the production of plastics [14,15].

Despite its availability, acenaphthene is not used nearly enough in our country. It might be used in large amounts for the purposes indicated above.

The present paper deals with a study of the vapor-phase oxidation of acenaphthene, mainly to naphthalic anhydride.

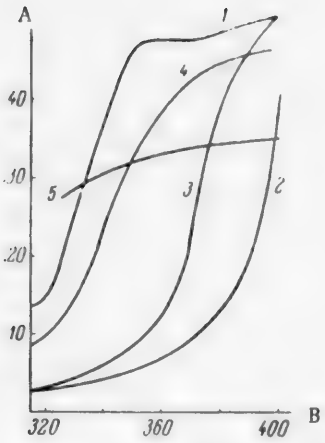

Fig. 1. Effects of diferent catalysts on the acenaphthylene contents of the distillate: A) acenaphthylene content, B) temperature (°C); catalysts: 1) vanadium pentoxide, 2) vanadium pentoxide with K_2SO_4, 3) iron vanadate with K_2SO_4, 4) copper vanadate with K_2SO_4, 5) manganese dioxide.

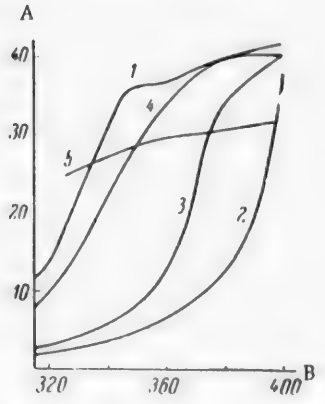

Fig.2. Effects of different catalysts on the yield of acenaphthylene: A) yield of acenaphthylene (%), B) temperature (°C); designations of curves as in Fig.1.

We studied the oxidation of acenaphthene by air over vanadium catalysts and manganese dioxide at 320-425°. The effects of temperature, contact time, and acenaphthene: air volume ratio on the yields of different oxidation products were studied in the experiments. The results are plotted in Fig. 1-3 and summarized in Tables 1 and 2.

Oxidation of acenaphthene over vanadium pentoxide (Catalyst No.1) by small amounts of air yields mainly a mixture of acenaphthylene with unchanged acenaphthene, and is always accompanied by formation of variable amounts of naphthalic anhydride, regardless of the amount of air. The anhydride yield increases with temperature and increasing amount of air, reaching a maximum (29%) at 350-360°, and then decreases. The oxidation product formed from acenaphthene under these conditions is easily distilled under vacuum, when naphthalic anhydride remains as a residue in the distillation flask. In the best experiments the acenaphthylene content of the distillate did not exceed 60%, and its total yield calculated on the acenaphthene taken is about 40%.

On addition of potassium sulfate to vanadium pentoxide (Catalyst No.2) the oxidation of acenaphthene by small amounts of air presents a very different picture from that described above. With this catalyst appreciable amounts of acenaphthylene are formed only at temperatures above 360-380°, and this is accompanied by formation of naphthalic anhydride in amounts increasing rapidly with increase of temperature. In the oxidation of acenaphthene by large amounts of air over vanadium pentoxide with potassium sulfate, the main reaction product is naphthalic anhydride. The results of oxidation of acenaphthene by small amounts of air over copper vanadate with potassium sulfate (Catalyst No.4) or iron vanadate with potassium sulfate (Catalyst No.3) differ little from the results of oxidation of acenaphthene over vanadium pentoxide alone (Catalyst No.1) under similar conditions.

The oxidation of acenaphthene over manganese peroxide (Catalyst No.5) at 230-400° takes a peculiar course. In this case, formation of acenaphthylene begins at a considerably lower temperature than over vanadium pentoxide, and is not accompanied by formation of naphthalic anhydride. At 325° the acenaphthylene content in the reaction products is higher than it is with the other catalysts, and reaches 28-30%, whereas in presence of the other catalysts it hardly reaches 3-15% at this temperature. However, the yield of acenaphthylene in presence of manganese peroxide changes little with increase of temperature and does not rise above 33%, whereas in presence of the other catalysts increase of temperature has a fairly pronounced effect and the acenaphthylene yield rises from 3-11% to 40-42%.

Increase of the amount of air over manganese peroxide does not lead to any appreciable increase of the acenaphthylene yield or to formation of naphthalic anhydride but merely results in complete combustion of acenaphthene.

Of all the catalysts tested, iron vanadate with potassium sulfate (Catalyst No.3) gave the best yield of naphthalic anhydride in the oxidation of acenaphthene at 350-370°, with acenaphthene to air in 1:100 ratio

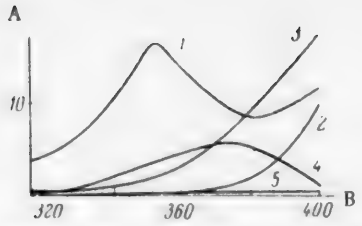

Fig.3. Effects of different catalysts on the formation of nondistillable residue: A) yield of residue (%), B) temperature (°C); designations of curves as in Fig. 1.

by volume, and a contact time of 2.9 seconds. Under these conditions part of the acenaphthene is burned completely, while naphthalic anhydride of a high degree of purity is formed (melting point 268°) in a yield of 75-80% of the theoretical.

EXPERIMENTAL

The reactor used for studying the oxidation of acenaphthene consists of a massive steel cylinder 295 mm long and 75 mm in diameter (Fig. 4). It contains two parallel canals 20 mm in diameter running axially through the reactor and interconnected at the top under the lid. One canal is packed with the catalyst (88 cc) while the other serves as a preheater and additional mixer for acenaphthene vapor and air. At the top the reactor has a screw lid with sockets for a thermometer and a thermoregulator. The reactor is electrically heated; the temperature is controlled within ±1° by means of a thermoregulator. The reactor is connected to two air preheaters, which are electrically heated stainless-steel tubular coils, and the acenaphthene evaporator. Each preheater is equipped with a thermoregulator. The acenaphthene evaporator is immersed in a salt thermostat (53% KNO_3, 40% $NaNO_2$, 7% $NaNO_3$) where its temperature(160-270°) is maintained to within ±0.5°. Hot air enters the reactor in two streams. One stream enters the evaporator, where it passes through the layer of fused acenaphthene and becomes saturated with its vapor. The feed rate of acenaphthene into the reactor is controlled by the velocity of this stream and the acenaphthene temperature in the evaporator. The other stream of air serves to dilute the mixture of air and acenaphthene vapor at the entry into the reactor to the required acenaphthene : air ratio. The other parts of the unit are clear from the diagram.

Preparation of catalysts. Pumice in the form of 4-7 mm pieces was used as support for all the catalysts. Some of the catalysts contained considerable amounts of potassium sulfate, the influence of which on the activity of vanadium catalysts is reported in the literature [16].

Catalyst No.1. Ammonium vanadate (15 g) was dissolved with warming in 400 ml of water, and 300 ml (bulk volume) of pumice was put into the hot solution. The solution was evaporated with continuous stirring, and the catalyst was then dried at 125°. Before use it was activated by hot air at 400° for 2-3 hours.

Catalyst No.2. This was prepared and activated in the same manner as Catalyst No.1, but 11.4 g of potassium sulfate was added to the ammonium vanadate solution before addition of the pumice.

Catalyst No.3. Potassium sulfate (7.6 g) and 10 g of ammonium metavanadate were dissolved in 250 ml of water with warming. A solution of 7 g of ferric chloride ($FeCl_3 \cdot 6H_2O$) in 100 ml of water was added to this solution, and 200 ml of pumice was put in immediately. The resultant mass was evaporated almost to dryness with continuous stirring and then dried at 125°. The catalyst was activated by hot air at 400° for 3-4 hours until it was completely free of ammonium chloride.

Catalyst No.4. This was prepared as Catalyst No.3, but instead of ferric chloride 7 g of cupric chloride ($CuCl_2 \cdot 2H_2O$) was taken. The dried catalyst was activated by hot air at 360° for 3 hours.

Catalyst No.5. Manganese carbonate (12 g) was dissolved in 16 ml of concentrated nitric acid with 200 ml of water. The solution was warmed and filtered. To the filtrate 200 ml of pumice was added and the mixture was evaporated to dryness. The dry catalyst was heated to 250° and treated with hot air at that temperature until magnesium nitrate was completely decomposed. The catalyst was then activated by hot air at 400° for 1-2 hours.

Acenaphthene was oxidized in presence of these catalysts, both with small (up to 1:15 ratio) and large (up to 1:150 ratio) amounts of air at 320-435 . The experiments were conducted in series with 5-6 experiments in each. Each series consisted of experiments at different temperatures but under otherwise equal conditions, with the same catalyst.

It had been noticed that fresh vanadium catalysts become "conditioned" (undergo changes of activity) at the start of operation, and therefore the results of the first 5-6 experiments were disregarded. Usually 20-22 of acenaphthene was oxidized in each experiment. The evaporator was filled with acenaphthene, weighed,

TABLE 1

Oxidation of Acenaphthene by Small Amounts of Air over Catalyst No.1

Temperature of expt. (°C)	Acenaphthene taken (g)	Duration of expt. (min)	Amount of air (liters/min)	Yield of reaction product (g)	Amount distilled under vacuum (g)	Acenaphthylene content in distillate (%)	Yield of acenaphthylene (%)	Amt. of residue (naphthalic anhydride (%)
320	21.1	20	0.75	20.2	19.4	10.1	9.35	3.9
340	21.9	20	0.75	20.6	18.8	26.3	23.8	6.8
360	21.3	20	0.75	20.7	18.0	24.8	21.2	11.1
380	21.6	20	0.75	20.8	19.1	30.1	27.0	6.4
400	21.4	20	0.75	21.0	19.5	37.9	34.9	6.3
320	21.1	35	0.69	20.1	18.2	18.8	16.4	8.1
340	20.6	37	0.69	20.0	16.0	39.9	31.1	16.9
360	20.5	37	0.69	19.7	14.9	44.9	32.9	20.9
380	20.8	36	0.69	19.4	13.3	48.9	31.7	27.4
400	20.5	35	0.69	19.7	15.0	52.8	39.0	19.8
320	21.5	19	1.33	19.8	18.7	13.9	12.2	4.2
340	21.1	18	1.33	19.9	17.6	37.1	31.4	10.0
360	21.4	18	1.33	19.2	16.4	46.8	36.2	13.3
380	21.3	18	1.33	19.2	17.2	48.9	40.0	7.8
400	21.0	18	1.33	18.8	16.2	50.9	39.7	11.7
320	21.6	35	1.33	20.2	18.8	13.4	11.8	6.6
340	21.9	36	1.33	18.9	16.0	37.5	28.8	13.3
360	21.0	35	1.33	18.8	12.6	52.8	31.5	29.1
380	21.7	35	1.33	18.9	12.7	57.9	34.3	26.8
400	21.7	35	1.33	18.3	13.1	60.1	36.8	23.6

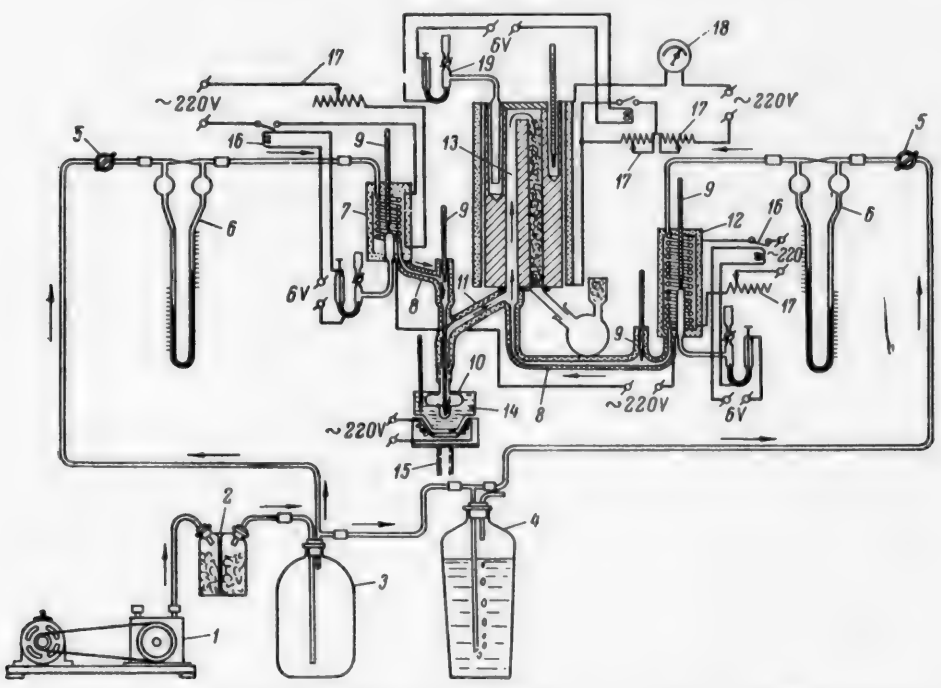

Fig. 4. Apparatus for contact oxidation of acenaphthene: 1) air blower, 2) filter, 3)receiver, 4) pressure regulator, 5) fine-regulation valves, 6) flow meters, 7) primary-air preheater, 8) air ducts, 9) thermometers, 10) acenaphthene evaporator, 11) evaporator bend, 12) preheater, 13) mixing chamber, 14) salt thermostat, 15 screw turntable, 16) relay, 17) rheostats, 18) ammeter, 19) thermoregulator.

connected to the reactor, and immersed in the thermostat in which a predetermined temperature was maintained. The second air stream was then adjusted to the required rate, and only then was the first stream passed through the evaporator. The instants at which the air supply into the acenaphthene evaporator was started and stopped were taken as the start and the end of the experiment respectively. The reaction product was collected in a weighed glass receiver. The receiver was fitted with a cotton-wool plug at the outlet in order to prevent loss of product with the stream of exit gas.

TABLE 2

Vapor-Phase Oxidation of Acenaphthene over Iron Vanadate with Potassium Sulfate, Catalyst No. 3

Temperature of expt.(°C)	Volume ratio of acenaphthene to air	Contact time (sec)	Yield of naphthalic anhydride (%)
350	1 : 94	2.9	79.7
350	1 : 93	2.9	81.2
360	1 : 100	2.9	76.6
370	1 : 91	2.9	76.4
370	1 : 96	1.86	77.8
370	1 : 115	2.9	77.1
370	1 : 111	1.46	74.5
380	1 : 37	2.85	63.4
380	1 : 64	2.9	76.2
380	1 : 99	2.9	78.2
400	1 : 102	2.9	69.8
400	1 : 76	3.74	60.2
435	1 : 112	2.9	33.9

Oxidation of acenaphthene over vanadium pentoxide by small amounts of air (Table 1) gave a low-melting product containing a small amount of naphthalic anhydride. When this product was distilled at 10-20 mm, acenaphthylene and unchanged naphthene were distilled off in the 135-145° range, while naphthalic anhydride remained as residue in the distillation flask.

Since the yellow color of the distillate is caused by the presence of acenaphthylene in acenaphthene, we developed a colorimetric method for estimation of acenaphthylene and tested it with artificial mixtures of acenaphthylene and acenaphthene. A standard solution containing 0.2 g of acenaphthylene in 100 ml of ethyl alcohol is the most suitable for work with the KOL-1M colorimeter with a No.7 light filter (effective wave length 449). The error of the colorimetric determinations (with artificial mixtures) does not exceed 2-3%. The residue in the distillation flask consisted mainly of naphthalic anhydride; this was demonstrated as follows. A mixture of 5 g of residue, 5 g of sodium carbonate, 25 ml of nitrobenzene, and 150 ml of water was boiled for 1 hour under reflux. Nitrobenzene was then distilled off in steam, and the undissolved residue was filtered off. From the soda filtrate 2.6 g of naphthalic anhydride was precipitated by mineral acid. To test for the presence of acenaphthene quinone in the undissolved residue, 25 ml of nitrobenzene, 25 ml of 40% sodium bisulfite solution, and 150 ml of water were added to the residue and the mixture was heated with a mechanical stirrer on the water bath for 1 hour. The liquid was cooled, the nitrobenzene was separated off, the bisulfite solution was acidified with sulfuric acid and boiled for 15-20 minutes until sulfur dioxide was completely removed. Not even a trace of acenaphthene quinone separated out of the solution.

In addition to naphthalic anhydride, the residues retain certain amounts of acenaphthene and acenaphthylene, which in our procedure are distilled in steam together with nitrobenzene.

It follows from the foregoing that, even when small amounts of air are used, acenaphthene is oxidized partially as far as naphthalic anhydride.

The effects of different catalysts on the oxidation of acenaphthene by small amounts of air are shown in Fig. 1-3.

All the five series of experiments, the results of which are plotted in these graphs, were conducted at 1:7.5 ratio of acenaphthene to air, with a contact time of 3.5 seconds.

In experiments with large amounts of air, with all our vanadium catalysts the oxidation products contained considerable amounts of naphthalic anhydride together with a little acenaphthylene. A part of the acenaphthene was burned. These products melted at fairly high temperatures and could not be distilled under vacuum. Acenaphthylene was distilled out of them in steam, and naphthalic anhydride was extracted in warm soda or alkali solution. When acenaphthene was oxidized by large amounts of air under fairly harsh conditions over Catalyst No.3, pure naphthalic anhydride in the form of well-defined large colorless laminar crystals of m.p. 268° collected in the receiver. The yield reached 75-80% of the the theoretical.

When the oxidation was performed with the same amount of air and the same contact time, but at a temperature 10-20° lower, the yield of naphthalic anhydride was somewhat higher, but its quality was worse.

This is illustrated in Table 2, which contains the results of certain experiments on oxidation of acenaphthene to naphthalic anhydride by large amounts of air over Catalyst No.3.

SUMMARY

1. Naphthalic anhydride is formed in 30-80% yield by catalytic vapor-phase oxidation of acenaphthene at 320-400° over vanadium pentoxide on pumice.

2. Addition of potassium sulfate to vanadium pentoxide sharply raises the activity of the catalyst, increasing the yield of naphthalic anhydride to 50-60%.

3. Even better results are obtained in presence of iron vanadate with potassium sulfate on pumice. With this catalyst the yield of naphthalic anhydride of m.p.268° is 75-80%.

4. Oxidation of acenaphthene over manganese oxide on pumice as catalyst yields a low-oxidation product with small amounts of air, or combustion products with large amounts of air.

LITERATURE CITED

[1] A. Behr and A. Van-Dorp, Ann. 172, 263 (1874).

[2] C. Graebe and E. Gfeller, Ber. 25, 652 (1892).

[3] G. Charrier and A. Moggi, Gazz 57, 736 (1927).

[4] H. Paillard and A. Duckert, Helv. Chim. Acta, 16, 773 (1933).

[5] U.S. Patent 2379032; C. A. 4631 (1945).

[6] U.S. Patent 1935054; Zbl. II, 3492 (1934).

[7] U. S. Patent 1844390; Zbl. II, 618 (1932).

[8] Ger. Patent 441163; Frdld. XV, 350 (1928).

[9] French Patent 649292; Zbl. II, 1120 (1919).

[10] U. S. Patent 1844392; Zbl. II, 305 (1933).

[11] U. S. Patent 1844395; Zbl. II, 1836 (1932).

[12] British Patent 318617; Zbl. I, 3357 (1930).

[13] British Patent 318618; Zbl. I, 3357 (1930).

[14] J. Jones, J. Appl. Chem. 1, 568 (1951).

[15] M. Kaufmann and F. Williams, J. Appl. Chem. 1, 489 (1951).

[16] I. I. Ioffe, Questions of Chemical Kinetics, Catalysis, and Reactivity [in Russian] (Moscow, 1955) p. 232.

Received January 8, 1958.

PREPARATION OF FORMALDEHYDE BY OXIDATION OF METHANE, CATALYZED BY NITROGEN OXIDES

N. S. Enikolop'yan, N. A. Kleimenov, L. V. Karmilova,
A. M. Markevich, and A. B. Nalbandyan

In the first part of this investigation [1], we studied the conditions of formaldehyde formation in the oxidation of methane catalyzed by small amounts (0.1%) of nitric oxide.

This paper contains the results of further investigations performed with reaction vessels arranged in series, and also by a recirculation scheme. The reaction vessels used were packed and treated with potassium tetraborate. Nitrogen oxides were used as the homogeneous catalyst.

EXPERIMENTAL

Experiments with Reaction Vessels in Series*

In this series of experiments, the original gas–air mixture (CH_4 33.3%, air 66.6% NO 0.1%) was passed consecutively through three reaction vessels. The formaldehyde was collected in water in absorbers placed at the exit from each reactor. The reaction vessels were porcelain tubes 30 mm in diameter, heated in electric furnaces. They were packed with "Mazda" hard-glass beads. The results of these experiments are presented in the table, where the last column gives the yields of CH_2O calculated on the CH_4 taken.

It is seen from these results that under these conditions 7.4% of methane by volume is oxidized to formaldehyde, and 9-12% to carbon monoxide. Methyl alcohol was not determined in the reaction products in these experiments. If up to 20% methyl alcohol, calculated on formaldehyde, is formed [1,2], the useful conversion of methane reaches 9% on the amount originally taken.

Experiments in a Circulation Unit

Two circulation schemes were used in the experiments – closed and continuous.

In the closed-circulation scheme the original gas–air mixture, confined in the apparatus, was passed repeatedly through the reaction vessel. Formaldehyde was collected in water in an absorber placed at the exit of the reaction vessel. The contact time and temperature in the reactor were kept constant. After a definite number of cycles the spent mixture was passed out into the atmosphere and the system was refilled with fresh mixture.

The yields of formaldehyde for different numbers of cycles were determined, and the distribution of the reaction products between different cycles was studied. The lower limit of CH_2O yield per molecule of NO catalyst was also determined. The number of cycles in such a system, with contraction disregarded, is defined as the ratio of the amount of gas passed through the reactor to the total amount of circulating mixture.

The results of one series of experiments are plotted in Fig. 1.

*A. A. Anisonyan, S. Ya. Beider, and N. I. Vinnikova, of the All-Union Scientific Research Institute of Gases, MNP, assisted in this part of the work.

Contents of O_2, CO, CO_2 and CH_2O in the Gas–Air Mixture in a System of Three Consecutive Reactors

Reactor No.	At entry into reactor (vol.%)			At exit from reactor (vol.%)				CH_2O (% by vol. on CH_4 taken)
	O_2	CO	CO_2	O_2	CO	CO_2	CH_2O	
1	13.9—14.0	0	0	10.0—11.5	0.7—1.5	0.1—0.3	0.9—0.93	2.7—2.8
2	10.0—11.5	0.7—1.5	0.1—0.3	9—10	1.5—2.5	0.2—0.4	0.83	2.5
3	9—10	1.5—2.5	0.2—0.4	7.5—9	3—4	0.5—0.7	0.70	2.1
	Formaldehyde obtained			—	—	—	2.46	7.4

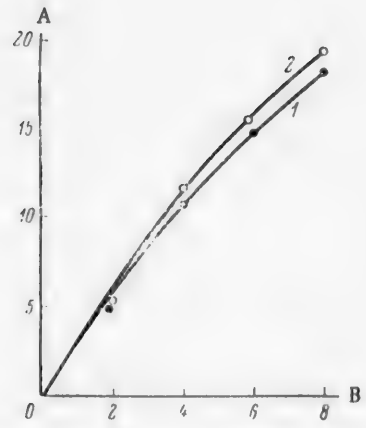

Fig.1. Yield of formaldehyde in closed circulation at t = 580° with an original mixture containing (%): CH_4 28, air 71.4, NO 0.6; A) contents of CH_2O and CO (in % on CH_4 by volume), B) number of cycles; curves: 1) yield of CH_2O, 2) accumulation of CO.

It follows from these results that in 8 cycles 18.5% of the methane taken is oxidized to formaldehyde, and a little more (19.7%) is converted to carbon monoxide. In some instances, when the circulating mixture was supplemented with air or oxygen, up to 32% of the original methane could be converted into formaldehyde.

It was shown earlier [1] that under the optimum conditions the molecular yield of formaldehyde in a single pass was about 10 per molecule of homogeneous catalyst.

In repeated circulation in a closed system an increase of the useful conversion of methane and a corresponding increase of the formaldehyde yield per molecule of NO could be expected if nitrogen oxides are a true catalyst and do not undergo chemical changes during the reaction.

To confirm this hypothesis, experiments were performed with a mixture containing 18% CH_4, 9% O_2, 73% N_2 and 0.1% NO. Small amounts of methane and oxygen in equimolecular proportions were fed in order to maintain a constant pressure in the system. The experiments were performed at 550 and 590°. It was found that 20 and even 30 molecules of formaldehyde are formed per molecule of NO.

An important disadvantage of closed circulation is that the process must be stopped at intervals and the system recharged with fresh air–gas mixture. Continuous circulation is preferable in this respect.

In the continuous-circulation scheme, the gas circulating in the system was continuously enriched with fresh original gas–air mixture at the entry into the reactor. The spent gas from the absorber was simultaneously removed from the system. Under these conditions, the number of cycles is defined as the ratio of the amount of circulating gas to the amount of fresh gas–air mixture. When the number of cycles is n, the composition of the gas entering the reaction vessel always corresponds to the (n–1)th cycle, i.e., the contents are much lower than in the fresh mixture. Because of this the yield of CH_2O is appreciably lower in continuous circulation than in a system of reactors in series, where the concentrations of the reacting gases decrease gradually from stage to stage.

The principal circulation experiments were concerned with a study of the dependence of the formaldehyde yield on the composition of the mixture and the number of cycles. The experiments were performed with different methane–air mixtures and different numbers of cycles. The temperature in these experiments was varied between 565 and 680°. The amount of nitrogen oxides fed in was calculated to give a concentration of 0.1% by volume in the circulating mixture. The main results are presented in Fig. 2 and 3. It is seen that, for example, with 10-fold circulation of a mixture containing 22% CH_4, up to 21% of the methane passed is converted into

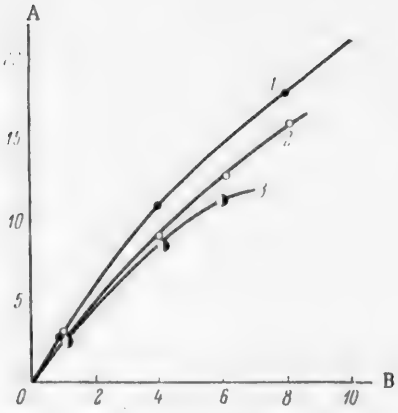

Fig. 2. Yield of formaldehyde in continuous circulation of different original methane–air mixtures containing 0.1% NO: A) content of CH_2O (in % on CH_4 by volume), B) number of cycles; CH_4 content (%) and temperature (°C) respectively: 1) 22 and 620, 2) 33.3 and 640, 3) 40 and 650.

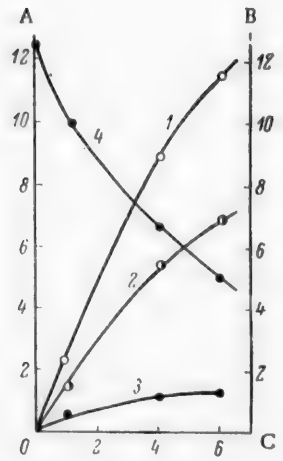

Fig. 3. Yields of formaldehyde and other oxidation products, and consumption of oxygen in continuous circulation at t = 650° of an original mixture containing (%): CH_4 40, air 60, NO 0.1; A) contents of CH_2O, CH_3OH and CO (in % by volume on CH_4), B) O_2 concentration in the circulating gas (vol. %), C) number of cycles; curves: 1) yield of CH_2O, 2) formation of CO, 3) formation of CH_3OH, 4) fall of oxygen concentration.

formaldehyde. Hence the useful conversion of methane reaches 280 g per 1 m^3 of methane if the methyl alcohol formed is disregarded. Under these conditions about 11.5% of the original hydrocarbon is converted into carbon monoxide. The formaldehyde concentration in the gas before absorption was 0.4-0.45%.

With 4-fold circulation of the same mixture the formaldehyde yield reaches 11%. In circulation of a mixture containing 33.3% methane, about 10% of the CH_4 is converted into formaldehyde in 4 cycles, and if the number of cycles is increased to 8 the yield on the methane passed can be raised to 16%.

The experimental results show that if the methane content of the original mixture is raised from 22 to 40% the useful conversion of methane is decreased somewhat (Fig. 2). At the same time, the formaldehyde content of the gas leaving the reactor rises from 0.4-0.45 to 0.9%, which raises the productivity of the unit and makes absorption of the formaldehyde easier. As expected, the yields of formaldehyde and methyl alcohol are not proportional to the number of cycles. The relative degree of useful conversion of methane per cycle decreases with increase of the number of cycles.

A special series of experiments was performed, with chemical determination of nitrogen oxides in the feed and spent mixture and the absorption liquor, in order to calculate the material balance of the homogeneous catalyst.

These experiments showed that losses of nitrogen oxides as the result of unavoidable absorption in the absorber may be from 2 to 16% of the amount fed in, in accordance with the circulation conditions (flow velocity, temperature of the experiment, oxygen content of the mixture).

It was shown that 84-98% of the nitrogen oxides is found in the exit gases. It follows from all these results that nitric oxide is not consumed to any extent in the reaction, and acts as a homogeneous catalyst.

SUMMARY

1. In a study of the possibility of raising the degree of useful conversion of methane by oxidation to formaldehyde in a system of reactors in series and with circulation, it was shown that in presence of small amounts (0.1-0.12%) of NO in a system of three consecutive reactors the useful conversion of methane can be raised to 7.4%, and in a closed-circulation system it can be raised to 20% and over.

2. The distribution of the reaction products and oxygen consumption in mixtures of different compositions was studied in relation to the number of cycles under conditions of continuous circulation. It is shown that with 10-fold circulation the useful conversion of methane into formaldehyde in lean mixtures (CH_4 = 22%) can be raised to 21%. It is shown that the productivity of the process can be raised and the formaldehyde content of the gas increased by circulation of mixtures enriched with natural gas.

3. The relative formaldehyde yield per volume of homogeneous catalyst present can be raised to 30 under circulation conditions.

4. The extent of unavoidable losses of catalyst in the system has been determined. It is shown that nitrogen oxides are not consumed in the reaction but act as a homogeneous catalyst.

LITERATURE CITED

[1] N. S. Enikolopyan, N. A. Kleimenov, L. V. Karmilova, A. M. Markevich, and A. B. Nalbandyan, J. Appl. Chem. 32, No.4, 913 (1959).*

[2] L. V. Karmilova, N. S. Enikolopyan, and A. B. Nalbandyan, J. Phys. Chem. 30, 798 (1956).

Received September 30, 1957.

*Original Russian pagination. See CB Translation.

REACTIONS OF METALS WITH ORGANIC THIO AND THIOPHOSPHORUS ADDITIVES IN OILS*

G. V. Vinogradov, M. M. Kusakov, P. I. Sanin, E. A. Razumovskaya, and A. V. Ul'yanova

The commonest antiwear(antiseize) additives are mixtures of compounds containing sulfur, phosphorus, and chlorine, or compounds containing all these elements. It is important to determine the functional demarcation between the action of sulfur, phosphorus, and chlorine compounds and also the mutual influence of these compounds, or of sulfur, phosphorus, and chlorine atoms in the molecule of the additive, on interaction with the metal and the antiwear effect. Reliable information on the mechanism of joint action of sulfur and chlorine compounds is now available. Investigation of the same question in relation to phosphorus and sulfur compounds is important.

The definition of the lower temperature limit of additive—metal interaction under static conditions depends on the sensitivity of the method. Comparison of the binding of modifying elements on the metal surface, detected under static conditions at low temperatures, with the results of dynamic (wear) tests is possible only at low sliding velocities when it is permissible (at least in the first approximation) to disregard the change of temperature in the volume of the lubricant film enclosed between the friction surfaces. Despite the arbitrary definition of the lower temperature limit of additive—metal interaction, its determination is significant for comparing the activities of different compounds.

Modification of frictional surfaces by the action of antiwear (antiseize) additives, which is their main function, presupposes that their reactivity is sufficiently high, as the restoration of the frictional surfaces damaged as the result of wear must generally proceed at a high rate. It seems likely that at moderate temperatures the shift of equilibrium in the direction of decomposition of the additive is primarily due to its interaction with the metal. The condition that the reactivity of the additives must be high implies that they should decompose more or less readily at elevated temperatures, and the rate of the decomposition reaction may exceed the rate necessary for modification of the frictional surfaces during wear. Reactions taking place within the volume of the lubricant may become significant. The upper temperature limit of additive effectiveness is determined by the rapid, metal-catalyzed, thermal decomposition of the additives which commences at increased temperatures.

The volume temperatures of solutions of organic sulfur and phosphorus compounds have a strong influence on the results of wear tests. The causes of this are, on the one hand, changes in the conditions of heat transfer from the friction zone, and, on the other, changes in the chemical activity of the substances dissolved in the oils with respect to the metal. The nature of such changes may be investigated under static conditions [1].

This paper contains the results of an investigation of the interaction of chromium—manganese—silicon steel and electrolytic copper with organic thio and phosphorus compounds dissolved in a nonpolar (naphthene—paraffin) bright stock fraction isolated from a mixture of high-grade Surakhany and Karachukhur petroleums. This product had the following characteristics: density $d_4^{20} = 0.8812$, average molecular weight M = 543, refractive index $n^{20}D = 1.4859$, kinematic viscosities $\gamma_{20} = 750$, $\gamma_{50} = 105$ and $\gamma_{100} = 14.5$ centistokes.

*Paper presented at the Conference on Lubrication and Wear, held in London in October 1957.

Activities of the Preparations

Additive	Specific activity (pulses/minute · g)	
	Steel	copper
Elemental sulfur	$3.1 \cdot 10^{10}$	$3.5 \cdot 10^{10}$
Didecyl sulfide	$6.5 \cdot 10^{9}$	$8.8 \cdot 10^{9}$
Didecyl disulfide	$6.5 \cdot 10^{9}$	$8.8 \cdot 10^{9}$
Tributyl trithiophosphite (S^{35})	$4.7 \cdot 10^{7}$	—
Tributyl trithiophosphite (P^{32})	$1.5 \cdot 10^{8}$	—
Tributyl phosphite (P^{32})	$4.1 \cdot 10^{8}$	—

Organic thio compounds with tagged sulfur were prepared by the usual methods. The original radioactive substances were elemental sulfur S^{35} and BaS containing radioactive sulfur. Tributyl phosphite containing the P^{32} isotope was synthesized from butyl alcohol and PCl_3 containing radioactive phosphorus. The reaction was carried out in presence of pyridine. Tributyl trithiophosphite containing tagged sulfur was prepared by the action of PCl_3 on butyl mercaptan in presence of pyridine [2]. Butyl mercaptan was prepared by the action of butyl bromide on thiourea containing S^{35} in presence of ethyl alcohol, with subsequent decomposition of the complex formed (alkyl isothiourea hydrobromide) by aqueous caustic soda. Tributyl trithiophosphite containing tagged phosphorus was prepared by the same method, but contained the P^{32} isotope.

The investigations were carried out by the method described previously [1]. The amounts of sulfur or phosphorus which interacted with the metal were calculated from the results of determinations of the activity of standard solutions of the radioactive preparations applied onto metallic disks. Since the standard and working determinations were carried out under the same conditions, it was not necessary to take the differences in scattering of electrons by steel and copper into account. Standard benzene solutions of preparations containing S^{35} or P^{32} of known specific activity were placed in definite amounts on the disk surfaces by means of a micropipet. After the solution had spread and the solvent evaporated, the radioactivity was determined under the same conditions as used for disks immersed in oil containing the additives. The S^{35} and P^{32} concentrations in the standard solutions were chosen so that the activity of the disks after evaporation of the solvent was at least 2000 pulses/minute. The activities of the preparations, measured on the disk surfaces and calculated per g of a mixture of stable and radioactive isotopes, are given in the table.

The table shows what small amounts of sulfur and phosphorus can be determined on the metal surfaces [3-5].

The results of experiments with steel and solutions containing 0.6% of elemental sulfur are plotted in Fig. 1. When Fig. 1 is examined it must be remembered that, in the case of Curves 1 and 3, 100/pulses/minute · cm^2 corresponds to $1.4 \cdot 10^{-9}$ g of sulfur (the total amount of the stable and radioactive isotopes); in Curve 2, 100 pulses/minute · cm^2 corresponds to $1.8 \cdot 10^{-9}$ g of sulfur. It is clear from Fig. 1 that interaction between steel and sulfur begins even at room temperature. Similar results were obtained with copper, but with the difference that the interaction of sulfur was much more intensive with copper than with steel. The amount of sulfur bound on the surface was tens of times greater for copper than for steel even at room temperature.

Intensive interaction of sulfur with steel even at low temperatures causes sulfur solutions to have peculiar antiwear properties; such solutions differ in nearly every respect from solutions of sulfides, disulfides, and other similar compounds.

Fig. 2 shows the results of experiments (each of 2 hours) at different temperatures, with solutions containing didecyl sulfide and didecyl disulfide at concentrations such that the oil contained 1% sulfur.

The difference between these experiments, in which the effect of temperature on the amounts of phosphorus and sulfur bound by the metal (in a definite constant time) was determined, and the kinetic experiments was that in the former instance a new metal disk was used each time, whereas in the kinetic studies the experiments at any one temperature were performed with the same disk.

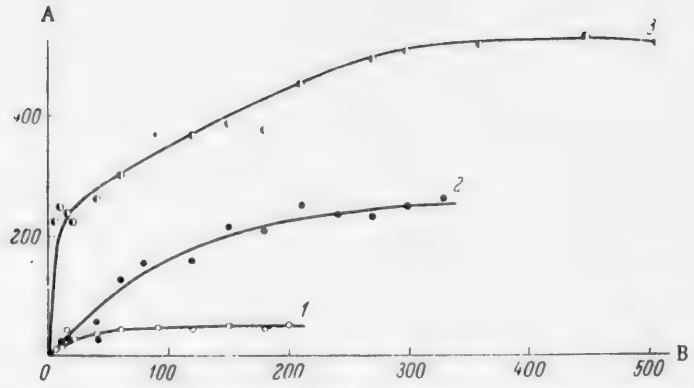

Fig. 1. Binding of elemental sulfur by steel: A) activity (pulses/minute · cm^2), B) time (minutes); temperature (°C): 1) 40, 2) 60, 3) 130.

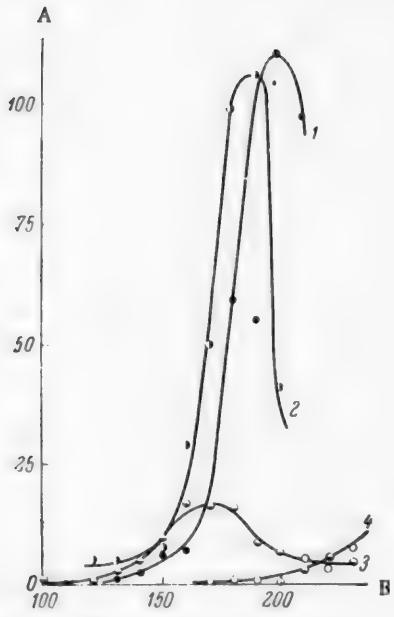

Fig.2. Effect of temperature on the amount of sulfur bound by copper and steel: A) total amount of radioactive and stable isotopes (mg), B) temperature (°C); 1) didecyl sulfide on copper, 2) didecyl disulfide on copper, 3) didecyl disulfide on steel, 4) didecyl sulfide on steel.

It is evident from Fig. 2 that the reactivity of the disulfide, is considerably higher than that of the sulfide, because of the greater mobility of the sulfur atoms in the former. This difference is especially significant in the case of steel, i.e., the less reactive metal. The difference between alkyl and aryl sulfides on the one hand, and disulfides on the other, with respect to their interaction with steel is in qualitative agreement with the results of tests of their solutions in naphthene–paraffin bright stock fractions, performed in friction machines. The fact that the binding of sulfur on the metal surface has a temperature maximum confirms the view advanced above, according to which there is an upper temperature limit of additive effectiveness, which corresponds to development of decomposition processes of the additive in the volume of the oil. In fact, it is easy to detect at high temperatures the liberation of gaseous substances, containing radioactive sulfur, from the oil.

In all cases, sulfur was bound irreversibly, i.e., chemically, on steel and copper. This was found in experiments in which the washed and dried activated disks were placed in a solvent under constant conditions, kept in it for 2 hours and again subjected to the same treatment; their activity was then determined. Experiments with tributyl phosphite solutions (concentration 0.1 M) showed that P^{32} is bound on steel from these solutions even at 20° (Fig.3). In accordance with the temperature, the surface becomes saturated, or the activity begins to increase at a constant rate, or the process may become self-accelerating. At temperatures above 140°, the additive undergoes decomposition accompanied by formation of a precipitate.

Experiments with tributyl trithiophosphite tagged with P^{32} and S^{35} respectively are of considerable interest. The experiments were carried out with solutions (concentration 0.1 M) in contact with steel disks for 2 hours. It was found that phosphorus is bound by steel much more rapidly than sulfur. Binding of phosphorus by steel could be detected even at room temperature, whereas binding of sulfur could be detected only at temperatures above 100°. Under the experimental conditions used, the amount of phosphorus bound by steel at 20° was 4.2 mg/cm^2. This is about 0.01% of the total phosphorus in solution. The amounts of phosphorus and sulfur bound by the steel surface increase with temperature, reach maximum values, and then decrease. When the binding of phosphorus

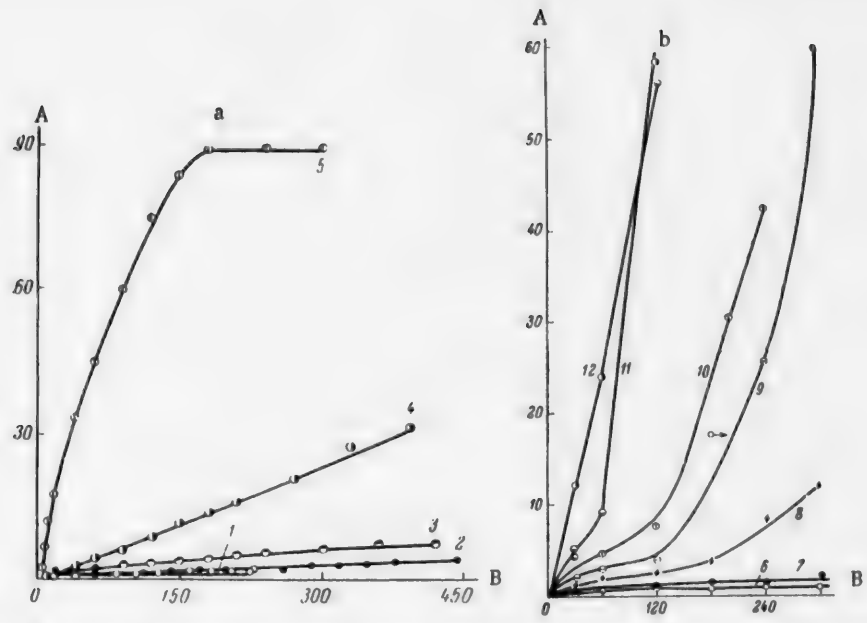

Fig. 3. Binding of phosphorus from tributyl phosphite solution by steel: A) total amount of radioactive and stable isotopes (mg/ cm^2), B) time (minutes); temperature (°C): 1) 20 2) 40, 3) 60, 4) 80, 5) 100, 6) 110, 7) 120, 8) 130, 9) 140, 10) 150, 11) 160, 12) 170.

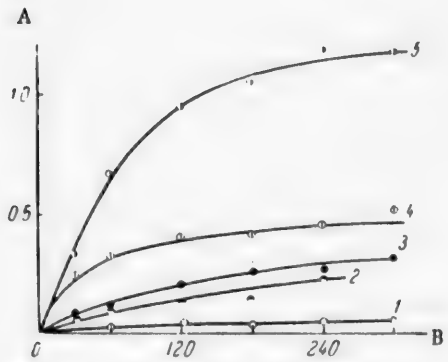

Fig. 4. Binding of phosphorus from tributyl trithiophosphite solution by steel: coordinates as in Fig. 3; temperature (°C) 1) 20, 2) 40, 3) 60, 4) 80, 5) 150.

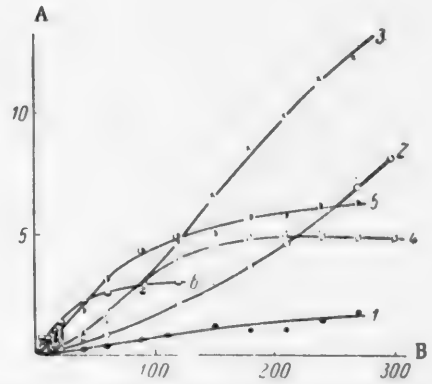

Fig.5. Binding of sulfur from tributyl trithiophosphite solution by steel; coordinates as in Fig. 3; temperature (°C): 1) 120, 2) 130, 3) 140, 4) 150, 5) 160, 6) 170.

by the steel disks was at a maximum (at about 160°), about 4% of the total phosphorus in solution had reacted. The amount of sulfur which reacted under the same conditions was 0.02%.

The results of kinetic studies of the interaction of steel with tributyl trithiophosphite tagged with P^{32} and S^{35} are plotted in Fig. 4 and 5. It is seen that at temperatures of about 140° and over, tributyl trithiophosphite begins to decompose after some time (with liberation of gaseous sulfur-containing products), and the increase of the activity of the disk surfaces accordingly slows down or ceases entirely.

The results of the static experiments described above are in excellent qualitative agreement with the results of wear tests on solutions of organic thiophosphorus compounds and mixtures of organic thio and phosphorus compounds [4-6]. The above experiments showed that phosphorus in organic phosphites has much higher reactivity toward steel than sulfide or disulfide sulfur, including sulfur linked with phosphorus. Therefore a film of iron phosphide is readily formed on the steel surface (preferentially to a sulfide film). This explains why, in absence of seizing and sharp rises of temperature, the properties of the steel surface are influenced predominantly by phosphorus under such conditions. It is only when the frictional surfaces begin to seize(at very high temperatures in regions of their contact) that the influence of sulfur and the formation of iron sulfide films become apparent. As iron sulfide has some measure of plasticity, the seizing conditions are made somewhat milder – the running-in of the frictional surfaces under seizing conditions becomes easier. In presence of organic phosphorus compounds only, seizing conditions become especially severe. It follows from this that the effects of sulfur and phosphorus in organic sulfur and phosphorus compounds with regard to antiwear activity are not only functionally differentiated, but mutually supplementary.

The experiments described above for steel disks were repeated with disks of copper. It was found that there is a sharp difference between steel and copper with regard to sulfur, whereas phosphorus is bound with approximately the same intensity by copper and steel disks. The binding of sulfur increases more rapidly on copper than on steel with increase of temperature. At all temperatures, more sulfur than phosphorus is bound by the surfaces of the copper disks; moreover, the amount bound is considerably greater (by several orders of magnitude) than on steel. These results show that the nature of the metal has a significant influence on the conditions of interaction between it and organic sulfur and phosphorus compounds in hydrocarbon solutions; the results given above for steel are specific and characteristic of metal of a given composition and thermochemical treatment. At the same time, experiments with such different metals as copper and steel show that many metals are effective acceptors not only of sulfur but also of phosphorus from organic thiophosphorus compounds.

SUMMARY

1. The lower temperature limit of interaction between oil additives and metals is determined by the start of binding of sulfur and phosphorus by the metal surface. This definition depends on the sensitivity of the method.

2. The activity of an additive toward a metal may increase with temperature up to a certain limit. This limit corresponds to a temperature which may in this sense be regarded as the upper temperature limit of additive serviceability or the temperature of highest activity of the additive. At higher temperatures the sulfur and phosphorus compounds dissolved in the oil decompose with formation of compounds less active toward the metal.

3. There is a functional demarcation between the effects of the different active principles (sulfur and phosphorus) in antiwear additives for oils. Phosphorus in organophosphorus additives prevents seizing by raising considerably the load values at which seizing occurs, while sulfur in organic sulfur compounds has an especially prominent effect under seizing conditions, making them considerably milder and preventing scoring, which is not characteristic of phosphorus.

LITERATURE CITED

[1] G. V. Vinogradov, M. M. Kusakov, Yu. S. Zaslavskii, and É. A. Razumovskaya, J. Acad. Sci. USSR 9, 33 (1955).

[2] A. Hippert and E. Reid, J. Am. Chem. Soc. 60, 2370 (1938).

[3] G. V. Vinogradov, M. M. Kusakov, P. I. Sanin, Yu. S. Zaslavskii, É. A. Razumovskaya, A. V. Ul'yanova, and D. V. Ryabova, Chemistry and Technology of Fuel 6, 14 (1956).

[4] G. V. Vinogradov, in Proceedings of the First Conference on Chemistry and Applications of Organophosphorus Compounds [in Russian] (Izd. AN SSSR, Moscow, 1957) p. 139.

[5] G. V. Vinogradov, M. D. Bezborod'ko, O. E. Morozova, P. I. Sanin, and A. V. Ul'yanova, Chemistry and Technology of Fuel 5, 47 (1956).

[6] O. E. Morozova, G. V. Vinogradov, and M. D. Bezborodko, in the book: Chemistry of Organic Sulfur Compounds Present in Petroleum Products [in Russian] (Ufa, 1958) 4, p. 182.

Received January 22, 1958.

JOINT POLYCONDENSATION OF PHENOXYACETIC ACID AND p-CHLOROPHENOL WITH FORMALDEHYDE

A. A. Vansheidt, N. N. Kuznetsova, and Z. I. Kulikova

In order to raise the selectivity of carboxylic cation exchangers based on phenoxyacetic acid (KFU resins) [1] for large organic ions, ion-exchange resins with a lowered carboxyl group content were synthesized by joint polycondensation of phenoxyacetic acid and formaldehyde with phenol and resorcinol.

It was found that the insoluble condensation products, containing bound phenol or resorcinol in addition to phenoxyacetic acid, do indeed have higher exchange capacities for streptomycin and other antibiotics than KFU resin.

However, the joint condensation of these substances (because of the high reactivity of phenol, and especially of resorcinol) resulted in a violent reaction, so that the process was difficult to carry out even on a small industrial scale.

We therefore attempted to replace these compounds by the less reactive p-chlorophenol in joint condensation with phenoxyacetic acid and formaldehyde; because of the presence of a halogen atom in the nucleus, it might also be easier to determine the composition and structure of the polycondensation products and also possibly to modify their sorptional properties in the desired direction.

It is known that p-chlorophenol [2] reacts with formaldehyde in an acid medium with formation of novolacs.

The resins were synthesized from phenoxyacetic acid, p-chlorophenol, and paraform rather than formaldehyde solution, as p-chlorophenol is difficultly soluble in water.

It was found that p-chlorophenol reacts at approximately the same rate as phenoxyacetic acid with paraform. Thus, when a mixture consisting of 1 mole of phenoxyacetic acid and 0.9 mole of formaldehyde (as paraform) is heated in presence of 0.1% H_2SO_4, about 80% of the formaldehyde is combined within 25 minutes after addition of the formaldehyde, while after 55 minutes the formaldehyde has reacted almost completely.

In the case of p-chlorophenol about 77% of the formaldehyde is combined in 25 minutes, and after 45 minutes, formaldehyde cannot be detected in the reaction mixture.

For joint polycondensation of all three reagents the mixture was heated at 100-105° for 3 hours in presence of 1.5% sulfuric acid until the formaldehyde was completely combined; three different molar proportions: 2.0, 1.0, and 0.5, were used, and the amount of formaldehyde in the original mixture was 0.8 mole per mole of phenol derivatives in all cases.

Under these conditions, resins were obtained in 95-96% yield; after unconverted monomers had been removed and the resins were dried they were hard but brittle fusible substances, soluble in acetone, ether, alcohol, phenol, and aqueous alkalies (Table 1).

It follows from Table 1 that the melting points of the soluble resins vary between 95 and 110°, i.e., in relatively narrow limits, and their average molecular weight, determined cryoscopically, is between 620 and 710. Table 1 also contains the results of elementary analysis of the resins, their COOH group contents, and values calculated from the resin yields on the assumption that the resins were formed by polycondensation of formaldehyde with phenol derivatives analogously to phenol–formaldehyde novolacs

$$n\mathrm{CH_2O}+(n+1)\mathrm{C_6H_5OH} \rightarrow n\mathrm{H_2O}+\mathrm{H[C_6H_3(OH)CH_2]_nC_6H_4OH}, \quad (1)$$

i.e., with liberation of equivalent amounts of water for the formaldehyde and phenols.

It is clear from Table 1 that the amounts of Cl, COOH groups, C and H found and calculated were similar for each of the resins.

It follows that the components reacted in the proportions in which they were present in the original mixtures. For phenolic components (Φ) of different compositions, Equation (1) can be written in the following general form:

$$n\mathrm{CH_2O}+(n+1)\Phi \rightarrow n\mathrm{H_2O}+(\Phi+\mathrm{C})_n\Phi, \quad (2)$$

where C is carbon, and Φ may represent phenoxyacetic acid (PA) of M = 152, or chlorophenol (CP) of M = 128, or mixtures of them with molecular weights of 136, 140, or 144 for CP:PA ratios of 2.0, 1.0 and 0.5 respectively.

This equation shows that with a molar CH_2O : PA ratio of 0.8, as used in our experiments, the average degree of polymerization of the resins should be 4, as $\frac{1}{0.8} = \frac{n+1}{n}$, and hence n = 4. Their molecular weights can be calculated from the polycondensate formula $(\Phi+12)_n\Phi$ if the values of n and Φ are known.

Thus, the average molecular weights of our resins can be calculated on the assumption that n = 4 from the average molecular weights of the phenolic components of the original mixtures, which are 136, 140, and 144; we then find from Equation (2) that the calculated molecular weights of the resins formed at CP:PA ratios of 2, 1, and 0.5 are 728, 748, and 768 respectively; these values are either close to or rather higher than the molecular weights found cryoscopically in phenol (Table 1).

In addition, the soluble resins (I and II) were converted into their acetates by treatment with acetic acid in pyridine on heating. The acetates were also analyzed completely. The calculated data were found on the assumption that the OH groups in the resins were completely acetylated.

Table 1 shows that the experimental and calculated values were in good agreement; this confirms the hypothesis that the OH group contents of the original resins were equivalent to the chlorine contents found.

TABLE 1

Composition and Properties of Soluble Resins and Their Acetates, Formed by Joint Polycondensation of Chlorophenol (CP), Phenoxyacetic Acid (PA), and Formaldehyde

Conditions and analytical data	Polycondensates			Acetates	
	I	II	III	I	II
Molar CP : PA ratio in original mixture	2.0	1.0	0.5	2.0	1.0
Melting point (°C)	103—109	106—109	94—101	95—105	104—109
Average weight of phenolic unit	136	140	144	—	—
Molecular weight:					
found	708	620	678		
calculated	728	748	768		
Cl (in %)					
found	15.8	11.5	7.8	13.80	10.80
calculated	16.2	11.8	7.7	13.60	10.40
COOH (in %):					
found	10.1	14.6	19.6	8.2	11.7
calculated	10.3	15·0	19.5	8.6	13.0
C (in %):					
found	61.18	62.70	63.30	61.15	61.24
	61.28	62.93	63.70	60.82	61.31
calculated	61.40	62.45	63.50	60.70	61.80
H (in %):					
found	4.27	4.58	4.25	4.78	4.85
	4.30	4·50	4.68	4.59	4.67
calculated	4.10	4.35	4.45	4.35	4.40

The soluble resins can therefore be regarded as polymer homologs of different molecular weights, the molecules of which consist on the average of 5 phenoxyacetic acid and chlorophenol residues cross linked by means of CH_2 bridges at the aromatic nuclei.

Hardening of soluble resins. When the soluble resins are heated with paraform at 110° in presence of 4% sulfuric acid for 6-7 hours they greatly increase in viscosity but still remain soluble. On further heating at 120-140° the resins become rubberlike, and then hard and insoluble as the result of conversion into space polymers.

The hardened resins (KFUKh), after crushing and removal of insoluble impurities, consisted of brown grains of satisfactory mechanical strength which swelled in aqueous alkalies and had the properties of weakly acidic ion exchangers, stable to the action of acids and weak alkali solutions. Their exchange capacity was about 3 meq/g, or about one half of the capacity of the previously described KFU resins made from phenoxyacetic acid and formaldehyde. These resins (according to the results obtained in the Physicochemical Laboratory of the Institute of High-Molecular Compounds of the Academy of Sciences USSR) had high exchange capacity (close to 100%) with respect to large organic ions (streptomycin, collimycin, and other antibiotics)

Table 2 contains data on certain resin samples made from equimolecular amounts of p-chlorophenol and phenoxyacetic acid, but hardened with different amounts of paraform (from 1.9 to 0.45 mole CH_2O per mole of phenoxyacetic acid).

TABLE 2

Characteristics of KFUKh Resins Hardened with Different Amounts of Paraform

Moles CH_2O per mole PA taken	Resin yield (%)	K_{sw} of Na form in water	Capacity (meq/g)	Found %					Found (moles per 100 g resin)		
				C	H	Cl	OH	COOH	Cl	OH	COOH
1.9	90	2.5	—	—	—	10.0	4.9	—	0.28	0.29	—
1.4	93	3.1	2.9	62.8	5.5	10.7	5.0	13.5	0.30	0.29	0.29
1.1	85	3.2	—	—	—	9.9	4.7	—	—	—	—
0.9	85	3.6	—	—	—	10.6	5.2	—	0.30	0.30	—
0.65	80	3.8	—	—	—	10.9	5.2	—	0.31	0.30	—
0.55	69	4.5	3.0	62.5	5.2	10.7	4.7	13.5	0.30	0.28	0.30
0.45	65	14.0	2.9	62.2	4.7	10.9	4.8	13.2	0.30	0.28	0.29
	Calculated		3.2	63.1	4.3	11.5	5.6	14.8			

TABLE 3

Characteristics of Hardened Resins Made with Different Proportions of Chlorophenol and Phenoxyacetic Acid.

Resin No.	Molar ratio of components in original mixture		Moles CH_2O/mole PA + CP taken for hardening	Yield (%)	K_{sw} of Na form		Exchange capacity (meq/g)		Contents (%)					Molar CP : PA ratio in polymer
	CP:PA	CH_2O: nucleus			in water	in 1 N NaOH	found	calculated	C	H	Cl	OH	COOH	
I	2 : 1	0.8	2.0	55	2.2	4.0	2.6	—	63.80	5.2	13.4	5.5	11.7)	1.3 : 1
							—	2.2	61.40	4.1	16.2	7.9	10.4)	
II	1:0	0.8	1.4	93	3.1	3.3	3.0	—	62.85	5.5	10.7	5.0	13.3)	1 : 1
							—	3.3	63.05	4.3	11.5	5.6	14.8)	
III	1 : 2	0.8	2.0	95	2.0	2.0	4.3	—	64.20	4.8	7.1	3.6	19.3)	1 : 2.0
							—	4.3	64.00	4.5	7.7	3.6	19.3)	

It follows from Table 2 that the swelling coefficient of the resins (in 1 N NaOH solution) increases from 2.5 to 14 with decrease of the amount of paraform added, while the yield and mechanical strength decrease. A particularly large increase of the swelling coefficient (from 4.5 to 14) and decrease of mechanical strength was observed on decrease of the amount of formaldehyde from 0.55 to 0.45 mole per mole of phenoxyacetic acid. With regard to the composition of the hardened resins, Table 2 shows that their chlorine, hydroxyl, and carboxyl contents, in moles per 100 g of resin, changed little with variations in their degree of cross linking, and in all cases these groups were present in equimolecular proportions, i.e., the resins contained phenoxyacetic acid and p-chlorophenol residues in the same proportions as those in which the components were present in the original mixture.

However, the amounts of Cl, OH, and COOH groups found in all the samples were somewhat less than the amounts calculated on the assumption that the hardened resins are weakly cross-linked space polymers, close in composition to linear polymers of the structure

$$[-(C_6H_3(OCH_2COOH)-CH_2)-(C_6H_2ClOHCH_2-)]n$$

We also prepared insoluble resins with other proportions of chlorophenol to phenoxyacetic acid. Details are given in Table 3, which gives the yields and degrees of swelling of the resins and their OH and COOH group contents in relation to the proportions of the phenolic components in the original mixture.

Resins II and III were obtained in good yields; the yield of Resin I, made with excess of p-chlorophenol, was 55%, probably because the bifunctional p-chlorophenol, which cannot give rise to cross-linked polymers, was predominant in this case.

The chlorine and OH contents found show that the composition of insoluble Polymer I does not correspond to the composition of the original mixture, as the polymer has a much lower content of p-chlorophenol units than the original mixture of the soluble resin. Thus, it follows from the last column of Table 3 that Polymer I contains only 1.3 and not 2 p-chlorophenol units per phenoxyacetic acid unit. The probable explanation is that the original polymer is heterogeneous not only with respect to molecular weight but also in composition, and when it hardens only the components containing trifunctional phenoxyacetic acid units can be cross linked, whereas components containing few or no phenoxyacetic acid units are not involved in formation of the cross-linked polymer and are removed from the hardened product during alkali treatment. This probably accounts for the low yield of Resin I and its lower chlorine content.

As stated earlier, the solution viscosity greatly increases during the hardening process immediately before gelation while the resin remains soluble, evidently owing to formation of linear polymers of higher molecular weight.

It was therefore of interest to isolate and investigate these intermediate hardening products, in order to obtain some idea of the changes in the composition and molecular weight of the soluble resins during further interaction with formaldehyde.

Data are presented below on the composition and molecular weight of a soluble resin formed from equimolecular amounts of chlorophenol and phenoxyacetic acid, and isolated during hardening immediately before gelation.

Molecular weight – 1128, m. p. 165-170°.

Contents (%): Cl – 10.0, COOH – 13.5, H – 4.75.

This resin hardly differed in composition from insoluble Resin II (Table 3), but was soluble in aqueous alkalies, phenol, and acetone. However, it did not melt but merely softened at 165-170°. Its molecular weight was only double that of the original soluble resin.

Thus, when a space polymer is formed from a linear polymer, the molecules first grow by joining with each other to form soluble polymers of higher molecular weight, and the latter are converted into space polymers only

after their degree of polymerization has reached 6-7 , which corresponds to about 7-8 aromatic residues in the chains.

EXPERIMENTAL

Synthesis and hardening of soluble resins. One mole of phenoxyacetic acid and one mole of p-chlorophenol were heated together at 80° until a clear solution was formed; to this 0.05 mole of sulfuric acid (97-98%) was added with stirring, followed by gradual addition of 1.6 mole of formaldehyde (as paraform) in such a manner that the temperature in the flask did not exceed 100°. After addition of the paraform the reaction was continued at 100-105° until a sample of the resin hardened at room temperature.

Unchanged p-chlorophenol and formaldehyde were then removed from the resin by steam distillation, the resin was transferred to a filter, washed with distilled water to remove phenoxyacetic acid until neutral to litmus, and then dried under vacuum to constant weight. The yield was 286 g (96% of the theoretical). The synthesis of resins with different proportions of p-chlorophenol and phenoxyacetic acid was effected similarly.

For preparation of the insoluble product, after the end of the reaction the resin (in the same flask) was washed three times with equal volumes of distilled water and dried at a bath temperature of 105-110°. During the drying 22.4 g of 50% sulfuric acid was added. The drying was stopped when the temperature in the flask reached 110°. After this, 42 g of paraform was added in the form of a fine powder. When the paraform dissolved, the resin was poured out onto trays of acid-resisting stainless steel which were placed in an oven where the resin was kept first at 110° for 7 hours and then at 120° until it hardened at that temperature. The resin was then crushed to a grain size of 5-7 mm; the resin was subjected to further hardening in granular form at 140° for 2.5-3 hours until the required swelling coefficient was reached.

The hardened product was crushed down to ≤ 1 mm grain size and treated first with 0.5 N NaOH solution to remove all soluble organic impurities, and then with 0.5 N H_2SO_4 solution to convert it into the H form; it was then washed with water until the wash waters were neutral to Methyl orange, and dried to the air-dry state at 50-60°. The yield of resin was 150 g. The resin in the H form consisted of brown grains, insoluble in alkalies and organic solvents, with an exchange capacity of 3 meq/g and a swelling coefficient of 3-4.

To obtain the resin in the Na form it was covered with 0.5 N NaOH solution, left for 12 hours, and washed with distilled water to a negative reaction to phenolphthalein in the wash waters.

Determination of OH and COOH groups in the insoluble products. The OH-group content was determined by our modification of the Verley acetylation method [3].

0.5 g of resin (grain size 0.1-0.085 mm) was heated in a Verley flask with 10 ml of acetylation mixture, consisting of 12 g of acetic anhydride and 88 g of pyridine (free from moisture), on a boiling water bath for 4 hours. The mixture was then cooled to room temperature and 50 ml of distilled water was added to decompose unchanged acetic anhydride. On the following day the resin was filtered off. 20 ml samples of the filtrate were titrated with 0.2 N NaOH solution in presence of phenolphthalein. A blank experiment was performed at the same time.

The OH-group contents of the resins were calculated from the formula:

$$\% \text{ OH} = 3 \frac{(a - b) \cdot n \cdot \cdot 17}{q \cdot 10},$$

where a is the number of milliliters of 0.2 N NaOH taken in the blank titration, b is the number of milliliters of 0.2 N NaOH taken for titration of the filtrate sample, N is the normality of the solution, and q is the weight of resin (in g).

After the filtration the resin sample on the filter was washed with water to a negative reaction to litmus in the wash waters, rinsed into a flask with 100 ml of acetone, and titrated with 0.2 N NaOH solution in presence of 100 ml of 0.5 N sodium acetate solution:

$$\% \text{ COOH} = \frac{c \cdot 45 \cdot n.}{q \cdot 10},$$

here c is the number of milliliters of NaOH taken for titration of the sample.

On the other hand, the COOH group may be determined indirectly if the resin is not removed by filtration from the acetylation mixture decomposed by water. In this case, both the free acetic acid and the carboxyl groups in the resin are titrated.

From the chlorine content found, the number of milliliters of NaOH equivalent to the OH-group content can be calculated.

Then

$$\% \text{ COOH} = \frac{a - (b - c) \cdot n \cdot}{q \cdot 10},$$

where a is the number of milliliters of NaOH taken in the blank titration, b is the number of milliliters of NaOH taken for titration of the sample, and c is the number of milliliters of NaOH equivalent to the OH-group content.

In the case of the resin made from equimolecular amounts of phenoxyacetic acid and p-chlorophenol the volume of NaOH taken in titration of different samples was always the same as in the blank titration. This showed that the resin actually contained one mole of phenoxyacetic acid per mole of p-chlorophenol, as OH groups are determined by back titration and COOH groups by direct titration.

No such agreement was found for resins made from p-chlorophenol and phenoxyacetic acid taken in other proportions.

Determination of the molecular weights of soluble resins. The molecular weights of the resins were determined cryoscopically in phenol (Table 4).

Tests of the alkali resistance of resins. The resin in the H form was covered with 5 times its own volume of 1 N NaOH solution. After a certain time the solution was analyzed for chloride. Chloride was not detected even after the resin had been in contact with the alkaline solution for a month, while the chlorine content of the resin was close to that found before the alkali treatment. The swelling coefficient of the resin (Na and H forms) in water and alkali did not change; this shows that the resin is not broken down at the cross links by alkali treatment.

However, the alkali solution was always slightly colored during treatment of the resin, even if 0.2-0.5 N solution was used.

Preparation of acetates of soluble resins. Resin I or II (5 g) was dissolved in 100 g of acetylation mixture (consisting of 88 g pyridine and 12 g acetic anhydride) in a flask under reflux, and heated on a boiling water bath for 2 hours. The contents of the flask were then poured out gradually with stirring into 5% HCl solution containing 1.2 moles of HCl. The acetate was then filtered off, washed with water on the filter to a negative reaction to Methyl orange in the wash waters, and dried under vacuum to constant weight.

TABLE 4
Determinations of Molecular Weight

Resin	Weights taken		Δt (°C)	M (found)
	phenol	resin		
I	51.93	1.8329	0.417	617
		2.8459	0.633	629
II	55.66	0.8294	0.153	710
		1.9722	0.333	770
III	42.34	0.6600	0.167	678
		1.3515	0.343	677
Intermediate product in hardening	40.73	0.8340	0.133	1119.3
		1.5502	0.243	1138.7

SUMMARY

1. It is shown that joint condensation of formaldehyde with phenoxyacetic acid and p-chlorophenol in presence of sulfuric acid yields resins, which are either soluble or insoluble in aqueous alkalies and organic solvents according to the amount of aldehyde taken and the reaction conditions, and which contain residues of all the original reagents in their chains.

2. Soluble resins formed in presence of 0.8 molecule of CH_2O per aromatic nucleus were low-melting polymers of the phenol–formaldehyde novolac type of molecular weight 600-700, and with different proportions of phenoxyacetic acid and p-chlorophenol residues in the chain, dependent on the composition of the original mixture.

3. When the soluble resins were heated with paraform in presence of sulfuric acid, the viscosity of the reaction mixture increased owing to the formation of soluble polymers of higher molecular weight (M = 1100); this was followed by gelation and formation of infusible and insoluble space polymers as the result of cross linking of the resin at the phenoxyacetic acid residues by the action of formaldehyde.

4. The insoluble resins were mechanically strong, capable of limited swelling within wide limits (dependent on the amount of formaldehyde taken for hardening), and could take up metal cations and antibiotics from aqueous solutions.

5. The exchange capacity of these weakly acidic ion exchangers varied from 2 to 4 meq/g, in accordance with the relative contents of phenoxyacetic acid and p-chlorophenol; a resin with an exchange capacity of 3 meq/g (KFUKh), made from phenoxyacetic acid and p-chlorophenol in equimolecular proportions, had very high selectivity for streptomycin and other antibiotics.

LITERATURE CITED

[1] A. A. Vansheidt and N. N. Kuznetsova, J. Appl. Chem. 32, No.4, 868 (1959).*

[2] W. J. Burke et al., J. Polymer Sci. 20, 75 (1956); W. J. Burke, S. H. Ruetman, C. W. Stephens and Alex Roschthal, J. Polymer Sci. 22, 477 (1956).

[3] A. A. Vansheidt and N. N. Kuznetsova, J. Appl. Chem. 30, 1850 (1957).*

Received November 3, 1958.

*Original Russian pagination. See C. B. translation.

CATALYTIC CONDENSATION OF COMPRESSED ACETYLENE WITH AROMATIC AMINES IN THE LIQUID PHASE

N. S. Kozlov and S. Ya. Chumakov

The Perm' Agricultural Institute

Favorskii and Shostakovskii [1] have shown that compressed acetylene may be used for synthesis of vinyl ethers. The conditions for safety with the use of acetylene under pressure in an autoclave were found in their investigations. In a number of publications, the use of compressed acetylene is recommended for various organic syntheses, such as the reactions of acetylene with aldehydes, ketones [2], alcohols, and acids [3].

In the present investigation, the reactions of compressed acetylene with primary aromatic amines were studied for the first time. It had been shown by one of us earlier [4] that in presence of copper, mercury, or silver salts acetylene reacts with primary aromatic amines. In the present investigation all three variants of this reaction were studied, namely: 1) condensation of acetylene with primary aromatic amines, when the end products are quinaldine and its derivatives; 2) condensation of acetylene with a mixture of an aromatic amine and acetone, when the end products are 2,4-dimethylquinoline and its homologs; and 3) condensation of acetylene with a mixture of a primary aromatic amine and an aromatic aldehyde, when α-phenylquinoline or its homologs are formed. The catalysts used were cuprous chloride, mercuric chloride, copper acetylide, and mercury salts of organic acids.

Among the serious disadvantages in our earlier work [5] was the long time required for complete saturation of the reaction mass with acetylene. In some instances about 30 hours was needed.

With the use of compressed acetylene we were able to shorten the saturation time to 2-3 hours. It was also found that under these new reaction conditions the end products were considerably influenced by the specific effects of copper and mercury catalysts. If the reaction between compressed acetylene and aromatic amines is effected in presence of mercuric chloride or the mercury salts of acetic, propionic, or butyric acids, the principal reaction products are ethylideneamine bases, and the end products are quinaldine and its homologs. If the reaction is effected in presence of cuprous chloride or copper acetylide, a resinous substance is formed; distillation of this, in the reaction with aniline for example, yields quinaldine and an appreciable amount of indole. We consider that the reaction proceeds in two directions simultaneously. First, the reaction of aniline with acetylene yields ethylideneaniline, which is then converted into quinaldine.

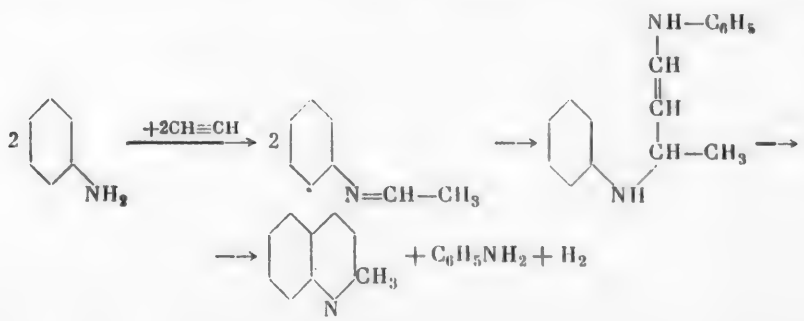

Second, aniline and acetylene yield vinylaniline, which polymerizes to polyvinylaniline; indole is formed by the action of heat on the latter.

In relation to this, we developed a new variant of indole synthesis.

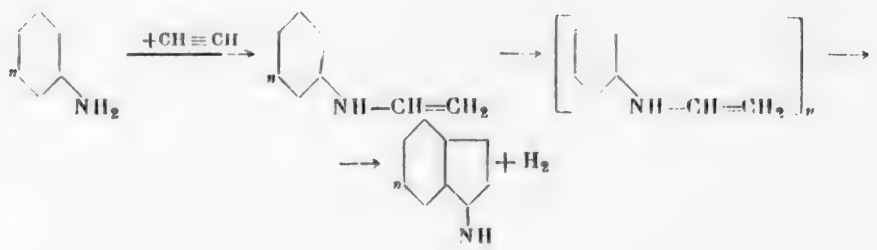

EXPERIMENTAL

Method. Weighed quantities of primary aromatic amine and catalyst were put in an autoclave 0.75 liter in capacity. Acetylene was blown through the autoclave, and the latter was then connected to an acetylene cylinder by means of a flexible steel tube and filled with acetylene at 10-12 atmos pressure; it was then shaken mechanically at room temperature or after being warmed to not over 30°. Absorption of acetylene was indicated by the fall of pressure in the autoclave. Fresh portions of acetylene were introduced into the autoclave at intervals, and the reaction was terminated when the acetylene pressure in the autoclave ceased to drop. In all the experiments, saturation of the reaction mass with acetylene was complete in 2-3 hours.

The reaction products were treated by one of two methods: 1) the reaction mass was transferred to a Wurtz flask together with the catalyst, and distilled; 2) the product was separated from the catalyst be means of a solvent, and the residue was distilled after evaporation of the solvent. Quinoline bases were isolated by one of two methods from the reaction products, which were obtained in the form of fractions of wide boiling ranges: 1) the fraction was diazotized, and the quinoline bases were isolated by the usual methods; 2) the reaction product was dissolved in 10% hydrochloric acid and treated with potassium ferrocyanide; the quinoline bases were precipitated as complex salts, isolated by the action of alkali, and extracted in ether.

Experiment No. 1. The autoclave was charged with 50 g of aniline and 5 g of mercuric chloride, and acetylene was pumped in under 10-12 atmos pressure. Rapid absorption of acetylene commenced after the autoclave had been heated by steam to 25-30° with shaking. The saturation was complete after 2.5 hours. Distillation of the reaction products gave: 1st fraction, to 190°, 21 g; 2nd fraction, 190-260°, 30 g; residue, 4 g. The 1st fraction consisted of aniline with a small admixture of quinaldine. From the 2nd fraction, 14 g of quinaldine was isolated, b.p. 245-248°, $d_4^{20} = 1.056$, $n_4^{20} = 1.611$. From it the picrate of m.p. 191° and quinophthalone of m.p. 232-233° were prepared. The 2nd fraction contained only small amounts of secondary amines. It was found in special experiments that it contained about 15% aniline. The quinaldine yield was 18.2% on the aniline taken, or 31.3% on the converted aniline. If the aniline present in the 2nd fraction is taken into account, the yield of quinaldine becomes considerably higher.

In an experiment with 50 g of aniline and 10 g of mercuric chloride, 50 ml of benzene had to be added as solvent, as the reaction mass lost its fluidity. Rapid absorption of acetylene began when the autoclave was shaken, without preliminary heating. As in the preceding experiment, the reaction mass absorbed 16 g of acetylene. This experiment yielded 16 g of quinaldine, and 19 g of aniline was recovered. The quinaldine yield was 20.8% on the aniline taken, or 33.4% on the converted aniline.

Experiment No. 2. For this experiment, 50 g of aniline and 5 g of finely divided cuprous chloride was taken. The reaction mass absorbed 14 g of acetylene in 2.5 hours. The reaction products yielded 19 g of unchanged aniline and 14 g of quinaldine, which is 18.2% on the aniline taken or 29.4% on the converted aniline.

When the 190-270° fraction, obtained in a yield of 31 g, was treated with 10% hydrochloric acid solution, 7.5 g of a substance insoluble in the acid was obtained. This substance was extracted in ether, dried, and distilled after evaporation of the ether. The following products were obtained: 1st fraction, 230-245°, 3 g; 2nd fraction, 245-260°, 3.5 g; residue, 1.0 g. Redistillation of the 1st and 2nd fractions yielded 1.5 g of a substance with b.p. 250-254°. On standing, this crystallized (m.p. 51-52°) and gave a positive color test for indole; it gave

a red picrate of m.p. 184-185° and an acetyl derivative of m.p. 182°. It was found by means of the picrate reaction and by treatment of an ether solution of the 1st and 2nd fractions with $NaHSO_3$ solution that it contained up to 50% of indole in some experiments. The indole yield was 5.15% on the aniline taken, or 8.4% on the converted aniline.

The results were very similar if 10 rather than 5 g of cuprous chloride catalyst was taken. Absorption of acetylene by the reaction mass was complete after 1.5-2 hours. The quinaldine yield was 21.4% on the aniline taken, or 35.4% on the converted aniline, and the indole yield was 5 or 7.5% respectively.

Experiment No.3. The reaction mass consisted of 50 g of aniline and 3 g of copper acetylide. The saturation was continued for 3 hours, during which time the reaction mass absorbed 13 g of acetylene. Treatment of the reaction products yielded 16 g of unchanged aniline and 35 g of a fraction boiling in the 190-260° range. From this, 18 g of quinaldine and 2 g of indole was isolated. The quinaldine yield was 23.4% on the aniline taken, or 36.4% on the converted aniline.

Experiment No.4. A mixture of 25 g of p-toluidine, 50 ml of alcohol, and 5 g of copper acetylide absorbed 7 g of acetylene in 2 hours. Treatment of the reaction products yielded 10 g of p-toluidine and 8 g of dimethylquinoline; the substance of m.p. 58-60° gave a picrate of m.p. 186°. The yield of 2,6-dimethylquinoline was 21.7% on the p-toluidine taken, or 36.4% on the converted p-toluidine. In addition, 2 g of a neutral substance of b.p. 240-270° was obtained; this gave a color test for indole, but was not studied in detail.

At the same time and under the same conditions a series of experiments was carried out on the condensation of aromatic amines with compressed acetylene in presence of mercury salts of organic acids [5]. In an experiment with 50 g of aniline and 15 g of mercuric acetate, 22 g of a substance of m.p. 126-127° was isolated from the resinous reaction product. This substance is the Eckstein–Eibner base, and is converted into quinaldine when heated. Kjeldahl determination of nitrogen in the substance of m.p. 126-127° gave 11.87% and 12.04% nitrogen; the calculated value for ethylideneaniline base is 11.76%.

In an experiment with 30 g of p-toluidine, 30 ml of alcohol, and 15 g of mercuric acetate the reaction product yielded 11 g of substance with m.p. 115-117°; when this was heated, the formation of 2,6-dimethylquinoline was detected. Kjeldahl determination of nitrogen in the substance of m.p. 115-117° gave 10.7 and 10.66% nitrogen; the calculated value for α-8-di-p-toluino-α-butylene is 10.53%. Similar results are obtained if mercuric propionate or butyrate is used instead of the acetate.

Experiment No.5. A reaction mass consisting of 50 g of aniline, 50 ml of acetone, and 10 g of mercuric chloride was saturated for 3 hours with acetylene under 10-12 atmos pressure. After evaporation of the unchanged acetone on the water bath, the reaction product was treated as in the preceding experiments. 20 g of unchanged aniline was recovered, and 27 g of a 190-300° fraction was obtained. The reaction product yielded 5 g of quinaldine and 6 g of a substance of b.p. 262-264°, which formed a picrate of m.p. 191-192°, $d_4^{20} = 1.050$, $n_4^{20} = 1.5990$. These constants correspond to published data for 2,4-methylquinoline [6a]. Similar results were obtained when cuprous chloride was used as catalyst instead of mercuric chloride.

Experiment No. 6. A reaction mass consisting of 50 g of p-toluidine, 50 ml of acetone, and 10 g of cuprous chloride was saturated with acetylene in the autoclave. Distillation of the reaction products gave: 1st fraction, up to 205°, 14 g; 2nd fraction, 205-250°, 18 g; 3rd fraction, 250-300°, 25 g. Treatment of the 2nd and 3rd fractions yielded 6 g of 2,6-dimethylquinoline and 10 g of 2,4,6-trimethylquinoline of m.p. 39-40°; the picrate melted at 201°.

Experiment No. 7. A reaction mass consisting of 25 g of aniline, 50 ml of alcohol, 15 g of benzaldehyde, and 5 g of cuprous chloride was saturated with acetylene in the autoclave. Distillation of the reaction product yielded 15 g of a fraction boiling in the 250-350° range which crystallized completely. Recrystallization from alcohol gave 11 g of substance of m.p. 82-83°, which formed a picrate of m.p. 191-192°. The constants of this substance agree with data for α-phenylquinoline [6b]. The formation of some quinaldine was also detected.

Experiment No.8. A mixture of 24 g of p-toluidine, 15 g of benzaldehyde, 50 ml of alcohol, and 7 g of cuprous chloride was treated with acetylene in the usual manner to give 7 g of substance with m.p. 68°, which formed a picrate of m.p. 207°. The constants of this substance corresponded to literature data for 6-methylphenylquinoline [6b].

SUMMARY

The catalytic condensation of primary aromatic amines and mixtures of primary aromatic amines with

acetone or benzaldehyde with compressed acetylene in an autoclave was studied. Mercuric chloride, cuprous chloride, and copper acetylide were tested as catalysts. The intermediate reaction products were ethylideneamine bases, and the end products were the corresponding quinoline bases—quinaldine and its homologs, and α-phenylquinoline and its homologs; in presence of copper catalysts indole was formed—a fact first observed by us in these reactions.

LITERATURE CITED

[1] M. F. Shostakovskii, Vinyl Ethers [in Russian] (Moscow, 1952) pp.5-20.

[2] I. N. Nazarov, I. L. Kotlyarevskii and V. F. Ryabchenko, J. Gen. Chem. 23, 1900 (1952).*

[3] Acetylene Chemistry (IL, 1954) [Russian translation].

[4] N. S. Kozlov and P. Ya. Fedoseev, J. Gen. Chem. 6, 250 (1936); 6, 1352, 1341; 7, 836 (1937); 8,413 (1938).

[5] L. E. Olifson, Bull. Chkalovsk Section, D. I. Mendeleev All-Union Chem. Soc. 2, 51 (1941); 3, 31 (1949).

[6] I. Heilbron, Dictionary of Organic Compounds a) I, 952; b) III, 452; c) II,792 [Russian translation].

Resubmitted March 25, 1959.

*Original Russian pagination. See C. B. translation.

BRIEF COMMUNICATIONS

STUDIES OF THE TEMPERING OF PORCELAIN

A. I. Avgustinik and V. M. Loginov*

We reported earlier that when porcelain insulators are fired by a high-speed procedure (12-14 hours inclusive of cooling) their mechanical strength is increased by as much as 60-80% in some instances [1]. It was found that the strength of the insulators increases if they are cooled in the 900-600° range at a rate of 300-400°/hour.

The increase in the strength of porcelain during rapid cooling is attributed by some workers to the residual stresses which arise in the transition of the vitreous phase in porcelain from the plastic into the elastic state [2-4]. This question has been discussed theoretically [5,6] and has been verified in the qualitative respect [4].

Certain patents [7] relate to the use of heat treatment tempering for increasing the strength of ceramics.

The purpose of the present investigation was to determine the causes of the increase of strength of porcelain insulators as the result of rapid cooling. The influence of rapid cooling was tested in two ways: with specimens (rods 12 and 22 mm in diameter and 80 mm long for bend tests, and disks 80 mm in diameter, with pits, for puncture tests), previously fired at 1320° in the "Proletarii" factory kiln, then heated in a Silit furnace and cooled rapidly; and with specimens (rods 10 mm in diameter and 80 mm long for static and dynamic bend tests, 25 · 25 mm cylinders for compressive tests) which were fired in a Silit furnace at 1330° and then either cooled slowly (during 5 hours) in the same furnace, or removed from the furnace and toughened by rapid cooling in a current of air at 20° (air velocity 10 m/second). In the second firing procedure the heating-up time was 3 hours and exposure at constant temperature either lasted 2, 4, or 6 hours, or did not take place at all; a reducing atmosphere in the furnace was created by combustion of kerosene, and the medium had the following composition: CO 6%, CO_2 7%, and O_2 from 0.8 to 1%.

Porcelain body from the "Proletarii" insulator factory was used for the first series of experiments. The fired specimens were heated in a Silit furnace and exposed at various temperatures for 0.1, 1, and 2 hours, and then either cooled rapidly in a current of air at 20° (air velocity 5 or 10 meters/second) or allowed to cool naturally in air.

For the second series of experiments mixes were prepared in accordance with the "Proletarii" and Lomonosov factory formulations by joint wet grinding of the stone and clay materials in a ball mill. The phase composition of the porcelain in the second series of experiments was studied by means of x-ray ionization analysis with the use of comparison standards made from quartz, cristobalite, mullite, and the vitreous phase. ** Changes in the coefficient of linear expansion of the porcelain in the 560-590° range were also determined.

The results of static-bending tests on specimens of the first series are given in Fig. 1 and 2; the results of static and dynamic bending tests and compressive tests on specimens of the second series are given in Fig. 3.

Each result of the mechanical strength and electrical breakdown tests represents the average value for 8-10 determinations.

The results of phase analysis are presented in Table 1.

*Student R. N. Suvorova assisted in the work.

**The investigation was performed in the x-ray unit of the State for Planning and Research in the Cement Industry, under the guidance of P. F. Konovalov.

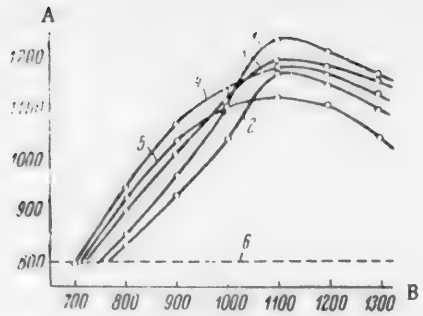

Fig. 1. Effects of heating temperature, exposure time, and air-feed rate on the bending strength of previously-fired porcelain specimens 12 mm in diameter: A) bending strength (kg/cm^2), B) temperature (°C); exposure time (hours)and feed rate (m/second) respectively: 1) 0.1, 10; 2) 0.1, 5; 3) 1, 10; 4) 2, 10; 5) 2, 5; 6) strength before

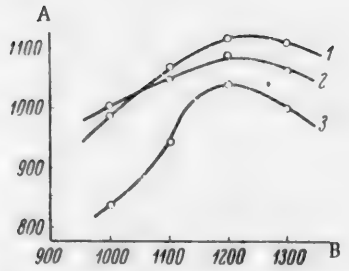

Fig.2. Effects of heating temperature and cooling rate on the bending strength of previously-fired porcelain specimens 22 mm in diameter: A) bending strength (kg/cm^2), B) temperature (°C); air feed rate (m/second): 1) 5; 2) 10; 3) cooled in stationary air; exposure time 2 hours at each tempering.

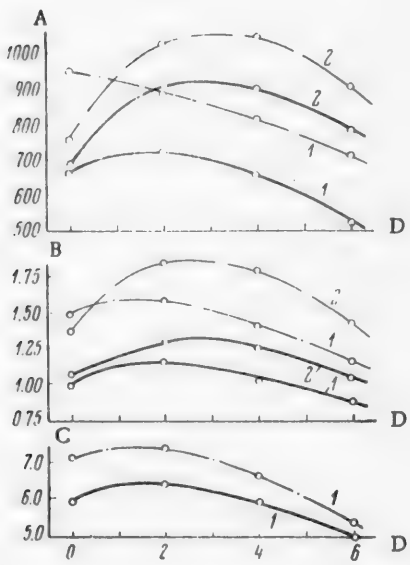

Fig. 3. Variations of mechanical strength of porcelains from the "Proletarii" (1) and Lomonosov (2) factories at different cooling rates in relation to the time of exposure at 1300°: A) bending strength (kg/cm^2), B) impact bend strength (kg-m), C) compressive strength (tons/cm^2), D) exposure at maximum temperature (hours); continuous curves refer to samples cooled during 5 hours, broken curves to samples cooled in an air stream at 10 meters/second; the lowest diagram relates to compressive-strength tests on specimens cooled in stationary air (upper curve).

Fig. 1 shows that the highest strength was obtained when previously-fired specimens were heated to 1100° with a very short exposure (0.1 hour)at that temperature, and then cooled rapidly in a current of air (at 10 m/second). For rods 12 mm in diameter the strength was 50% greater than that of specimens cooled slowly in the usual manner. For rods 22 mm in diameter heated to 1200° and cooled in a current of air (5 m/second), the strength increase was 40% (Fig. 2).

To test the effect of rapid cooling on the electrical strength of porcelain, previously fired disks were heated to 1100 and 1200°, held at those temperatures for 2 hours in the furnace, and cooled rapidly in a current of air (at 5 m/second). The specimens cracked if the air velocity was 10 m/second. The electrical strength was 27.7 and 27.2 kv/mm, as compared with 27.6 kv/mm before the heat treatment, i.e., it was unaffected by the treatment.

Analogous results were obtained in tests on specimens of the second series; the mechanical strength in static and dynamic bending and in compression was 15-30% higher when the specimens were cooled rapidly in a current of air at 10 m/second. The specimens used for compressive tests were cooled in stationary air.

This considerable increase of the mechanical strength of porcelain as the result of rapid cooling (from temperatures above 700°) can be described as tempering.

It may be assumed that the increase of the strength of porcelain during tempering is the consequence of stresses in it. The nature of these stresses and the course of their development present a complex problem, as is shown by the fact that, according to the data in Table 1,

the porcelain samples differed in phase composition whereas their strength characteristics were almost the same.

It was assumed that the stress field was nonuniform over the specimen cross section.

To test this assumption, all the side faces of both tempered and untempered specimens (prisms 20 · 18 mm in cross section) were ground down to 12 · 10 mm, while the length remained unchanged (80 mm). The specimens were previously fired in the works kiln at 1320°. To temper the specimens they were heated to 1200°, removed from the furnace, and cooled in a current of air (5 m/second). The test results are given in Table 2. It is clear from these results that the untempered specimens and tempered specimens with their sides ground down are equal in strength, whereas the strength is about 38% higher for tempered specimens with their external surfaces intact. It follows that increase of the strength of porcelain in these tempering experiments may be attributed to stresses which develop in the surface layers of the specimens.

TABLE 1

Phase Composition of Porcelain from the "Proletarii" and Lomonosov Factories after Firing at 1330° in a Silit Furnace

Porcelain	Length of exposure at 1330° (hours)	Phase composition from x-ray data (%)			Quartz content, from change of coeff. of linear expansion (%)	total porosity
		mullite, from 2.546 A line	quartz, from 1.82 A line	cristobalite, from 4.04 A line		
"Proletarii" factory	0	12.7	15.5	Traces	16.5	13.1
	2	15.4	10.4		—	6.6
	4	14.25	5.0		5.0	10.5
	6	12.0	3.4		—	13.43
Lomonosov factory	0	17.2	21.3		22.25	14.4
	2	22.5	14.9		—	5.9
	4	22.7	11.6		—	4.26
	6	25.0	10.7		10.1	5.47

TABLE 2

Results of Bending Tests on Specimens of Rectangular Section

Specimens	Number of specimens tested	Range of strength variations (kg/cm²)	Average strength (kg/cm²)
Not tempered, 20 × 18 mm	8	650—690	677
Tempered, 20 × 18 mm	8	850—1000	935
Not tempered, sides ground down, 12 × 10 mm	5	440—617	555
Tempered, sides ground down, 12 × 10 mm	5	512—623	554

SUMMARY

1. When porcelain specimens in the form of rods 12 and 22 mm in diameter, and of prisms 20 · 18 mm in cross section, and 80mm long are cooled rapidly at temperatures above 700° in a current of air at room temperature passed at a rate of 5-10 m/second, their mechanical strength is increased by 40-50%.

2. The increase of mechanical strength is caused by the development of stresses in the surface layers; this effect may be described as tempering and can be used for improving the service characteristics of ceramic objects [1].

3. The electrical strength of porcelain is not diminished by tempering.

LITERATURE CITED

[1] A. I. Avgustinik and V. M. Loginov, J. Appl. Chem. 31, No. 8, 1150 (1958).*

[2] W. Steger, Ber. Deut. Keram. Ges. 15, 3 (1934).

[3] B. Long, La Ceramique (April 1934).

[4] A. E. Fradkin and M. S. Kuznetsova, Trans. State Electr. Ceramic Inst. 1 (1956).

[5] L. Mattyasovszky-Zsolnay, J. Am.Ceram.Soc.40, 9 (1957).

[6] H. Marzahl, Electr. techn. Z.—A. 13, 1 (1954).

[7] U. S. Patent 2670573; Swiss Patent 297325.

Received October 10, 1958.

*Original Russian pagination. See C. B. translation.

POSSIBLE USE OF THE PGF-2 GAS ANALYSIS APPARATUS AS A UNIVERSAL INSTRUMENT FOR RAPID ESTIMATION OF THE EXPLOSION HAZARDS OF VARIOUS VAPOR–GAS–AIR MEDIA

A. N. Baratov

Central Scientific Research Institute of Fire Prevention

For safety under conditions in which inflammable gases or vapors may accumulate, it is necessary to ensure that their concentration in the air does not reach the lower explosibility limit. However, no universal apparatus is as yet available for estimation of the explosion hazards of the atmosphere in any building or space with adequate reliability and speed.

All instruments used for determination of the explosibility of gas–vapor–air media are essentially gas analysis instruments for determination of combustible gases and vapors in air. The explosion hazard is estimated by comparison of the concentrations found with literature data on the explosibility concentration limits.

The use of such instruments has the following serious disadvantages: 1) their applicability is restricted to the substances for which they are calibrated; 2) they cannot be used for direct determination of explosibility, as it is first necessary to know the lower explosibility limits for the media in question; 3) the probability of error in estimation of explosibility is fairly high because of the great discrepancies between the limits cited by different authors; 4) determinations of explosion hazards are not reliable because the actual estimation is performed some time after sampling; 5) it is virtually impossible to use such instruments with a number of substances (high-boiling liquids of complex fractional composition) both because of difficulties in calibration and because of lack of data on the explosibility limits of such substances; 6) these instruments are not of universal applicability – it is essential to know what substance is present in the air, and to select an appropriately calibrated gas-analysis apparatus.

The PGF gas-analysis apparatus is the one most commonly used for determinations of the explosibility of industrial atmospheres. The basis of the apparatus is a wheatstone bridge, two arms of which are platinum spirals, contained in the measurement and the comparison chamber respectively, and the other two arms are constant resistances. The gas to be tested is collected in the measuring chamber by means of a piston pump incorporated in the apparatus, and undergoes catalytic combustion there. This results in an increase of temperature in this chamber relative to that of the spiral in the insulated comparison chamber. This disturbs the balance of the bridge, as shown by a galvanometer in the bridge circuit. The emf in the galvanometer circuit is proportional to the concentration of the combustible component in the sample.

It must be pointed out that the operation of this instrument as practiced at present is not free from the defects listed above.

Nevertheless, the PGF gas-analysis apparatus can be used as the basis of an instrument which could be used for direct estimation of the explosibility of vapor–gas–air mixtures containing various inflammable gases, vapors, or mixtures of them.

This possibility depends on the fact that the combustion temperature of gas–vapor–air mixtures containing combustible components in concentrations corresponding to the lower explosibility limit is constant for all combustible gases and liquids. Since it is the combustion temperature of the sample in the gas-analysis apparatus

which ultimately determines its content of the combustible component, it may be assumed that the readings of the apparatus will be the same for different gases and vapors in any combustible mixture containing a combustible component in a concentration corresponding to the lower explosibility limit.

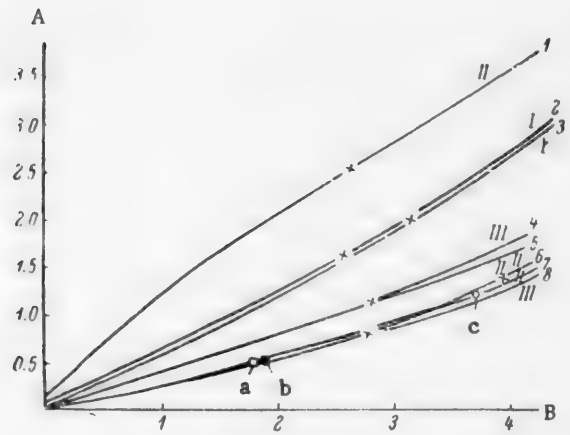

Calibration curves for PGF-2 gas-analysis apparatus : A) amount of gas(vol %), B) instrument readings; I, II, III) datum points for the curves; 1) methane, 2) ethyl alcohol, 3) hydrogen, 4) acetylene, 5) propane, 6) ethylene, 7) B-70 gasoline, 8) butadiene; a,b,c) lower limits for B-70 gasoline from different literature sources.

The constancy of the combustion temperatures of gas mixtures at the lower limit is explained as follows. The lower explosibility limit represents the minimum concentration of the combustible component in the air at which spontaneous propagation of the flame is still possible. This concentration does not exceed 5% of the volume of the mixture for most substances. According to the laws of thermal explosion, the lower limit is reached at equilibrium between the gain of heat owing to the exothermal oxidation reaction and loss of heat from the reaction zone. Since we are concerned with dilute combustible mixtures, it may be assumed that heat losses under equal conditions are determined by the conditions of heat transfer virtually through air, i.e., they are equal. In the light of the condition indicated above for thermal explosion, it may be assumed that the calorific capacity of a volume element of all such mixtures will also be the same. Therefore the maximum heat effect and accordingly the maximum combustion temperature should also be the same for all mixtures.

To confirm this, we calculated the theoretical combustion temperatures of a number of individual substances at concentrations corresponding to the lower limit in air.

Since the combustion temperatures of mixtures of the limiting composition are relatively low, dissociation of the combustion products may be disregarded in these calculations. The theoretical temperature of combustion in the presence of excess air was calculated for each substance. The following results were obtained.

Substance	Combustion temperature (°C)
Methane	1646
Ethane	1644
Propane.	1648
Hexane	1648
Ethanol	1650

Comparison of the calculated values confirms our hypothesis that the combustion temperatures of mixtures of the limiting composition are equal (the greatest difference between the theoretical combustion temperatures of the substances listed in the above table is 0.24-0.4%).

Additional evidence in favor of our hypothesis that the readings of the PGF gas-analysis apparatus are constant and that therefore the apparatus is of universal applicability for determination of the explosibility of various gas–vapor–air media in tests of combustible gas mixtures of the limiting composition is provided by calibration curves for the PGF apparatus, plotted by the designers of the apparatus for different vapors and gases, and shown in the diagram. The points marked on the curves correspond to 50% values of the lower limiting concentrations of the vapors and gases by volume.

It is evident from the graph that, despite the fact that the calibration curves were plotted for different

standard temperatures of the heated spirals, these points correspond to roughly the same scale reading for nearly all the substances. The exceptions are points for B-70 gasoline and ethylene, which are at appreciable distances from the mean value along the abscissa axis. This is probably because, first, a low value of the lower limit was taken for B-70 gasoline and, second, because the calibration curves were not determined under identical test conditions .

It follows from the foregoing that if on the scale of the galvanometer in the bridge a mark is made corresponding to the reading obtained for a combustible mixture containing any combustible component at a concentration of 50% of the lower concentration limit, when the apparatus is introduced into the test atmosphere and switched on it will immediately indicate whether the hazardous concentration is reached.

The design and construction of the apparatus are considerably simplified, as several datum points are no longer required, the apparatus becomes universally applicable (i.e., suitable for any combustible component), and it is no longer necessary to calibrate the apparatus for different substances. The accuracy is also increased considerably, as it is not necessary to find lower explosibility limits, and errors in selection of reference data on explosibility limits are thereby eliminated.

SUMMARY

By analysis of the critical conditions of thermal explosion and by direct calculation of theoretical combustion temperatures it is shown that the combustion temperatures of different gas–vapor–air mixtures containing the lower limiting concentrations of combustible components are equal. This relationship forms the basis of the recommended use of the PGF-2 gas-analysis apparatus as a universal instrument for determination of the explosibility of various vapor–gas–air mixtures for safe work with explosive gases.

Received March 3, 1958.

REDUCTION OF NICKEL AND COBALT FERRITES BY HYDROGEN

M. G. Zhuravleva, V. N. Bogoslovskii, and G. I. Chufarov

The Sverdlovsk Institute of Metallurgy, Ural Branch of the Academy of Sciences, USSR

Ferrites are complex oxides of the general formula MFe_2O_4, where M is a bivalent metal ion. They may be formed in a number of metallurgical processes by interaction of individual oxides. In some cases their formation is desirable, as in the refining of copper, because copper is thereby freed from nickel, but in others they have an adverse effect, such as in zinc production. Attention should also be drawn to the technological uses of ferrites as materials with good magnetic properties together with high resistivity.

Tumarev [1] studied reduction of mixtures of oxides and chemical compounds by carbon monoxide, and Mishin and Kabanova [2] investigated the reduction of cobalt ferrite by carbon monoxide. The phase composition of the solid products of reduction of cobalt ferrite by hydrogen was studied by Simanov, Klyachko-Gurvich, and Gerasimov [3].

According to published data [4,5], ferrite formation in mixtures of $NiO + Fe_2O_3$ and $CoO + Fe_2O_3$ commences at 700-800°. The reaction is rapid at 1100° and is largely complete in 3 hours. However, for final completion of the process at this temperature a time of 25-30 hours is required.

We prepared ferrites of nickel and cobalt by the action of heat on equimolecular mixtures of $NiO + Fe_2O_3$ and $CoO + Fe_2O_3$ in air at 1200° for 3 and 30 hours.

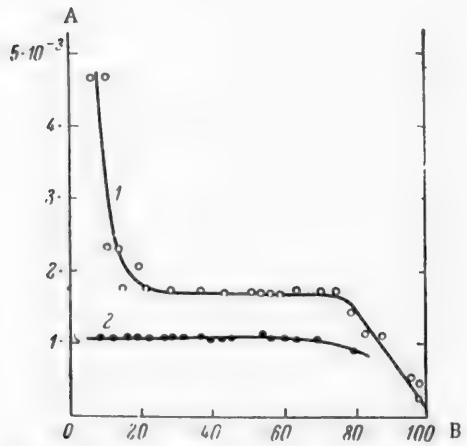

Fig. 1. Reduction of nickel ferrite by hydrogen at 400°: A) reduction rate $K \cdot 10^{-3}$ (grams O_2 minute), B) degree of reduction (%); 1) ferrite after 3-hour sintering, 2) ferrite after 30-hour sintering.

It was found by x-ray structural analysis of the ferrites that when oxide mixtures are heated for three hours conversion to ferrite is incomplete and the samples contain certain amounts of unchanged oxides. The ferrites formed after 30-hour sintering of the mixtures are single phases and have a spinel structure with lattice parameters of 8.376 ± 0.003A for cobalt ferrite and 8.333 + 0.005A for nickel ferrite.

The ferrites were reduced by hydrogen at 200 mm pressure in the 300-500° temperature range in a closed apparatus in which hydrogen was circulated over a heated ferrite sample. The water vapor formed was frozen in a trap cooled in liquid nitrogen. The rate of reaction was determined from the fall of pressure. Hydrogen was added into the system at intervals and its pressure varied within narrow limits.

The curves in Fig. 1 and 2 represent the rates of reduction of nickel and cobalt ferrites at the same temperature. It is clear that the two ferrites are reduced at approximately the same rate.

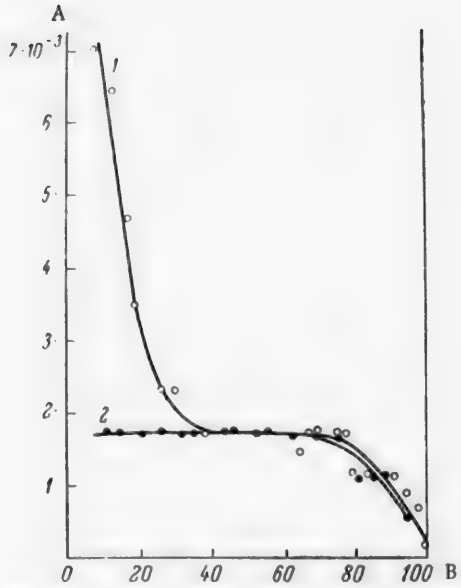

Fig. 2. Reduction of cobalt ferrite by hydrogen at 400°: A) reduction rate $K \cdot 10^{-3}$ (grams O_2/minute), B) degree of reduction (%); 1) ferrite after 3-hour sintering, 2) ferrite after 30-hour sintering.

Fig.3. Equilibrium composition of the gas in the reduction of nickel and cobalt ferrites by hydrogen at 400°: A) H_2O content (%), B) degree of reduction (%); 1) cobalt ferrite, 2) nickel ferrite.

In the case of ferrites formed by 3-hour sintering the reduction rate is high at the initial stage, and it then drops sharply at 20-25% reduction in the case of nickel ferrite and at 30-40% reduction in the case of cobalt ferrite. The initial drop is due to the presence of unchanged oxides, and is not found on curves for ferrites formed by 30-hour sintering.

The content of water vapor in the equilibrium gas phase during reduction of cobalt and nickel ferrites is independent of the extent of reduction, and is 7% H_2O for nickel ferrite and 9% H_2O for cobalt ferrite (Fig.3).

The solid reaction products were studied by means of x-ray structural analysis at different stages of reduction.

It was found that the spinel phase is present right through the reduction process, i.e., the ferrite is reduced as a single chemical compound without previous decomposition into oxides. Determinations of the lattice parameter of the spinel phase showed it to be constant within the limits of experimental error at different degrees of reduction. Constancy of the lattice parameter is consistent with the fact that the composition of the equilibrium gas phase does not change during the reduction. The metallic phase formed by reduction consists of a solid solution of nickel in iron, containing about 30 atomic % of nickel; this concentration corresponds to the nickel–iron ratio in the ferrite.

These experiments on reduction kinetics and x-ray investigations of the products formed in the reduction of nickel and cobalt ferrites by hydrogen at 400° showed that no appreciable diffusional processes take place within the crystal lattice. The lattice parameters of the spinel and metallic phases do not alter during reduction. The reduction is effected by migration of ions over the external surfaces of the crystals and over the interphase boundary; such migration proceeds quite freely at such temperatures, and the reduction rate is therefore considerable. At higher temperatures the extent of volume diffusion increases and its role in the arrangement of the crystal lattice becomes more significant [3].

LITERATURE CITED

[1] A. S. Tumarev, Problems of Metallurgy [in Russian] (Izd. AN SSSR, 1953) p.33.

[2] V. D. Mishin and L. M. Kabanova, Trans. Ural Polytech. Inst. 58, 128 (1957).

[3] Yu. P. Simanov, L. L. Klyachko-Gurvich, and Ya. I. Gerasimov, Bull MGU 10, 9 (1950) .

[4] T. I. Bulgakova, Ya. I. Gerasimov, Yu. P. Simanov, and L. L. Klyachko-Gurvich, J. Gen. Chem. 18, 154 (1948).

[5] Ya. I. Gerasimov, T. I. Bulgakova, and Yu. P. Simanov, J. Gen. Chem. 19, 219 (1949).*

Received May 9, 1958

*Original Russian pagination. See C. B. translation.

FILMS OF SEMICONDUCTING TIN DIOXIDE WITH INCREASED CONDUCTIVITY

A. Ya. Kuznetsov, A. V. Kruglova, and B. P. Kryzhanovskii

In recent years transparent semiconducting films of tin dioxide on glass have been widely used in science and technology. These films are used in the production of nondimming and nonicing sight glasses in aviation and land and sea transport, as transparent electrodes in various photoelectric and electroluminescent devices, as highly economical heating elements of small dimensions, and for many other purposes. There are essentially two methods for application of these semiconducting films on glass: by pulverization and by pyrolysis of tin chlorides [1-3]. In the first method, a glass surface heated to 600-650° is treated with alcoholic stannic chloride solution, when the process of film formation can be schematically represented by the following equations:

$$SnCl_4 + 2H_2O \rightarrow SnO_2 + 4HCl,$$

$$SnO_2 + \text{reducing agent (alcohol)} \rightarrow Sn,\ SnO.$$

In the second method, glass heated to 400° is treated with vapor of the hydrolysis products of stannous chloride. The main reactions of film formation are

$$SnCl_2 + H_2O \rightarrow SnO + 2HCl,$$

$$2SnO + O_2 \rightarrow 2SnO_2,$$

$$2SnO \rightarrow Sn + SnO_2.$$

In each case a film of semiconducting tin dioxide is formed, not of the exact stoichiometric composition because of the presence of Sn and SnO [2,4,5].

These methods give transparent conducting films, the specific surface resistance of which reaches hundreds of ohms, on the glass surface. Films of lower resistance, obtained when the thickness is increased, exhibit considerable light scattering and are essentially semitransparent coatings.

There is a great technological demand for transparent coatings the specific surface resistance of which does not exceed some tens of ohms. It was therefore necessary to find ways of increasing sharply the surface conductivity of SnO_2 films with retention of a high degree of transparency. Two solutions of this problem were studied: variation of the stoichiometric composition of the tin oxide by the presence of excess metal, and introduction of extraneous impurities into the SnO_2 lattice.

Variation of the stoichiometric ratio by thermal disproportionation of the tin monoxide present in the film to the metal and dioxide [4] gave only slight increases of conductivity with retention of transparency. An effective increase of film conductivity was achieved by introduction of extraneous impurities. It was found experimentally that the conductivity of tin dioxide films is increased sharply both by introduction of quinquevalent metal atoms capable of replacing tin atoms in the SnO_2 lattice (Sb), and by introduction of halogens (F) replacing oxygen atoms. However, introduction of metal atoms appreciably lowers the film transparency while increasing conductivity. Thus, with addition of antimony a highly conducting film thermally stable up to 800° was obtained, but its transparency was considerably lower [5].

Films of SnO_2 containing fluorine atoms have high transparency and conductivity. Fluorine was introduced into the films by addition of 3-10% NH_4F by weight to the $SnCl_2$ powder in treatment of glass by the vaporized pyrolysis products of stannous chloride (in the pyrolysis method), or by addition of 0.5% by weight of NH_4F to the alcoholic solution of stannic chloride in the pulverization method. Unfortunately, the amount of NH_4F in solution cannot be increased because of the low solubility of ammonium fluoride in alcohol, and therefore it is not possible to increase film conductivity very much in this manner.

Surface Resistivity and Light Transmission of Glasses Coated with SnO_2 Films with Added Ammonium Fluoride and Made from Pure $SnCl_2$

Glass type	Without added NH_4F				With 5% NH_4F added (glass not etched)		Amount of $SnCl_2$ evaporated (g)
	glass not etched		glass etched				
	ρ_s(ohms)	light transmission (%)	ρ_s (ohms)	light transmission (%)	ρ_s(ohms)	light transmission (%)	
Sheet	400	56	376	85	100	87	8
	270	52	250	83	50	82	10
	85	40	70	75	12	77	20
Pyrex	500	59	470	86	95	89	8
	200	50	200	82	45	78	12
	110	47	100	80	18	77	22

The greater increase in the conductivity of tin oxide films was obtained by the pyrolysis method (see table). In this case, addition of fluorine raised the conductivity of the film to $\kappa \simeq 3 \cdot 10^3$ ohm^{-1}cm^{-1}; transparent coatings 0.25 thick with specific surface conductance not exceeding 10 ohms were obtained. The increase of conductivity was accompanied by an increase of transparency. It seems likely that the fluorine atoms partially oxidize the metallic tin atoms present in the film to SnF_2 and SnF_4. This naturally involves an increase of transparency. Since tin dioxide is an electronic semiconductor, the increase of conductivity on introduction of fluorine into the film may be explained as follows. A bivalent oxygen atom in the SnO_2 lattice is replaced by a univalent fluorine atom, which can bind only one valence electron of tin. The liberated second electron, previously bound by oxygen, can, under the influence of thermal energy, pass into the conductivity zone and increase the total conductivity.

Thus, the total conductivity of a semiconducting tin dioxide film is made up of two components

$$\varkappa_{total} = \varkappa_s + \varkappa_i ,$$

where κ_s is the conductivity caused by the presence of excess metal over the stoichiometric ratio for SnO_2; κ_i is the conductivity due to added fluorine atoms.

The lengthy preliminary treatment of glass by acid solutions for formation of silica films [2] can be avoided by the addition of ammonium fluoride to the original stannous chloride in pyrolysis (see table). The coating time and the amount of stannous chloride volatilized can also be reduced sharply by addition of ammonium fluoride.

SUMMARY

If ammonium fluoride is added to stannous chloride in the pyrolysis method, the conductivity of the semiconducting tin dioxide films is greatly raised, the light transmission of the coatings is improved, the coating time and consumption of stannous chloride are appreciably reduced, and lengthy acid pretreatment of glasses is avoided.

LITERATURE CITED

[1] A.Ya. Kuznetsov, A.V. Kruglova, and B. P. Kryzhanovskii, Industrial Lab. 8 (1956).

[2] K. S. Evstrop'ev, A. Ya. Kuznetsov, I. G. Mel'nikova, and B. P. Kryzhanovskii, Optico-Mechanical Ind. 1 (1957).

[3] E. Umblia Glass 32, 12, 598 (1955).

[4] B. P. Kryzhanovskii, A. Ya. Kuznetsov, and A. V. Kruglova, Optico-Mechanical Ind. 2 (1957).

[5] B. P. Kryzhanovskii and A. Ya. Kuzentsov, Optico-Mechanical Ind. 6 (1957).

Received July 10, 1958.

TEXTILE -BASED MEMBRANE SEMIULTRAFILTERS

S. G. Mokrushin and V. I. Borisikhina

The S. M. Kirov Polytechnic Institute of the Urals

It was shown in the preceding paper [1] that collodion ultrafilters of different pore sizes can be made on a paper base.

The purpose of the present work was to prepare textile-based semiultrafilters of definite predetermined pore sizes.

Collodion solutions with additives developed by us were used for impregnation of the textile fabrics. Collodion was applied to the base (textile fabric) in a vacuum apparatus by the Bechhold method [2]. The pore radii in the prepared semiultrafilters were determined by Manegold's method [3]. The effective filtration area in the Zsigmondy funnel was 10.87 cm^2. The filtration vacuum was 15 mm. The experimental temperature was 14-15°.

Data on semiultrafilters made with different textile (cotton) supports [4] are presented in the table.

Effect of the Type of Fabric on Properties of Semiultrafilters

Filter base	Code of fabric	Thickness of semi-ultrafilter (mm)	Filtration time of 100 ml H_2O(sec)	Average diameter of filter pores (mμ)	Notes
"Byaz' " (sheeting)	33	0.026	65	788	Surface of semiultrafilter uneven, thickenings at thread crossings
Calico	62	0.025	67	780	Close, hard, occasional surface irregularities
Cambric	100	0.023	69	706	The same
Zephyr	370	0.023	82	650	Dense, with smooth and even surface
"Rogozhka" (coarse canvas)	400	0.029	67	800	Thick, coarse, surface streaked and uneven
Bandage cloth	422	0.022	69	716	Difficulties in treatment
Batiste	429	0.021	70	680	Dense, with smooth and even surface

The fabrics were impregnated with a 6% solution of nitrocellulose motion-picture film containing 1% of malonic ester and 0.5% of glycerol.

In addition to the fabrics listed in the table, numerous others were tested, such as natural silk pongee, linen, and various staple-fiber, viscose, glass, and others.

The experiments showed that the best semiultrafilters are obtained with batiste, zephyr, and fine calico. Raised, diagonal, and hackled fabrics, and fabrics with knotted threads are unsuitable, because the thread irregularities give rise to faults on the surface of the finished semiultrafilters Before use the fabric must be washed

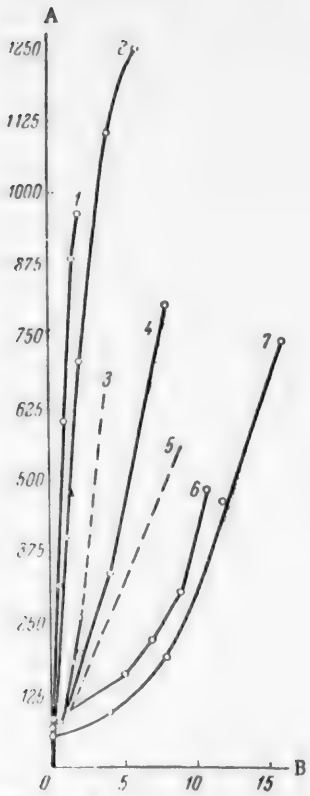

Effects of additives on pore size in semiultrafilters: A) average pore size (mμ), B) content of additive (%); additives: 1) malonic ester, 2) mixture (1:1) of acetoacetic and malonic esters, 3) acetoacetic esters, 4) mixture (1:1) of acetoacetic ester and ethyl acetate, 5) ethyl acetate, 6) glycerol, 7)acetone.

in dilute ammonia solution, rinsed in water, and then boiled in dilute hydrochloric acid solution. Chloride ions were washed out in hot distilled water, and finally the moist fabrics were ironed with a hot iron.

Circles (filters) of suitable diameter were cut from the prepared fabrics; small curved metal clamps were attached to their lower edges to facilitate impregnation of the fabrics with the collodion solution and the subsequent drying and gelatination.

It was found that semiultrafilters based on thin dense fabrics are satisfactorily reproducible.

The pore size may be varied by addition of appropriate amounts of esters to the original collodion solution.

The diagram shows the effects of different additives on pore size of ultrafilters made on a batiste support.

In this case the original solution was a 4% solution of nitrocellulose motion-picture film in alcohol–ether mixture containing 0.5% of glycerol.

For characterization of textile-based semiultrafilters it was important to determine the changes produced in pore size and state of the filter surface by the action of strong acids, bases, and concentrated salt solutions.

According to Yander and Zakovskii [5], such changes can be easily investigated by repeated determinations of the "water number," which is the time required for filtration of 100 ml of distilled water. The distilled water and the reagent solutions used in the tests were previously passed through an ultrafilter with 60 mμ pores to remove any suspended matter.

For determinations of the "water number", acids (1-2 N sulfuric, nitric, hydrochloric), concentrated salt solutions (ferric chloride, copper sulfate, and others), and alkali solutions were passed repeatedly through the semiultrafilters. The "water number" remained virtually constant in each experiment.

SUMMARY

A method for preparation of semiultrafilters of various predetermined pore sizes on textile supports has been developed; it was found that semiultrafilters of especially high quality are obtained on a batiste support.

LITERATURE CITED

[1] S. G. Mokrushin and V. I. Borisikhina, J. Appl. Chem. 25, No. 11, 1182 (1952).*

[2] H. Bechhold, Z.phys. Chem. 60, 257 (1907).

[3] N. Bjerrum and E. Manegold, Koll. Z. 43, 5 (1927).

[4] Ministry of Trade USSR, Price List No. 30 [in Russian] (State Trade Press, Moscow, 1957).

[5] G. Yander and I. Zakovskii, Membrane, Cellulose, and Ultrafine Filters [in Russian] (ONTI, Chem Theoret. Press, Leningrad, 1937).

Received August 18, 1958

*Original Russian pagination. See C. B. translation.

CORROSION RESISTANCE OF CERTAIN ELECTRODEPOSITED ALLOYS UNDER NEAR-TROPICAL CONDITIONS

N. P. Fedot'ev, P. M. Vyacheslavov, E. G. Kruglova, and S. Ya. Grilikhes

During recent years, interest has greatly increased in the electrolytic method for production of coatings of binary and ternary alloys. Some of these, such as tin–zinc and tin–cadmium alloys, are used abroad as protective coatings in tropical climates. It is known that under tropical conditions a zinc coating rapidly becomes covered with a loose deposit of basic salts. Tin coatings withstand atmospheric attack, but are somewhat porous at thicknesses up to 25μ, which weakens their protective action. If tin–zinc alloys are used, the advantages of both metals can be utilized—the porosity of tin coatings is diminished and their rate of corrosion reduced [1].

Tin–zinc alloys have been studied in great detail by a number of workers [1-3]. Tin–cadmium alloys gave good results in tests in a salt spray chamber. Tests of specimens, coated with tin–copper electrodeposited alloy containing 45-50% tin, for 4000 hours in fresh water showed that coatings 10μ thick effectively protect steel against corrosion and are unchanged in external appearance [2]. If the tin content is less than 30% such coatings protect steel, but themselves darken appreciably. A technological process for deposition of such alloys has been worked out in adequate detail by Fedot'ev et al. [4] and Lainer [5]. The electrodeposition conditions and corrosion resistance of zinc–cadmium alloys was studied by Kudryavtsev et al., who showed that an alloy containing 83% cadmium and 17% zinc has the highest resistance to corrosion [6].

The information available on ternary electrodeposited alloys is very incomplete. There are reports of their use as protective and decorative coatings, but no data on their corrosion resistance under severe conditions are available.

The purpose of the present investigation was to determine the relative stability to corrosion, under near-tropical conditions, of the following electrodeposited alloys: tin–zinc, tin–cadmium, tin–copper, zinc–cadmium, copper–tin–zinc, and copper–tin–cadmium.

Conditions of alloy deposition. Preliminary experiments on deposition of tin–zinc alloys showed that alloys containing 70-80% tin give the best results with regard to corrosion resistance at high humidities (98-100%) and large fluctuations of temperature (25-35°). The following conditions were established for the deposition of these alloys:

Alloy composition (%)			Electrolyte composition (g/liter)		
Tin	Zinc	Tin	Zinc	KCN_{free}	$NaOH_{free}$
80	20	32–36	1.5–2.0	20–22	10–11
70	30	32–36	2.5–3.0	20–22	10–11

The zinc and zinc–tin coatings were passivated in order to increase their corrosion resistance. Zinc coatings were treated for 5-10 seconds in a solution containing 150 g of ammonium dichromate and 10 g of sulfuric acid per liter. The following two solutions were used for passivation of the alloys: 1) chromic anhydride 20 g/liter, sulfuric acid 0.25 g/liter; solution temperature 60-70°, treatment time 15-30 seconds; 2) sodium

dichromate 3 g/liter, caustic soda 10 g/liter, OP-10 (polyethylene glycol ether) 5 g/liter; solution temperature 90-95°, treatment time 5-10 seconds.

Solution 2 is recommended for passivation of tin coatings [7]. The auxiliary OP-10 was added to improve wetting of the metal surface. When treated in the acid solution the specimens darkened somewhat. The surface became lighter in the alkaline solution. Ammonium chromate solution was not used for passivation of the alloys, as it did not show any appreciable advantages in preliminary corrosion tests.

Preliminary corrosion tests on tin–cadmium electrodeposited coatings showed that coatings containing 40-60% tin have the highest resistance. The following electrolyte compositions were established for deposition of alloys of these compositions:

Tin content of coating (%)	Electrolyte composition (%)					
	$Sn(BF_4)_2$	$Cd(BF_4)_2$	NH_4BF_4	HBF_4	H_3BO_3	Glue
40	24	240–250	50–60	50–70	18–20	0.5–1.0
60	30	240–250	50–60	50–70	18–20	0.5–1.0

The cathodic current density was 1.5-2.0 amp/dm^2, electrolyte temperature 18-25°.

The coatings were passivated by means of an acid solution containing 150 g of ammonium dichromate and 10 g of sulfuric acid per liter, and the alkaline solution 2 detailed above.

Cadmium–zinc alloy was deposited from an electrolyte of the following composition: cadmium (calculated as metal) 27 g/liter, zinc (calculated as metal) 6 g/liter, potassium cyanide (free) 20 g/liter; cathodic current density 1.5 amp/dm^2, anodic current density 0.5 amp/dm^2, electrolyte temperature 18-25°. The anodes were zinc and cadmium plates. The area ratio of the zinc and cadmium anodes was 1:4.

Coatings containing 18-20% zinc were formed under these conditions. They were passivated by means of a solution containing 150 g of ammonium dichromate and 10 g of sulfuric acid per liter.

Coatings containing 40, 60, and 80% tin were chosen for corrosion tests on tin–copper alloys. They were deposited from electrolytes of the following compositions:

Tin content of coating (%)	Electrolyte composition (g/liter)			
	Tin	Copper	KCN_{free}	$NaOH_{free}$
40	45	10	18	13
60	45	7–8	20	9–10
80	45	4–5	20	8–9

The cathodic current density was 1.5 amp/dm^2, the anodic current density was 3-4 amp/dm^2, electrolyte temperature 18-25°. The anode material was an alloy of 50% tin and 50% copper in the first two electrolytes, and pure tin in the third. The specimens coated with the alloy containing 80% tin were passivated in solution 2.

Copper–tin zinc and copper–tin–cadmium alloys were deposited from the electrolytes shown on the following page.

Corrosion tests were carried out with specimens of carbon steel (St3) coated with the above-named alloys in layers 20μ thick. The tests were performed in a TVK-2 heat and humidity unit under near-tropical conditions. For 9 hours the temperature in the chamber was maintained at 35 ± 2°, and the relative humidity at 98%. During the subsequent 15 hours the temperature was lowered to 22-25°, and dew was deposited. This cycle was repeated every 24 hours. The tests were continued for 84 days.

Composition of coating (%)			Electrolyte composition (g/liter)					
Tin	Copper	Zinc	Tin	Copper	Zinc	KCN_{free}	$NaOH_{free}$	Cathodic current density (amp/dm^2)
18.1	78.2	3.7	30	20	2	25	8	5
14.2	78.7	7.1	30	20	2	25	8	10
26.6	66.2	7.2	30	20	2	25	8	2
52.2	38.1	9.7	30	10	5	21.6	8	5
Tin	Copper	Cadmium	Tin	Copper	Cadmium	KCN_{free}	$NaOH_{free}$	Cathodic current density (amp/dm^2)
35.5	53.7	10.8	30	20	1	24	8	2
27.9	62.7	9.4	30	20	1	24	8	5
35.6	37.6	26.8	30	10	1	25	7	5

The corrosion resistance of the coatings was estimated by visual inspection. Changes in the color of the coating and appearance of pits and corrosion sites were noted The visual inspection was accompanied by determination of weight changes of the specimens. The following results were found in the tests. A uniform dark gray deposit of corrosion products, which could not be rubbed off, formed on all specimens coated with tin–zinc alloy. The weight increased in all cases, which also shows the presence of dense, nonflaking corrosion products. The behavior of zinc coatings was considerably worse – loose, easily crumbled white deposits were formed on them.

Of the Sn–Zn alloys tested, the coating containing 80% tin and 20% zinc and passivated in the acid solution had the highest resistance to corrosion.

The following conclusions may be drawn from the results of tests on tin–cadmium coatings. The darkening of the surface increases with decrease of the tin content of the coating. Increase of the tin content lowers the protective power of the coating and favors corrosion of the basis metal. If an acid solution is used for passivation, the specimens darken somewhat, but the surface shows much less change in the tests than that of specimens passivated in the alkaline solution. Alloys containing 40-60% tin and passivated in the acid solution had the best resistance to corrosion.

A nonpassivated cadmium coating did not withstand the test; over 50% of its surface was covered with dark corrosion patches. Passivated cadmium had a better decorative appearance after the tests than tin–cadmium alloy coatings; only isolated small points were seen on the surface. There was considerable corrosion of the basis metal in specimens coated with tin. Copper–tin alloys containing from 40 to 75% tin were almost unattacked in the tests, but there was considerable corrosion of the basis metal. Similarly, ternary alloy coatings were almost free of corrosion, but gave poor protection to the basis metal.

The zinc–cadmium alloy containing 83% cadmium had the best corrosion resistance of all the alloys tested.

SUMMARY

The relative corrosion resistance and protective power of electrolytic binary and ternary alloy coatings, and of zinc and cadmium coatings were determined under conditions simulating a tropical climate (in a heat and humidity chamber).

The tested coatings can be arranged in order of decreasing corrosion resistance as follows: passivated zinc–cadmium alloy (83% Cd), passivated cadmium, passivated tin–zinc alloy (20% Zn), passivated tin-cadmium alloy (60-40% Cd), copper–tin alloy (40-75% Sn), copper (38-78%)–tin (18-52%)–zinc (3-10%) alloy, copper (37-53%)–tin (27-35%)–cadmium (9-26%) alloy, nonpassivated zinc and cadmium.

LITERATURE CITED

[1] J. W. Cuthbertson, Metalloberflache 9 (1955).

[2] P. M. Vyacheslavov, Alloy Electrodeposited Coatings [in Russian] (Mashgiz, 1955).

[3] A Whittaker, Machinery 84, 639 (1954).

[4] N. P. Fedot'ev, P M. Vyacheslavov, and E. I Orlova, J Appl Chem. 23, No. 4, 380 (1950)*

[5] V. I. Lainer and N. T. Kudryavtsev, Fundamentals of Electroplating [in Russian] (Metallurgy Press, 1957).

[6] N. T. Kudryavtsev and E. F. Pereturina, J. Appl. Chem. 26, No. 2, 155 (1953).*

[7] H. Britton, Metaux (Corrosion Inds.) 30, 134 (1955).

Received September 19, 1958.

*Original Russian pagination. See C. B. translation.

CORROSION OF METALS IN THIONYL CHLORIDE

V. A. Titov, Yu. A. Babkin, and I. M. Balandin

The Moscow Steel Institute

The bivalent SO radical is known as thionyl. Thionyl chloride is the acid chloride of sulfurous acid, $SOCl_2$, and is used in the production of dyes, color film, pharmaceutical products, etc.

Thionyl chloride reacts with atmospheric moisture to form SO_2 and HCl (very corrosive gases). The corrosive action of thionyl chloride has not been studied at all as yet, and it was therefore of great interest to study the corrosion resistance of a number of various metallic materials to it in order to determine whether they can be used for the production of process equipment.

The experiments were performed both under laboratory conditions and directly in the works. The materials chosen for the tests were the commonest types of stainless steel, a nickel-based alloy of the Hastelloy type, and a number of pure metals including titanium.

Corrosion Rates of Various Metals in Pure and Crude Thionyl Chloride

Metal	Corrosion rate (mm/year)	
	in thionyl chloride	in crude material
ÉI-461	0.01	0.0072
1Kh18N9T	0.02	0.0135
Kh17	0.08	0.0146
St 3	0.17	1.16
Titanium (VT-1D)	6.8	39.2
Copper (M-3)	11.5	14.8

Three specimens of each metal, 50 x 20 x 2 mm in size, were cut from a sheet, cleaned with emery paper, degreased in acetone, and used in the tests.

The laboratory experiments were performed with pure thionyl chloride in jars with ground-glass stoppers. The works trials were carried out with crude thionyl chloride of the composition: $SOCl_2$ 80%, dissolved gases 2.7%, chlorides 17.3%. Three specimens of the same metal were placed in a perforated glass cylindrical capsule divided into three sections by glass partitions. The capsules containing the specimens were placed in a perforated lead pipe installed in a tank with circulating crude thionyl chloride.

The duration of the tests was the same, 456 hours, in the laboratory and under works conditions. In the first case the temperature of the medium was kept at 20 ± 0.5°, and in the second it varied from 40 to 45°.

The corrosion kinetics of different metals in pure thionyl chloride was studied. The test results are presented in the table and plotted in Fig. 1 and 2.

The results of the experiments show that copper and titanium are not resistant to pure thionyl chloride. Copper (Curve 1, Fig. 1) was attacked rapidly, as protective films were not formed on the copper specimens.

Titanium is more resistant than copper to thionyl chloride. Its corrosion rate fell somewhat with time (Curve 2, Fig. 1), because of the formation of films consisting of corrosion products on the surface of the titanium specimens. It was found that the rate of corrosion of copper in thionyl chloride was 11.5 mm/year, and of titanium, 6.8 mm/year.

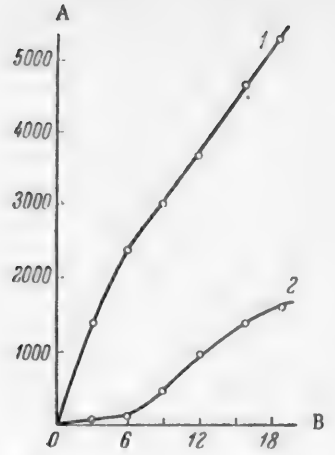

Fig. 1. Kinetics of the corrosion of copper (1) and titanium (2) in pure thionyl chloride: A) weight loss (g/m^2), B) duration of test (days).

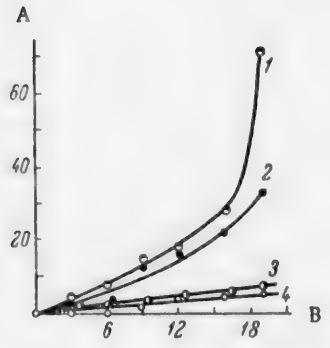

Fig. 2. Kinetics of the corrosion of St 3 (1), Kh17 (2), 1K18N9T (3), and EI-461 (4) steels in pure thionyl chloride: A) weight loss (g/m^2), B) duration of test (days).

The corrosion of ÉI-461 alloy (Line 4, Fig. 2) and 1Kh18N9T steel (Line 3, Fig. 2) was slight throughout the experiments. The corrosion rates were 0.01 and 0.02 mm/year respectively.

Curves 1 and 2 in the same diagram represent the corrosion kinetics of St 3 steel and Kh17 stainless steel respectively. The course of Curve 1 indicates an appreciable acceleration of corrosion with time. The corrosion rate of St 3 steel was 0.17 mm/year. The chrome steel corroded at a lower rate than St 3 steel, but at an appreciably higher rate than 1Kh18N9T chrome – nickel steel.

Thus, the corrosion resistance of ÉI-461 alloy is 17 times that of St 3, and the resistance of 1Kh18N9T steel is 8.5 times that of St 3. On the other hand, under these test conditions St was 40 times as resistant as titanium and about 70 times as resistant as copper.

The results of tests of the same metals in crude thionyl chloride are given in the table. It is seen that the corrosion rates of titanium and copper are respectively 33 and 12 times the corrosion rate of St 3. The lowest corrosion rate in crude thionyl chloride was again found for ÉI-461 alloy (0.0072 mm/year). Somewhat higher rates (0.0135 to 0.0146 mm/year) were found for the stainless steels.

Thus it was found that under works conditions the corrosion resistance of ÉI-461 alloy was more than 160 times that of St 3, while stainless steels were about 80 times as resistant as St 3.

On the basis of these results the tested metals can be divided into three groups in accordance with their corrosion resistance to thionyl chloride. The first group includes resistant materials: ÉI-461 alloy and stainless steels, the second includes St 3, and the third contains the nonresistant materials copper and titanium.

The high corrosion rates of titanium and copper indicate that these metals did not become passive in thionyl chloride, and were therefore attacked fairly rapidly; under works conditions their corrosion was greater because of the higher temperature and motion of the medium. Conversely, under these conditions the readily-passivated stainless steels showed smaller weight losses than in laboratory tests. Evidently the continuous renewal of the solution resulted in formation of more effective passive films, which gave better protection to the metal against corrosion, despite the higher temperature of the medium.

SUMMARY

1. ÉI-461 alloy proved to be resistant to crude and pure thionyl chloride; its rate of corrosion did not exceed 0.01 mm/year. Because of the cost of this alloy its use is justified only for particularly important small components.

2. The tested grades of stainless steel had fairly high corrosion resistance to thionyl chloride. 1Kh18N9T steel is recommended for construction of works equipment; it has good corrosion resistance, high plasticity and impact viscosity, and good weldability.

3. ST 3 steel, and especially copper and titanium, are unsuitable construction materials for equipment used in the production of thionyl chloride.

Received May 30, 1958.

INFLUENCE OF THE STRUCTURE OF ALCOHOLS ON THE FILM FORMING PROPERTIES OF THEIR ESTERS

Z. I. Edlinskii (Z. Jedlinski)

The Polytechnic Institute, Gdansk, Poland

The polymerization and film-forming properties of fatty-acid esters of α-methylglucoside were described in the preceding communications. It was suggested that the high tendency to polymerization of these substances is caused, among other factors, by the cyclic structure and spatial configuration of α-methylglucoside. To confirm this hypothesis, a series of fatty-acid esters of various polyhydric alcohols was synthesized and their properties were compared with the properties of the corresponding α-methylglucoside esters.

Unsaturated esters of α-methylglucoside, pentaerythritol, glycerol, and mannitol were prepared and their ability to form space polymers in films was studied. The results confirmed Drinberg's views [3] on the influence of the structure of alcohols on the film-forming properties of their esters.

In accordance with the theory advanced by Carothers [4] and Drinberg [3] concerning the influence of functionality of esters on the polymerization process, the rates of drying and polymerization of esters are influenced by the number and positions of the double bonds in the original fatty acids and by the number of hydroxyl groups in the alcohol. Increase of the functionality of the monomer due to a high content of esterifiable hydroxyl groups in the alcohol increases the rate of conversion into a space polymer without influencing the increase in the aging rate of the films. The results of the present investigation show that, in addition to functionality, the the spatial structure of the monomer has a definite significance. The spatial structure of the alcohol radical in the monomer influences the rates of polymerization and drying of the unsaturated aliphatic ester. The mechanism of this process can be represented on the assumption that unsaturated acid residues can be distributed more uniformly in space in esters of cyclic alcohols than in esters of polyhydric alcohols of linear strucutre. Accordingly, the acyl groups in such polyesters, which have considerable mobility around the ester linkage at the earliest stage of polymerization or copolymerization, have greater possibility of contact and further interaction by means of the double bonds, and this leads to rapid formation of a polymer.

EXPERIMENTAL

Esters of fatty acids were made by the azeotropic esterification method [2], fatty acids of linseed or cameline oil being heated with the corresponding alcohols in xylene. The catalysts were zinc oxide or lead oxide (litharge) taken in the proportion of 0.5% by weight of the fatty acids. The esterification temperature was maintained at 175-185°, and raised to 200° during the last few hours.

The reaction was continued for about 8 hours. The acidity and the amounts of water liberated were determined during the reaction.

The reaction between pentaerythritol and fatty acids was found to be the most rapid. In the reaction with acids of cameline oil, a product with acid number 0.2 was obtained after 8 hours of heating. The esterification product of glycerol had acid number 4.0, that of α-methylglucoside, 4,4, and of mannitol, 5.8. The properties of the esters are given in Table 1.

The polyhydric alcohol esters were heated with lead–manganese drier to 180° under the same conditions and converted into varnishes. The drier had the following composition (in g): linseed oil 100, litharge 9, manganese oxide 3, white spirit 200.

TABLE 1

Properties of Esters of α-Methylglucoside, Pentaerythritol, Glycerol, and Mannitol

Esters of	Numbers			Drying time in air (hr)
	acid	saponification	hydroxyl	
α-Methylglucoside and acids of cameline oil	4.4	164.8	49.2	75
Pentaerythritol and acids of cameline oil	0.2	172.1	30.5	80
Mannitol and acids of cameline oil	5.8	182.7	51.1	144
Glycerol and acids of cameline oil	4.0	185.0	–	140

TABLE 2

Properties of Varnishes and Coatings

Binders	Drying time in air (hr)	Film hardness [5]	Strength [5]	
			flex (mm)	impact (kg·cm)
Ester of α-methylglucoside and acids of cameline oils	18	0.086	1	50
Ester of pentaerythritol and acids of cameline oil	26	0.084	1	50
Ester of mannitol and acids of cameline oil	36	–	1	–
Raw cameline oil	33	0.120	1	50
Raw linseed oil	22	0.120	1	50

The amount of drier used was calculated to give 0.4% of lead in the final varnish.

The properties of the varnishes and films are given in Table 2

DISCUSSION AND CONCLUSIONS

The experimental results confirm the theory of Carothers [4] and Drinberg [3] concerning the influence of functionality on polymerization and drying of polyesters, but this theory does not take sufficiently into account the influence of alcohol structure on chemical activity and ability to form cross-linked polymers.

It was demonstrated in the case of unsaturated esters of α-methylglucoside that the spatial configuration of the alcoholic radical in the ester has a considerable influence on the rates of conversion of the ester into a space polymer.

For the esters of different alcohols studied, the rate of drying in air diminishes in the following sequence: α-methylglucoside esters → pentaerythritol esters → glycerol esters → mannitol esters.

LITERATURE CITED

[1] Z. Jedlinski, Roczniki Chem. 30, 333 (1956).

[2] Z. Jedlinski, Przem. Chem. 12, 229 (1956).

[3] A. Ya. Drinberg, Trans. Leningrad Technol. Inst. 14, 7 (1957).

[4] W. H. Carothers, J. Am. Chem. Soc. 51, 2548 (1929).

[5] S. V. Yakubovich Testing Varnishes, Paints, and Coatings [in Russian] (1952).

Received June 12, 1958.

COMBINATION OF THE ESTER INTERCHANGE AND POLYCONDENSATION REACTIONS IN SYNTHESIS OF POLYETHYLENE TEREPHTHALATE

B. V. Petukhov and A. A. Konkin

The All-Union Scientific Research Institute of Artificial Fibers

The manufacture of "lavsan" polyester fiber commences with the production of polyethylene terephthalate.

The synthesis of polyethylene terephthalate (PETP) from the dimethyl ester of terephthalic acid (DMT) is usually effected in two stages [1]: ester interchange to convert DMT to the diglycol ester by the action of ethylene glycol.

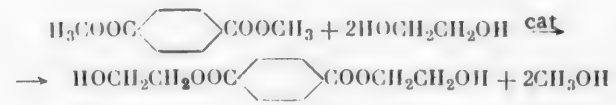

and polycondensation of the latter to PETP

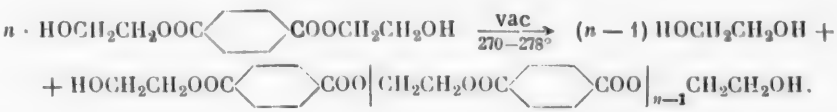

It is stated that in synthesis by the ester-interchange method it is essential that the first stage (the reaction between the methyl ester and glycol) is continued until the full calculated amount of methyl alcohol has been liberated. Otherwise the unconverted methyl ester groups restrict chain growth, remaining as end groups [2]. The addition of more than 2 moles (usually 2.5) of ethylene glycol per mole of DMT is regarded as an obligatory condition for completion of ester interchange at the first stage.

We carried out experiments in which the amount of ethylene glycol was less than 2 moles per mole of DMT, and the ester interchange at the first stage was not taken to completion owing to deficiency of ethylene glycol.

Specific Viscosity of Polyethylene Terephthalate

Glycol : DMT ratio		Specific viscosity of polymer
moles/mole	g/g	
2.5	0.8	0.28_0
2.0	0.64	0.27_5
1.8	0.57	0.26_4
1.5	0.48	0.26_7
1.3	0.41	0.25_5

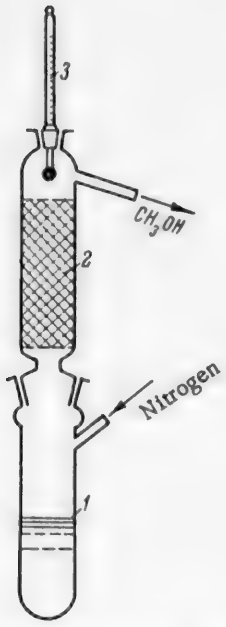

Fig. 1. Apparatus for ester interchange : 1) reaction vessel, 2) column, 3)thermometer.

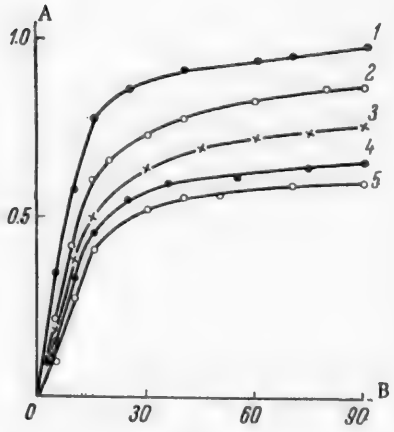

Fig. 2. Kinetics of ester interchange : A) extent of reaction, B) time (minutes); ratio of glycol to DMT (moles/mole): 1) 2.5 : 1, 2) 2 : 1, 3) 1.8 : 1, 4) 1.5 : 1, 5) 1.3 : 1.

The ester-interchange reaction was carried out in the apparatus shown in Fig.1 in presence of 0.05% (on the weight of DMT) of zinc acetate catalyst. A current of nitrogen was used to provide an inert atmosphere in the vessel. The lower part of the apparatus, into which 50 g of DMT was put in each experiment, was immersed in a bath of Wood's alloy at 200°.

Evolution of methyl alcohol began after the mixture melted. During the entire process, which lasted 1.5 hours, the bath temperature was raised steadily to 270°. The height of the column was chosen so as to give almost complete separation of the glycol—methyl alcohol mixture; the glycol flowed back into the lower reaction vessel down the glass packing, washing crystals of sublimed DMT down with it.

The extent of the ester-interchange reaction was determined as the ratio of the amount of methyl alcohol liberated to the theoretical amount calculated from the equation given above.

The polycondensation was effected in a separate vessel, fitted with a stirrer with a reliable gland, for 2.5 hours at 270 ± 1° under a residual pressure of 0.5mm. The specific viscosity of the polymer was determined in a solution in cresol, of a concentration of 0.5 g/100 ml, at 20°.

It is seen in Fig. 2 that almost the theoretical amount of methyl alcohol was liberated in the ester-interchange reaction only in the experiment in which 2.5 moles of ethylene glycol per mole of DMT was taken. At lower glycol contents in the mixture the ester interchange does not go to completion at that stage; in all the experiments the amount of methyl alcohol liberated was 85-90% of the amount which should be liberated for the amount of ethylene glycol taken. Therefore a product containing a considerable amount of unconverted methoxy groups was subjected to the subsequent polycondensation.

Polycondensation yielded blocks of polyethylene terephthalate, the specific viscosities of which are given in the table.

These results show that products of quite high molecular weight were obtained in all the experiments; this would not occur if the unconverted methoxy groups were completely retained and blocked the chain ends. Therefore it may be assumed that because of the high and increasing viscosity of the melt, and despite the high temperature, vacuum, and stirring, the ethylene glycol liberated during polycondensation is not removed immediately from the reaction zone, but takes part repeatedly in ester interchange. The amount of ethylene glycol taken initially can then be less than 2 moles per mole of DMT.

SUMMARY

1. In the synthesis of polyethylene terephthalate polymer from dimethyl terephthalate the ester interchange need not be taken to completion and the initial amount of ethylene glycol may be less than 2 moles per mole of dimethyl terephthalate.

2. The ethylene glycol liberated during the subsequent ester interchange is capable of converting the remaining methoxy groups.

LITERATURE CITED

[1] J. R. Whinfield and J. T. Dickson, British Patent 578079.

[2] R. Hill (editor), Fibers from Synthetic Polymers (IL, Moscow, 1957) p. 140 [Russian translation].

Received January 20, 1958.

PREPARATION OF LACTIC ACID ESTERS

R. M. Gel'dshtein

In chemical industry, liquid mixtures are very frequently separated by distillation of one of the components in the form of an azeotropic mixture with a solvent (azeotropic distillation). This method is especially convenient for use with mixtures the components of which do not withstand high temperatures. In such cases the solvent not only increases the volatility of the distilled substance but also dilutes the mixture and so prevents local overheating and resinification of the high-boiling component.

We used azeotropic distillation to concentrate lactic acid and to prepare its esters, which are finding increasing uses as solvents. The simplest method for preparation of these esters is ordinary esterification of lactic acid by alcohols [1-5]. A disadvantage of the method is the need to use anhydrous alcohols and concentrated (75-85%) lactic acid, which is prepared either by evaporation of the dilute acid under vacuum, or by the action of a current of air blown through it at a high temperature [4,6]. This involves considerable losses of lactic acid, both by volatilization in steam and as the result of side reactions which take place at high temperatures [6,7]. In addition, crude lactic acid has to be purified before being concentrated, and this complicates the process further and increases losses of lactic acid.

Esters have not been prepared directly from crude lactic acid. Until recently, the procedure used in the reagent industry for synthesis of lactates from the crude acid was to prepare the calcium salt, which was then treated with sulfuric acid in presence of the corresponding alcohol [8]. This method is inconvenient, as the reaction mass has to be heated to 200°, and this causes resinification of the product. We were able to simplify the esterification of lactic acid by the McDermott method [5] by the use of a water trap for continuous return of the benzene–alcohol mixture into the reaction flask. This made it possible to prepare esters from technical alcohols and technical 60-65% lactic acid which is easily prepared if water is removed in the form of an azeotrope with benzene from crude 35% acid. This method was used to prepare the ethyl (in 30% yield on lactic acid), isopropyl (in 15% yield), butyl, isobutyl, amyl, and isoamyl (in approximately 50% yield) esters of lactic acid.

EXPERIMENTAL

A 5-liter flask equipped with a stirrer and seal, and a water trap [9], was charged with 1.1 kg of lactic acid (calculated for the 100% acid) and 1.2 kg of benzene. The mass was boiled on a glycerol bath with stirring until the amount of water corresponding to the formation of 60-65% acid collected in the water trap At this stage, 1 kg of ethyl alcohol (or 1.3 kg of technical isopropyl alcohol), 300 g of benzene, and 20 g of sulfuric acid (sp.gr. 1.84) were added and the boiling was continued until water ceased to collect in the water trap. Water which remained in the lactic acid, introduced with the alcohol, and formed during esterification was distilled over at this stage. The reaction mass was neutralized at room temperature by barium hydroxide in presence of Congo Red. The precipitate was filtered off on a Buchner funnel. Benzene was evaporated from the filtrate, and the residue was distilled under vacuum.

For preparation of esters of higher alcohols (butyl, amyl, and others) it is more convenient and rapid to use the corresponding alcohol rather than benzene to concentrate the lactic acid, as azeotropic mixtures of butyl or amyl alcohol with water contain 4-5 times as much water as the azeotropic mixture of benzene and water [10]. Therefore, to concentrate the acid, 1.5 kg of alcohol is put in instead of benzene, and after removal of the water 1 kg of alcohol is put in instead of benzene, and after removal of the water 1 kg of benzene and 20 g of sulfuric acid are added and the synthesis is continued as described above.

SUMMARY

1. A convenient method is proposed for concentrating lactic acid by distillation of water in the form of an azeotrope with benzene.

2. A water trap was used in esterification of lactic acid; this simplified the synthesis and made it possible to use aqueous alcohols and unpurified 60% lactic acid.

LITERATURE CITED

[1] E. Clemensen and Arnold H. Heitman. Am. Chem.J. 42, 328 (1909).

[2] H. Wuyts and R. Bailleux, Zbl. I, 817 (1920).

[3] L. I. Simon and L. Piaux, Zbl. II, 1457 (1924).

[4] German Patent 278487; Zbl. II, 1012 (1914].

[5] Organic Syntheses, Vol. II (IL, Moscow, 1949) p. 267 [Russian translation].

[6] F. Krafft and W. A. Dyes, Ber. 28, 2589 (1895).

[7] J. Wislicenus, Ann. Chem. 164, 181, 189 (1872).

[8] German Patent 171835; Zbl. II, 470 (1906).

[9] C. Weygand, Organic Preparations (I IL, Moscow, 1951) p. 72 [Russian translation].

[10] L. Horsley, Tables of Azeotropes (IL, Moscow, 1951). p. 30 [Russian translation].

Received February 17, 1958.

ALKYLATION OF AVTOL-6 (LUBRICATING OIL) DISTILLED BY CHLORINATED PARAFFIN IN PRESENCE OF DRY GUMBRIN AND GASEOUS HYDROGEN CHLORIDE

I. F. Radzevenchuk

Recent investigations of the chemical composition of lubricating oils have confirmed that these oils contain low-cyclic hydrocarbons with long side chains [1-3]. It is becoming increasingly evident that such hydrocarbons cause the oil to have a flat viscosity–temperature curve (a high viscosity index) and low density[2].

The paraffin-chain content of aromatic hydrocarbons in oil can be increased by alkylation by means of chlorinated paraffin wax.

It was shown in earlier papers that the viscosity properties of Avtol can be improved by alkylation [4], and the extracts from selective purification can be converted into oils [5]. This reaction was carried out in presence of aluminum chloride – a very active but costly catalyst. Alkylation of benzene by alkyl halides has been effected in presence of gumbrin and gaseous hydrogen chloride. The reaction took place at 70°, and good yields of alkyl benzenes were obtained [6].

In the present investigation it was decided to replace aluminum chloride by a cheaper catalyst – dry gumbrin and gaseous hydrogen chloride. It was expected that under these conditions aromatic hydrocarbons with long side chains would also be formed, so that the oils would have flat viscosity–temperature curves.

Important factors for success in the reaction are preliminary heat treatment of the clay and the action of gaseous hydrogen chloride on the clay suspension in the alkylation reagents (oil and chlorinated paraffin).

The gumbrin must be dried until the water between the layers has been removed [7]. It was dried at 160° to constant weight, and lost 14.2% of water in the process. It is possible that after removal of the water its place between the montmorillonite lattice layers was taken by the mixture of the alkylation reagents. It is known that montmorillonites are capable of absorbing organic liquids [8]. Oil and chlorinated paraffin come into close contact with the active centers of the aluminosilicate (gumbrin) and the catalytic reaction becomes more probable. A second and no less important condition is the action of dry gaseous hydrogen chloride on a suspension of dry gumbrin in the alkylation reagents. The temperature at which the hydrogen chloride is passed influences the activity of the catalyst formed in this process. It was noticed that the reaction proceeded better when the temperature was raised to 70-90°. It is possible that adsorption of hydrogen chloride was accompanied by chemical reaction between surface hydroxyl groups of the montmorillonite lattice and hydrogen chloride. Miesserov et al. [9] attribute the increased activity of aluminum oxide in isomerization reactions after treatment with hydrogen chloride to this reaction.

EXPERIMENTAL

Avtol-6 distillate from Lok-Batan petroleum contained 30% aromatic hydrocarbons. The kinematic viscosity was 80.6 centistokes at 37.8°, and 7.61 centistokes at 98.9°; the viscosity index was 47.1, $d_{15}^{15.6}$ = = 0.9200. Chlorinated paraffin was prepared from white Groznyi paraffin wax which solidified at 52°. A current of chlorine was passed through the Groznyi paraffin wax until the weight increased by 12-13%. The product was dissolved in ligroine, cooled, and unchanged paraffin was removed from it by filtration. Ligroine was not distilled off, but used as a solvent in the alkylation reaction.

The alkylation was carried out as follows: a mixture of Avtol-6 distillate with 23% of chlorinated paraffin was put in a three-necked flask equipped with a stirrer, reflux condenser, and inlet tube for gaseous hydrogen chloride. A current of dry hydrogen chloride, made directly from NaCl and H_2SO_4 was passed in at 80° with stirring; after 10 minutes 10% of nonactivated gumbrin, dried at 160° to remove interlayer water, was introduced quickly into the flask. Gaseous hydrogen chloride was passed through the suspension of gumbrin in the alkylation reagents at 80° for 5 hours. The hydrogen chloride supply was then discontinued and the oil was left to settle for 12 hours at room temperature. The settled gumbrin was colored black by the oily tar which permeated it. The oily layer was washed with hot water and treated by 10% activated gumbrin at 240°. The solvent (ligroine) and part of the oil was distilled off during this treatment. Filtration gave a clear oil in 90% yield. Its constants are given in Table 1, together with constants for oil made by alkylation in presence of aluminum chloride.

TABLE 1

Constants of Oils Made by Alkylation in Presence of Aluminum Chloride and Dry Gumbrin, and of Gaseous Hydrogen Chloride

Catalyst	Content of chlorinated paraffin (%)	Kinematic viscosity (centistokes)		Viscosity index	Yield on oil taken (%)	Solidification point (°C)
		98.9°	37.8°			
$AlCl_3$	23	5.8	41.1	91.3	90	+4
Clay + HCl	23	5.73	39.5	91.4	90	+5

Table 1 shows that the oil formed in presence of dry gumbrin and gaseous hydrogen chloride has constants similar to those for the oil made by alkylation in presence of 2% aluminum chloride. For fuller characterization of the changes as the result of alkylation, the alkylation product (clay + HCl) and the distillate treated with 2% $AlCl_3$ were separated into fractions by the chromatographic method.

The chromatographic separation was effected as follows: solutions of the oils in ligroine (purified by means of sulfuric acid and boiling below 50°) were passed through glass tubes packed with activated gumbrin. Each oil gave three adsorption zones in the gumbrin – grayish black, brown, and pale gray. The pale gray adsorption zone was first eluted by means of ligroine. This gave the first (colorless) fraction. The brown adsorption zone gave the second fraction. The third fraction was obtained by elution with alcohol–benzene mixture in the cold. No such fraction was obtained from Avtol-6 distillate treated with 2% aluminum chloride. The fourth fraction was obtained by extraction of the adsorbent by hot alcohol–benzene mixture in a Soxhlet apparatus. The third and fourth fractions were obtained in very small amounts and were not analyzed in detail. The constants of the original oils and of the fractions obtained by chromatographic separation are given in Tables 2 and 3.

TABLE 2

Constants of the Alkylation Product (Gumbrin + Gaseous Hydrogen Chloride) and Its Fractions

Product	Yield (%)	Color	Kinematic viscosity (centistokes)		Viscosity index	$n_D^{2.7}$	Solidification temperature (°C)	M
			98.9°	37.8°				
Alkylation product (gumbrin + HCl)	—	Brown	5.73	39.40	91.5	1.4939	+5	—
Fraction 1	47	Colorless	5.71	32.30	97.2	1.4922	+8	—
Fraction 2	43	Colorless	5.67	39.62	87.1	1.5622	+8	355

TABLE 3

Constants of Avtol-6 Distillate after Treatment with 2% Aluminum Chloride, and of its Fractions

Product	Yield (%)	Color	Kinematic viscosity (centistokes)		Viscosity index	n_D^{27}	Solidification temperature (°C)
			98.9°	37.8°			
Avtol-6 distillate + 2% Al_2Cl_3	—	Brown	7.35	78.50	47.7	1.5070	—20
Fraction 1	60	Colorless	6.26	52.24	63.9	1.4952	—20
Fraction 1	30	"	6.98	63.38	31.7	1.5170	—20

It follows from the tables that alkylation changed the amounts and relative proportions of the principal hydrocarbon fractions. The amount of the first fraction decreased by 13%, with a corresponding increase in the yield of the second fraction, which should contain more-easily adsorbable hydrocarbons, which are more valuable as oil components. Evidently these were formed as the result of alkylation. They have a higher viscosity index (this increased by 65 units) and a somewhat different refractive index. Addition of 1% of the alkylation product to standard Avtol lowered its pour point by 6°, while 1% of Fraction 3 lowered it by 8°. The depressant effect of the alkylation product and the differences in the yields and constants of the fractions obtained by chromatography indicate that the composition of the oil is changed by alkylation in presence of gumbrin and gaseous hydrogen chloride.

SUMMARY

1. Alkylation of Avtol-6 distillate by chlorinated paraffin in presence of dry gumbrin and gaseous hydrogen chloride yielded a product with a high viscosity index (91.4).

2. Aluminum chloride can be replaced in the alkylation reaction by dry gumbrin and gaseous hydrogen chloride, without any appreciable decrease in the oil quality and yield.

LITERATURE CITED

[1] L. G. Zherdeva, F. T. Sidlyaronok and N. I. Velizarova, Chemistry and Technology of Fuel 1, 17 (1956).

[2] L. G. Zherdeva, A. A. Karaseva and E. V. Voznesenskaya, Chemistry and Technology of Fuel 1, 50 (1956).

[3] N. I. Chernozhukov and L. P. Kazakova, Chemistry and Technology of Fuel 1, 57 (1956).

[4] I. F. Radzevenchuk, J. Appl. Chem. 29, No. 11, 1697 (1956)*.

[5] I. F. Radzevenchuk, J. Appl. Chem. 30, No. 6, 966 (1957).*

[6] I. F. Radzevenchuk, J. Gen. Chem. 28, 2423 (1958).*

[7] K. G. Miesserov, Progr. Chem. 29, 279 (1953).

[8] F. V. Chukhrov, Colloids in the Earth's Crust [in Russian] (Izd. AN SSSR, 1955) p. 538.

[9] K. G. Miesserov, O. E. Morozova, and A. A. Petrov, J. Gen. Chem. 25, 2204 (1955).*

Received February 6, 1958.

*Original Russian pagination. See C. B. translation.

PREPARATION OF PROPIONIC ACID FROM ACRYLONITRILE

I. N. Nazarov and G. A. Shvekhgeimer

The N. D. Zelinskii Institute of Organic Chemistry

The demand for propionic acid has greatly increased during recent years, as many synthetic anesthetics contain ester groups with propionic acid residues.

The simplest and most convenient synthesis of propionic acid is by acid hydrolysis of propionitrile. A cheap and available source of propionitrile is required for the large-scale use of this reaction. Acrylonitrile is such a source:

$$CH_2{=}CHCN \xrightarrow{H_2} CH_3CH_2CN \xrightarrow{H_2O} CH_3CH_2COOH.$$

However, this simple and short series of conversions has not been used as yet for production of propionic acid. The probable explanation is the lack of a sufficiently convenient and simple method for hydrogenation of acrylonitrile to propionitrile. For example, Reppe and Hoffman [1] performed the hydrogenation at 130-200° under 30 atmos pressure in presence of a copper catalyst.

Winans [2] described a more convenient method – hydrogenation with the aid of pyrophoric nickel at 20-75° and 6 atmos hydrogen pressure, but he gave neither the hydrogenation rate nor the yield of propionitrile.

We used a catalyst consisting of 5% palladium deposited on calcium carbonate [3]. The hydrogenation was effected under constant hydrogen pressure (10 atmos) with continuous stirring of the mixture. The catalyst was used in the proportion of 1% on the weight of acrylonitrile taken (0.05% of palladium). The reaction was strongly exothermic and cooling was necessary. One portion of catalyst was sufficient to hydrogenate six batches of acrylonitrile at a satisfactory rate. The yield of propionitrile was 97% of the theoretical.

The palladium can be recovered completely from the spent catalyst.

Saponification of the nitrile to propionic acid was effected by a modification of the method of Beckurts and Otto [4]; the yield of propionic acid was about 95%.

EXPERIMENTAL

Hydrogenation of acrylonitrile. 212 g (4 moles) of freshly distilled acrylonitrile (b.p. 75-76.5°) and 2.1 g of palladium catalyst (prepared by the usual method [3]) was placed in an autoclave 1.2 liters in capacity. The autoclave was fitted with a propeller stirrer and a device for continuous supply of hydrogen at constant pressure. The temperature rose spontaneously to 60-70° a few minutes after the start of hydrogenation. The reaction temperature was maintained at 60-70° by regulation of the stirrer speed and by cooling of the autoclave in cold water. The hydrogenation was performed at a constant pressure of hydrogen (10 atmos) and was complete after 45 minutes. The cooled reaction mass was decanted from the catalyst and distilled.

Distillation gave 210 g of propionitrile (95.5%) of b.p. 94-97° and 8.7 g of a low-boiling fraction (b.p. 83-94°).

The catalyst entrained during decantation was returned to the autoclave. The catalyst retained adequate activity in hydrogenation of six batches of acrylonitrile of 212 g each (hydrogenation of the last batch took 1.5 hours).

The low-boiling fractions were dried over magnesium sulfate and an additional amount of propionitrile was obtained from them. The total yield of propionitrile was 97%.

Saponification of propionitrile. To 980 g of concentrated sulfuric acid (sp.gr. 1.830), 275 ml of water was added with stirring; the temperature of the mixture rose to 107°. To this diluted sulfuric acid at 107°, 550 g of propionitrile (b.p. 94-97°) was added with vigorous stirring at a rate such that the mixture boiled briskly throughout. The temperature of the mixture first rose to 141° and then began to fall; at the end of the nitrile addition it had fallen to 127°. An emulsion was formed before the end of the nitrile addition. All the nitrile was added during 1 hour 15 minutes. The mixture was then stirred at 134-142° for 2 hours. The propionic acid was distilled off under moderate vacuum (about 100 mm) and then redistilled under atmospheric pressure.

The yield was 700 g of propionic acid of b.p. 135-139°.

The yield of propionic acid was about 95% of the theoretical.

SUMMARY

A method for preparation of propionic acid from acrylonitrile is described; it consists of two consecutive stages: a) hydrogenation of acrylonitrile to propionitrile, and b) saponification of propionitrile to propionic acid.

LITERATURE CITED

[1] W. Reppe and U. Hoffman, German Patent 552978 (1930); Zbl. II, 1236 (1932); French Patent 723936 (1931); Zbl. II, 1235 (1932).

[2] C. F. Winans, U. S. Patent 2334140 (1943); C. A. 38, 2666 (1944).

[3] M. Busch and H. Stove, Ber. 49, 1064 (1916).

[4] H. Beckurts and R. Otto, Ber. 10, 262 (1877).

Received January 16, 1958.

REACTIONS OF NITRO OLEFINS WITH BARBITURIC ACID

V. A. Kon'kova and V. V. Perekalin

Derivatives of barbituric acid (barbiturates) are widely used as highly effective narcotics of low toxicity. The most active of these are substituted at the methylene group, and are mainly alkyl and often mixed derivatives (veronal, barbamyl, nembutal, luminal, and others [1]).

Despite the enormous number of investigations relating to the synthesis and studies of pharmacological properties of barbiturates, little is known about products containing nitro and amino groups in the alkyl radicals linked to the methylene carbon atom [2].

In the course of our work on the chemistry of unsaturated nitro compounds we synthesized nitroalkyl derivatives of barbituric acid by reactions of the latter with various unsaturated nitro compounds.

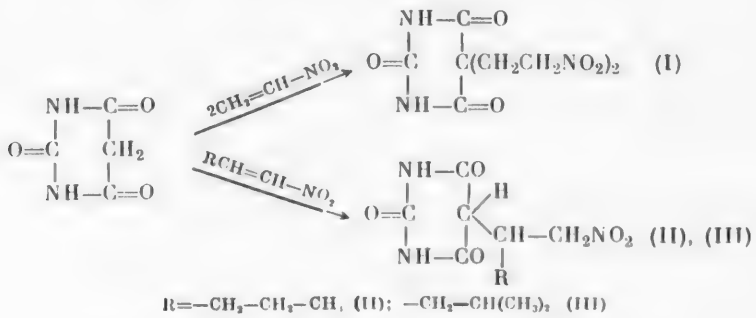

R=—CH_2—CH_2—CH, (II); —CH_2—$CH(CH_3)_2$ (III)

5,5-(2',2'-dinitrodiethyl)barbituric acid (I). 1.75 g of barbituric acid (0.013 mole) and 1.9 g of nitroethylene (0.026 mole) in 30 ml of anhydrous methanol were left overnight at room temperature in presence of a few drops of triethylamine. The odor of nitroethylene disappeared at the end of this time. The liquid was filtered and the solution was evaporated down to a small volume under vacuum.

In addition to a compound which melted at 157° (with decomposition), obtained in 38-40% yield, a high-melting substance was isolated. The compound (I), m.p. 182-183° (decomp.) was isolated from methanol after repeated recrystallization.

Found % C 35.24, 35.34; H 4.13, 4.17; N 20.53, 20.54. $C_8H_{10}O_7N_4$. Calculated % C 35.04, H 3.65, N 20.44.

The substance was hydrogenated over palladium catalyst. The amine was isolated in the form of its hydrochloride.

5-[1-(nitromethyl)butyl(1)] barbituric acid (II). 1.28 g of barbituric acid (0.01 mole) and 1.16 g (0.01 mole) of nitropentene in 25 ml of anhydrous methanol were heated for 10 hours at 60-70° in presence of a few drops of triethylamine. After evaporation of the solvent a substance was obtained of m.p. 136°, yield 1.7 g (65-69%). Substance (II) of m.p. 154° (decomp.) was isolated after repeated crystallization from methanol acidified with 10% hydrochloric acid.

Found % C 44.41, 44.73; H 5.82, 5.79; N 17.31, 17.20. $C_9H_{13}O_5N_3$. Calculated % C 44.44, H 5.35, N 17.28.

5-[(1-nitromethyl-3-methyl)butyl]barbituric acid (III). 1.56 g of barbituric acid (0.012 mole) together with 1.57 g of nitroisohexylene (0.012 mole) in 25 ml of ethanol were heated for 9 hours at 60-65° in presence of a few drops of triethylamine. A substance was obtained in a yield of 0.97 g (30%), m.p. 149-150°. Substance (III) of m.p. 159-160° was isolated from ethanol acidified with 10% hydrochloric acid.

Found %: C 46.86, 46.83; H 5.83, 5.66; N 16.83, 16.72. $C_{10}H_{15}O_5N_3$. Calculated %: C 46.69, H 5.83, N 16.34.

5,5-[(2'-nitroethyl-1-nitromethyl)butyl]barbituric acid. 1.5 g of (II) and 0.5 g of nitroethylene were heated together in anhydrous methanol for 3 hours at 60° in presence of a few drops of triethylamine. The odor of nitroethylene disappeared during the heating. Substance (IV) of m.p. 154° was isolated. A mixed sample with (II) gave a depression of melting point.

Found %: N 17.71, 17.76. $C_{11}H_{16}O_7N_4$. Calculated %: N 17.72.

LITERATURE CITED

[1] S. V. Anichkov and M. L. Belen'kii, Textbook of Pharmacology [in Russian] (State Medical Press, 1955).

[2] M. J. Kamlet, J. Am. Chem. Soc., 77, 4896 (1955).

Received July 10, 1958.

BOOK REVIEW

W. L. Faith, D. B. Keyes and R. L. Clark. INDUSTRIAL CHEMICALS.

Second Edition, New York, Wiley, 1957, 844.

The book under review contains technical and economic information on the main products of the chemical industry of the United States of America. The first edition of this book was published in 1950. Considerable changes have taken place since that time. In particular, the production of certain new chemical products of exceptional importance, such as polyethylene, has been extensively developed, and therefore the second edition of the book has been appreciably expanded (35 names of chemical products have been added and only one omitted).

The following change in presentation has been made in the second edition: instead of maps showing location of producing firms, lists and location (town and state) of firms in the U.S.A. are given for each product.

The book consists of 140 articles, each of which contains information on a particular chemical product. Most of the articles are 5-6 pages in length, but the articles on some products (such as "Acetylene," "Hydrogen," "Acetic Acid," "Phenol," "Ethyl Alcohol," etc.) extend to 10-15 pages; the articles are arranged in alphabetical order.

A detailed subject index makes it easy to use the book and to locate required data. An index of chemical firms in the U.S.A. is also given at the end of the book.

All the articles follow the same plan: for each chemical product the general technological production scheme is given, the production process and the principal chemical reactions are outlined, the consumption of the necessary materials is given, the principal physical and chemical properties of the products are listed, and applications and packaging forms are given. In addition, graphs show the production of each substance in the U.S.A. during the past 20 years (1935-1955) and price variations over 20 years (1936-1956). Economic aspects of the production of various chemicals are also considered very briefly. Producing firms are listed at the end of each article.

Two or more production methods are described in some instances. For example, the article "Barium Carbonate" (pp. 129-132) contains brief descriptions of two methods for production of $BaCO_3$ – from barium sulfide and carbon dioxide, and from barium sulfide and sodium carbonate. In the case of acetylene, three production methods are given. Several production methods are described in the article "Acetic Acid."

The selection of the articles is occasionally of a random character and does not entirely correspond to the title of the book. For example, together with data on important products of the chemical industry made on the large scale (acetylene, ammonia, caustic soda, sulfuric acid, chlorine, etc.) the book contains articles on substances (aspirin, vanillin, penicillin, and others) which are dubious members of the class of industrial chemicals. At the same time there is no information on such a substance as sodium hypophosphite, which is becoming important in chemical nickel plating. There is no information on aluminum fluoride, which is becoming increasingly important in chemical technology.

In our opinion, tables would have been preferable to graphs for showing the production of industrial chemicals and price changes. Tabular data are more convenient to use than graphs. Such a change would not increase the size of the book.

All the articles are of the summary type.

On the whole, the book is written at the modern technological level. It is a useful brief reference work for chemical engineers, planners, and economists.

I. Ya. Volkind

Physical Chemistry

PHYSICAL CHEMISTRY Section
of the
PROCEEDINGS OF THE ACADEMY OF SCIENCES
OF THE USSR (DOKLADY)

including all reports on:

Chemical Kinetics
Interface Phenomena
Electrochemistry
Absorption Spectra
and related subjects

As in all sections of the Proceedings, the papers are by leading Soviet scientists. Represents a comprehensive survey of the most advanced Soviet research in physical chemistry. The 36 issues will be published in 6 issues annually. Translation began with the 1957 volume. Translation by Consultants Bureau bilingual chemists, in the convenient C. B. format.

Annual subscription	**$160.00**
Single issues	**35.00**
Individual articles	**5.00**

Cover-to-cover translation, scientifically accurate. Includes all diagrammatic and tabular material integral with the text; clearly reproduced by multilith process; staple bound.

CONSULTANTS BUREAU, INC.
227 W. 17th St., NEW YORK 11, N. Y.

PROCEEDINGS OF THE FIRST ALL-UNION CONFERENCE ON RADIATION CHEMISTRY, MOSCOW, 1957

THIS UNPRECEDENTED RUSSIAN CONFERENCE on Radiation Chemistry, held under the auspices of the *Division of Chemical Sciences, Academy of Sciences, USSR* and the *Ministry of Chemical Industry*, aroused the interest of scientists the world over. More than 700 of the Soviet Union's foremost authorities in the field participated and, in all, fifty-six reports were read covering the categories indicated by the titles of the individual volumes listed below. Special attention was also given to *radiation sources used in radiation-chemical investigations.*

Each report was followed by a general discussion which reflected various points of view in the actual problems of radiation chemistry: in particular, on the *mechanism of the action of radiation on concentrated aqueous solutions,* on the *practical value of radiation galvanic phenomena,* on the *mechanisms of the action of radiation on polymers, etc.*

The entire "Proceedings" may be purchased as a set, or individual volumes may be obtained separately as follows:

Primary Acts in Radiation Chemical Processes
(heavy paper covers; 5 reports, approx. 38 pp., illus., $25.00)
Radiation Chemistry of Aqueous Solutions
(heavy paper covers, 15 reports, approx. 83 pp., illus., $50.00)
Radiation Electrochemical Processes
(heavy paper covers, 9 reports, approx. 50 pp., illus., $15.00)
Effect of Radiation on Materials Involved in Biochemical Processes
(heavy paper covers, 6 reports, approx. 34 pp., illus., $12.00)
Radiation Chemistry of Simple Organic Systems
(heavy paper covers, 9 reports, approx. 50 pp., illus., $30.00)
Effect of Radiation on Polymers
(heavy paper covers, 9 reports, approx. 40 pp., illus., $25.00)
Radiation Sources
(heavy paper covers, 3 reports, approx. 20 pp., illus., $10.00)

PRICE FOR THE 7-VOLUME SET
: $125.00

NOTE: *Individual reports from each volume available at $12.50 each. Tables of Contents sent upon request.*

CB translations by bilingual scientists include all photographic, diagrammatic, and tabular material integral with the text.

CONSULTANTS BUREAU, INC.
227 WEST 17TH STREET, NEW YORK 11, N. Y